TECHNISCHE UNIVERSITÄT MÜNCHEN

Lehrstuhl für Grundwasserökologie

Insights into the microbial physiology of bacteria capable of degrading pollutants in contaminated groundwater ecosystems

Sviatlana Marozava

Vollständiger Abdruck der von der Fakultät Wissenschaftszentrum Weihenstephan für Ernährung, Landnutzung und Umwelt der Technischen Universität München zur Erlangung des akademischen Grades eines

Doktors der Naturwissenschaften

genehmigten Dissertation.

Vorsitzende(r): Univ.-Prof. Dr. B. Küster

Prüfer der Dissertation:

1. Univ. - Prof. Dr. R.U. Meckenstock
2. Prof. Dr. W.F.M. Röling
   (VU University Amsterdam/Niederlande)

Die Dissertation wurde am 16.05.2013 bei der Technischen Universität München eingereicht und durch die Fakultät Wissenschaftszentrum Weihenstephan für Ernährung, Landnutzung und Umwelt am 31.08.2013 angenommen.

TECHNISCHE UNIVERSITÄT MÜNCHEN

Lehrstuhl für Grundwasserökologie

Insights into the microbial physiology of bacteria capable of degrading pollutants in contaminated groundwater ecosystems

Sviatlana Marozava

Vollständiger Abdruck der von der Fakultät Wissenschaftszentrum Weihenstephan für Ernährung, Landnutzung und Umwelt der Technischen Universität München zur Erlangung des akademischen Grades eines

Doktors der Naturwissenschaften

genehmigten Dissertation.

Vorsitzende(r): Univ.-Prof. Dr. B. Küster

Prüfer der Dissertation:

1. Univ. - Prof. Dr. R.U. Meckenstock
2. Prof. Dr. W.F.M. Röling
   (VU University Amsterdam/Niederlande)

Die Dissertation wurde am 16.05.2013 bei der Technischen Universität München eingereicht und durch die Fakultät Wissenschaftszentrum Weihenstephan für Ernährung, Landnutzung und Umwelt am 31.08.2013 angenommen.

Summary

Natural environments provide microorganisms with conditions very different to well established laboratory cultivation systems such as batch cultures. One of the main differences is that substrates in the environments are typically presented at low concentrations what limits bacterial growth significantly. By contrast, in batch experiments with excess of substrates bacteria approach maximum growth rates. These two different scenarios are characterized by contrasting physiological states. For example, when exposed to excess of organic carbon enteric bacteria are known to utilize favourable substrates preferentially and to block consumption of less preferred substrates via carbon catabolite repression (CCR). During carbon limitation they relieve CCR and utilize many substrates simultaneously. The current study aimed to examine the physiology of two strictly anaerobic environmentally important bacteria, the Gram-negative iron-reducing *Geobacter metallireducens* and the Gram-positive halorespiring *Desulfitobacterium hafniense* Y51, under various limiting conditions.

It was hypothesised that *G. metallireducens* behaves similar to enteric bacteria when subjected to high or low concentrations of mixed carbon substrates. Firstly, *G. metallireducens* was cultivated in batch with single and mixed carbon sources in the presence of Fe(III) citrate. Secondly, in order to investigate the physiology of the strict anaerobe *G. metallireducens* under conditions close to natural, it was cultivated in chemostats with biomass retention (retentostats) at acetate and acetate plus benzoate as electron and carbon sources in the presence of Fe(III) citrate as electron acceptor. During exponential growth phase in batch, *G. metallireducens* showed preferential consumption of acetate and ethanol over benzoate but simultaneous consumption of benzoate and toluene, as well as of butyrate and benzoate. In contrast, during cultivation in retentostats with acetate plus benzoate, *G. metallireducens* was able to utilize these two substrates simultaneously. To reveal overall physiological changes caused by different conditions applied, a global nano-liquid chromatography-tandem mass spectrometry (nano-LC-MS/MS) based proteomics approach was performed using label-free quantification. The benzoyl-CoA pathway was found to be subjected to incomplete CCR during early and late exponential growth phase with a mixture of acetate plus benzoate. Peripheral pathways involved in toluene, ethanol, and butyrate degradation were differentially abundant only with the corresponding substrates. However, they were detected at low levels on all conditions tested. Proteins expressed at low growth rates were compared to high growth rates on corresponding substrates (acetate or acetate plus benzoate). In the course of cultivation, growth rates below 0.003 h^{-1} were achieved (approximately 70 times lower than growth rates obtained during exponential growth phase).

Carbon limitation was characterized by the increased abundances of several catabolic pathways involved in the degradation of carbon substrates not present in the medium (ethanol, butyrate, fatty acids, and several xenobiotics). A growth rate-specific physiology was reflected in the changed abundances of energy-, chemotaxis-, oxidative stress-, and transport-related proteins.

In order to investigate further whether *G. metallireducens* derepresses less preferred catabolic pathways under natural conditions, it was introduced into an indoor groundwater aquifer which was fed with a constant source of toluene. However, after 2.5 months of incubation *G. metallireducens* was nearly undetectable. Therefore, a follow-up proteomic approach was unfeasible.

In contrast to experiments with *G. metallireducens, D. hafniense* Y51 was cultivated in chemostats under limitation of electron donor (lactate) or acceptor (fumarate) and/or ammonium at dilution rates of 0.02 h^{-1} as well as in batch cultures with substrate excess. Under limiting conditions in chemostats, *D. hafniense* Y51 showed complete utilization of residual electron donors and/or acceptors. Extracted proteins were isotope-code labelled (ICPL) and compared to one another. The analysis of significantly different protein ratios revealed increased abundances of enzymes of the CO_2 fixation pathway as well as enzymes related to utilization of some alternative electron donors and acceptors under all conditions applied. Moreover, ammonium limitation was characterized by an increase in ammonium scavenging proteins.

In conclusion, the results obtained indicate that during exponential growth in batch *G. metallireducens* prefers easily degradable substrates over aromatic compounds. However, there is no complete CCR on the molecular level. Moreover, during cultivation in retentostats *G. metallireducens* derepresses peripheral metabolic pathways that are typical for habitats where specific types of substrates such as fatty acids or aromatics prevail. Additionally, extremely low growth rates mimic environmental conditions to a great extent, implying that *G. metallireducens* expresses many adaptive mechanisms in its natural habitats. Expression of alternative metabolic pathways by *D. hafniense* Y51 in response to limitations is another example of an adaptive physiology of pollutant-degrading microorganisms.

Zusammenfassung

Eine der wesentlichsten Abweichungen von den üblichen Laborbedingungen ist die niedrige Substratkonzentration in der Umwelt, die das Bakterienwachstum signifikant einschränkt. In den üblichen Batch-Experimenten ist das Substrat dagegen im Überschuss vorhanden, wodurch maximale Wachstumsraten hervorgerufen werden.

Diese beiden Szenarios sind durch gegensätzliche physiologische Zustände gekennzeichnet. So stellen z.B. enterale Bakterien die Verstoffwechselung weniger günstiger Substrate durch Katabolit-Repression ein (Carbon Catabolite Repression, CCR), wenn besser geeignete Substrate im Überschuss vorhanden sind. Unter limitierenden Bedingungen wird hingegen die CCR eingestellt und zahlreiche verschiedene Substrate gleichzeitig genutzt.

Die vorliegende Studie untersucht die Physiologie zweier strikt anaerober und umweltrelevanter Bakterien unter verschiedenen, limitierenden Bedingungen. Untersucht wurden das Gram-negative und eisenreduzierende Bakterium *Geobacter metallireducens* und das Gram-positive, halorespirierende Bakterium *Desulfitobacterium hafniense* Y51. Dabei wurde von der Hypothese ausgegangen, dass *G. metallireducens* sich ähnlich verhält wie ein enterales Bakterium, wenn es hohen, niedrigen Substratkonzentrationen oder einem Substratmix ausgesetzt wird.

Zum einen wurde dazu *G. metallireducens* in Batch-Experimenten mit einzelnen und gemischten Substraten auf Fe(III)-Citrat kultiviert. Zum anderen wurde *G. metallireducens* in einem Chemostat kultiviert, um die Physiologie unter umweltähnlichen Bedingungen zu studieren. Ein Chemostat mit Biomasse-Rückhaltung (Retentiostat) wurde dabei Acetat und Acetat plus Benzoat als Elektronen- und Kohlenstoffquelle betrieben. Fe(III)-Citrat diente als Elektronenakzeptor für die strikt anaerobe Atmung.

Während des exponentiellen Wachstums zeigte *G. metallireducens* eine bevorzugte Nutzung von Acetat und Ethanol in der Gegenwart von Ethanol, aber auch eine gleichzeitige Nutzung von Benzoat und Toluol, sowie von Benzoat und Butyrat. Im Gegensatz dazu nutzte *G. metallireducens* während der Kultivierung in Retentiostaten mit Acetat und Benzoat beide Substrate simultan.

Um die unterliegenden physiologischen Anpassungen unter den verschiedenen Kultivierungsbedingungen aufzuklären, wurde das globale Proteom der Bakterien untersucht. Dazu wurde Nano-Liquid Chromatographie-Tandem Mass Spektrometrie zur Label-freien Identifikation der Proteine eingesetzt (nano-LC-MS/MS). Dabei zeigte sich, dass der Benzoyl-CoA Stoffwechselpfad während der beginnenden und endenden exponentiellen Wachstumsphase eine unvollständige CCR aufweist, wenn Acetat und Benzoat gemeinsam

verwendet werden. Periphere Stoffwechselwege, die Toluol, Ethanol und Butyrat verwendeten, wurden in unterschiedlichem Umfang genutzt, aber nur, wenn das jeweilige Substrat zugegeben wurde. In niedrigen Konzentrationen waren diese Pfade jedoch unter allen getesteten Bedingungen aktiv. Die Proteine, die bei niedrigen Wachstumsraten gebildet wurden, wurden mit den Proteinen verglichen, die bei normalen Batch-Kultivierungen gebildet wurden (Acetat oder Acetat plus Benzoat). Während der Kultivierung wurden Wachstumsraten von unter 0.003 h^{-1} gemessen, und damit ca. 70-mal geringere als die Wachstumsraten während der exponentiellen Phase. Die Kohlenstofflimitierung steigerte signifikant die Abundanz diverser katabolischer Stoffwechselpfade, deren eigentliche Substrate in dem Medium nicht vorhanden waren (Ethanol, Butyrat, Fettsäuren und einige Xenobiotika). Die spezifische Physiologie der Wachstumsraten spiegelte sich wieder in veränderten Abundanzen der Proteine für den Energiestoffwechsel, für Chemotaxis, oxidativen Stress und Transportsysteme. Um darüber hinausgehend zu untersuchen, ob *G. metallireducens* weniger günstige katabolische Stoffwechselwege unter natürlichen Bedingungen unterdrückt, wurde das Bakterium in einen Toluol-kontaminierten Modellaquifer eingesetzt. Nach 2,5 Monaten Inkubation konnte *G. metallireducens* jedoch nicht mehr nachgewiesen werden, so dass eine Untersuchung des Proteoms nicht möglich war.

Im Gegensatz zu den Experimenten mit *G. metallireducens* wurde *D. hafniense* Y51 in einem Chemostat kultiviert. Dabei wurden der Elektronendonor (Lactat), der -akzeptor (Fumarat) und/oder Ammonium limitierend bei Verdünnungsraten von 0.02 h^{-1} hinzugefügt. Außerdem wurden Batch-Experimente unter Substratüberschuss wie oben beschrieben durchgeführt.

Im Chemostat, unter limitierenden Bedingungen, zeigte *D. hafniense* Y51 eine vollständige Nutzung von verbleibenden Elektronendonoren und –akzeptoren. Die extrahierten Proteine wurden mittels Isotopkodiertem Protein Labelling (ICPL) markiert und miteinander verglichen. Die Auswertung der signifikant verschiedenen Proteinverhältnisse zeigte unter allen Bedingungen zunehmende Vorkommen von Enzymen des CO_2 Fixierungsweges. Zudem war die Ammonium-Limitation von einem Anstieg der Proteine der Stickstoff-Fixierung gekennzeichnet, und von Proteinen, die hochaffin für Ammonium waren.

Aus den vorliegenden Ergebnissen lässt sich die generelle Schlussfolgerung ziehen, dass *G. metallireducens* einfach abbaubare Substrate aromatischen Verbindungen vorzieht. Trotzdem wies das Bakterium nur eine unvollständige CCR auf molekularer Ebene auf. Darüber hinaus unterdrückte es während der Kultivierung im Retentiostat periphere metabolische Stoffwechselwege, die typisch für Umgebungen sind, in denen Substrate wie Fettsäuren oder

Aromaten dominieren. Die extrem niedrigen Wachstumsraten simulierten weitestgehend Umweltbedingungen, so dass die Vermutung naheliegt, dass *G. metallireducens* viele dieser Anpassungsmechanismen in seiner natürlichen Umgebung ausführt. Die Expression alternativer metabolischer Stoffwechselwege durch *D. hafniense* Y51 als Antwort auf die limitierenden Bedingungen ist darüber hinaus ein weiterer Beleg für die Anpassungsfähigkeit der Physiologie schadstoffabbauender Mikroorganismen.

Table of contents

Additional material can be found on the CD attached

Abbreviations

ANOVA - analysis of variance
BTEX - benzene, toluene, ethylbenzene, and xylene
CcpA - catabolite control protein A
CCR – carbon catabolite repression
cis-DCE - 1,2-dichlorethene
CRP - cyclic AMP receptor protein
DGGE – denaturing gradient gel electrophoresis
DOC – dissolved organic carbon
EDTA - ethylenediaminetetraacetic acid
EI – enzyme I of phosphoenolpyruvate-dependent phosphotransferase system
EII - enzyme II of phosphoenolpyruvate-dependent phosphotransferase system
FDR – false discovery rate
GC-MS – gas chromatography coupled to mass spectrometry
HPLC – high pressure liquid chromatography
HPr - histidine protein
ICPL – isotope-coded protein labelling
LC-MS/MS – liquid chromatography-tandem mass spectrometry
PAGE – polyacrylamide gel electrophoresis
PAHs - polyaromatic hydrocarbons
PBS buffer - phosphate buffered saline
PCA – principal component analysis
PCE – perchloroethylene
PCR – polymerase chain reaction
PHB - poly-β-hydroxybutyric acid
PRDs - PTS-regulatory domains
PTS - phosphoenolpyruvate-dependent phosphotransferase system
PVDF - polyvinylidene difluoride
SDS - sodium dodecyl sulphate
TAE buffer – Tris base, acetic acid and EDTA buffer
TCA - 1,1,1-trichloroethane
TCA – tricarboxylic acid cycle
TCE – trichloroethylene
T-RFLP – terminal restriction length polymorphism
UV –ultra violet
VC – vinyl chloride
W-L – Wood–Ljungdahl pathway

1 Introduction

1.1 Role of microorganisms in the degradation of pollutants in contaminated groundwater

The environment has been experiencing pollution with thousands of different xenobiotics since the chemical industry started to develop. Artificial compounds such as insecticides, herbicides, detergents and others possess not only a significant toxicity but also a high stability in the environment due to their low chemical activity at moderate temperatures. Nowadays, a gradual accumulation of contaminants in the environment is taking place. Lack of, or slow biodegradation of xenobiotics by microorganisms is one of the main problems in cleaning the environment.

A major part of xenobiotics released into the environment is comprised of chlorinated solvents (Arneth et al., 1989; Hirata et al., 1992) and petroleum hydrocarbons (US-EPA, 1998). Chlorinated solvents have been used extensively as degreasing agents in household activities and industry. The most abundant chlorinated compounds found in groundwater are methylene chloride, trichloroethylene (TCE), perchloroethylene (PCE), and 1,1,1-trichloroethane (TCA) (Arneth et al., 1989) which enter the environments mainly through the leaching from landfills (Arneth et al., 1989). Chlorinated compounds and their degradation intermediates have high toxicity (Kimbrough, 1972) and are considered to be carcinogenic for animals and humans (Holliger et al., 1998).

Aromatic hydrocarbons which are often petroleum derived pollutants are frequently found in contaminated aquifers. These compounds have benzene ring, where all C-atoms are sp^2-hybridised and which possess a delocalised π-electron system over the ring. Therefore, the chemical stability of aromatic hydrocarbons is high due to the mesomeric delocalisation energy. Aromatic hydrocarbons can be divided into mono- (e.g., benzene, toluene, ethylbenzene, and xylene (BTEX)) and polyaromatic hydrocarbons (PAHs) (naphthalene, anthracene, etc). The most frequent cause of contamination is leakage from underground pipelines, oil tanks, and landfills, spillages from overfilling or accidents during fuel transferring.

Removal of pollutants from contaminated groundwater is important not only for provision of high quality drinking water but also for the preservation and effective functioning of groundwater ecosystems. Conventional methods for removing, reducing, or mitigating toxic substances introduced via anthropogenic activities include pump and treat systems (McKinney and Lin, 1996), incineration (Lisk, 1988), containment (Haest et al., 2010), soil

vapour extraction, and ozone or hydrogen peroxide injection (Bhuyan and Latin, 2012). Usage of such treatment methods is costly, involves risks of creation of toxic gases, irreversible damage of the indigenous communities, etc. On the other hand, natural attenuation is a perspective alternative which offers significant cost reduction during remediation as well as it is an environmentally friendly approach. Natural attenuation consists of physico-chemical processes (dilution, sorption, dispersion, etc.) and biodegradation by intrinsic microbial community (Johnson et al., 2003).

Environmental microorganisms are able to metabolize many organic pollutants because evolutionary they have developed pathways to biodegrade naturally occurring analogues of anthropogenic contaminants. For example, compounds such as aromatic hydrocarbons and organohalogens are wide spread in nature. The first chemicals have been formed geochemically over geological period of time by the reactions of buried biomass and became major oil components. Moreover, some aromatic amino acids or monoterpens can be produced by anaerobic bacteria (Widdel and Rabus, 2001). Halogenated alkanes are released in massive quantities by volcanoes and forest fires. They are also produced by marine algae, some fungi, evergreen cypress, etc. (Gribble, 1994). Therefore, certain microorganisms which have been selected by evolution to utilize naturally occurring recalcitrant compounds can play an important role in the natural attenuation of groundwaters contaminated with pollutants of analogous nature.

Many studies demonstrated the importance of microorganisms in natural attenuation. Just to name a few, it has been shown that *Geobacter* sp. play an important role in the anaerobic oxidation of benzene in a petroleum-contaminated aquifer in Bemedji, Minnesota (Rooney-Varga et al., 1999), *Comamonadaceae* degrade BTEX in petroleum hydrocarbon contaminated sites in Hungary (Tancsics et al., 2010). Most of the xenobiotics have been subjected to the biodegradation at Vejen site, Denmark after 10 years from the beginning of the observations (Baun et al., 2003). Intrinsic bacterial communities showed degradation of BTEX under iron-reducing conditions in a contaminated aquifer at Banisveld, the Netherlands (Röling et al., 2001). Biodegradation of 1,2-dichlorethene (*cis*-DCE) and vinyl chloride (VC) has been observed in river sediments contaminated with chlorinated aliphatic hydrocarbons originating from polluted groundwater in the industrial area of Vilvoorde, Belgium (Kuhn et al., 2009).

However, degradation of contaminants frequently requires biostimulation and/or bioaugmentation in addition to the natural attenuation (Scow and Hicks, 2005) due to the lack

of important nutrients or key players in the environment. The rates of microbial biodegradation depend strongly on redox conditions and nutrient bioavailability (Röling and van Verseveld, 2002). In many polluted environments oxygen is being depleted very fast and much slower anaerobic processes prevail due to the low oxygen concentrations in groundwaters. Therefore, aromatic hydrocarbon-degrading microorganisms are obliged to use alternative electron acceptors, such as nitrate, sulphate, Fe(III) oxides, etc., while halorespiring-bacteria require usage of easily degradable electron donors. The low levels of compounds essential for redox reactions can decrease bioremediation significantly. Moreover, natural environments are characterized by low contents of such important nutrients for bacterial physiology as nitrogen and phosphorus. Therefore, the addition of electron acceptors and electron donors which are limited in the environment might increase the degradation rates of pollutants by natural communities (Tyagi et al., 2011). Furthermore, introduction of the microorganisms with specific degrading capabilities which are absent from the contaminated aquifers or are in low abundances can enhance biodegradation as well. However, the latter strategy must be carried out with caution as many stress conditions in the environment can lead to unsuccessful results (Perelo, 2010).

Another important aspect which contributes to slow bioremediation is the presence of high concentrations of easily degradable substrates which might hinder degradation of pollutants in the environments. Such an effect can be explained by preferential consumption of the substrates which are degraded faster, and/or energetically more favourable than, e.g., aromatic compounds. Additionally, catabolic pathways involved into biodegradation can be repressed by preferred substrates. For example, it has been shown that ethanol utilization is preferred over BTEX consumption in oxic and anoxic mesocosm experiments (Ruiz-Aguilar et al., 2002; Da Silva et al., 2005), degradation of benzene was reduced in the presence of ethanol and acetate in oxic (Schaefer et al., 2010b) and anoxic microcosms with sulphate as electron acceptor (Rakoczy et al., 2011); ethanol and/or acetate inhibited utilization of BTEX significantly under denitrifying and iron-reducing conditions in anaerobic mesocosms (Chen et al., 2008). Preferential consumption of acetate and ethanol over recalcitrant pollutants leads to the removal of electron acceptors that can be used for mineralization of aromatic compounds available in the environment (Chen et al., 2008). Therefore, investigation of physiology of the main players in the biodegradation under combinations of different carbon sources is of importance as it can provide valuable information for future enhancement of *in situ* bioremediation.

1.2 Carbon catabolite repression

In the environment, microorganisms are often exposed to a mixture of carbon sources where accurate regulation of uptake and metabolism of these substrates is essential to enable survival of the fittest. Carbon catabolite repression (CCR) is a well-established gene regulation system for such a global metabolic control in bacteria. It prioritizes the usage of a preferred carbon source over the other, when both are present. As a result, gene expression of less preferred carbon sources is repressed and bacteria exhibit higher growth rates while utilizing the most energy efficient carbon substrates (Vinuselvi et al., 2012) .

1.2.1 CCR in *E. coli* and *B. subtilis*

CCR has been studied since the early 1940s when J. Monod discovered diauxic growth of *Bacillus subtilis* (Monod, 1942). CCR involves global and operon-specific regulation (inducer exclusion and induction prevention) of catabolic pathways (Gorke and Stulke, 2008). The most studied representatives of global regulators are the cyclic AMP receptor protein (CRP)-dependent CCR specific for Gram-negative bacteria and the catabolite control protein A (CcpA)-dependent CCR typical for Gram-positive bacteria (Figure 1-1) (Warner and Lolkema, 2003; Gorke and Stulke, 2008; Fujita, 2009). CRP and CcpA are transcriptional regulators of the type of CRP/FNR and LacI/GalR, respectively. Both regulators are connected to the phosphoenolpyruvate-dependent phosphotransferase system (PTS), which is involved in the uptake of carbohydrates in the Gram-negative Enterobacterium *Escherichia coli* and the Gram-positive Firmicute *B. subtilis*. Therefore, PTS plays a connecting role between the substrate uptake and global regulation in *E. coli* and *B. subtilis*.

The main components of PTS are enzyme I (EI), histidine protein (HPr) and enzyme II (EII) (Figure 1-1) (Warner and Lolkema, 2003). In Gram-negative bacteria, the phosphorylative state of the substrate specific EII regulates the expression of catabolic proteins together with activity of different permeases. For example, during active uptake of glucose in *E. coli*, dephosphorylated EII^{Glu} binds to permeases of other carbohydrates and blocks their activity. This mechanism is also known as inducer exclusion. In the absence of glucose, EII^{Glu} is phosphorylated and subsequently influences the levels of cAMP in the cell which binds to the CRP regulator and leads to expression of catabolic genes (global regulation) (Warner and Lolkema, 2003) (Figure 1-1).

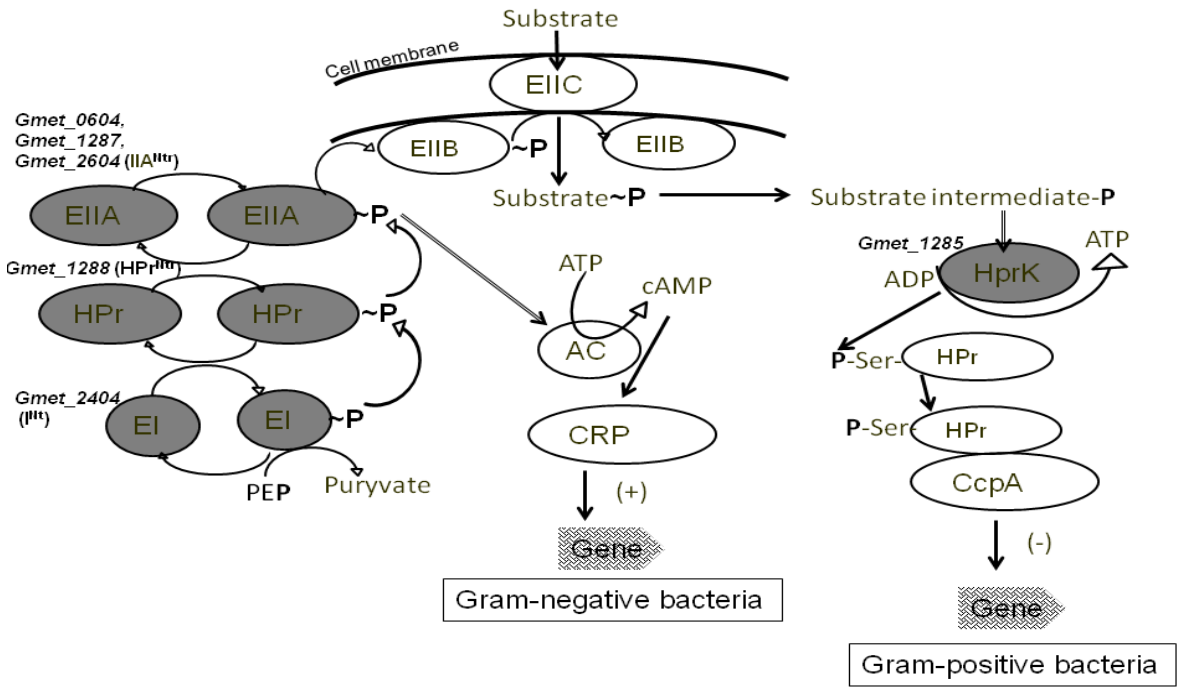

Figure 1-1 Schematic representation of the general scheme of CCR in Gram-positive and Gram-negative bacteria (modified from (Warner and Lolkema, 2003)). On the left side is the PTS transfer chain of phosphoryl-groups from enzyme EI to the substrate, where EI is enzyme I of PTS, PEP – phosphoenolpyruvate, HPr - histidine protein, EIIA, EIIB and EIIC - membrane bound proteins of PTS, AC - adenylate cyclase, CRP and CcpA - transcriptional regulators, HprK - Hpr kinase. Highlighted in grey are PTS orthologues encoded in the genome of *G. metallireducens* together with their gene numbers.

In Gram-positive bacteria, the primary sensor of CCR is Hpr kinase which can be activated not only by intermediates of transported substrates but also by other metabolites present in the cell (Figure 1-1) (Warner and Lolkema, 2003). The phosphorylation of a serine residue of the HPr protein by HPr kinase plays an important role in CCR. In the presence of glycolytic intermediates P-Ser-HPr binds to the CcpA regulator and prevents transcription of catabolic genes (Warner and Lolkema, 2003). Inducer exclusion is also found in Gram-positive bacteria, e.g., P-Ser-HPr binds to the transporters of alternative substrates in the presence of glucose and blocks their activity (Deutscher, 2008).

Another operon-specific mechanism of CCR is induction prevention, which is based on the prevention of the activity of operon-specific transcriptional regulators (Gorke and Stulke, 2008). In *E. coli* and *B. subtilis*, specific transcription factors containing duplicated PTS-regulatory domains (PRDs) control the expression of operons encoding PTS-substrates catabolic genes. The activity of these factors is regulated by components of the PTS (EII

and/or HPr). In order to be activated or deactivated, PRD-containing regulators should be phosphorylated at one of their PRDs by EII or HPr (Deutscher, 2008; Gorke and Stulke, 2008).

However, the extensive analysis of 250 bacterial genomes (Cases et al., 2007) showed the absence of many permease components of PTS in other groups of bacteria, suggesting that substrate transfer by PTS in *Enterobacteriaceae* and *Firmicutes* is rather an exception than a rule. Moreover, many bacteria contain paralogues to known PTS enzymes: I^{Ntr}, NPr (HPr paralogue), IIA^{Ntr} (PtsN) (Boel et al., 2003) (Figure 1-1). It is suggested that they could be involved not only in CCR (Aranda-Olmedo et al., 2006; Carmona et al., 2009; Daniels et al., 2010) but also in potassium metabolism (Lee et al., 2007), control of the intracellular accumulation of polyhydroxyalkanoates (Velazquez et al., 2007), iron regulation (Paustian et al., 2002), down regulation of pyruvate dehydrogenase activity (Pflueger-Grau et al., 2011), and even virulence (Higa and Edelstein, 2001; Bartfeld et al., 2009). Interestingly, many Gram-negative Proteobacteria encode Hpr kinase which is absent from Gram-negative enteric bacteria but present in Gram-positive bacteria (Boel et al., 2003). These organisms lack functional PTS together with the transcriptional regulator CcpA (Boel et al., 2003). For the majority of bacteria the more appropriate role of PTS was suggested to be an assessment of the concentrations of carbon sources in the environment (Cases et al., 2007).

The above mentioned transcriptional regulators CRP and CcpA are not exclusively the only regulators which are taking part in CCR. A set of various important regulators has been identified. Other global regulators involved in glucose-mediated CCR in *Enterobacteriaceae* are Mlc, MtfA, ArcA/B, Cra, Fnr (Deutscher, 2008). In *B. subtilis*, CcpB participates in the repression of *xyl* and *gnt* operons (Chauvaux et al., 1998), CcpC regulates the expression of aconitase and citrate synthase (Blencke et al., 2006), CcpN controls the expression of gluconeogenic genes (Servant et al., 2005), and the Crh protein (an analogue of HPr) is suggested to regulate the glycolytic flux (Landmann et al., 2011).

In the last years, more and more reports appear on PTS-independent CCR. For example, in *Streptomyces coelicolor*, glucose kinase is a trigger enzyme and an essential player in global carbon control (Kwakman and Postma, 1994; Gorke and Stulke, 2008). In *Pseudomonads* and *Acinetobacter baylyi*, the global regulator Crc binds to the mRNA transcripts of the regulators of catabolic pathways (Muller et al., 1996; Fischer et al., 2008; Gorke and Stulke, 2008; Moreno et al., 2009a).

To summarize, CCR is rather a complicated mechanism. It is operated via a PTS system in bacteria utilizing sugars, where CCR is regulated globally or via phosporylative states of certain PTS components. However, many bacteria do not encode a full set of PTS-related proteins, suggesting that preferential consumption of carbon sources might require (an)other mechanism(s). The question of CCR regulation becomes critical for microorganisms degrading pollutants in the environment which might not specialize on consumption of sugars.

1.2.2 CCR in environmentally relevant bacteria

1.2.2.1 Easily degradable carbon sources vs. aromatic compounds

The investigation of the CCR phenomenon is particularly interesting for environmentally relevant microorganisms capable of hydrocarbon degradation under anoxic conditions. Organic contaminants are poorly degraded in the absence of oxygen due to the reduced degradation rates with other electron acceptors and, especially, the lack of the reactive co-substrate oxygen. Moreover, contaminated sites often contain a wide range of pollutants together with fermentation products, humic acids, etc. For such environments, it is relevant to know whether easily degradable substrates will repress pollutant degradation pathways or not, e.g., in order to design effective bioremediation strategies.

Some studies have already been conducted on CCR in environmentally relevant anaerobic bacteria. The strict anaerobes *Clostridium acetobutylicum* (Grimmler et al., 2010) and the Gram-negative thermophilic anaerobic bacterium *Thermotoga neapolitana* (Vargas and Noll, 1996; Nguyen et al., 2001) showed CCR of xylose and L-galactose by glucose. Facultative anaerobes performed different strategies in the utilization of the aromatic compound benzoate with other substrates. The repression by succinate, malate and acetate was observed for *Azoarcus* sp. strain CIB (Barragan et al., 2004), while in *Thauera aromatica* there was simultaneous utilization of both substrates (Heider et al., 1998; Trautwein et al., 2011), and in *Aromatoleum aromaticum* EbN1 preferential consumption in the presence of succinate was observed (Trautwein et al., 2011). In the Gram-negative β-proteobacterium, *Ralstonia eutropha*, acetate itself and not its metabolite acetyl-CoA partially inhibited phenol degradation (Ampe et al., 1998), while catechol, an intermediate of benzoate degradation inhibited the consumption of acetate (Ampe and Lindley, 1995). In addition, malate was shown to inhibit the degradation of TCE in *R. eutropha* (Ayoubi and Harker, 1998).

Therefore, environmentally relevant microorganisms perform different strategies for utilization of aromatic compounds in the environment. Pollutants can be subjected to CCR by

aliphatic acids and/or glucose or they can be utilized simultaneously or even preferred over easily degradable substrates.

In contrast to the observations on substrate consumptions, only limited amount of knowledge exists on the driving mechanisms.

1.2.2.2 Mixture of aromatic compounds

Despite structural similarity, there are observations on preferential utilization of one aromatic substrate over another aromatic compound when a bacterium is exposed to their mixture. Mainly, benzoate plays a role of an inhibitor. For example, in *Acinetobacter calcoaceticus*, benzoate is preferred over *p*-hydroxybenzoate and phenol. Phenol utilization is repressed by benzoate itself, probably through inhibition of MphR, the transcriptional activator of phenol hydroxylase (Zhan et al., 2009). *Cis*,*cis*-muconate, an intermediate product of benzoate degradation in this bacterium, has been found to repress degradation of *p*-hydroxybenzoate (Gaines et al., 1996). In the Gram-positive bacterium, *Rhodococcus* sp. strain DK17, benzoate showed strong inhibition of phthalate degradation via unknown mechanism (Choi et al., 2007). In *P. putida*, the transcriptional regulator BenR, an AraC/XylS family member, blocked the expression of the transporter of *p*-hydroxybenzoate when benzoate was present (Cowles et al., 2000).

Hence, although degradation of many aromatic compounds including benzoate proceeds through the common intermediate benzoyl-CoA, benzoate seems to be a preferred substrate in the mixture of aromatic compounds. Such an observation can be explained by the fact that it takes only one reaction to convert benzoate to benzoyl-CoA while for many other aromatic compounds, e.g., toluene and phenol, more degradation steps are involved. Microorganisms might optimize their physiology in such a way that they prefer to consume the aromatic compound which requires less energetic costs and provides sufficient amount of ATP when being utilized.

1.2.2.3 Mechanisms of CCR in xenobiotics degrading bacteria

Hitherto, mechanisms of repression of the xenobiotic-degrading pathways have been examined in few microorganisms only. Nevertheless, the diverse strategies in optimization of carbon consumption have been identified for some bacteria. The mechanisms of repression are stated below and based, principally, on the blockage of expression of the degrading pathways by global regulators, preferred substrates, or catabolic metabolites. It is worth

mentioning, that in all investigated mechanisms, the release from the repression is usually observed after removal of the preferred substrates.

With respect to research conducted on CCR in environmentally relevant microorganisms, the Gram-negative γ-Proteobacterium *Pseudomonas* sp. is one of the most studied bacteria. In *Pseudomonas* sp., regulation of catabolic pathways differs from the well-described mechanisms of *E. coli* and *B. subtilis*. The global transcriptional regulator CRP-like protein is present within its genome but seems to lack CCR activity (Rojo, 2010). However, another global regulator Crc which belongs to a family of endonucleases–exonucleases–phosphatases (Rojo, 2010) was found to be important for an optimized growth. It exhibits succinate-mediated CCR over not only carbohydrates and aromatic compounds, but also some amino acids (Moreno et al., 2009b; Rojo, 2010). Crc binds to the mRNAs of transcriptional activators of degradation pathways of less preferred substrates, e.g., alkanes and benzoate, and inhibits their translation (Rojo, 2010). Repression of toluene and xylene degradation pathways by glucose or succinate in *P. putida* is also mediated by Crc together with PtsN (an analogue of EIIA) (Cases et al., 1999; Aranda-Olmedo et al., 2006). Recently, it has been shown that Crc targets not only inducers of less preferred substrates but also their uptake systems and enzymes of the corresponding pathways (Hernández-Arranz et al., 2012).

Sometimes, repression of catabolic pathways in *P. putida* does not require global regulators: preferred substrates themselves may function as direct inhibitors. For example, fumarate, succinate, and citrate inhibit induction of 3-chlorocatechol degradation by the ClcR transcriptional activator via direct binding to this activator (McFall et al., 1997). Phenol degradation is also suggested to be inhibited via similar mechanism, where organic acids (succinate, lactate, acetate) and glucose repress the PhlR activator of phenol degradation (Muller et al., 1996). Moreover, *m*-xylene degradation is inhibited by metabolites of the Entner-Doudoroff pathway (Velazquez et al., 2004) and is mediated by the phosphorylated form of the PtsN protein, an analogue of EII^{Ntr} of *E.coli* (Cases et al., 1999).

Recently, it has been shown that sRNAs take part in the mediation of CCR in *P. aeruginosa* and *P. putida*. CbrAB/Crc system in *P. aeruginosa* regulates the expression of proteins related to the degradation of acetate, aromatic acids, and branched-chain amino acids (Sonnleitner et al., 2012). The latter mechanism involves sRNA CrcZ. In the presence of preferred substrate such as succinate, the expression level of *crcZ* is very low, but when this substrate is depleted, the concentration of *crcZ* increases. It binds to the global regulator Crc and it removes Crc from the transcriptional activators of less preferred substrates and as a result the CCR is

relieved (Sonnleitner et al., 2009). Next to CrcZ, CrcY was also found to be involved in the control of the free levels of Crc in *P. putida* (Moreno et al., 2012). Interestingly, recently it has been shown that the repression of catabolic genes by Crc in *P. putida* is reduced at low temperatures (10 C°) relative to high (30 C°). The relief in repression is facilitated by the increased levels of sRNAs CrcZ and CrcY at low temperatures (Fonseca et al., 2012). Therefore, it is possible that under natural conditions where temperatures are below those applied in the laboratories, *Pseudomonas* sp. does not exhibit CCR, and the inhibition of the degradation of less preferred substrates could be just a laboratory artefact. However, this aspect requires further investigations.

Crc-mediated CCR was also suggested to play a role in the repression of protocatechuate degradation by acetate and succinate in another γ-Proteobacterium *Acinetobacter baylyi*. The repression acts post-transcriptionally as in *P. putida*. However, in contrast to *P. putida* where Crc blocks activity of the target mRNAs via binding to them, it involves the degradation of *pca-qui* transcripts which encode protocatechuate 3,4-dioxygenase (Zimmermann et al., 2009). Moreover, in the presence of acetate and succinate Crc was found to be a negative regulator of a number of aromatic hydrocarbon-degrading pathways involved in the utilization of compounds such as *p*-hydroxybenzoate, vanillate, hydroxycinnamates, benzyl esters, benzoate, salicylate, and anthranilate (Bleichrodt et al., 2010).

Besides the examples described above, there are reports on CCR in two aerobic members of β-proteobacteria, *Cupriavidus necator* JMP134 and *Acidovorax* sp. KKS102. In *C. necator* JMP134, benzoate directly represses the degradation of 4-hydroxybenzoate supposedly via inhibition of the activity of PobR, the transcriptional regulator of 4-hydroxybenzoate degrading genes (Donoso et al., 2011). While in *Acidovorax* sp. KKS102, the pE promoter of the *bph* operon of the PCB/biphenyldegrading pathway is repressed by succinate, fumarate, or acetate. In the absence of these substrates, the pE promoter is activated by BphQ protein, a member of the two-component regulatory system BphP/ BphQ (Ohtsubo et al., 2006).

In contrast to *Pseudomonas*, transcriptional regulators of the CRP-FNR family were shown to play an important role in regulation of expression of the xenobiotic-degrading genes in some bacteria. Thus, it has been shown that in the presence of glucose, CRP-like protein of the Gram-positive aerobic Actinobacterium *Rhodococcus* sp. strain TFB represses the expression of the genes responsible for the degradation of tetralin (Tomas-Gallardo et al., 2012) while in another Gram-positive halorespiring and strict anaerobic Firmicute *Desulfitobacterium hafniense* DCB-2, the CRP-FNR like protein CprK plays a role of an activator. It binds

halogenated phenolic compounds and subsequently activates genes involved in their degradation (Pop et al., 2004; Kemp et al., 2013). In the facultative anaerobic α-Proteobacterium *Rhodopseudomonas palustris*, two members of the CRP-FNR family, AadR (Dispensa et al., 1992) and HbaR (Egland and Harwood, 2000), activate the expression of ´the genes involved in the anaerobic 4-hydroxybenzoate and benzoate degradation, respectively.

Unfortunately, until now, mechanisms of CCR in anaerobic microorganisms have been extensively studied only in the facultative anaerobic β-Proteobacterium *Azoarcus* sp. CIB where P_N promoter of the benzoate-degrading genes (*bzd*)genes is subjected to CCR by succinate (Durante-Rodriguez et al., 2008). Therefore, further accumulation of knowledge on the molecular basis of repression or activation of xenobiotics degradation in strict anaerobes, microorganisms which play a major role in bioremediation, is required. The currently collected information on CCR can be used to draw possible hypotheses on regulating mechanisms of carbon consumption in strict anaerobes.

1.3 *In situ* physiology of microorganisms

Natural environments provide microorganisms with conditions different to well-established laboratory cultivation systems, such as batch. The particular characteristic of the majority of the habitats is that there is no single substrate but a mixture of different carbon sources of low and high molecular weight at very low concentrations (Konopka, 2000; Langwaldt et al., 2005). For example, in marine and lacustric environments (Munster, 1993), the content of dissolved organic carbon (DOC) can be as low as 0.4-4000 nM, while in groundwaters it can "increase" up to 75-180 µM (Fredrickson and Madylin, 2001; Langwaldt et al., 2005). However, microorganisms are still able to survive under such oligotrophic environmental conditions. The important question to ask is: how do they do that? Studies on the physiology of microorganisms *in situ* can assist in answering this question. Nevertheless, they are challenged with complications in growth monitoring, difficulties in DNA and protein extractions, and constant fluctuations of the environmental parameters. Therefore, different systems to study the physiology of microorganisms in the laboratory under more stable conditions have been developed.

1.3.1 Systems to study physiology of microorganisms

Physiological studies on microorganisms used to be conducted in two common cultivation systems: batch and chemostat. These two methods have profoundly different approaches in

understanding how microorganisms grow under low nutrient concentrations (Kovarova-Kovar and Egli, 1998).

Batch is a closed system where conditions change constantly due to a gradual utilization of substrates with subsequent exhaustion. Bacterial cultures exhibit different growth phases which are characterised by various physiological parameters, such as cell numbers, cell sizes, DNA and protein content, and etc. (Wanner and Egli, 1990). Batch has been used extensively to estimate maximum specific growth rates [μ_{max}] on different substrates and biomass produced per amount of substrate of interest (growth yield). Therefore, cultivations in batch can provide information on the physiological capabilities of microorganisms under different growth conditions. The major drawbacks of batch cultivation are that microorganisms exhibit short term maximum specific growth rates with a rapid transition to stationary phase. As a result, no long term steady state conditions are possible.

In contrast to batch, chemostats provide a possibility to cultivate microorganisms at constant conditions where growth rates and physico-chemical parameters are fixed (Hoskisson and Hobbs, 2005). The particular feature of chemostat is cultivation at low growth rates and high cell densities which significantly facilitate performances of various physiological analyses. Moreover, continuous cultivations in chemostat is considered to be a more appropriate method to imitate oligotrophic conditions in ecosystem (Kovarova-Kovar and Egli, 1998). According to Kovarova-Kovar and Egli (1998) the most suitable experimental approach to study physiology of microorganisms under natural conditions is to carry out continuous cultures with mixed substrates and/or mixed cultures. However, the lowest growth rate provided by chemostat cultivation that can be reliable appears to be $0.02\ h^{-1}$. At lower dilution rates, there is inhomogeneity in substrate concentrations due to the inability to equally distribute the amount of inflow per all bacterial cells (van Verseveld et al., 1984).

Continuous cultures with biomass retention (retentostats) may permit to achieve extremely low growth rates (Lin et al., 2009; Goffin et al., 2010) with doubling times approaching up to one year.It indicates that bacterial physiology exhibited during cultivation in retentostats might be very different to the one in chemostats (Konopka et al., 1998). The difference between chemostats and retentostats is the filter unit in the reactor which leads to the retention and accumulation of bacterial cells. While microorganisms keep on dividing, they receive lower substrate amounts per cell which leads to the subsequent lower growth rates with time. Cultivation of different microorganisms in retentostats has been carried out extensively in the 80’s and 90’s, mainly in order to answer the questions of maintenance and stringent response

at growth rates close to zero (Chesbro et al., 1979; Arbige and Chesbro, 1982; Muller and Babel, 1996; Tappe et al., 1996; Konopka et al., 1998; Tappe et al., 1999). The recent development of advanced "omics" techniques provides new opportunities to investigate the physiology of microorganisms at low growth rates from a different perspective, looking at global response through analysis of gene expression and metabolite regulations (Goffin et al., 2010), membrane composition, and isotope fractionation (Davidson et al., 2009).

1.3.2 Strategies to survive in oligotrophic environments

The physiology of microorganisms in the environment is different to laboratory conditions due to such environmental factors as resource limitations, competition, predation, and heterogeneity. Microorganisms are never at steady state. Their population numbers constantly increase and decrease (Jannasch and Egli, 1993) in response to the availability of carbon and energy (Kovarova-Kovar and Egli, 1998). Therefore, the state of microorganisms under natural conditions can be described somewhere in between a closed batch culture and an open continued culture (Jannasch and Egli, 1993).

Various limitations occur in natural habitats: nitrogen, phosphorus, carbon, and energy limitations (Elser et al., 1995). Carbon limitation can be considered as the most crucial for microorganisms as 50% of their biomass consists of this element. For heterotrophic bacteria (except of photoheterotrophic), substrates which contain carbon are sources of carbon and energy. Many environments are energy-limited as bacteria are constantly seeking energy and therefore reduce their natural energy resources. Munster (1993) reported that the concentrations of free amino acids and carbohydrates in freshwater habitats are in the nM range (Munster, 1993). Meanwhile, groundwaters contain only from 0.5 to 5% of DOC utilizable by heterotrophic bacteria (Morita, 1990; Egli, 2010). Surprisingly, the majority of bacteria (70-90%) have been shown to be active and able to grow under such oligotrophic environmental conditions (Egli, 2010).

Bacterial populations which are exposed to carbon/energy limitations are characterized by small cell sizes and extremely low growth rates. The strategies they apply to survive can be divided into the following:

(i) *Enhanced substrate affinity and effectiveness of substrate utilization*. The limiting substrates need to enter a cell through a barrier of several cell layers. In order to facilitate that, Gram-negative microorganisms can enhance abundance of their porin proteins which form large pores in the cell membrane and, therefore, increase membrane permeability (Konopka, 2000). However, it has been shown

that the permeability of the cell membrane decreases in *E.coli* cultivated in chemostats at growth rates below 0.3 h^{-1} (Liu and Ferenci, 1998). This observation suggests that at growth rates below certain levels, bacteria may enter into a protecting status, i.e., by reducing the pore size they minimize amount of putative damaging molecules that can enter a cell. Changes in the cell envelope are suggested to be tightly regulated under starving conditions; otherwise, it may lead to a cell death. The ColRS system has been shown to be involved in such a regulation in *P. putida* (Putrins et al., 2011). In order to increase the scavenging of limiting nutrients, bacteria turn on the synthesis of high affinity ABC transporters (ATP-binding cassette). In contrast to low-affinity permeases, ABC transporters require energy to transfer substrates. This expensive strategy is paid back by the energy released from the utilization of the transported nutrient (Goelzer and Fromion, 2011). The overall abundance of proteins involved in the initial steps of degradation of the limiting substrate is increased in order to enhance the effectiveness of substrate utilization (Harder and Dijkhuizen, 1983b).

(ii) *Expression of stress factors*. In recent work, it was argued that nutrient limitation, being a stress condition, triggers general stress response in bacteria (Wick and Egli, 2004) (Ihssen and Egli, 2004). The resistance to a variety of stresses is mediated by the σ^s factor (RpoS). RpoS prepares cells to future environmental challenges, such as oxidative stress, osmotic stress, temperature and pH instability, biofilm formations, or control of virulence (Wick and Egli, 2004). Therefore, being energy-limited, bacteria are able to survive and compete. However, as shown for *E. coli*, the drawback of RpoS is the repression of high-affinity enzyme systems (Ferenci, 2001). Hence, bacteria are faced with a problem: the increased protective capabilities lead to a loss of high affinity transport of limiting substrates.

(iii) *Adjustment of RNA content to low growth rates*. It was shown for *E. coli* that under starving conditions the concentration of the alarmone (p)ppGpp, a major growth control protein in *E. coli* (Potrykus et al., 2011), increases. (p)ppGpp participates in breaking down the stable RNAs and consequently leads to the decreased translation rates (Gerdes et al., 2005). As it was suggested by Gerdes et al. (2005), the advantage of such a decrease is not only in the adjustment of the

cell metabolism to realistic nutrient concentrations but also in the elimination of translational errors.

(iv) *Accumulation of storage compounds.* Some bacteria have been shown to accumulate poly-β-hydroxybutyric acid (PHB) at low growth rates (Matin et al., 1979). Such strategy is advantageous for survival during extreme carbon limitations and starvation.

(v) *Co-expression of alternative catabolic pathways and mixed substrates growth*. Microorganisms may express many catabolic enzyme systems even for those carbon sources which are not present in the environment at that moment. In such a way, heterotrophic bacteria do not restrict themselves to one particular carbon source but are ready to utilize substrates that may appear in their habitats (Kovarova-Kovar and Egli, 1998). As a consequence of the co-expression of various catabolic pathways bacteria are able to utilize several carbon substrates simultaneously at low growth rates (Kovarova-Kovar and Egli, 1998). Moreover, microorganisms grow faster at low substrate concentrations when utilizing mixtures of growth-controlling substrates simultaneously than when growing with a single compound only (Kovarova-Kovar and Egli, 1998).

1.3.3 Derepression of catabolome and mixed substrates utilization at low growth rates

Monod established his principles of CCR by showing that *E. coli* exhibits repression of lactose degradation in the presence of glucose when cultivated in batch (Monod, 1942). However, later it has been discovered that when *E. coli* was cultivated at low dilution rates in carbon-limited chemostats glucose and lactose were consumed simultaneously (Silver and Mateles, 1969). It was suggested that external concentration of glucose was too low to cause CCR of lactose utilization (Silver and Mateles, 1969). In the late 70's, the fresh water bacteria *Pseudomonas* sp. and *Spirillum* sp. have been shown to exhibit increased activity of such enzymes of central metabolism as aconitase, isocitrate dehydrogenase and glucose 6-phosphate dehydrogenase at low growth rates when cultivated in lactate- and succinate-limited chemostats (Matin et al., 1976). Such an increase in activity was suggested to be related to the relief from carbon catabolite control. Later, Egli and co-workers developed this concept further by showing that catabolite derepression occurs also for enzymes which are involved in the initial steps of the degradation of alternative substrates, i.e., substrates which are not present in the medium at the moment (Ihssen and Egli, 2005). The absence of CCR

was confirmed for *E. coli in vitro* in glucose-limited chemostats where *E. coli* was able to consume other sugars without a lag phase (Lendenmann and Egli, 1995). Such a strategy was formulated by Thomas Egli as following: "be prepared for bad times and have all the tools ready in case you need them" (Egli, 2010). This suggests that it is advantageous for microorganisms to express various catabolic enzymes during nutrient limitation in order to be able to act fast and compete under starvation when new substrates appear in the environment.

Derepression of catabolic proteins has been well described for the copiotroph *E. coli* on different levels. Thus, proteome analysis of glucose-limited *E. coli* (Wick and Egli, 2004) showed that it overexpressed the transporters involved not only in the glucose transport but also in the transport of alternative substrates. At low growth rates *E. coli* upregulated expression of such catabolic enzymes as aldehyde dehydrogenase and tagatose-biphosphate aldolase which degrade substrates other than glucose. Investigation of *E. coli* catabolome showed that cells taken from glucose-limited chemostats were able to oxidize 25 carbon compounds not present in the medium in contrast to the exponentially grown cells from a batch. Moreover, *E. coli* cultivated at low growth rates in chemostats under the complex substrate mixture of Luria-Bertani browth (LB) medium, was able to oxidise even higher number of alternative substrates (Figure 1-2) (Ihssen and Egli, 2005). However, it is important to mention that derepression of catabolic pathways was not absolute and some substrates were not utilized by glucose-limited cells in the study of Ihssen and Egli (2005). For example, cells taken from glucose-limited chemostats did not show significant increase in oxygen uptake rate when exposed to arabinose and glutamine (Ihssen and Egli, 2005). Transcriptome analysis of glucose-limited *E. coli* (Franchini and Egli, 2006) confirmed previous observations established in Egli's research group clearly indicating increased expression of transporting and catabolic enzymes related to utilization of alternative substrates. Regulation of derepression of catabolic pathways was suggested to be mediated by elevated cAMP levels and endoinduction (Ihssen and Egli, 2005; Franchini and Egli, 2006).

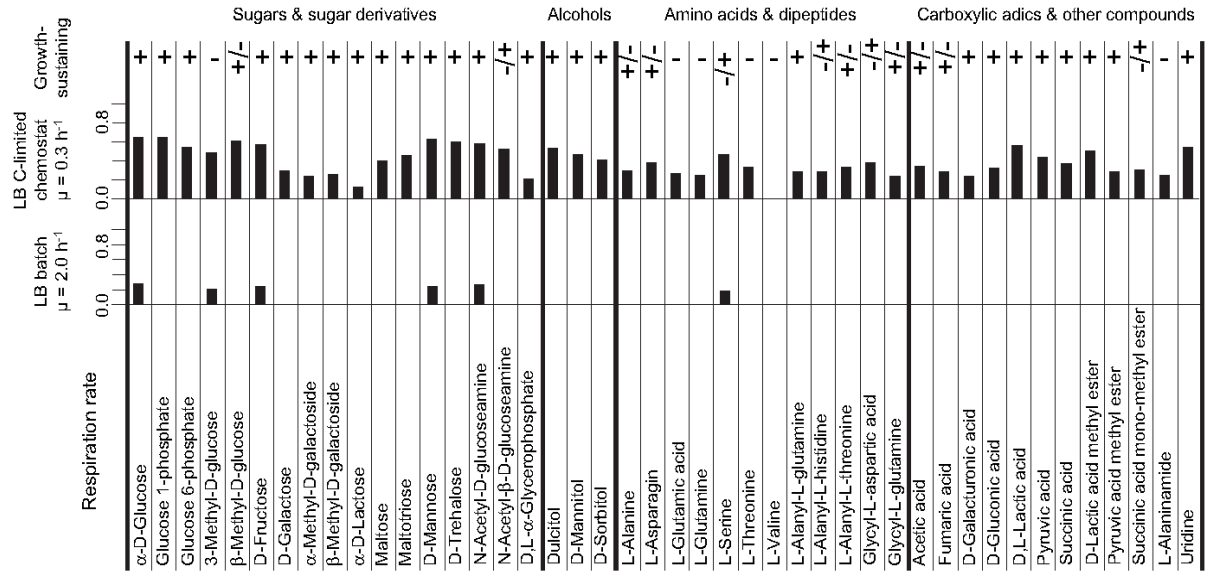

Figure 1-2 Respiration rates exhibited by chloramphenicol-treated *E. coli* MG 1655 cells in BIOLOG plates with various substrates. Cells were sampled during excess (the early exponential growth phase in batch culture ($\mu > 1.9$ h^{-1})) or limitation (carbon-limited LB chemostat culture ($D = \mu = 0.3$ h^{-1})) of LB medium. The bars represent respiration rates normalized to biomass (Egli, 2010).

Various reports exist on the expression of the diverse transporting and degrading systems for substrates absent from the cultivation medium in bacteria, other than *E. coli*, cultivated under carbon limitation. Thus, already in 1984, Sepers showed that two heterotrophic strains which were isolated from a freshwater basin, expressed enzymes for utilization of alternative substrates at low dilution rates in chemostats (Sepers, 1984). For example, at a growth rate of 0.1 h^{-1} and below, the uptake of alternative substrates such as aspartate, leucine, glycine, amino acids mixture, glucose, and acetate was detected in strain HIS 42 cultivated in chemostat with histidine as a sole source of carbon. Another strain, HIS 53, cultivated in chemostat with aspartate at a dilution rate of 0.01 h^{-1} and below, was able to utilize alternative substrates such as glycine, alanine, valine, isoleucine, leucine, proline, serine, methionine, phenylalanine, ornithine, glucose, and acetate. At a very low dilution rate of 0.001 h^{-1} this strain showed capabilities of the highest respiratory activity on such alternative carbon sources as propionate, butyrate, oxalate, succinate, lactate, glycollate, glycerate, citrate, α-ketoglutarate, glycerol, benzoate. Later, it was demonstrated that *P. putida* CA-3 cultivated in continuous chemostat under phenylacetate limitation also expressed the *sty* operon responsible for expression of genes for styrene utilization (O'Leary et al., 2002). In *P. putida* KT2442 cultivated at a dilution rate of 0.1 h^{-1}, the genes encoding for the transport of various amino acids as well as different ABC transporters were upregulated in carbon-limited vs.

nitrogen-limited chemostats (Poblete-Castro et al., 2012). The pathogenic Gram-negative *Yersinia pestis* upregulated transporters for alternative substrates during nutrient exhaustion in batch (Pieper et al., 2008). The enzymes involved in the utilization of alternative substrates were also shown to be expressed in the aromatic hydrocarbon-degrading facultative anaerobic bacterium "*Aromatoleum aromaticum*" EbN1 (Trautwein et al., 2012) and in the facultative anaerobic Gram-positive bacterium *Lactobacillus plantarum* (Goffin et al., 2010).

Furthermore, relief from CCR at low dilution rates has been shown as well for yeasts and fungi. For example, two different carbon substrates methanol and glucose were utilized simultaneously by the methylotrophic yeast *Hansenula polymorpha* cultivated in carbon-limited chemostats at low dilution rates (Egli et al., 1986). In the filamentous fungus *Aspergillus nidulans*, the formation of β-galactosidase activity was no longer repressed by glucose at the low dilution rates of 0.045 and 0.015 h^{-1} (Ilyes et al., 2004). As a consequence of the relief from the carbon catabolite control at low growth rates, induction of exocellular protease activity has been observed for various bacteria. For example in *Vibrio* SA1, aminopeptidase was produced at a dilution rate of 0.19 h^{-1} in lactate-limited chemostat (Wiersma and Harder, 1978). In *Bacillus licheniformis* cultivated in chemostat, citrate limitation triggered high production of exocelular protease (Frankena et al., 1988). The protease formation was highest at low dilution rates in glucose-limited chemostats with *Clostridium sporogenes* (Allison and Macfarlane, 1990).

All examples described above show that relief from CCR under carbon limiting conditions and low dilution rates is not only a phenomenon of well-described *E. coli* but also occurs in a wide range of microorganisms. As a result, bacteria are prepared to utilize several substrates simultaneously in contrast to batch conditions where they prefer only readily utilizable carbon sources. For instance, in experiments of Lendenman et al. (1996), *E. coli* was cultivated in chemostat with six different carbon sources at low concentrations and cells were able to utilise all these carbon sources simultaneously. Remarkably, steady-state concentrations of the substrates were proportional to the ratio of the substrates in the mixture and they were lower than steady-state concentrations of individual carbon sources used for single-substrate growth. Therefore, the utilization efficiency of the substrates was increased. Such simultaneous utilization of the substrates is advantageous because individual substrate concentrations which occur in nature are extremely low and are frequently below threshold concentrations. However, the increased efficiency of microorganisms in the utilization of mixed substrates

may lower substrate threshold concentrations for the induction of the degrading enzymes (Kovarova-Kovar and Egli, 1998).

A difference in behaviour of microorganisms when exposed to substrate excess and substrate limitation is suggested to be explained by different determinants of competitive abilities (Lendenmann and Egli, 1998). Thus, at high substrate concentrations the maximum specific growth rate [μ_{max}] determines the competitive ability and microorganisms utilize substrates supporting the highest growth rates. At low substrate concentrations, the substrate affinity constant (K_s) plays a major role in the ability of microorganisms to utilise carbon sources (Lendenmann and Egli, 1998). Thus, it is obvious that under carbon-limiting conditions, the simultaneous derepression of many different catabolic enzymes is not wasteful but allows an organism to respond quickly to changes in the substrate availability.

Such a derepression of the catabolome at conditions close to natural can be used in bioremediation strategies. Several studies demonstrated that additional, easily degradable substances may enhance the degradation of pollutants. For example, degradation of methylene chloride was increased in the presence of acetate by *Pseudomonas* sp. (LaPat-Polasko et al., 1984) and 3-phenylpropionic acid was consumed simultaneously with glucose in *E. coli* cultivated in chemostat (Kovarova et al., 1997). The addition of 250 µM benzoate enhanced the biodegradation of 35µM naphthalene in enrichments taken from river Rhine polluted with aromatic compounds cultivated anaerobically in sediment columns (Langenhoff et al., 1996). The addition of a mixture of organic and amino acids at low concentrations (in the range of 1-10 µM) increased the growth yields on toluene by 54% for *P. putida* (Dinkla and Janssen, 2003). Therefore, further studies on environmentally relevant microorganisms, especially obligate anaerobes which play important role in the degradation of pollutants, and their capabilities in substrate utilization under naturally occurring low growth rates may enhance our insights into the optimization of the bioremediation strategies.

1.4 Model microorganisms

To date, the physiology of a model strictly anaerobic aromatic hydrocarbon-degrading microorganism *Geobacter metallireducens* has not been investigated under extremely low growth rates. Additionally, the lack of knowledge exists on global expression of catabolic enzymes by anaerobic halorespiring bacterium *Desulfitobacterium hafniense* Y51 under various limiting conditions.

Iron-reducing *Geobacter* species have been demonstrated to be abundant in environments polluted with hydrocarbons and rich in Fe(III) (Lovley et al., 2004). *Geobacter metallireducens* strain GS-15 has been isolated from the freshwater sediments from the Potomac river, Maryland (Lovley and Phillips, 1988). *Geobacter* species have a versatile physiology and are used in many aspects. For example, besides being major players in degradation of aromatic compounds in the presence of Fe, they are capable of generating electricity (Lovley et al., 2011) and are used in uranium bioremediation (Wilkins et al., 2009). *G. metallireducens* was shown to be able to degrade 11 aromatic compounds, including the common petroleum derived pollutants such as toluene, phenol, *p*-cresol (Lovley et al., 1993) and benzene (Zhang et al., 2012). Moreover, *G. metallireducens* also utilizes fermentation products such as acetate, butyrate, and ethanol. In the natural habitats where *G. metallireducens* was identified, the aromatic pollutants derived from, for example, oil spillages might be mixed with naturally occurring fermentation products. Such a scenario requires more knowledge on the response of *G. metallireducens* to mixtures of different carbon substrates. Therefore, physiological studies with *G. metallireducens* at conditions close to natural are important to enable improvements in bioremediation or bioaugmentation strategies.

G. metallireducens is a Gram-negative bacterium. It possesses a CRP analogue within its genome (Gmet_0750, which has 51.5% similarity to CRP of *E. coli* K-12) together with a HPr kinase analogue (Gmet_1285 with 62.3% similarity to HPr kinase of *B. subtilis*) (Figure 1-1). This combination is supplemented with genes coding for the nitrogen PTS in *E. coli*: PTS I^{Ntr} (Gmet_2404 with 55.6% similarity to PtsP of *E. coli* K-12), PTS IIA^{Ntr} (Gmet_2604 with 51% similarity to PtsN of *E. coli* K-12), HPr^{Ntr} (Gmet_1288 with 66.7% similarity to catabolite repression HPr-like protein of *B. subtilis*) and only three genes coding for enzymes of PTS system similar to *E. coli*: PTS EI (Gmet_1289) and two genes coding for components of PTS EIIA, Gmet_0604 with 50.1% similarity to the putative PTS system enzyme IIA component of *E. coli* K-12, and Gmet_1287 with 56.5% similarity to PTS enzyme IIAB of *E. coli* K-12 (Figure 1-1). The mixed and not fully represented PTS of *G. metallireducens* suggests a mechanism of CCR different to enteric bacteria. *G. metallireducens* has a HprK homologue but lacks known PTS EII permeases, suggesting that it is not able to transport sugars via PTS (54). However, as it has been mentioned earlier in the introduction, the same components of PTS such as HPr kinase PTS I^{Ntr}, PTS IIA^{Ntr}, and HPr^{Ntr} might play a role in the regulation of carbon consumption in *G. metallireducens*.

Desulfitobacterium hafniense Y51 was isolated in Japan from soil contaminated with chlorinated ethenes and is a strictly anaerobic Gram-positive bacterium which belongs to the *Clostridia* (Suyama et al., 2001). *D. hafniense* Y51 utilizes electron donors such as formate, lactate, pyruvate, and vanillate (Peng et al., 2012). In addition to utilization of PCE as an electron acceptor, it can also utilize sulphite, sulphate, fumarate, nitrate (Villemur et al., 2006) and nitrite (Peng et al., 2012). PCE and TCE are dehalogenated to *cis*-1,2-DCE by *D. hafniense* Y51. Moreover, *D. hafniense* Y51 possesses within its genome the *O*-demethylation operons (Nonaka et al., 2006) and should be able to dechlorinate chlorinated hydroquinone metabolites (Villemur et al., 2006).

Like *G. metallireducens*, *D. hafniense* Y51 does not utilize sugars (Nonaka et al., 2006). However, in contrast to *G. metallireducens*, only one component of the PTS was found to be present in its genome. It is *DSY1020*, a homologue of the PTS lactose/cellobiose IIC component of *B. subtilis* (with 49.6% similarity). Thus, unlike *G. metallireducens*, *D. hafniense* Y51 possesses a putative PTS EIIC permease. This observation makes it a possible candidate for the control of carbon metabolism in *D. hafniense* Y51 as in *B. subtilis* where EII permeases have been shown to be involved in catabolite control of transcription factors (Gorke and Stulke, 2008). However, as *D. hafniense* Y51 uses halogenated compounds as electron acceptors, it is appealing to reveal global regulators which might be involved in the preferential reduction of terminal electron acceptors.

Some other CCR-related proteins similar to known global regulators have been identified in the genome of *D. hafniense* Y51. Thus, it possesses a homologue of the negative regulator of gluconeogenesis CcpN (*DSY3082*) (Servant et al., 2005) which shares 73.6% similarity with the CcpN-regulator of *B. subtilis*. Within its genome, *D. hafniense* Y51 encodes only one CRP-FNR transcriptional regulator *DSY3063* similar to CprK1 regulator of *D. hafniense* DCB-2 (*Dhaf_0678*). As mentioned earlier, CprK1 positively regulates the expression of the halorespiring genes (Gabor et al., 2006) and might be also important for the regulation of reduction of halogenated compounds in *D. hafniense* Y51. Additionally, *D. hafniense* possesses some homologues to the global stress response regulators. For example, it encodes the transcriptional repressor CodY (*DSY2548*) and the putative uncharacterized protein *DSY4842* with 52.3% and 55.9% similarity to sigma L (RpoN) of *B. subtilis* and *Listeria monocytogenes EGD-e*, respectively. In *L. monocytogenes EGD-e*, sigma L is responsible for growth under environmental stress conditions (Raimann et al., 2009), while in *B. subtilis* it is involved in the regulation of cold shock adaptation pathways (Wiegeshoff et al., 2006). The

transcriptional repressor CodY (*DSY2548*) controls the expression of the catabolic genes under starvation in the stationary growth phase (Sonenshein, 2005).

Therefore, although *D. hafniense* does not encode known players of CCR, a few candidates for carbon metabolism under different growth conditions can be revealed.

1.5 Objectives

This thesis aims to highlight the *in situ* physiology of environmentally relevant, strictly anaerobic microorganisms capable of degrading toxic compounds in contaminated groundwater. The iron-reducing Gram-negative bacterium *G. metallireducens* and the halorespiring Gram-positive bacterium *D. hafniense* Y51 were chosen as promising candidates due to their substantial importance in bioremediation. The achieved knowledge might bring better understanding of biodegradation processes as well as further optimization of bioremediation and bioaugmentation technologies.

The major part of the work has been conducted on *G. metallireducens*. Cultivation in batch under excess of various carbon sources was chosen as a reference system. Retentostat was established as a model system for investigation of *in situ* physiology. The physiological response of *G. metallireducens* to acetate or acetate plus benzoate limitation in retentostat was compared to its behaviour under carbon excess in batch with the respective substrates. Further, *G. metallireducens* was introduced into a model aquifer contaminated with aromatic compound toluene in order to investigate its physiology under conditions maximally close to natural. Moreover, the physiological response of *D. hafniense* Y51 to various limitations in chemostats was also investigated and compared to the physiology of *G. metallireducens* under carbon limitation.

The physiology of the bacteria mentioned above was investigated on the level of expressed proteomes. Thus, proteins expressed by *G. metallireducens* and *D. hafniense* Y51 were analysed via label-free proteomics (LC-MS-MS coupled to UPLC) and isotope-stable labelling (ICPL), respectively.

This thesis contains the following specific objectives:

i) Examination of the physiology of *G. metallireducens* under high carbon substrate concentrations during exponential growth in batch. The aim was to reveal whether easily degradable substrates such as acetate or ethanol inhibit utilization of aromatic compounds in *G. metallireducens* and to investigate

which catabolic pathways are expressed when *G. metallireducens* is cultivated at high concentrations of single (acetate, benzoate, butyrate, ethanol, toluene) and mixed (acetate plus benzoate) carbon substrates. It was hypothesized that *G. metallireducens* would prefer the easily degradable substrate acetate and ethanol over aromatic compounds as well as high concentrations of the preferred substrates will inhibit the expression of pathways involved in the degradation of aromatic compounds on the proteomic level.

ii) Investigation of the physiology of *G. metallireducens* under acetate and acetate plus benzoate limiting conditions at extremely low growth rates in retentostat in order to disclose whether slow growing anaerobic microorganism like *G. metallireducens* relieves CCR under carbon limitation similarly to the fast growing aerobic copiotroph *E. coli.* Detailed insights into the behaviour of *G. metallireducens* at low growth rates which occur in nature were aimed to be achieved. Simultaneous consumption of the two different substrates acetate and benzoate together with expression of many alternative catabolic pathways was expected under carbon limitation.

iii) Introduction of *G. metallireducens* into an indoor model groundwater mesocosm exposed to a constant source of toluene in order to mimic a real scenario of contaminated groundwater and investigate whether *G. metallireducens* is able to compete with indigenous communities, and to biodegrade contaminant of interest. It was expected that as the members of *Geobacteraceae* family are highly abundant in iron-containing aquifers polluted with aromatics, *G. metallireducens* will survive and degrade toluene under the conditions applied.

iv) Cultivation of another strict anaerobe *D. hafniense* Y51 under various nutrient limiting conditions (ammonium, lactate and fumarate limitations) in order to give insights onto the physiology of this model bacterium under limiting conditions as well as to examine whether relieve from CCR is observed in the anaerobic halorespiring bacteria.

2 Material and methods

2.1 Organisms and cultivation media

2.1.1 Cultivation of *G. metallireducens* in batch

Geobacter metallireducens (strain GS-15/ATCC 53774/DSM 7210) was purchased from the Deutsche Sammlung von Mikroorganismen und Zellkulturen GmbH (DSMZ), Germany. Microorganisms were cultivated under anoxic conditions in a mineral medium (DSMZ Geobacter medium 579) with DSMZ trace element solution SL10: 1 ml l^{-1} and DSMZ 7 vitamins solution: 0.5 ml l^{-1}. Single substrates were added in concentrations of acetate (5 mM), benzoate (1 mM), butyrate (20 mM), ethanol (20 mM), toluene (1 mM) with Fe(III)-citrate (50 mM) as an electron acceptor. For diauxic experiments the following concentrations were used: 2 mM acetate plus 0.6 mM benzoate, 2.5 mM acetate plus 0.5 mM toluene, 4 mM butyrate plus 2 mM acetate, 2.5 mM acetate plus 2 mM ethanol, 4 mM butyrate plus 2 mM ethanol, 4 mM butyrate plus 0.5 mM benzoate, 1 mM ethanol plus 0.6 mM benzoate together with 50 mM Fe(III)-citrate. All inoculations were performed in three replicates. 80 ml medium was dispensed into sterile 100 ml bottles. The bottles were flushed with N_2/CO_2 (80 % / 20 %) and sealed with butyl rubber stoppers. For experiments with toluene bottles were sealed with viton rubber stoppers. All incubations were performed at 30°C in the dark. Growth was determined via monitoring of Fe(II) production. For inoculation cells were pre-grown with the same substrate as in single substrate experiments. For dual substrate experiments the pre-cultivation conditions chosen for the inoculation were: acetate for experiments with acetate plus benzoate or acetate plus toluene; benzoate for experiments with toluene plus benzoate or ethanol plus benzoate; ethanol for experiments with ethanol plus butyrate or ethanol plus acetate; butyrate for experiments with acetate plus butyrate or benzoate plus butyrate. Preliminary experiments showed that the carbon source used to grow the inoculum did not influence the profile of substrate consumption in experiments with mixed substrates (data not shown).

For proteomic analysis, cells were sampled during early exponential growth phase which was estimated based on the information of produced Fe(II), except for the last biological replicate of the condition acetate plus benzoate, where cells were sampled in the late exponential phase.

2.1.2 Cultivation of *G. metallireducens* in retentostats

Cultivation of *G. metallireducens* in retentostats was done in three replicate runs with 2.5 mM acetate plus 0.7 mM benzoate as two carbon sources and in two runs for 5 mM acetate as a single carbon source. The recycling fermenter was built by the electronics and mechanics

workshops of the Faculty of Earth and Life Sciences, VU University Amsterdam, the Netherlands (Schrickx et al., 1995; Lin et al., 2009). The fermenter vessel had a maximum capacity of 2 l with a working volume of 1.5 l. The fermenter was operated under anoxic conditions. A N_2 and CO_2 mixture (90:10) was flushed through a titanium (III) citrate solution in order to remove any traces of oxygen. Then, it was pumped into the reactor with constant rate of 2 l per hour. The medium inside the reactor was stirred constantly at 200 rpm. Medium was pumped out through the retention unit wrapped into 0.22 µm pore size filter to retain biomass. The pH of the culture was maintained at 6.8 by the addition of 2 M HCl or 2 M NaOH. The temperature was controlled at 30 °C. The gas outlet was connected to a bottle filled with water to avoid oxygen entering the system. The fermenter and medium reservoir were kept dark by wrapping with aluminium foil. The fermenter was inoculated with 10% volume taken from exponentially growing pre-cultures and cultivated under batch conditions until the Fe(II) concentration reached 30-40 mM indicating complete carbon source consumption. Then, the feed peristaltic pump was switched on (medium supply rate of 50 ml h^{-1}) and the fermenter was operated in a retentostat mode.

Acetate and benzoate were chosen as electron donors because acetate is an important primary product of fermentation of natural organic matter in anoxic sediments (Lovley, 1997) and benzoate is a wide spread model compound for investigation of aromatic compounds metabolism in anaerobic bacteria (Wischgoll et al., 2005; Heintz et al., 2009). Fe(III) citrate was selected as an electron acceptor for cultivation because iron is an important electron acceptor in anoxic environments and polluted aquifers (Roling et al., 2001). However, iron in the form of Fe(III) citrate is soluble and should not block the filter unit of the retentostat.

For proteomic analysis, cells were sampled several times in the course of the retentostat cultivation (see Figure 3-7 and Figure 3-9). Two biological replicates were investigated per condition of acetate, three biological replicates per condition of acetate plus benzoate.

2.1.2.1 Determination of growth rate and biomass production rate in retentostats

The growth rate was estimated according to the following formula:

$$\mu = \frac{r_x(t)}{x(t)} \qquad \text{Equation 2-1}$$

where $r_x(t)$ is the biomass production rate and $x(t)$ is the biomass as a function of time.

Biomass production rate ($r_x(t)$) can be estimated with two equations:

(i) Based on published values for maintenance energy (m_s) and maximum growth yield (Y_{xsm}) which were already estimated for *G. metallireducens* cultivated under carbon limitation in retentostats (Lin et al., 2009):

$$r_x(t)_{fit} \equiv \frac{dx(t)}{dt} = m_s Y_{xsm}\left(\frac{r_s}{m_s} - x_0\right)e^{-m_s Y_{xsm} t} \qquad \text{Equation 2-2}$$

where t is the time (h), $x(t)$ is the biomass as a function of time t, m_s is the maintenance energy (mmol/biomass unit*h), Y_{xsm} is the maximum growth yield (biomass units per mmol of limiting substrate), r_s is the addition rate of the growth-limiting substrate (mmol h^{-1}).

The Equation 2-2 was based on the Pirt equation (Equation 2-3) (Pirt, 1965), where substrate utilization is transferred into energy to support growth and maintenance :

$$r_s = r_s(\text{maintenance}) + r_s(\text{growth}) \qquad \text{Equation 2-3}$$

where r_s(maintenance) is the rate of utilization of substrate for maintenance, r_s(growth) is the rate of utilization of substrate for growth (van Verseveld et al., 1986).

Subsequently, Equation 2-3 can be presented as following:

$$\frac{ds}{dt} = \frac{ds}{dt_M} + \frac{ds}{dt_G} \qquad \text{Equation 2-4}$$

For substrate utilization in retentostats Equation 2-4 can be transferred as following according to (van Verseveld et al., 1986):

$$r_s(t) = m_s x_t + \frac{r_x(t)}{Y_{xsm}} \qquad \text{Equation 2-5}$$

because

$$\frac{dx}{dt} = \mu x_t = -\frac{Yds}{dt} \qquad \text{Equation 2-6}$$

therefore,

$$\frac{ds}{dt_G} = -\mu\frac{x_t}{Y_{xsm}} \qquad \text{Equation 2-7}$$

and

$$\frac{ds}{dt_M} = -m_s x_t \qquad \text{Equation 2-8}$$

where m_s is the maintenance energy in mmol biomass unit*h^{-1}, x_t is the biomass at time t in biomass unit, and r_s is the addition rate of growth-limiting substrate (mmol h^{-1}).

Equation 2-5 can be presented as following:

$$r_x(t) = \frac{dx}{dt} = \left(x_t - \frac{r_s}{m_s}\right)(-m_s Y_{xsm}) \qquad \text{Equation 2-9}$$

The solution of integration is the following:

$$\int_{x_0}^{x} \frac{1}{x_t - \frac{r_s}{m_s}}\, dx = \int_0^t -m_s Y_{xsm} dt$$

Knowing that $\int \frac{1}{x+a} dx = \ln(x+a)$, and $\int kx dt = kxt + C$, we have

$\ln\left(x_t - \frac{r_s}{m_s}\right) = -m_s Y_{xms} t + C$, therefore

$x_t - \frac{r_s}{m_s} = e^C \; e^{-m_s Y_{xsm} t}$

If t =0, then $e^C = \left(x_0 - \frac{r_s}{m_s}\right)$

Therefore,

$$x_{t\,fit} = \frac{r_s}{m_s} + (x_0 - \frac{r_s}{m_s}) e^{-m_s Y_{xsm} t} \qquad \text{Equation 2-10}$$

The Equation 2-10 can be inserted into Equation 2-9 which, finally, gives Equation 2-2:

$$r_x(t) = \left(x_t - \frac{r_s}{m_s}\right)(-m_s Y_{xsm}) =$$

$$\left(\left(\frac{r_s}{m_s} + \left(x_0 - \frac{r_s}{m_s}\right) e^{-m_s Y_{xsm} t}\right) - \frac{r_s}{m_s}\right)(-m_s Y_{xsm}) =$$

$$m_s Y_{xsm} \left(\frac{r_s}{m_s} - x_0\right) e^{-m_s Y_{xsm} t}$$

(ii) Based on experimental residual substrate concentrations measured in the outflow from the reactor according to (Lin et al., 2009).

Assuming that during growth *G. metallireducens* uses carbon substrates only for respiration and incorporation into biomass, the following formula for the rate of incorporation of substrates into biomass ($r_{x(substrate)}(t)$) can be derived as:

$$r_{x(substrates)}(t) = f * ((C1\ mol\ substrates\ consumed) - (C1\ mol\ substrates\ for\ respiration)) \qquad \text{Equation 2-11}$$

where f is the flow of the medium into the retentostat and equals 0.05 l/h.

Therefore, $r_{x(substrates)}(t)$ was calculated as the following for two different growth conditions in retentostats:

- for growth with one single substrate (acetate):

$$r_{x(acetate)}(t) = f * (2([Acetate]_{in} - [Acetate]_{out}(t)) - 0.125[Fe(II)]_{out}(t)) \quad \text{Equation 2-12}$$

where $[Acetate]_{in}$ is the acetate concentration in the medium supply (mM), $[Acetate]_{out}(t)$ is the acetate concentration in the filtrate at time *t* (mM), $[Fe(II)]_{out}(t)$ is the Fe(II) concentration in the filtrate at time *t* (mM), 2 – is the coefficient of transfer into C-mM for acetate ($C_2H_4O_2$), 0.125 is the fraction of mol of acetate directed into respiration according to stoichiometry (1 mol of acetate corresponds to the production of 8 mol of Fe(II), therefore the fraction of acetate for respiration equals 1/8).

- for growth with double substrates (acetate plus benzoate):

$$r_{x(acetate\ plus\ benzoate)}(t) = f * (2([Acetate]_{in} - [Acetate]_{out}(t)) + 7([Benzoate]_{in} - [Benzoate]_{out}(t)) - (\frac{0.25*2[Acetate]_{in}+0.23*7[Benzoate]_{in}}{2[Acetate]_{in}+7[Benzoate]_{in}}) * Fe(II)_{out}(t)) \quad \text{Equation 2-13}$$

where, $[Benzoate]_{in}$ is the benzoate concentration in the medium supply (mM), $[Benzoate]_{out}(t)$ is the benzoate concentration in the filtrate at time *t* (mM), 7 is the coefficient of transfer into C-mM for benzoate ($C_7H_6O_2$), 0.25 is the fraction of C-mM of acetate directed into respiration according to stoichiometry (2/8=0.25), and 0.23 is the fraction of C-mM of benzoate directed into respiration according to stoichiometry (7/30=0.23). It is important to note for a clarification, that the last part of Equation 2-13 takes into account that the various carbon sources do not consume the same amount of Fe(II) per C-substrate.

The stoichiometries of the acetate and benzoate degradation with Fe(III) citrate as an electron acceptor are the following (free energy values under standard conditions at pH=7, $\Delta G^{0'}$, for acetate and benzoate degradation coupled to iron reduction were calculated from published ΔG^0_f (Thauer et al., 1977) values (Supplementary material, Table 7-1):

Acetate: $C_2H_3O_2^- + 3H_2O + 8Fe(III) \rightarrow CO_2 + HCO_3^- + 8Fe(II) + 8H^+$ Equation 2-14

$$\Delta G^{0'} = -819 \text{ kJ mol}^{-1}$$

Benzoate: $C_7H_5O_2^- + 13H_2O + 30Fe(III) \rightarrow 6CO_2 + HCO_3^- + 30Fe(II) + 30H^+$ Equation 2-15

$$\Delta G^{0'} = -3{,}070 \text{ kJ mol}^{-1}$$

Due to the attachments of cells to the walls of the reactor and to the filter as well as due to the occasional leakages of the filter itself it was impossible to measure the cell biomass accurately. The actual biomass production rate was therefore calculated based on the substrate utilization (Equations 2-12 and 2-13). However at some time points, the measured Fe(II) was lower than Fe(II) theoretical (calculated from residual substrate concentrations), which was giving unrealistic negative substrate incorporation rates. As an alternative, a simulation of the biomass production rate ($r_x(t)_{fit}$) was estimated according to the first approach (Equation 2-2) based on the published values of m_s and Y_{xsm} for *G. metallireducens* under carbon limiting conditions (-0.016 and 0.053, respectively) (Lin et al., 2009).

2.2 Cultivation of *G. metallireducens* in the indoor aquifer

2.2.1 Preparation of dialysis bags and inoculum for mesocosm experiment

G. metallireducens was pre-cultured in batch with acetate as an electron donor and Fe(III) citrate as an electron acceptor. 50 ml of the full grown culture were harvested under anaerobic conditions. Cell pellets were re-suspended in *Geobacter* medium and further used to inoculate dialysis bags under anaerobic conditions.

Dialysis bags were self-made by heat-sealing out of toluene resistant, autoclavable 0.2 µm pore size polyvinylidene difluoride (PVDF) membrane material (Microdyn-Nadir). Each bag was 1.5 cm in diameter and 25 cm long. Natural sediment from the South Bavarian area (Bruckmül) with sand grains having size of about 0.5-4 mm in diameter were used for the bags. The sediments were re-suspended in water and sterilized three times. One liter Schott bottles filled with anoxic water (boiled for 10 minutes and then flushed with N_2 gas until they cool down) where used for transferring the dialysis bag into. Sediments, dialysis bags, Schott bottles, and stock solution of ferric hydroxide were transferred into the anaerobic chamber and left inside overnight to establish anoxic conditions. The sediments were mixed with 5 ml of 0.4 M ferric hydroxide and used to fill the dialysis bags and they were placed into the Schott bottles which were closed with butyl stoppers before being sterilized by autoclaving. The *Geobacter* cell pellet was then used to inoculate the sterile and anoxic dialysis bags in the anaerobic chamber and then mixed to spread the cells along the bags.

2.2.2 Placement of inoculated dialysis bags into the indoor aquifer

Inoculated bags were inserted in parallel into two cartridges (A and B) and placed at the end of an indoor aquifer (Figure 2-1). The indoor aquifer was installed previously by Dr. Marco Hünniger and Dr. Susanne Smidt in the Institute of Groundwater Ecology, Helmholtz

Zentrum München. The indoor aquifer had dimensions of 5 m long and 0.8 x 0.7 m in diameter. The indoor aquifer was packed with the sediment taken previously from South Bavarian area (Bruckmül) and constantly flushed with natural groundwater from wells of Helmholtz Zentrum München site at a flow of 1 m per day.

The cartridge A contained the dialysis bags inoculated with *G. metallireducens* into sterilized (three bags) and unsterile sediment (one bag); the cartridge B (control cartridge) contained dialysis bags with unsterile sediment without *G. metallireducens* (two bags) and with *G. metallireducens* (one bag). Construction of dialysis bags and their installation into the indoor aquifer were carried out by Dr. Housna Mouttaki and Dr. Marco Hünniger. Constant source of toluene (with final concentration of up to 3 mM in the groundwater reaching the dialysis bag) was placed 15 cm before the cartridges (Figure 2-1).

Dissolved oxygen concentrations in the water were measured weekly via fluorescent sensors. The sensors were installed by Dr. Marko Hünniger in front of the cartridges in the indoor aquifer (Figure 2-1). The sensors contained oxygen sensitive foil. Fluorescence light was produced when the foil was coming into the contact with oxygen. Further, fluorescence light was measured by a second set of sensors.

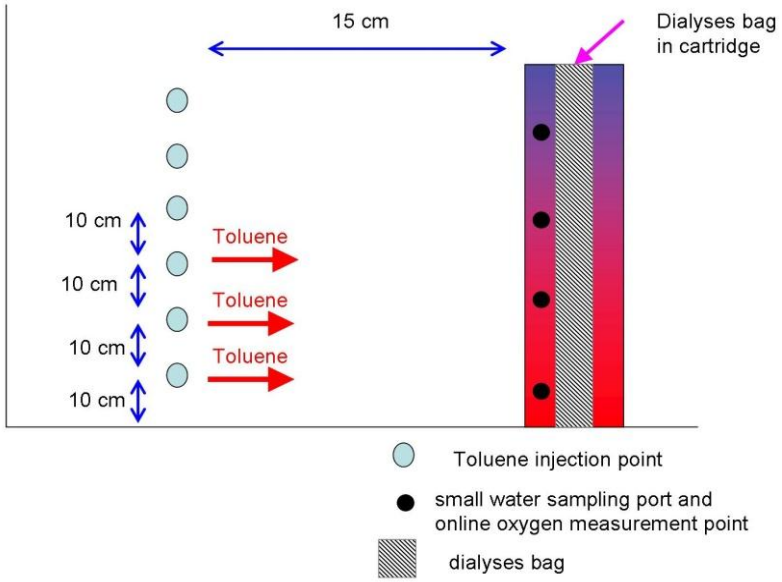

Figure **2-1** Experimental set up of mesocosm experiment (by Dr. Marko Hünniger).

2.3 Cultivation of *D. hafniense* Y51 in batch

Culture of *D. hafniense* Y51 was kindly provided by Prof. Dr. Hauke Smidt, laboratory of Microbiology, Wageningen Universiteit (WU), the Netherlands.

D. hafniense was cultivated under anoxic conditions in the presence of N_2/CO_2 atmosphere (90:10). Batch cultures were conducted in a modified *Desulfitobacterium hafniense* medium 720, (DSMZ; Braunschweig, Germany), containing (per liter): 1.0 g NH_4Cl, 0.4 g K_2HPO_4, 0.1 g $MgSO_4$ x $7H_2O$, 1 ml resazurine stock solution (0.5% w/v), 1 ml trace element solution SL-10, 1 ml selenite/tungstate solution, 0.01% yeast extract, and HCl-cysteine (0.8 mM) as an oxygen scavenger. The medium was supplemented with sodium lactate (20 mM) and sodium fumarate (30 mM) as an electron donor and acceptor, respectively. The medium was dispensed into 1 l serum bottles, sealed with butyl rubber stoppers and autoclaved at 121ºC for 15 min. After cooling, 1 ml of $CaCl_2$ x $2H_2O$ stock solution (0.3 M), 30 ml of bicarbonate solution (1.0 M), 1 ml of vitamin solution and 1 ml of vitamin B_{12} (5 mg/100 ml), were added separately from sterilized anaerobic stock solutions. The final pH of the medium was 7.0±0.2. 1% of inoculum was used for inoculation. The cultivation was carried out at 35ºC in the dark.

Maximum growth rate and mass balance analysis were estimated in two independent batch replicates. Cells harvested at the early exponential growth phase were used for proteomic analysis.

2.4 Cultivation of *D. hafniense* Y51 in chemostats

The chemostat set-up was built by the electronics and mechanics workshops Faculty of Earth and Life Sciences, VU University Amsterdam, the Netherlands.

Medium for continuous culturing had the same composition as the medium used for batch cultures except for varying the concentrations of limiting nutrients according to the selected type of limitation (electron donor-, electron acceptor- or/and ammonium- limiting conditions) (see below).

Oxidation of lactate in the presence of fumarate was expected to follow Equation 2-16.

$$C_3H_6O_3 + H_2O + 2C_4H_4O_4 \rightarrow C_2H_4O_2 + 2C_4H_6O_4 + CO_2 \qquad \text{Equation 2-16}$$

$$\Delta G^{0'} = -224.8 \text{ kJ/mol}$$

Limiting conditions were constructed in such a way that the ratio of fumarate to lactate was as following: 3.2-3.8:1 under lactate- (chemostats L1 and L2), 0.6-1.5:1 under fumarate- (chemostats F1, F2, F3 and F4), and 1.7-1.9:1 under fumarate plus ammonium-limitation (chemostats A1 and A2). In the latter limitation, ammonium (i.e., NH_4Cl) was omitted from the medium.

Fermentor vessels had a working volume of 1 l. The medium supply was made and kept anoxic. A gas mixture of N_2 and CO_2 (95:5) was flushed through the culture at 2 l h^{-1} and stirred at 330 rpm. Traces of oxygen in the gas mixture were removed by flushing it through a strong reducing titanium (III) citrate solution (Zehnder, 1989). The gas outlet was connected to a water-filled column, which kept the fermentor at a slight over pressure, in order to avoid possible leakage of oxygen into the fermentor. Culture pH (7.0±0.2) was controlled by the addition of 1 M HCl or NaOH. The temperature was maintained at 35ºC. The dilution rate for all continuous cultures was set to 0.02 h^{-1}. Both fermentor and medium reservoirs were kept dark by wrapping with aluminum foil.

Chemostat experiments were initiated with 10% inoculum taken from a pre-culture cultivated under the same batch conditions.

The fermentor was first operated in the batch mode for two days. When nearly all lactate or fumarate was consumed, the fermentor was switched to the chemostat mode. The operating conditions were maintained constantly for at least five volume changes prior to the analysis of steady-state mass balances and sampling for proteomics.

2.4.1 Determination of physiological parameters

Carbon (*Crec%*) and electron (*erec%*) recoveries for utilized substrates were calculated based on the following reactions:

$$Crec\% = \frac{2 * [Acetate] + \left[CO_{2_{prod}}\right] + [Biomass]}{3 * [Lactate] + [Yeast\ extract] + [CO_{2_{con}}]} \text{x}100\% \qquad \text{Equation 2-17}$$

$$erec\% = \frac{8 * [Acetate] + 0 * \left[CO_{2_{prod}}\right] + 4.2 * [Biomass] + 14 * [Succinate]}{12 * [Lactate] + 4.25 * [Yeast\ extract] + 0 * \left[CO_{2_{con}}\right] + 12 * [Fumarate]} \text{x}100\% \qquad \text{Equation 2-18}$$

where [Acetate] and [Biomass] are the total acetate and biomass produced, [mM]; $CO_{2_{prod}}$ is the amount of CO_2 theoretically produced, estimated on the basis of measured acetate according to Equation 2-16, [mM]; [Lactate] and [Yeast extract] is the amount of lactate and yeast extract consumed [mM]; $CO_{2_{con}}$is the amount of CO_2 theoretically consumed for

biomass production, [mM]; [Fumarate] and [Succinate] are the amount of fumarate consumed and succinate produced [mM], respectively. Coefficients in *Crec%* and *erec%* indicate the number of carbon and reduction grades in the corresponding compounds, respectively. Reduction grades of compounds were estimated based on the following reduction grades of key elements C = 4, H = 1, O = -2 and N = -3.

The theoretical biomass production from CO_2 fixation was estimated according to the following equation:

$$CO_2 + 2.1H_2 + 0.2NH_3 \rightarrow CH_{1.8}N_{0.2}O_{0.5} + 1.50H_2O \qquad \text{Equation 2-19}$$

where $CH_{1.8}N_{0.2}O_{0.5}$ (Roels, 1983) is the theoretical biomass which was estimated as the difference between total measured biomass and the theoretical biomass derived from the complete utilization of yeast extract. The amount of C-mM in yeast extract was calculated according to the formula $CH_{1.9}O_{0.45}N_{0.25}$ (Zollars, 2010) and was constant in all chemostats (4.6 C-mM). The lactate incorporation into biomass was neglected for carbon and electron recovery estimations.

In addition, modifications of the estimations of *Crec%* and *erec%* were done for chemostats where expected residual lactate and residual fumarate were consumed. The residual consumption of lactate in fumarate-limited chemostats and fumarate in lactate-limited chemostats was assumed to proceed according to Equation 2-20, and Equation 2-21-Equation 2-22, respectively.

$$C_3H_6O_3 + H_2O \rightarrow C_2H_4O_2 + 2H_2 + CO_2 \qquad \text{Equation 2-20}$$

$$C_4H_4O_4 + 4H_2O \rightarrow 4CO_2 + 6H_2 \qquad \text{Equation 2-21}$$

$$6H_2 + 6C_4H_4O_4 \rightarrow 6C_4H_6O_4 \qquad \text{Equation 2-22}$$

Molecular growth yield (Y) was calculated as following:

$$Y = \frac{X}{S_0 - S} \qquad \text{Equation 2-23,}$$

where X is the biomass (g dw/l), S_0 is the initial substrate concentration [mM], S is the consumed substrate [mM], μ is dilution rate D (h^{-1}).

2.5 Analytical measurements

2.5.1 Fe(II) determination

Fe(II) was measured using the ferrozine assay according to Braunschweig et al. (Braunschweig et al., 2012). Culture samples were diluted 1:10 with 1M HCL, shaken for 30 min at 25ºC and 1200 rpm. Then, 100 µl of the diluted sample were added to 100 µl of ferrozine solution (ammonium acetate (500 g l^{-1}) and 0.1% (w/v) of ferrozine (1 g l^{-1}) in millipore water) and incubated for 15 min. Absorbance at 560 nm was measured using a Wallac 1420 Viktor^3 plate reader (Perkin Elmer, MA).

2.5.2 Acetate, butyrate, benzoate, toluene, and ethanol determination

Acetate and butyrate were measured by HPLC (Shimadzu, Japan) on an Aminex HPX87H column (Bio-Rad) with 0.5 mM H_2SO_4 as a mobile phase (column temperature: 50ºC, flow rate: 0.5 ml min^{-1}, UV detection at 220 nm). 0.5 ml of sample was treated with 55 µl of 35% perchloric acid, incubated for 10 min on ice, then 27 µl of 7 M KOH was added and stored at -20ºC. Before the measurements, the samples were thawed at room temperature, centrifuged at 13,000 rpm for 2 minutes in an Eppendorf centrifuge and the supernatant was filtered through Millipore filters (Millex-HV, 0.45 µm). Samples for benzoate measurements were treated with 1 M NaOH (1:10 dilution), incubated on ice for 10 min, and stored at +4ºC overnight. Before measurements, 80% ethanol was added in 1:1 ratio and samples were centrifuged for 2 min at 14,000 rpm in an Eppendorf centrifuge. Benzoate was analysed on a PFP Kinetex column. Elution took place isocratically with Millipore water with 1% acetic acid (solvent A) and methanol with 1% acetic acid (solvent B) (50:50, v:v) at a flow rate of 0.7 ml min^{-1} (UV detection at 236 nm). Toluene was measured on GC-MS as described elsewhere (Anneser et al., 2008). Ethanol was measured on GC-FID (Hewlett Packard 5890 Series II) equipped with a 30 m VOCOL column (Supelco, Bellefonte, Pennsylvania, USA) 0.25 mm inner diameter, with a film thickness of 1.5 µm and operated with nitrogen as a carrier gas at 1.6 ml min^{-1}. Sample application was performed by automated headspace injection of 1 ml from 10 ml headspace vials using a CombiPal Autosampler (CTC Analytics), and an injector temperature of 200°C. The temperature program started at 80°C (0.3 min), ramp 30°C min^{-1} to 160°C (3.67 min), and 60°C min^{-1} to 200°C (10.33 min).

2.5.3 Cell counting and dry weight

Cell numbers were measured using a Coulter Multisizer II (CoulterElectronics, England). Optical densities of bacterial biomass were measured at a wavelength of 660 nm. Cell

numbers were determined with a Multisizer^3 Coulter Counter (Beckman Coulter, CA, USA). Dry weight was measured as previously described by (van Verseveld et al., 1984).

2.6 Denaturing gradient gel electrophoresis (DGGE) analysis

Denaturing gradient gel electrophoresis (DGGE) analysis was performed by Martin Braster, a technical assistant in Cell Physiology department, VU Amsterdam. DGGE analysis of PCR-amplified 16S rRNA genes was used to control the purity of the continuous culture. FastDNA® SPIN Kit for Soil (Obiogene) was used for DNA extraction. The V3 region of the 16S rRNA gene sequence was amplified using universal 16S rRNA primers with attached GC clamp. DGGE was performed with a Bio-Rad Detection system. The PCR product was loaded onto a 1 mm thick polyacrylamide gel containing 30-55% linear denaturant gradient. A marker, consisting of 11 known clones was loaded in the wells of the gel as well. Electrophoresis was performed at a constant voltage of 200 V for 200 minutes in 1 x TAE running buffer at 60ºC. After electrophoresis, the gels were stained with 1 µl of Ethidium Bromide per 100 ml of 1 x TAE buffer and photographed under UV light using Kodak EDAS 290 camera.

2.7 Terminal restriction fragment length polymorphism (T-RFLP) analysis

T-RFLP analysis was done by amplifying a region of the 16S rRNA genes using universal primers with 5′-6-carboxyfluorescein (FAM) label (Ba27f-FAM as a forward primer and 907r as a reverse primer). PCR amplicons were purified by PCRExtract and GelExtract purification kit (5Prime, Hamburg, Germany). Restriction of purified amplicons was done with MspI restriction enzyme for 2 h at 37ºC. Further, digested amplicons were desalted using DyeEx Spin Columns (Qiagen, Hilden, Germany) and then denaturated for 5 min at 95ºC. Digested amplicons were subjected to capillary electrophoresis on ABI 3730 DNA analyzer (Applied Biosystems, Foster City, CA) as described by (Pilloni et al., 2011). PeakScanner (version 1.0) and GeneMapper (version 4.0) programs (Applied Biosystems, Foster City, CA) were used to analyze electropherograms generated by ABI 3730 DNA analyzer.

2.8 Determination of bacterial cell numbers in the sediments

Cells in the sampled sediment (0.5 ml) were fixed with 2.5 % glutardialdehyde and stored at 4ºC until further analysis. Glutardialdehyde was removed from the sediment via centrifugation for 10 min at 13,000 rpm in Eppendorf centrifuge. Fixed cells were disattached from the sediment via shaking in a swing mill (Retsch, MM 200) for 3 min at 20 Hz in the

presence of 1.5 ml of PBS buffer. Further, cells were separated from the sediment particles via gradient centrifugation at 11,000 rpm for 1 h at 4ºC in the presence of gradient medium Nycodenz with density of 1.3 g ml^{-1} (Nycomed Pharma AS, Oslo, Norway) in an ultracentrifuge (Optima XE-90, Beckman Coulter). After centrifugation the upper layer of the supernatant (1.5-2 ml) containing approximately 80% of the cells was collected. Harvested cells together with internal standard TruCount beads (TruCount tubes, Becton Dickinson, Heidelberg, Germany) were stained with SYBR-Green I (Molecular Probes, Invitrogen, Karlsruhe, Germany) at a ratio of 1:10,000 for 15 min and then subjected to flow cytometer (LSR II, Becton Dickinson, Heidelberg, Germany) equipped with a 488 nm and 633 nm laser. The following settings were used: forward scatter (FSC) 350 mV, side scatter (SSC) 300–370 mV, B530 (bandpass filter 350 nm) 500–580 mV. In order to minimise a background noise, the following thresholds were applied: 200 mV for FSC and SSC. The cell numbers were calculated according to the following formula (Nebe-von-Caron et al., 2000):

$$\frac{cells}{ml} = \frac{N_{bac} * \frac{N_{beads}}{vial} * V_{fractions}}{N_{beads} * V_{sample} * V_{sediment}} * 1.43 * 1.28 \qquad \text{Equation 2-24}$$

where N_{bac} is counted cell numbers in flow cytometer, N_{beads} is a number of beads in a TruCount tube, $V_{fractions}$ is the volume of supernatant taken after gradient centrifugation, V_{sample} is the volume taken for flow cytometer analysis, and $V_{sediment}$ is the volume of used sediment; 1.43 is a factor correcting for the release efficiency and 1.28 is a factor correcting for the loss during the gradient centrifugation.

2.9 Control of readiness to use alternative carbon substrates (Nitrate assay)

In order to check if *G. metallireducens* was prepared to degrade alternative carbon substrates when cultivated in retentostat under slow growth rates, cell biomass was harvested from the retentostat with acetate as a single substrate (2^{nd} run) at the end of the retentostat cultivation and centrifuged for 20 min at 4,500 rpm, 4°C, washed twice with *Geobacter* medium omitting electron acceptors and electron donors. Cell suspension was used to inoculate 10 ml serum tubes containing *Geobacter* medium with 5 mM $NaNO_3$ as electron acceptor and different carbon sources: 5 mM acetate, 1 mM benzoate, 10 mM butyrate, 5 mM lactate, 0.5 mM phenol, 0.5 mM *p*-cresol, 10 mM pyruvate, 0.5 mM benzylalcohol, 1mM toluene, or 20 mM ethanol and a blank without any carbon substrate. Each growth condition was presented with

three replicates containing 25 mg l^{-1} chloramphenicol and three replicates without growth inhibitor. The antibiotic chloramphenicol was used to block production of *de novo* proteins in order to see if degradation pathways for some carbon substrates were already expressed in retentostat. The results from chloramphenicol amended experiments were compared to the control experiments which did not contain the inhibitor. The analysis of NO_2^- produced was carried out 24 h after the inoculation of serum tubes.

2.10 Proteomic analyses

Cells were harvested by centrifugation at 3,345 g for 20 min, at 4°C; washed once with 1 x phosphate buffered saline (PBS) consisting of (per liter): 8.00 g NaCl, 0.20 g KCl, 0.24 g KH_2PO_4, 1.44 g Na_2HPO_4. Washed cells were centrifuged again at 12,000 rpm (Eppendorf centrifuge), 1 min, 4°C. Cell pellet was transferred into 1.5 ml sterile Eppendorf tube and stored at -80 °C until further analysis.

2.10.1 Label free proteomics

Protein extraction, separation, and digestion with subsequent LC-MS/MS analysis were done in the Department Proteomics, Helmholtz Centre for Environmental Research – UFZ by Dr. Jana Seifert and Kathleen Eismann and Christine Schumann.

Proteins for proteomic analyses were extracted by lysis buffer (2% sodium dodecyl sulphate (SDS), 20 mM Tris/HCl, pH 7.5) with sonication. The cell pellet was dissolved in SDS-lysis buffer and shaken for 5 min at 60°C and 1,400 rpm. Then, 20 mM Tris/HCL pH 7.5 buffer with 1 µl ml^{-1} benzonase (Novagen) (added directly before use), 0.1 mg ml^{-1} $MgCl_2$, 1 mM phenylmethylsulfonyl fluoride (PMSF) were added. Sonication was applied twice for 1 min (Ultrasound processor UP50H, Hielscher, Germany; 0.3 seconds per pulse, 30% duty) with sample cooling on ice between the rounds.

Protein concentration was determined using the Bradford protein assay (Bio-Rad) with bovine serum albumin as the standard (Bradford, 1976).

For one dimensional electrophoresis, 50 µg of protein extract were precipitated with a fivefold volume of ice-cold acetone (Laemmli, 1970). Acrylamide gels (12%) were stained with colloidal Coomassie Brilliant Blue G-250 (Roth, Kassel, Germany). The lanes of separated proteins were cut in 5 slices which were digested over night at 37°C with trypsin (Jehmlich et al., 2008b).

2.10.1.1 Protein identification

Three biological replicates were investigated per condition. Each biological sample was analysed in two technical replicates. Peptides were analysed by UPLC-LTQ Orbitrap-MS/MS as described by Bastida et al. (2010). The peptides were eluted over 50 min with a gradient of solvent B (8–40% ACN). Continuous scanning of eluted peptide ions was carried out between m/z range of 300 and 1,600, automatically switching to MS/MS CID mode on ions exceeding an intensity of 3,000. Identification was performed with MaxQuant (v. 1.2.2.5) (Cox and Mann, 2008) and its build-in database search algorithm Andromeda (Cox et al., 2011) using annotated protein sequences of *G. metallireducens* GS-15 (Uniprot, May 2011). Five gel slices of one gel band were defined as one experiment for LFQ calculations. Settings were the following: peptide modifications given were methionine oxidation as variable and cysteine carbamidomethylation as fixed. Further settings were: first search ppm of 20, main search ppm of 6, and maximum number of modifications per peptide 5, maximum missed cleavages 2 and a maximum charge for the peptide of 6. Parameters for identification were a minimum peptide length of 5 amino acids, a false discovery rate for peptides (1%), proteins and level of modification sites of 1%. A minimum of 1 unique peptide was required for protein identification as has been mentioned elsewhere (Ding et al., 2006) some proteins have only one tryptic peptide, which can be detected by mass spectrometry. Apart from unmodified peptides, only peptides with oxidized methionine and carbamidomethylized cysteine were used for quantification. Only unique or razor peptides were chosen for use in quantification. Miscellaneous settings switched on were re-quantify, keep low scoring versions of identified peptides, match between runs (time window of 2 min), label-free quantification and second peptides.

2.10.1.2 Statistical analysis

Statistical analysis of proteins identified with label-free proteomics was done by Dr. Robert Küffner from Teaching and Research Unit Bioinformatic, Institut für Informatik, Ludwig-Maximilians-Universität München.

(i) Normalization. After log-transformation, all individual batch cultures exhibited approximately normal intensity distributions. Between replicate substrate conditions, deviations of distributions were mostly due to differences in mean or variance. Protein intensity was normalized by matching mean $\overline{x}_j$ and standard deviation σ_j for each batch j by transforming measurements for each $x'_{i,j}$:

$$x'_{i,j} = \frac{(x_{i,j} - \overline{x}_j) * \sigma}{\sigma_j} + \overline{x} \qquad \text{Equation 2-25}$$

where $\overline{x}$ and σ correspond to mean and standard deviation across all proteins *i* and substrate conditions *j*, respectively.

*(ii) Determination and clustering of differentially expressed proteins***.** After normalization, a one-way analysis of variance (ANOVA) was applied for each protein to determine significant differences in expression between the six groups (=growth conditions) of six replicates each. Subsequently, conditions where proteins exhibit significant differential expression were identified via pairwise t-tests. Both statistical tests quantify the significance of differential expression events via p-values that, in case of large-scale datasets, need to be corrected for multiple testing to distinguish true discoveries from false positive random events. P-values from ANOVA and t-test were uniformly corrected by transforming them into respective false discovery rates (FDRs, i.e. the percentage of proteins with significant expression by chance) based on random permutations of the protein expression data. Each protein specific expression profile vector was randomized a hundred times and ANOVA as well as t-test were applied to the 100 randomized datasets as described above. For each p-value derived from the measured data, 100 p-values were derived from the permuted data. Then, a given p-value derived from measured data was transformed via FDR = 100 * number of permutations * number of true positives/number of false positives, where true and false positives refer to the number of p-values computed from measured and permuted data, respectively, that were less or equal than the given p-value. This approach to FDR calculation was adapted from significance analysis of microarrays (Tusher et al., 2001) and described in detail in (http://www-stat.stanford.edu/~tibs/SAM/sam.pdf). Subsequently a FDR threshold of 5% was applied to identify differentially expressed proteins and corresponding pairs of conditions. Six growth conditions resulted in 15 pairwise t-tests for each protein.

Further, in order to identify differences specifically caused by the growth rate, biological samples from retentostats and batch with acetate as a single carbon source and from retentostats and batch with acetate plus benzoate as two carbon sources were analysed separately via ANOVA with subsequent application of the t-test. Due to the lower number of conditions, perturbations were applied not to measurement vectors but to protein abundances within one vector. Protein abundances were randomized 100 times within each condition. FDRs were calculated as described above. However, FDR threshold was set to 2%.

(iii) Correspondence analysis. Correspondence analysis was conducted in order to visualize similarity between the conditions. Here, a two dimensional plot (drawn by the software PAST (Hammer et al., 2001)) depicts differentially expressed proteins as identified by ANOVA for each of the six conditions. The visualization measures the similarities between all data points based on Eigenvalues of Chi-squared distances (Hammer et al., 2001).

(iv) Hypergeometric test. Pathways enriched in differentially expressed proteins were identified by the hypergeometric test. Enrichment can be quantified via p-values based on the assumption of hypergeometric distribution as adapted from GO-analysis strategies (Alexa et al., 2006; Falcon and Gentleman, 2007). More specifically, given a pathway π and a pair of growth conditions *a* and *b*, the hypergeometric test estimates the significance of observing among the $K\pi$ pathway proteins $k\pi$ or more proteins that are significantly up-regulated in condition *a* as compared to condition *b*. For the purpose of representation, the p-values derived from the hypergeometric distribution were transformed into z-scores via the inverse cumulative distribution function.

(v) Hierarchical regulation analysis of TCA cycle

Hierarchical regulation analysis was performed by Dr. W. Röling from VU University, Amsterdam. Hierarchical regulation analysis quantifies the relative importance of changes in interactions of an enzyme with its substrate (products, effectors) [metabolic regulation] and in enzyme concentration [hierarchical regulation] for changes in flux through an enzyme (ter Kuile and Westerhoff, 2001; Rossell et al., 2005). The analysis uses a general description of enzyme activity:

$$v_i = f_i(e_i) * g_i(X) \qquad \text{Equation 2-26}$$

where, v_i is the rate through an enzyme *i*, which depends linearly on function f_i that depends on enzyme concentration e_i and function g_i that depends on substrate concentration *X*. From this equation a simple theorem can be derived:

$$1 = \frac{\Delta lnf(e)}{\Delta lnJ} + \frac{\Delta lng(X)}{\Delta lnJ} = \rho_h + \rho_m \qquad \text{Equation 2-27}$$

where *J* is the metabolic flux through the enzyme, ρ_h is the hierarchical regulation coefficient and ρ_m is the metabolic regulation coefficient.

Analysis is based on calculation of hierarchical coefficients because it is relatively easier to determine ρ_h than ρ_m as $f_i(e_i)$ is the enzyme concentration (normalized averaged protein abundances taken from proteomic data (see for details Supplementary material, Table 7-2B))

during exponential growth at maximum specific growth rate ($\mu_{max;}$ h^{-1}) and the flux *J* through the enzyme was calculated in terms of turnover of the intermediate acetyl-CoA according to the following equation:

$$J = \frac{\mu_{max}}{Y} \qquad \text{Equation 2-28}$$

where, *J* is flux [mmol acetyl-CoA $cell^{-1}$ h^{-1}], and *Y* is yield on acetyl-CoA [cells $mmol^{-1}$ of acetyl-CoA consumed] that is expressed as cells l^{-1} at stationary phase divided by mmol l^{-1} acetyl-CoA equivalents consumed in the stationary phase.

Therefore,

$$\rho_h = \frac{\Delta ln f_i(e_i)}{\Delta ln J} \qquad \text{Equation 2-29}$$

Fluxes and yields were expressed in acetyl-CoA equivalents, since acetyl-CoA is the first central intermediate in the degradation of all five carbon sources studied here (Supplementary material, Table 7-2A).

Calculations of residual substrate concentrations and Fe(II) produced in the stationary phase were based on experimental data (Supplementary material, Table 7-2A) and stoichiometric equations for butyrate, acetate, ethanol, benzoate and toluene degradation coupled to Fe(III) reduction (Equations 2-27 – 2-31).

Butyrate: $C_4H_7O_2^- + 6H_2O + 20Fe(III) \rightarrow 4CO_2 + 20Fe(II) + 19H^+$ Equation 2-30

Acetate: $C_2H_3O_2^- + 2H_2O + 8Fe(III) \rightarrow 2CO_2 + 8Fe(II) + 9H^+$ Equation 2-31

Ethanol: $C_2H_6O + 3H_2O + 12Fe(III) \rightarrow 2CO_2 + 12Fe(II) + 12H^+$ Equation 2-32

Benzoate: $C_7H_5O_2^- + 12H_2O + 30Fe(III) \rightarrow 7CO_2 + 30Fe(II) + 29H^+$ Equation 2-33

Toluene: $C_7H_8 + 14H_2O + 36Fe(III) \rightarrow 7CO_2 + 36Fe(II) + 36H^+$ Equation 2-34

Hierarchical coefficients ρ_h for each enzyme of TCA cycle were obtained from plotting enzyme concentrations at all growth conditions against their flux on respective carbon substrate in a logarithmic space (software Kaleidograph). Taking into consideration Equation 2-27, where $\rho_h + \rho_m = 1$, ρ_h coefficient with values close to one indicates importance of hierarchical regulation, while ρ_h close to zero indicates importance of metabolic regulation in flux changes though an enzyme. Moreover, hierarchical coefficients with negative values

indicate an antagonistic effect between the changes in enzyme concentration and changes in the flux though enzyme (with flux increase, enzyme concentration decreases) (Rossell et al., 2005).

2.10.2 Isotope-coded protein labelling (ICPL)

Prior to protein extraction, cells were thawed at room temperature. Protein extraction and stable isotope labelling were done with the ICPL Quadruplex kit (Serva, Heidelberg, Germany) according to manufacturer´s instructions. The cell pellet was dissolved in 400 µl of lysis buffer (guanidine-HCL) supplied by the kit followed by ultra-sonication. Protein concentration was determined using the Bradford protein assay (Bio-Rad) with bovine serum albumin as a standard (Bradford, 1976). Each sample used for ICPL labelling contained equal amounts of proteins with approximate concentrations of 5 mg ml-1.

Four different growth conditions were applied in this study (lactate, fumarate, ammonium-limited chemostats, and batch, see Table 3-4); therefore, four ICPL labels (ICPL-0, ICPL-4, ICPL-6, ICPL-10) were used (Table 2-1), resulting finally in ICPL ratios between the individual conditions for comparison. Ammonium and lactate-limiting chemostats were run in two biological replicates while fumarate limiting chemostats had four biological replicates. The labels used and analysis runs are indicated in Table 1. Proteins expressed in batch were used as a reference and were labelled with ICPL-0. Four labelling campaigns were carried out (Table 2-1), where 4944_A2 and 4944_A3 were conducted simultaneously, i.e. labelled samples were separated via SDS-PAGE, digested and analysed on LC-MS/MS. Runs 5120 and 4766 were analysed separately. In order to identify a contribution of technical variation into the overall variation between biological replicates, proteins expressed in chemostats F2 and A1 were labelled twice (Table 2-1).

Table 2-1

Arrangement of labelled proteins in labelling campaigns. A: ammonium plus fumarate limitation, F: fumarate limitation, L: lactate limitation.

Chemostats	F1	F2	F3	F4	A1	A2	L1	L2
ICPL label	ICPL-4	ICPL-4 ICPL-6	ICPL-4	ICPL-4	ICPL-10 ICPL-10	ICPL-10	ICPL-6	ICPL-6
Codes of labelling campaigns	4766	4944_A2 4944_A3	5120	4944_A3	4944_A3 5120	4944_A2	4944_A2	5120

2.10.2.1 LC-MS/MS analysis and data processing

For each analysis, the isotope-labelled proteins from the four different treatments were combined. The resulting mixture of labelled proteins per experiment was separated by 1D SDS-PAGE. After Coomassie Blue staining, each lane was cut in 5 to 6 slices and subjected to in-gel digestion with trypsin (Sigma Aldrich) as described previously (Merl et al., 2012).

The digested peptides were separated by nano-HPLC and analysed with a LTQ Orbitrap XL mass spectrometer (Thermo Scientific) as described (Gaupels et al., 2012). Except for up to ten most intense ions were selected for fragmentation in the linear ion trap. Furthermore, target peptides already selected for MS/MS were dynamically excluded for 60 seconds.

The MS/MS spectra were searched against the *Desulfitobacterium hafniense* database (Version: 2.4, 5017 sequences) using the Mascot search engine (version 2.3.02; Matrix Science) with the following parameters: a precursor mass error tolerance of 10 ppm and a fragment tolerance of 0.6 D. One missed cleavage was allowed. Carbamidomethylation was set as a fixed modification. Oxidized methionine and ICPL-0, ICPL-4, ICPL-6 and ICPL-10 modifications for lysine residues were set as variable modifications.

Data processing for the identification and quantification of ICPL-quadruplex labelled proteins was performed using Proteome Discoverer version 1.3.0.339 (Thermo Scientific). Proteome Discoverer generated automatically the ratios of signal intensities of peptide pairs labelled with different stable isotopes labels. All possible ratios for a given peptide within each labelling campaign were generated. The Mascot Percolator algorithm was used for the discrimination between correct and incorrect spectrum identifications (Brosch et al., 2009), with a maximum q value of 0.01. Subsequently, following the approach described in (Cox and Mann, 2008), protein ratios were calculated based on the median of all peptide ratios which were identified to belong to a corresponding protein. Proteins were further filtered: high peptide confidence and at least 2 peptides per protein (count only rank 1 peptide and count peptide only in top scored proteins).

2.10.2.2 Statistical analysis

- **Identification of significant protein ratios (Significance B analysis)**

In order to minimize the influence of outliers in Proteome Discoverer, the obtained protein ratios of each measurement were normalized by a median of all protein ratios detected in this measurement. Due to the variability in fumarate and lactate utilization patterns within

biological replicates (Table 3-4), statistical analysis was performed separately for normalized ratios of each replicate in Perseus statistical tool. According to Cox and Mann (2008), log 10 transformed protein ratios were used to quantify the probability of obtaining significantly different ratios from the main distribution. This significance (termed as Significance B according to Cox and Mann (2008)) was calculated for each protein group which was created based on intensity bins. Each bin contained equal amounts of proteins. Further, Significance B was corrected for multiple testing with false discovery rate (FDR) approach with significance cut off $p < 0.05$.

- **Principal component analysis (PCA)**

In order to visualize differences between the significant protein ratios, principal component analysis (PCA) was carried with the PAST software (Hammer et al., 2001). Missing values were subjected to iterative computation according to (Ilin and Raiko, 2010).

3 Results

3.1 Physiology of *G. metallireducens* at high substrate concentrations in batch

3.1.1 Utilization of substrate mixtures

In order to test whether *G. metallireducens* prefers aliphatic acids (acetate, butyrate) or alcohols (ethanol) over aromatic compounds (benzoate or toluene) and whether aromatic compounds can be consumed simultaneously, various batch experiments with single substrates and with mixtures of two substrates were conducted (Table 3-1).

G. metallireducens exhibited the highest maximum specific growth rate [μ_{max}] when grown with the single substrates ethanol or acetate (0.22 h^{-1} and 0.16 h^{-1}, respectively) (Supplementary material, Table 7-2). μ_{max} on benzoate was 0.11 h^{-1}, while on toluene or butyrate μ_{max} was the lowest with 0.07 $h^{-1}$and 0.05 h^{-1}, respectively (Supplementary material, Table 7-1).

Table 3-1. Batch experiments with dual substrate mixtures with indication of the type of consumption[a]

Pre-grown substrate	Co-substrate	Type of consumption	Lag phase (h)
Acetate (2mM)	Benzoate (0.6mM)	Preferential	None
Butyrate (3mM)	**Acetate** (2mM)	Preferential	None
Ethanol (2mM)	Acetate (2.5mM)	Preferential	None
Acetate (2.5 mM)	Toluene (0.5mM)	Preferential	13
Butyrate (4 mM)	Ethanol (2mM)	Simultaneous	None
Butyrate (4.5mM)	Benzoate (0.5mM)	Simultaneous	None
Benzoate (0.3mM)	Toluene (0.5mM)	Simultaneous	None
Benzoate (0.5mM)	**Ethanol** (1mM)	Preferential	36

[a]Substrates in bold are preferred substrates in the mixture

It was expected that if the substrate mixtures would be consumed simultaneously, the ratio of their consumption rates would be approximately equal to the ratio of the growth rates on the respective single substrates (see Supplementary material for calculations, chapter 7.1). This assumption was confirmed by experiment with a mixture of benzoate and toluene and was approximately 1:1 (Supplementary material, Table 7-3). However, this was not the case when

acetate plus benzoate or acetate plus toluene were supplied simultaneously. The ratio of the growth rates between acetate and toluene, or acetate and benzoate when used as sole substrates (9 and 6.4, respectively) was lower than the ratio of substrate consumption when these substrates were used together in a mixture (587.5 and 17,2, respectively) (Supplementary material, Table 7-3).

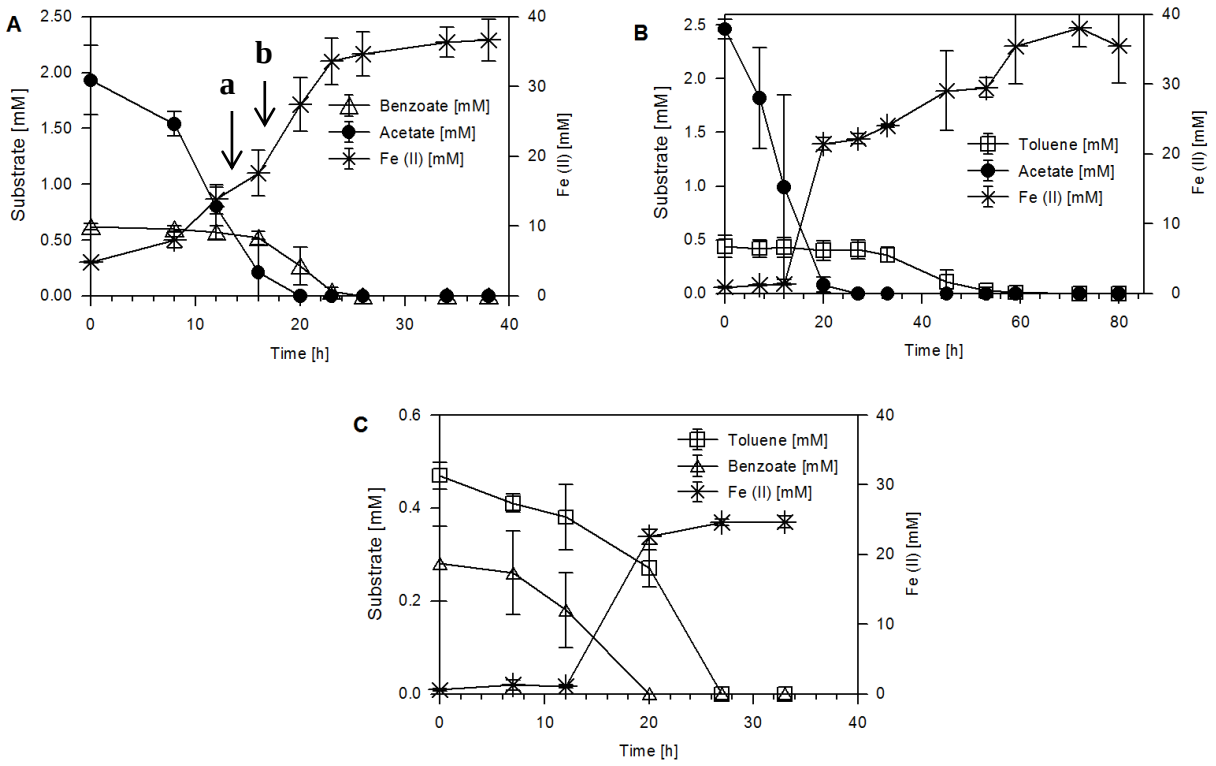

Figure 3-1. Substrate consumption by *G. metallireducens* in batch cultures with acetate plus benzoate (**A**), toluene plus acetate (**B**), toluene plus benzoate (**C**). Error bars indicate the standard deviations of three replicates. Arrows represent the sampling time for proteomics: **a** – early exponential phase, **b** - late exponential phase. Concentrations of substrates and Fe(II) are given in Table 1 of Appendix.

During acetate utilization, no benzoate or toluene degradation was observed, indicating that the substrates were not consumed according to their corresponding growth rates, but acetate inhibited toluene or benzoate utilization in a diauxic behaviour. Once acetate was depleted, benzoate utilization started immediately (Figure 3-1A). Four hours after complete removal of acetate, 52% of the benzoate was degraded. In contrast, *G. metallireducens* exhibited thirteen hours lag phase between consumption of acetate and toluene (Figure 3-1B). Cultivation of *G. metallireducens* on toluene plus benzoate showed a different pattern as the two substrates

were consumed simultaneously (Figure 3-1C; Table 3-1). However, benzoate was utilized at a higher rate and toluene was still present in the medium (58%) after full benzoate depletion.

In addition, acetate, ethanol, butyrate, and/or benzoate mixtures were tested for possible effects on substrate preference by *G. metallireducens* (Table 3-1, Figure 3-2). Among the tested conditions, only ethanol had a distinct repressing effect on the acetate and benzoate consumption (Figure 3-2B, and E) while butyrate and benzoate were consumed simultaneously (Figure 3-2D).

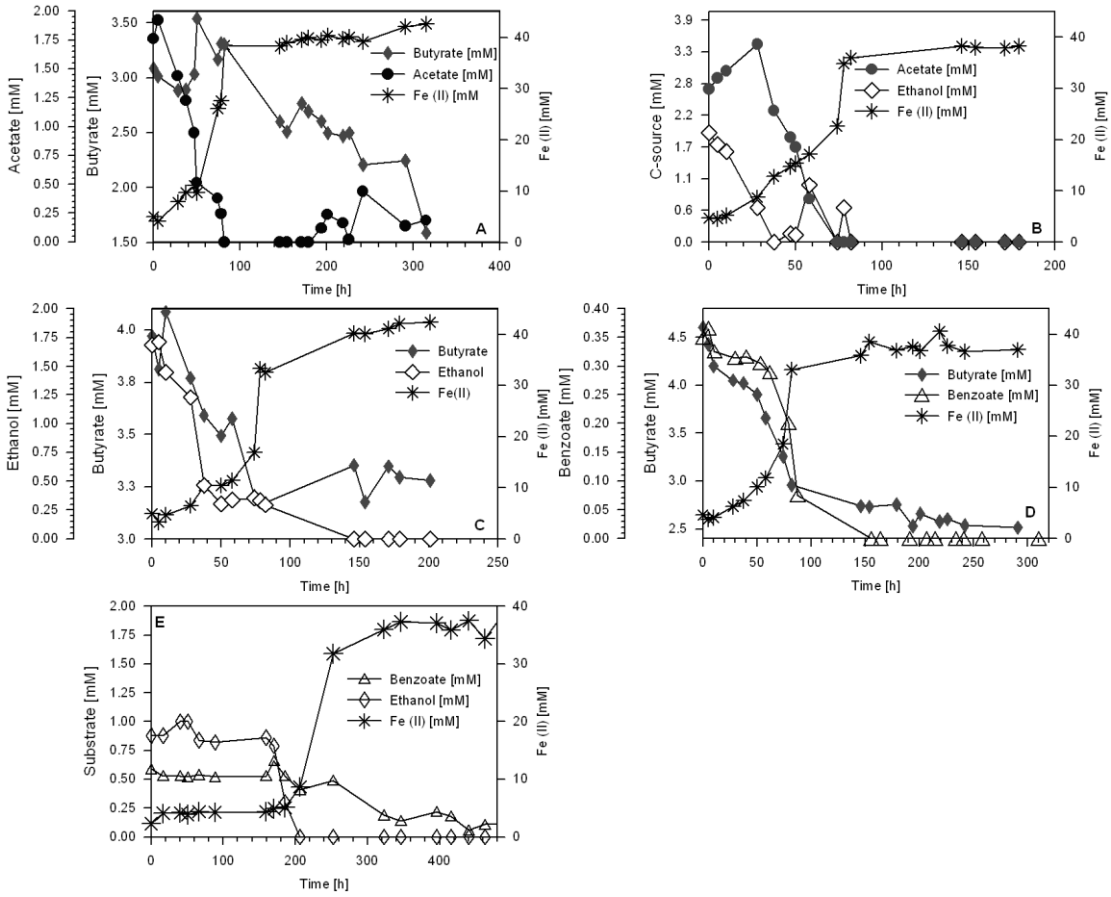

Figure 3-2. Growth of *G. metallireducens* with substrate mixtures. (**A**) Butyrate adapted cells exhibited preferential consumption of acetate. (**B**) Preferential consumption of ethanol in the presence of acetate. (**C**) Preferential consumption of ethanol in the presence of butyrate. (**D**) Simultaneous consumption of butyrate and benzoate. (**E**) Preferential consumption of ethanol by benzoate-adapted cells. Concentrations of substrates and Fe(II) are given in **Table 2** of Appendix.

3.1.2 Differential protein expression with different carbon sources

It was aimed to analyse which catabolic pathways were expressed on different carbon sources. LC-MS/MS analysis of proteomes of cells growing on five individual carbon sources (acetate, benzoate, butyrate, ethanol, and toluene) and one mixture of two substrates (acetate plus

benzoate) detected a total of 1477 proteins out of 3519 predicted for *G. metallireducens* in the Uniprot database. Samples for proteomic analysis were taken when cells were growing exponentially at the maximum specific growth rates [μ_{max}] (Supplementary material, Table 7-2). Eighty-four proteins were identified with one unique peptide; all others were identified with two or more. The cellular distribution of the identified proteins was in accordance to the predicted distribution (Figure 3-3), indicating appropriate representation of cytoplasmic and membrane proteins. At a false discovery rate (FDR) < 5%, 155 proteins were identified as differentially expressed (Table S1 in Additional material).

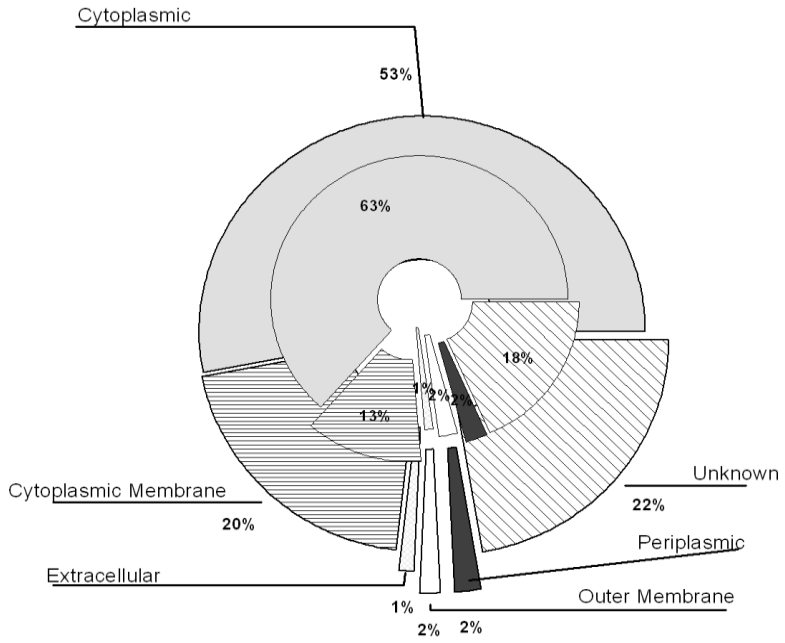

Figure 3-3. Cellular distribution of identified proteins (inner ring) vs. predicted (outside ring). Cellular distribution was predicted by Psort database. Annotated localization of detected proteins can be found in Additional material, **Table S2**.

3.1.3 Correspondence analysis of differentially expressed proteins on all substrates

Correspondence analysis of 155 differentially expressed proteins revealed a clear separation of the five different single substrate growth conditions: acetate, ethanol, butyrate, benzoate, and toluene (Figure 3-4). The two-substrate growth condition acetate plus benzoate was also examined. When the cells were sampled in the late exponential phase after complete depletion of acetate (Figure 3-1A), the two technical replicates showed similarity to the benzoate only

condition (Figure 3-4). When the cells were harvested during the acetate consumption phase, the protein expression pattern in one biological replicate exhibited the highest similarity to the acetate only condition while another replicate was positioned between the acetate and the benzoate only conditions (Figure 3-4).

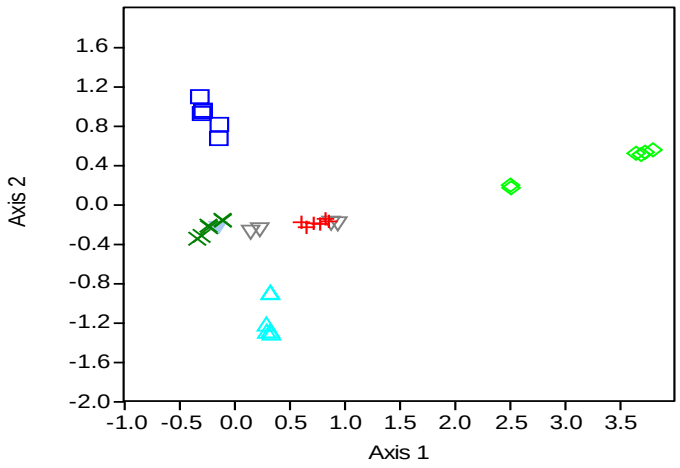

Figure 3-4. Correspondence analysis of 155 differentially expressed proteins across the different substrates. The first two axes with the highest eigenvalues retain 46% of the data. Symbols depict the different growth substrates: ◇ ethanol, △ toluene, ▼ acetate plus benzoate (early exponential phase, acetate consumption), ▽ acetate plus benzoate (late exponential phase, all acetate consumed), + benzoate, □ butyrate, × acetate. Normalized data used for correspondence analysis can be found in the Additional material, **Table S3**.

3.1.4 Protein expression clusters based on pairwise comparisons of protein abundances

All proteins that were identified as differentially expressed were sub-grouped based on chromosomal proximity of their corresponding genes. This revealed three major clusters (Figure 3-5 and Table 7-4 in Supplementary material) containing proteins involved in the degradation of benzoate, butyrate, or toluene, respectively. In addition to the shared functional annotation and chromosomal proximity, the clusters exhibited cluster-specific differential expression patterns. The remaining differentially expressed proteins not associated with any of the three clusters were compiled into a forth group designated as 'other'. The majority of the highly abundant proteins in the different clusters were involved in the degradation of their

corresponding carbon source(s) (Figure 3-5 and Table 7-4 in Supplementary material). The four clusters are described in more detail below.

(i) Toluene cluster. The expression profile of the toluene cluster proteins is characterized by the highest homogeneity compared to the other clusters: all thirteen proteins have a high abundance on toluene, but are present at lower abundances in all other tested conditions (Additional material, Table S4). Two proteins were detected with toluene only: zinc metalloendopeptidase Gmet_1854 (Q39UJ1) with unknown function and γ subunit of (R)-benzylsuccinate synthase BssC (Q39VF0), which is involved in activation of toluene (Biegert et al., 1996) (Additional material, Table S4). The α subunit of benzylsuccinate synthase BssA (Q39VF1) detected under all growth conditions was found to be abundant significantly on toluene only relative to all conditions (Supplementary material, Table 7-4). All six proteins predicted by Butler et al. (Butler et al., 2007) to be involved in β-oxidation of benzylsuccinate to benzoyl-CoA (BbsABCD and BbsEFGH) were increased in abundance with toluene as a sole carbon source. Besides, other proteins encoded by the genes located in the genomic toluene degradation island (Butler et al., 2007) were more abundant on toluene: electron transfer flavoproteins Gmet_1527 (Q39VG3), EtfA-5 (Q39VG4), EtfB-5 (Q39VG5), and aromatic hydrocarbon degrading-ATPase Gmet_1537 (Q39VF3). The latter protein is predicted to be involved in protein folding and stabilization and has 82.5% similarity to the chaperone BssE of *A. aromaticum* EbN1. Another abundant protein found in the toluene cluster is the aromatic hydrocarbon degrading-membrane protein Gmet_1535 (Q39VF5) which is predicted to be localized in the outer membrane and exhibits 58.9% similarity to the protein TodX involved in toluene uptake in *Pseudomonas putida* F1 (Wang et al., 1995; Hearn et al., 2008).

(ii) Benzoate cluster. The benzoate cluster contains 35 proteins (Figure 3-5). Most of them were highly abundant on benzoate, toluene, and, surprisingly, butyrate. Few proteins (eight out of thirty-five) had increased abundances on acetate plus benzoate during the early exponential phase with increased number of significantly abundant proteins (twelve) in the late exponential phase relative to acetate and ethanol (Figure 3-5). The only protein from the benzoate cluster which was detected with high abundance on benzoate relative to all other conditions tested was succinyl:benzoate coenzyme A transferase Gmet_2054 (Q39TZ1).

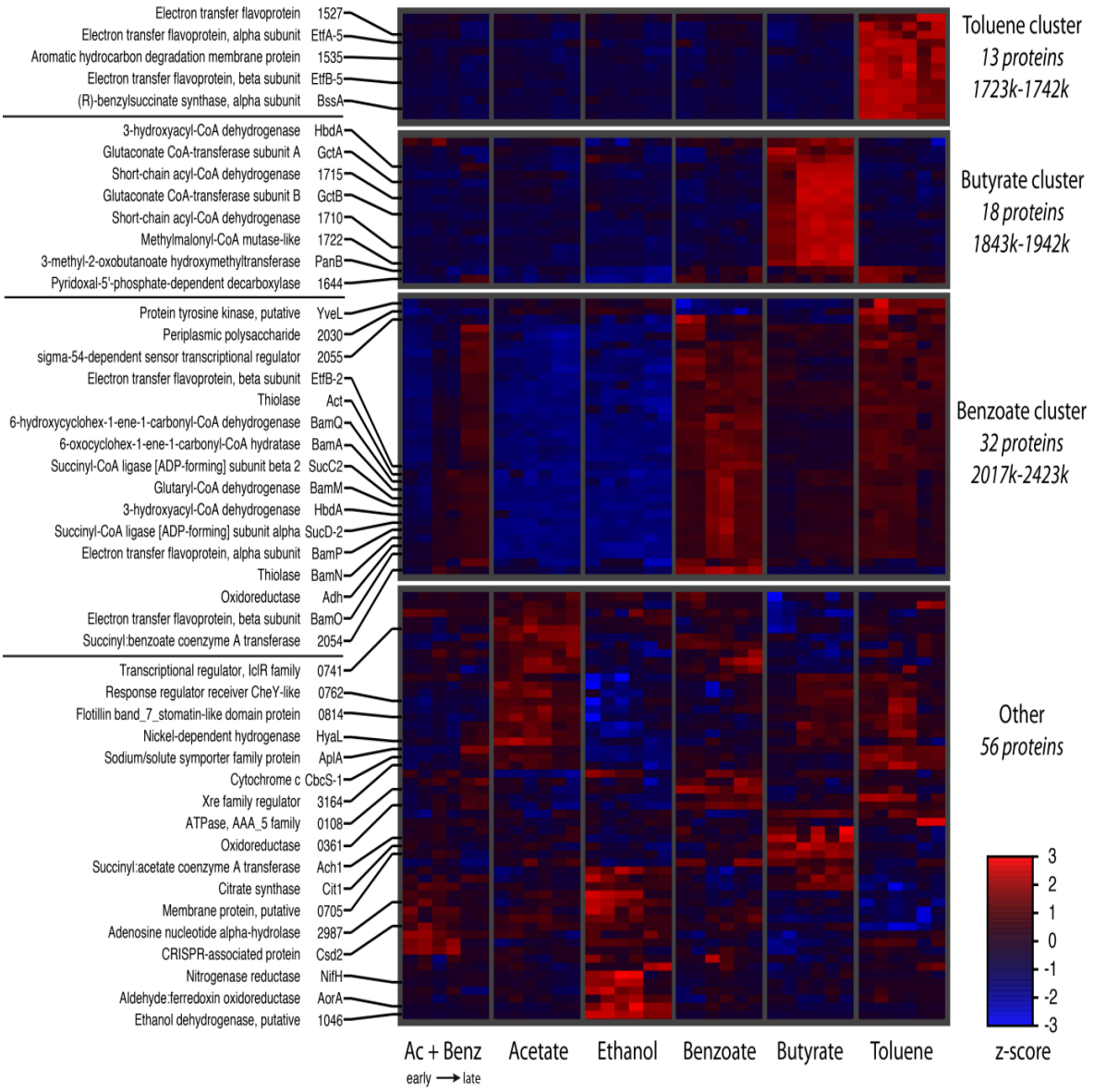

Figure 3-5. Heat map representing clustering of 118 differentially expressed proteins from *G. metallireducens* grown with a mixture of acetate plus benzoate and five single substrate (acetate, benzoate, butyrate, ethanol, and toluene). Clustering of proteins was based on the proximity of their encoding genes and co-expression. Gene coordinates of three distingished clustures are indicated on the right side of the figure. Cluster analysis was applied to each group separately and was based on z-score analysis with a range between 3 and -3. 46 proteins mentioned in the text are labeled in the graph. In addition to protein annotations, protein names (if available) or four digits of GMET ORF Ids are shown. Position of the replicates taken from early and late exponential phase on a mixture of acetate plus benzoate is indicated below the condition name. Proteins used for clustering can be found in Supplementary material, **Table 7-4**.

Benzoate-degrading proteins with significantly high abundances expressed during the late exponential phase on acetate plus benzoate relative to acetate and ethanol were the following: 6-hydroxycyclohex-1-ene-1-carbonyl-CoA dehydrogenase BamQ (Q39TP4), 3-hydroxyacyl-CoA dehydrogenase HbdA (Q39TX3), and three electron transfer flavoproteins EtfB-2

(Q39TX8), BamP (Q39TP3), and BamO (Q39TP2). Previous work showed that BamO was found to be induced on phenol (Schleinitz et al., 2009). The other proteins from the benzoate cluster were involved in fatty acid degradation (BamM (Q39TX0), BamN (Q39TX1), Adh (Q39TY6), Act (Q39TY7)) and TCA cycle (SucC2 (Q39TX6), SucD-2 (Q39TX7)). YveL protein (Q39U17) with putative function of capsule polysaccharide biosynthesis had significantly higher abundance on acetate plus benzoate relative to butyrate. Moreover, proteins from benzoate cluster such as BamQ, BamP, BamO, BamN, SucC2, and SucD-2 had increased abundances during early exponential growth phase with acetate plus benzoate relative to acetate or ethanol.

When *G. metallireducens* grew with toluene, the expression of the benzoate degradation cluster resembled its induction when *G. metallireducens* was grown with benzoate only (Figure 3-5) which is to be expected as toluene degradation proceeds via the benzoyl-CoA pathway. However, two proteins from the benzoate cluster involved in biosynthesis and degradation of surface polysaccharides and lipopolysaccharides had a relative higher abundance on toluene: polysaccharide export membrane protein Gmet_2030 (Q39U15) relative to acetate plus benzoate, benzoate and butyrate, and YveL (Q39U17) relative to acetate, benzoate and butyrate. These two membrane proteins are encoded by genes located in proximity to benzoate-degrading genes.

The majority of the proteins from the benzoate cluster had higher abundances on butyrate relative to acetate and ethanol conditions (Figure 3-5, Supplementary material Table 7-4).

(iii) Butyrate cluster. All butyrate cluster proteins were induced with butyrate as a substrate. However, two proteins within this cluster showed increased expression also on the other conditions. Pyridoxal-5'-phosphate-dependent decarboxylase Gmet_1644 (Q39V49) was increased in abundance on benzoate and toluene relative to acetate and ethanol and on acetate relative to ethanol. 3-methyl-2-oxobutanoate hydroxymethyltransferase PanB (Q39V51) was higher in abundance on toluene relative to acetate, ethanol and acetate plus benzoate, and on benzoate relative to ethanol (Supplementary material, Table 7-4). The first protein is involved in amino acid biosynthesis and butyrate metabolism, while the second one is taking part in pantothenate and CoA biosynthesis.

(iv) Other protein cluster. The fourth cluster represents a quite heterogeneous expression pattern as the proteins were not well correlated to the localization of their respective genes and were involved in various processes (Figure 3-5). Due to the lack of chromosomal proximity, some proteins were not included in the above clusters but nevertheless are likely to

play an important role in the physiology of *G. metallireducens* grown on the selected substrates.

As expected, ethanol induced putative ethanol dehydrogenase Gmet_1046 (Q39WT8) and aldehyde:ferredoxin oxidoreductase AorA (Q39WT9) with extremely high fold change in relation to the other conditions. Adenosine nucleotide alpha-hydrolase superfamily protein Gmet_2987 (Q39RC2) predicted to be involved in the biosynthesis of asparagine was highly expressed on ethanol in relation to all conditions except acetate plus benzoate. Moreover, ethanol induced higher abundance of nitrogenase iron protein subunit NifH (Q39XX0) relative to the benzoate condition. This protein is involved in biological nitrogen fixation (Bazylinski et al., 2000).

Butyrate induced two proteins from the TCA cycle: citrate synthase Cit1 (Q39WL2) and succinyl:acetate coenzyme A transferase Ach1 (Q39WL1). Moreover, oxidoreductase Gmet_0361 (Q39YS0) and a putative membrane protein Gmet_0705 (Q39XS7) were induced by butyrate as well.

Two proteins of energy metabolism, the nickel-dependent hydrogenase large subunit HyaL (Q39QD0) and a cytochrome c family protein CbcS-1 (Q39PV1) were highly abundant on toluene and less abundant on ethanol relative to all other conditions. These two proteins can be involved in the protection against oxidative stress. In *G. sulfurreducens,* an ortholog HyaL (95.9% identity) was shown to act as a protector against oxidative stress (Tremblay and Lovley, 2012) and CbcS-1 has a menaquinol oxidoreductase activity.

Cell envelope related flotillin band_7_stomatin-like domain protein Gmet_0814 (Q39XG8) with putative function of folding specificity was highly abundant on acetate relative to all conditions except for toluene. It was significantly abundant on toluene relative to acetate plus benzoate, butyrate, and ethanol.

ATPase, AAA_5 family Gmet_0108 (Q39ZG7) was highly abundant on benzoate and three times less abundant on toluene.

3.1.5 Differentially expressed catabolic pathways

Several catabolic pathways were found to be expressed on one growth condition although the respective substrates were not present (Figure 3-6).

The hypergeometric test was applied to all pairs of conditions in order to identify the set of catabolic pathways exhibiting a significant number of differentially expressed proteins. The analysis revealed simultaneous differential expression of several peripheral degradation

pathways with single substrates (Figure 3-6). For example, toluene, benzoate, and phenol-degrading pathways had higher abundances on toluene relative to acetate plus benzoate, acetate, and ethanol (Figure 3-6E); benzoate, propionate, and butyrate-degrading pathways had higher abundance on butyrate relative to acetate plus benzoate, acetate, ethanol (Figure 3-6C). However, not all pathways were differentially induced by one condition in relation to the other five growth conditions, e.g., proteins of fatty acid and phenol-degrading pathways were highly abundant on benzoate in relation to acetate and ethanol but not as compared to toluene, butyrate, and acetate plus benzoate (Figure 3-6B). Besides, expression of metabolic pathways on one substrate had a different order of expression in relation to another substrate. For example, benzoate degradation proteins had higher abundances on benzoate in relation to acetate and ethanol than in relation to butyrate (Figure 3-6B).

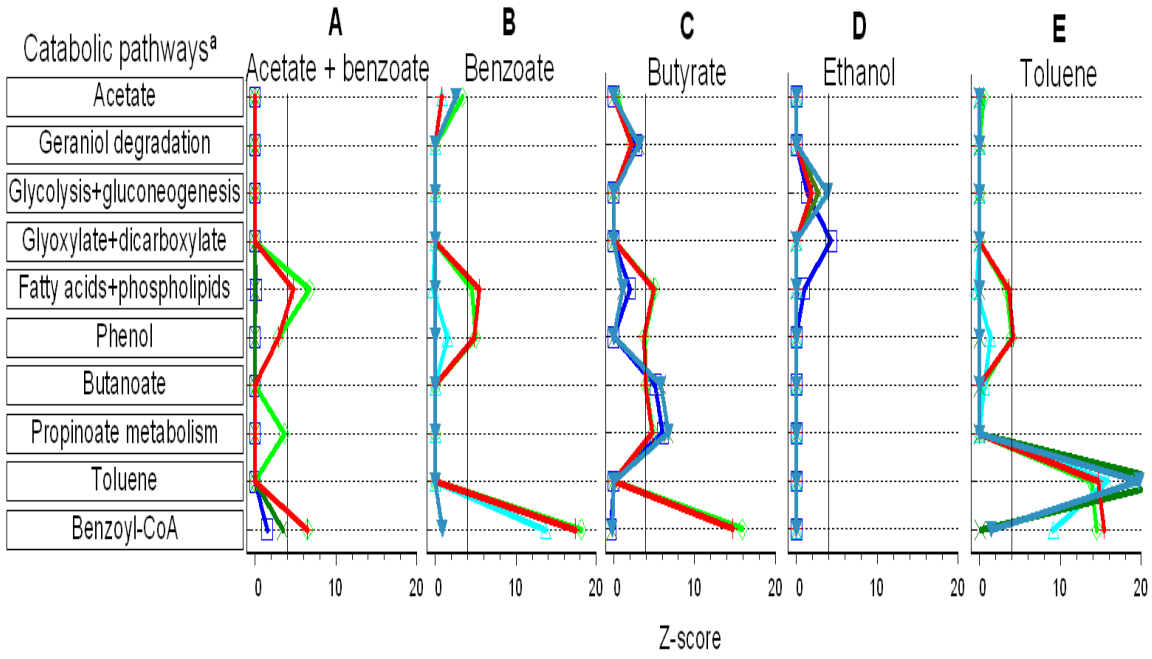

[a]Proteins taken for hypergeometric analysis were assigned to the respective pathway via the internet search tool DAVID.

Figure 3-6. Catabolic pathways found to be expressed on different growth conditions and representation of pairwise comparisons between the different growth conditions based on the metabolic pathways expressed. The x-axis represents the extend of relative expression of the catabolic pathways listed in the y-axis during the growth condition designated in the graph title (A-E) relative to another growth condition presented by the respective curve: acetate plus benzoate, acetate, benzoate, butyrate, toluene, ethanol. Pathways with z-scores > 4 (indicated by vertical solid line) are considered as significantly more abundant on one condition (A-E) relative to another (colored symbols). E.g., in panel A the lowest red circle indicates that the benzoyl-CoA pathway (depicted on the y-axis) is significantly higher expressed in the condition acetate plus benzoate (panel title) as compared to acetate. Z-scores of pairwise comparisons are given in Appendix, **Table 3**.

3.1.6 Regulatory proteins and carbon catabolite repression-related proteins

108 proteins with regulatory functions were detected, ten of which were differentially expressed across all conditions (Additional material, Table S5). Pairwise comparison revealed that six of them were found to be significantly abundant on one condition relative to another: sigma-54-dependent sensor transcriptional regulator with PAS sensor, Fis family protein Gmet_2055 (Q39TZ0) on benzoate relative to acetate and on toluene relative to acetate, Xre family regulator Gmet_3164 (Q39QU7) on benzoate relative to acetate plus benzoate, acetate, ethanol, and butyrate; CRISPR-associated protein Csd2 (Q39WR7) on acetate plus benzoate, acetate, benzoate, butyrate, and ethanol relative to toluene; response regulator receiver CheY-like Gmet_0762 (Q39XM0) on acetate relative to acetate plus benzoate and benzoate, as well as on butyrate and on toluene relative to acetate plus benzoate; IclR family regulator on acetate relative to benzoate and toluene Gmet_0741 (Q39XP1); S1 RNA-binding domain-containing transcriptional protein Tex (Q39Z96) on acetate plus benzoate, acetate, and benzoate relative to toluene and butyrate. A gene coding for sigma-54-dependent Gmet_2055 protein is located upstream of a gene coding for a succinyl:benzoate coenzyme A transferase which was highly abundant on benzoate, suggesting that this protein is positively regulated by Gmet_2055. The gene coding for IclR family like transcriptional regulator protein Gmet_0741 (Q39XP1) is located upstream of a solute:Na+ symporter (*aplA*) coding for a protein with acetate-permease activity AplA (Q39XP3). In contrast to growth with acetate and all other conditions tested, AplA is highly abundant on toluene (Table 7-4). The IclR regulator has lower abundance on toluene which might suggest a negative regulation of AplA by the IclR. The gene coding for Xre family regulator Gmet_3164 (Q39QU7) is located upstream of genes coding for two subunits of cytochrome c7 (*Gmet_3165* and *Gmet_3166*). However, the gene products of these subunits were not detected in our study.

Twenty-four PTS-like proteins were identified in the *G. metallireducens* genome. Eight gene products were found under all conditions and did not exhibit differential expression. However, Hpr^{Ntr} (Q39W50) and EIIA (Q39W51) were not detected on acetate plus benzoate.

3.1.7 Hierarchical regulation analysis of the TCA cycle

Clear effects of the substrates on growth rates and on expression of peripheral catabolic pathways was observed (Figure 3-5). Degradation of all carbon substrates studied here involves acetyl-CoA as a first central intermediate which enters the TCA cycle. Hierarchical regulation analysis (ter Kuile and Westerhoff, 2001) was employed to determine how changes

in flux through enzymes of the central TCA cycle are regulated as the result of growth on different substrates. Most of the calculated hierarchical coefficients (ρ_h) for enzymes of the TCA cycle were close to zero and/or had negative values (Table 3-2), revealing a dominant role for metabolic regulation (Rossell et al., 2005). The only exception was malate dehydrogenase with ρ_h = 0.9. Thus, changes in flux on the different growth substrates did not require substantial changes in the expression of TCA enzymes, but were mainly due to changes in concentrations of intracellular metabolites.

Table 3-2. Hierarchical regulation coefficients $\boldsymbol{\rho_h}$estimated for enzymes of the TCA cycle. $\boldsymbol{\rho_h}$ can take any value between -1 and 1. Standard errors were calculated between six growth conditions.

Enzyme	$\boldsymbol{\rho_h}$	Standard error
Citrate synthase	-0.13	0.56
Aconitase 1	-0.46	0.33
Aconitase 2	-1.01	0.30
Aconitate hydratase 2	0.22	0.35
Isocitrate dehydrogenase [NADP]	0.14	0.22
2-oxoglutarate dehydrogenase E1 component	-0.92	0.42
2-oxoglutarate ferredoxin oxidoreductase, alpha subunit	0.25	0.15
2-oxoglutarate ferredoxin oxidoreductase, beta subunit	-0.20	0.27
2-oxoglutarate ferredoxin oxidoreductase, gamma subunit	-0.33	0.33
Succinyl-CoA ligase [ADP-forming] subunit alpha	-1.05	1.32
Succinyl-CoA ligase [ADP-forming] subunit alpha	-0.08	0.38
Succinyl-CoA ligase [ADP-forming] subunit beta 1	-0.18	0.34
Succinate dehydrogenase subunit C	-0.61	0.20
Succinate dehydrogenase subunit A	-0.42	0.1
Succinate dehydrogenase subunit B	-0.30	0.23
Fumarase	-0.13	0.21
Malate dehydrogenase	0.90	0.56

3.2 Physiology of *G. metallireducens* during carbon limitation in retentostats

3.2.1 Cultivation in acetate limited retentostats

Acetate was used as an electron donor because it is a common product of fermentation in the natural environments (Lovley, 1997). During retentostat cultivation, acetate was not detected in the outflow (< 0.1mM; Figure 3-7C). However, the estimated Fe(II) concentration in the

filtrate was lower than the expected 40 mM (Figure 3-7C1 and Figure 3-7C2) that correspond to the complete consumption of 5 mM acetate according to the stoichiometric electron balance (Equation 2-14). For example, for the first replicate (run 1), 50% of the measurements had 60% of electron, while the second replicate (run 2) showed that 70% of measurements had 80% of electron recovery. Low Fe(II) concentrations might be due to the high electron flow into biomass or due to the Fe(II) precipitation in the reactor. Moreover, biofilm formation during the cultivation as well as accidental filter leakages produced the most likely wrong impression that the biomass was accumulating only until approximately 100 h and then declined (Figure 3-7A). The calculated biomass production rate based on acetate and Fe(II) concentrations in the filtrate ($r_x substrate(t)$) according to Equation 2-12 was much higher than the fitted biomass production rate estimated based on Equation 2-2 ($r_x(t)_{fit}$) due to the low values of the sampled Fe(II) which most likely precipitated. This means that the biomass production rate ($r_x substrate(t)$) according to Equation 2-12 could not be determined correctly and Equation 2-2 was used to estimate $r_x(t)_{fit}$ (Figure 3-7B).

Therefore, the growth rates μ (Equation 2-1) were estimated on the basis of the fitted biomass production rates ($r_x(t)_{fit}$) (Equation 2-2) and the fitted biomass ($x_{t\ fit}$) (Equation 2-10) with already published values of m_s and Y_{xsm} for carbon-limited *G. metallireducens* (Lin et al., 2009). The longest doubling times estimated were 292 h and 324 h for run 1 and run 2, respectively. In contrast, *G. metallireducens* grew 70 times faster in batch than in retentostats (see chapter 3.1).

3.2.2 Ability to use alternative substrates in acetate-limited retentostat

In order to identify the readiness of *G. metallireducens* to use alternative substrates at low growth rates, the cells from run 2 were harvested in the middle (100 h) and in the end (300 h) of the retentostat cultivation and subjected to substrate utilization tests. $NaNO_3$ was used as an electron acceptor to examine if *G. metallireducens* expressed active metabolic pathways. Produced NO_2^- was considered as an indicator for substrate consumption. Chloramphenicol treatment was used to check which enzymes were expressed in the cells by the time of harvesting from the acetate-limited retentostat. Previous attempts to adapt BIOLOG AN Microplates™ experiments (Ihssen and Egli, 2005) for cultivation of *G. metallireducens* failed due to its reactivity with the tetrazolium salt of BIOLOG plates even in the absence of the carbon substrate.

In the control tubes, the cells harvested after 100 h of cultivation in acetate limited-retentostat showed the highest NO_2^- production on butyrate, acetate and pyruvate relative to the blank

(Figure 3-8A). The chloramphenicol treated cells showed a similar pattern of NO_2^- production on butyrate and acetate with 73 (±33.5) µM and 85 (±5) µM of NO_2^- produced, respectively (Figure 3-8A).

Cells, which were harvested after 300 h of cultivation in the retentostat, contained iron precipitation because during the retentostat cultivation iron started to precipitate and accumulate in the reactor. As a consequence, the precipitates were carried over to the serum tubes. Therefore, besides produced NO_2^-, Fe(II) concentrations were also examined after 24 h of incubation in the serum tubes (Figure 3-8B and C). Analysis of NO_2^- production by cells taken from retentostat after 300 h of cultivation revealed similarly high concentration (in the range of 55-95 µM) in all chloramphenicol-amended tubes, including blank (Figure 3-8B). Fe(II) concentrations were similar in all chloramphenicol-treated experiments (Figure 3-8C). However, control experiments showed a different pattern, where some conditions (such as phenol, *p*-cresol, benzaldehyde, toluene, ethanol, and blank) induced higher production of Fe(II) (Figure 3-8B), while others (lactate, pyruvate, butyrate, benzoate, and acetate) induced consumption of NO_3^- (Figure 3-8B).

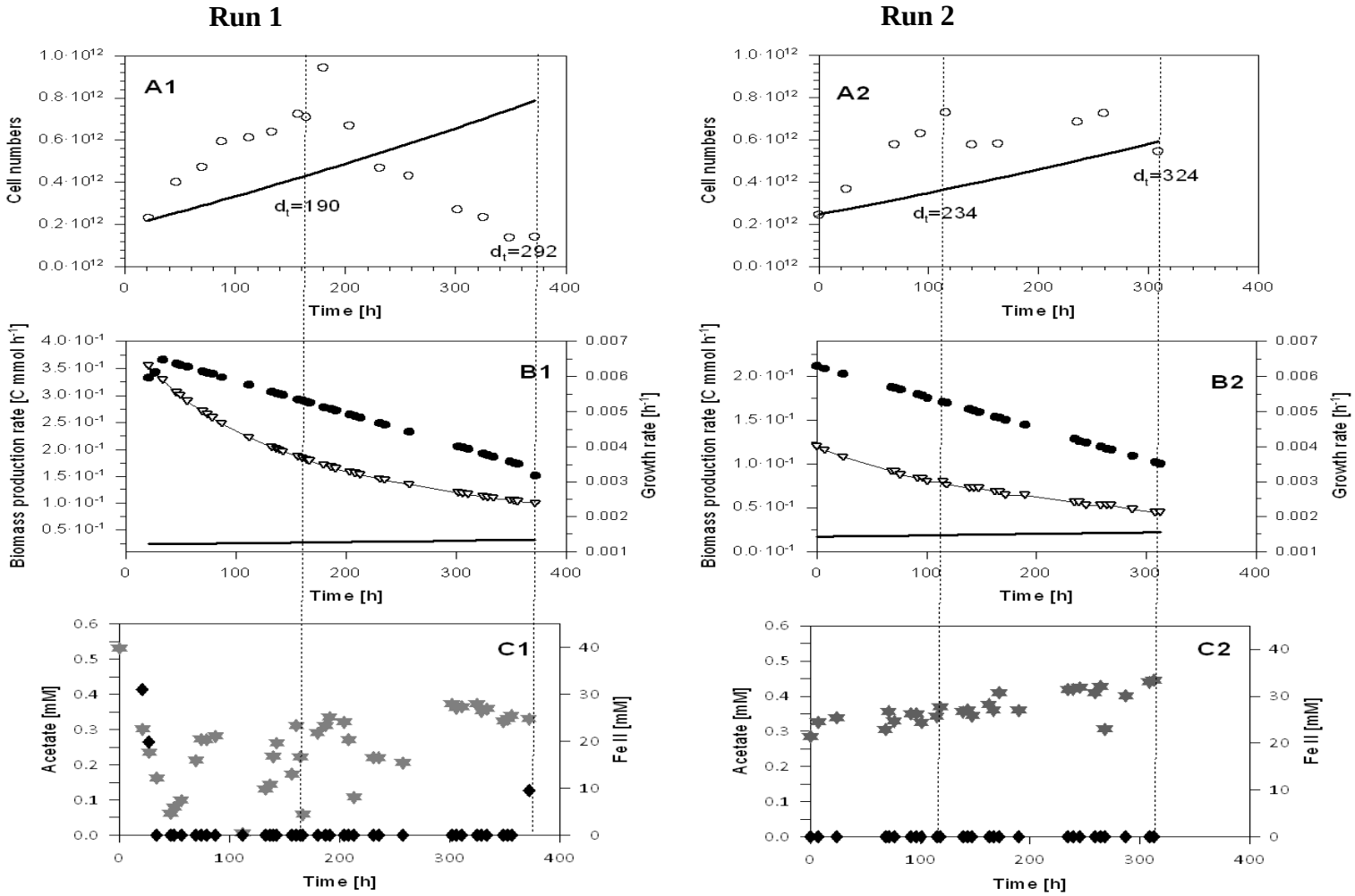

Figure 3-7 Growth of *G. metallireducens* in anoxic, acetate-limited retentostats (run 1 and run 2) with Fe(III)citrate as electron acceptor.

(A) Measured cell numbers (○) and fitted biomass *x(t)fit* (━) during retentostat cultivation. **(B)** Biomass production rate $r_{x(substrates)}(t)$ (●), growth rate μ (▽), fitted biomass production rate $r_x(t)_{fit}$ (━). **(C)** Fe(II) (☆) and acetate (◆) concentrations in the filtrate. Acetate detection limit was 0.1mM. (- - -) indicate the sampling points for proteomic analysis and the doubling times (d_t) during the sampling. The data used is given in Appendix, **Table 4**.

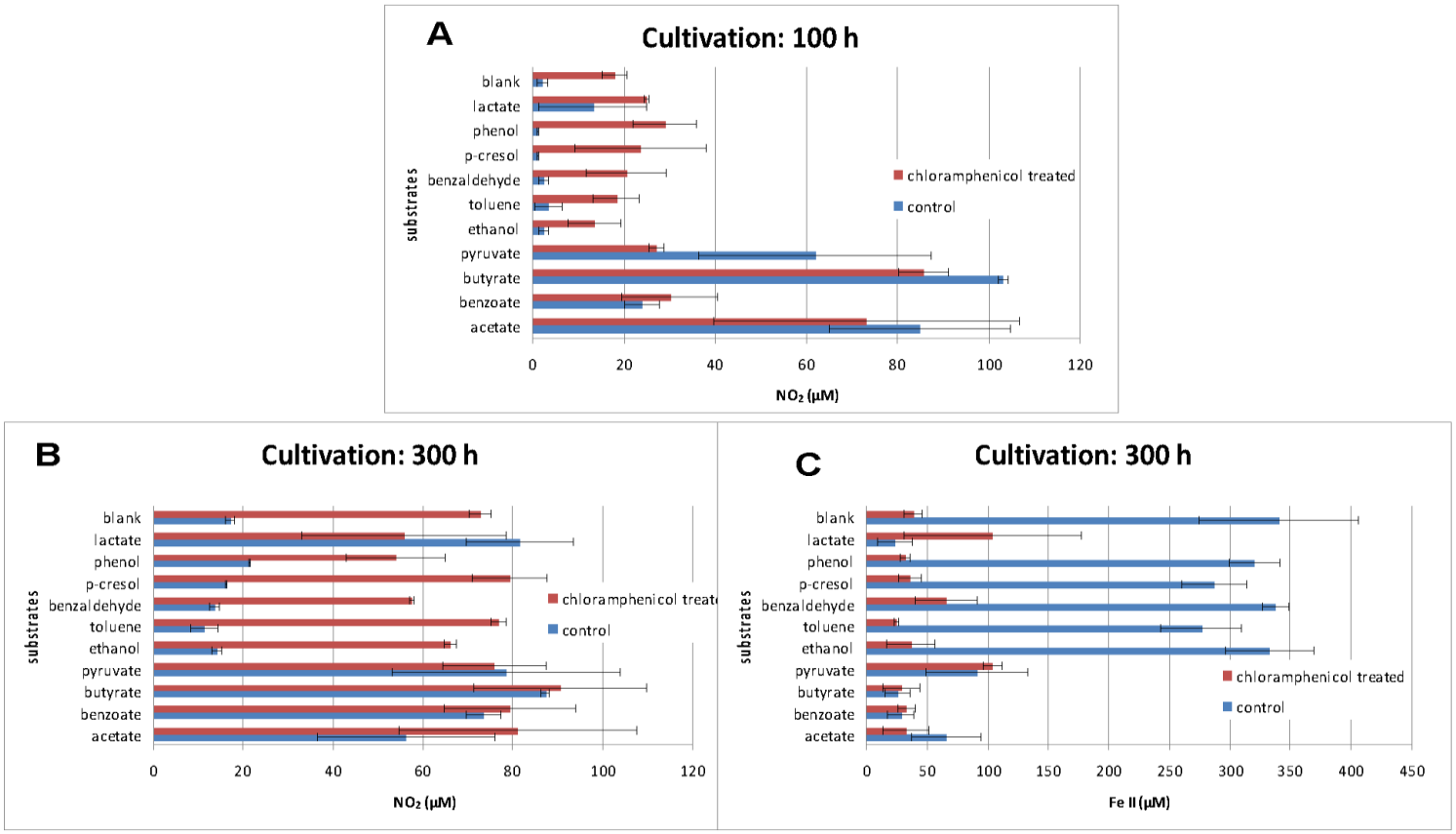

Figure 3-8

NO_2^- **(A, B)** and Fe(II) **(C)** production on various carbon sources by *G. metallireducens* sampled from acetate-limited retentostat (run 2) at different time points (after 100 h and 300 h of cultivation). The tubes were inoculated with either untreated or chloramphenicol inhibited cells.

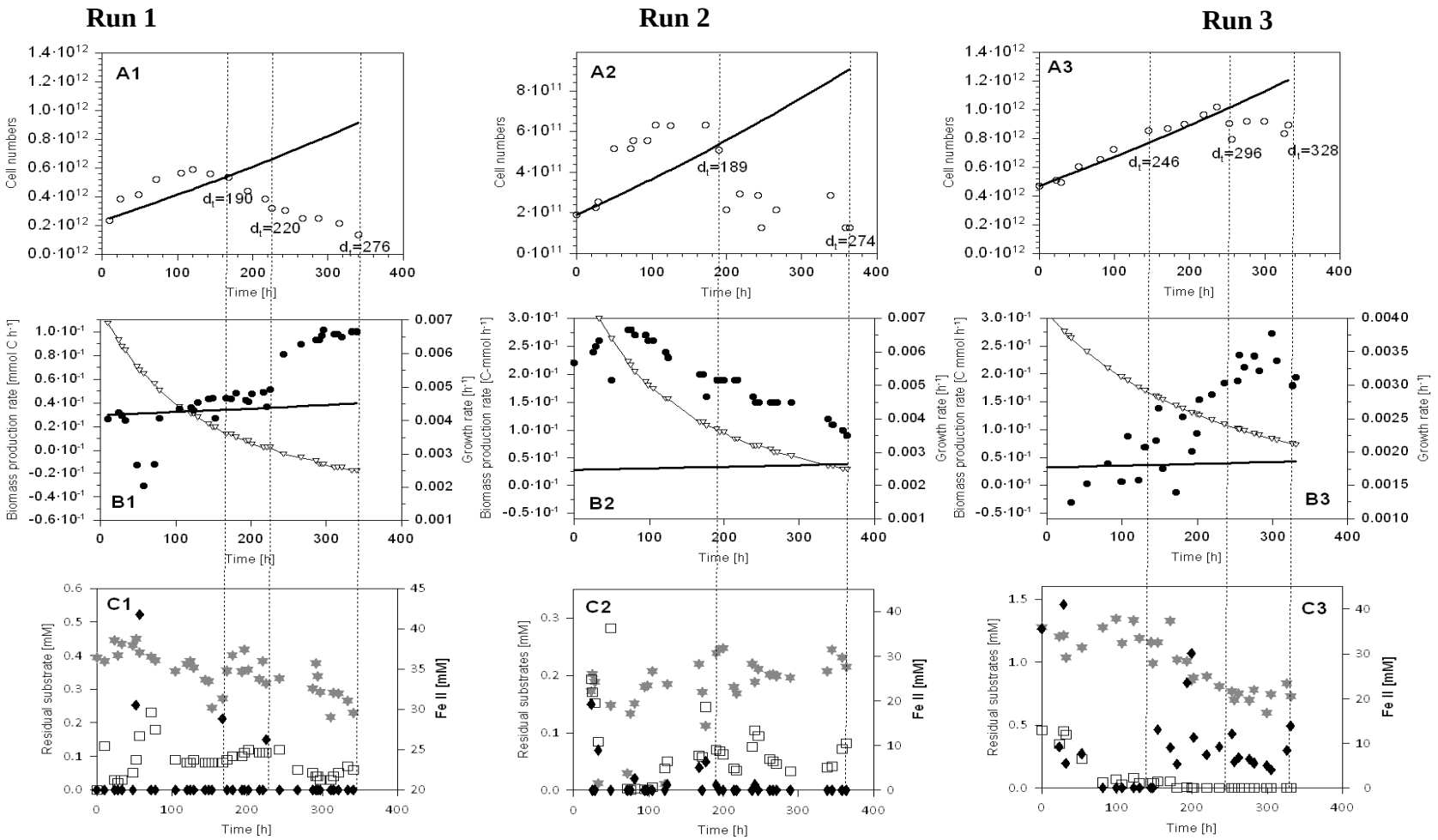

Figure 3-9. Growth of *G. metallireducens* in anoxic, acetate- and benzoate-limited retentostats (run 1, 2, and 3) with Fe(III)citrate as electron acceptor.

(A) Measured cell numbers (○) and fitted biomass *x(t)fit* (—) during retentostat cultivation. **(B)** Biomass production rate $r_{x(substrates)}(t)$ (●), growth rate μ (▽), fitted biomass production rate $r_x(t)_{fit}$ (—). **(C)** Fe(II) (☆) and acetate (◆), and (□) benzoate concentrations in the filtrate. Acetate detection limit was 0.1mM, benzoate detection limit was 20 µM limit was 20 µM. (- - -) indicates the sampling points for proteomic analysis and the doubling times (d_t) during the sampling.

The data used is given in Appendix, **Table 5**.

3.2.3 Cultivation of *G. metallireducens* in retentostats with two substrates (acetate plus benzoate)

In order to investigate if *G. metallireducens* is able to degrade two substrates at low growth rates simultaneously, benzoate and acetate were supplied at a constant rate (50 ml h^{-1}) to the reactor. Acetate (2.5 mM) and benzoate (0.7 mM) were supplied in approximately equal carbon content: 5 mM carbon and 4.9 mM carbon, respectively.

Two replicates (run 1 and run 2) showed similar patterns for substrate consumption in the medium: acetate was always below detection limit and the residual benzoate concentrations were in the range of 0.1 mM (Figure 3-9C1 and C2). *G. metallireducens* showed different behaviour in run 3 (Figure 3-9C3) where after 150 h of cultivation, the benzoate concentration decreased below detection limit (< 20 µM) and the residual acetate concentration increased up to 0.5 mM. However, the residual carbon concentrations were approximately similar in run 1 and 2 (0.7 mM) and run 3 (1 mM).

Fe precipitation and growth of biofilms on the walls of the reactor took place in the retentostat runs 1 and 2, resulting in a decrease of the dispensed cell numbers (Figure 3-9A and B). Run 3 showed good fitting of the counted cells to the simulated cell numbers. As for the acetate-limited retentostats, estimation of the growth rates was done based on $r_x(t)_{fit}$. The estimated lowest growth rates (Figure 3-9B) were similar for the run 1 and the run 2 with corresponding doubling times of 276 h (Figure 3-9A1) and 275 h (Figure 3-9A2), respectively. The highest doubling time (which corresponds to the lowest growth rate) for the run 3 was slightly higher (328 h) (Figure 3-9A3).

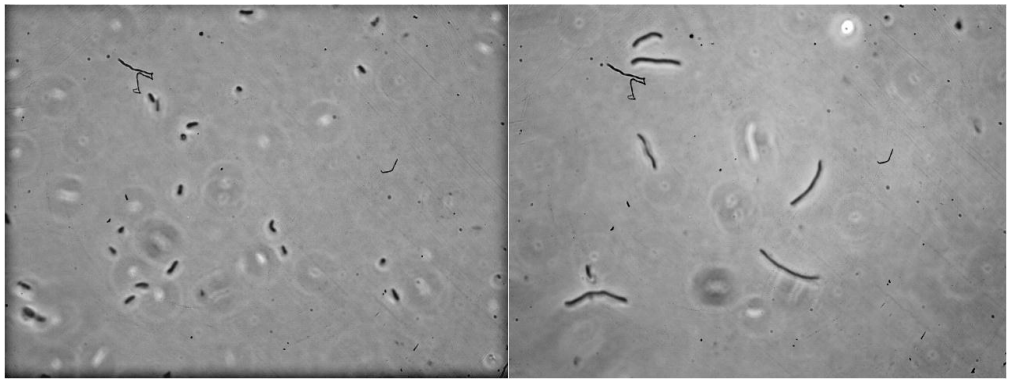

A **B**

Figure 3-10. Light microscopy photograph of *G. metallireducens* cultivated in acetate and benzoate limited retentostat at 50 h (A) and 300h (B) of cultivation.

Examination of cells with light microscopy revealed different morphologies in the beginning and in the end of cultivation in the retentostats with acetate plus benzoate (Figure 3-10). At low growth rates cells did not separate well resulting in elongated morphology.

Control of culture purity during the continuous cultivation in the retentostats did not show presence of any contamination (Figure 7-1 in Supplementary material).

3.2.4 Comparison of protein profiles across all conditions examined

Statistical analysis revealed 163 differentially expressed proteins with a false discovery rate (FDR) < 5% across all conditions and all sampling points examined (batch and retentostats with single and double carbon sources) (Additional material, Table S6). Pairwise comparisons showed that the major contribution to the differential expression of proteins was by enzymes related to benzoate degradation during the cultivation with acetate plus benzoate relative to the conditions with single substrate acetate. For example, nine proteins of benzoate degradation (five subunits of benzoyl-CoA reductase: BamF, BamC, BamE, BamH, and BamD; electron transfer proteins BamP, proteins of modified β-oxidation: BamQ, BamR and protein of lower pathway HbdA), four proteins annotated to fatty acids metabolism (BamM, BamN, Act and Adh) and one protein related to phenol degradation (BamO) had significantly lower abundances in retentostats with acetate as a single carbon source relative to retentostats where two substrates were used (Additional material, Table S6). Except for differences in abundances of the proteins related to benzoate degradation, the protein profiles expressed during cultivation of *G. metallireducens* in the retentostats with acetate or acetate plus benzoate were similar.

Furthermore, comparison of protein profiles across all conditions did not reveal major differences in physiological response to decreasing growth rates during retentostat cultivation (data not shown).

3.2.5 Comparison of protein profiles expressed at high (batch) and low (retentostat) growth rates within one growth condition (acetate or acetate plus benzoate)

In order to distinguish influence of growth rate on the physiology of *G. metallireducens*, protein profiles expressed at high and low growth rates were analysed for each growth substrate (acetate or acetate plus benzoate) separately. One-way ANOVA analysis of proteins expressed within each growth condition revealed 129 differentially expressed proteins with false discovery rate (FDR) < 2% on acetate (Table 7-5 in Supplementary material) and 118

proteins with false discovery rate (FDR) < 2% on acetate plus benzoate (Table 7-6 in Supplementary material). 39 proteins were detected to be differentially expressed on both growth conditions (acetate and acetate plus benzoate) (Table 3-3).

Table 3-3. Fold change of abundances of selected proteins[a] at different sampling times during retentostat cultivation with acetate and acetate plus benzoate[b]

ID	Annotation	Gene name	$^{A}t_0/^{A}b$	$^{A}t_1/^{A}b$	$^{A}t_2/^{A}b$	$^{AB}t_0/^{Ab}b$	$^{AB}t_1/^{AB}b$	$^{AB}t_2/^{AB}b$	$^{AB}t_3/^{AB}b$
Alcohols degradation									
Q39WT9	Aldehyde:ferredoxin oxidoreductase, tungsten-containing	aorA	126	456	368	132	1441	1468	1517
Q39WT8	Ethanol dehydrogenase, putative	Gmet_1046	167	118	629	528	774	428	262.8
Amino acid biosynthesis									
Q39RJ5*	Oxidoreductase, flavin-binding protein	Gmet_2911		18	1.4				
Q39V41	Efflux pump, RND family, inner membrane protein	Gmet_1652	5.4	12.1	18.6	12.3	21.6	47.8	23.7
Biosynthesis and degradation of polysaccharides									
Q39QV2	Alpha-glucan phosphorylase	Gmet_3159	4.3	17.2	10.8	3.2	6	7.3	3.9
Q39XE9	Alpha-amylase family protein	Gmet_0833	3.5	35.6	32.7	5.3	33.2	46.3	36
Biosynthesis of cofactors									
Q39RX2	BioD and DRTGG domain protein	Gmet_2784	9.1	26.9	39.7	2	12.8	29.5	14.5
Cell envelope									
Q39ZH8	Uncharacterized protein	Gmet_0097	0	0	0	0.4	0	0.3	0.3
Q39PY3	Lipoprotein, putative	Gmet_3486	0	0	0.1	0	0	0	0.1
Q39X72	Lipoprotein cytochrome c	Gmet_0910	12.4	32.1	23.2	8.9	78.3	232.8	280.8
Central intermediary metabolism									
Q39X36	N-acetylglutamate synthase	argA	0	0	0	0	0	0	0
Chemotaxis and motility									
Q39Z19	Twitching motility pilus retraction ATPase	pilT-2	4.5	5.7	5.2	3	4.5	8.3	4.3
Q39SS1	Methyl-accepting chemotaxis sensory transducer	mcp64H-2	8.6	11.6	30.3	8.1	12.1	16.1	18.8
TCA cycle									
Q39XG6	Pyruvate carboxylase	pyc	36	22.3	23.4	10.5	7.3	10.9	11.5
Q39WW6	Aconitate hydratase 1	acnA	33	95.3	52.7	10.6	44.6	87.8	389
Detoxification									
Q39XJ8	Organic solvent tolerance ABC transporter	Gmet_0784	0.7	0.2	0.1	0.9	0.2	0.1	0.1
Electron transport									
Q39UY1	Electron transfer flavoprotein, alpha subunit	etfA-7	0	0	0	0	0	0	0
Glyoxylate and dicarboxylate metabolism									
Q39S61	Hydroxypyruvate reductase, putative	hprA	2.4	18	19.5	3.5	12.2	17.3	13.3
Nucleotide biosynthesis									
Q39UH0	Non-canonical purine NTP pyrophosphatase	rdgB	0	0	0	0	0	0	0
Oxidative phosphorilation									
Q39QA3	ATP synthase subunit a	atpB	0	0	0.2	0.1	0	0	0.2

ID	Annotation	Gene name	$^{A}t_0/^{A}b$	$^{A}t_1/^{A}b$	$^{A}t_2/^{A}b$	$^{AB}t_0/^{Ab}b$	$^{AB}t_1/^{AB}b$	$^{AB}t_2/^{AB}b$	$^{AB}t_3/^{AB}b$
Q39QW7	NAD-dependent nucleoside diphosphate epimerase/dehydratase	Gmet_3144	3.8	8.9	6.2	5.4	8.9	12.6	6.2
Protein folding and stabilization									
Q39UM8	Peptidylprolyl cis-trans isomerase, PpiC-type	Gmet_1817	0	0	0	36.1	14.5	13.9	5.4
Protein synthesis									
Q39UK8	Translation initiation factor IF-1	infA	0	0.1	0	0.1	0	0.1	0
Q39U60	Elongation factor G 2	fusA-1	4.7	10.3	5.6	5.8	28.3	33.2	14.7
Q39VS9	Threonine--tRNA ligase	thrS	3.8	5.9	10.2	2.3	8.4	7.1	6.7
Regulatory functions									
Q39WN1	Transcription elongation factor GreA 1	greA1	0	0	0	0	0.1	0	0.1
Transcription									
Q39Y13	DNA-directed RNA polymerase subunit beta	rpoB	21.5	6.7	8.2	13	4.6	5.9	4.1
Q39Y12	DNA-directed RNA polymerase subunit beta	rpoC	21.2	8.3	9.7	12.3	4.4	5.9	4.5
Transport and binding proteins									
Q39VE3	Metal ion efflux pump, RND family, inner membrane protein	cusA	5.8	11.7	13	3.5	21.8	35.9	23.4
Q39VE2	Metal ion efflux pump, RND family, membrane fusion protein	cusB	7.4	25.1	21.7	5.7	85.5	101.3	52.2
Q39R73	ABC transporter, membrane protein	macB	8.6	35.9	49.2	9.9	87.4	184.2	98.3
Signal transduction									
Q39ZR5	Sensor histidine kinase, HAMP and PAS domain-containing	Gmet_0009	0	0	0	0	0	0	0
Unknown function									
Q39XS8	Uncharacterized protein	Gmet_0704	0	0	0	0.3	14.9	0	14.5
Q39X68	Uncharacterized protein	Gmet_0914	0.1	0.1	0	0	0	0	0
Q39T38	Uncharacterized protein	Gmet_2361	0.3	0.1	0	0.5	0.1	0	0.5
Q39Q16	Periplasmic protein YceI	Gmet_3449	0.5	0	0.1	0.2	0	0	0
Q39WC8	Peptidase, putative	Gmet_1209	3.9	5.6	3.1	11	6.9	8.2	5.3
Q39ZP4	Protein serine/threonine kinase PrkA	prkA	5	13.4	6.4	7.5	27.4	77.4	33
Q39RS7	DUF748 repeat protein	Gmet_2829	20.7	24.2	33.6	9.8	9	11.7	18.3

[a]Proteins with FDR < 2% differentially expressed in both conditions are presented. [b]Average of protein abundances expressed at t_x during retentostat cultivation were divided by average of protein abundance at exponential growth phase of corresponding condition. t_o,t_1,t_2,t_3 – sampling times during retentostat cultivation (see Figure 3-7 and Figure 3-9). Differentially expressed proteins relative to exponential growth phase (with FRD <5% derived from pairwise comparisons) are highlighted.

3.2.6 Growth rate specific functional groups of proteins: proteins detected only at high growth rates or low growth rates

The number of proteins detected at high and low growth rates only was approximately equal: 194 and 266 proteins, respectively. These proteins showed similar functional distribution at

and low growth rates (Figure 3-11, Additional material, Table S7). However, at high growth rates proteins had an additional functional group of cell division. Such functional groups as DNA metabolism and carbohydrate metabolism plus xenobiotics degradation (8% and 14% of proteins from overall detected only at high growth rates, respectively) were more abundant at high growth rates than at low growth rates. In contrast to high growth rates, low growth rates related proteins had a higher fraction of proteins with unknown function (32% vs. 26%), electron transport (13% vs. 8%), chemoxatis and motility (3% vs. 0.5%), and signal transduction (7% vs. 3%).

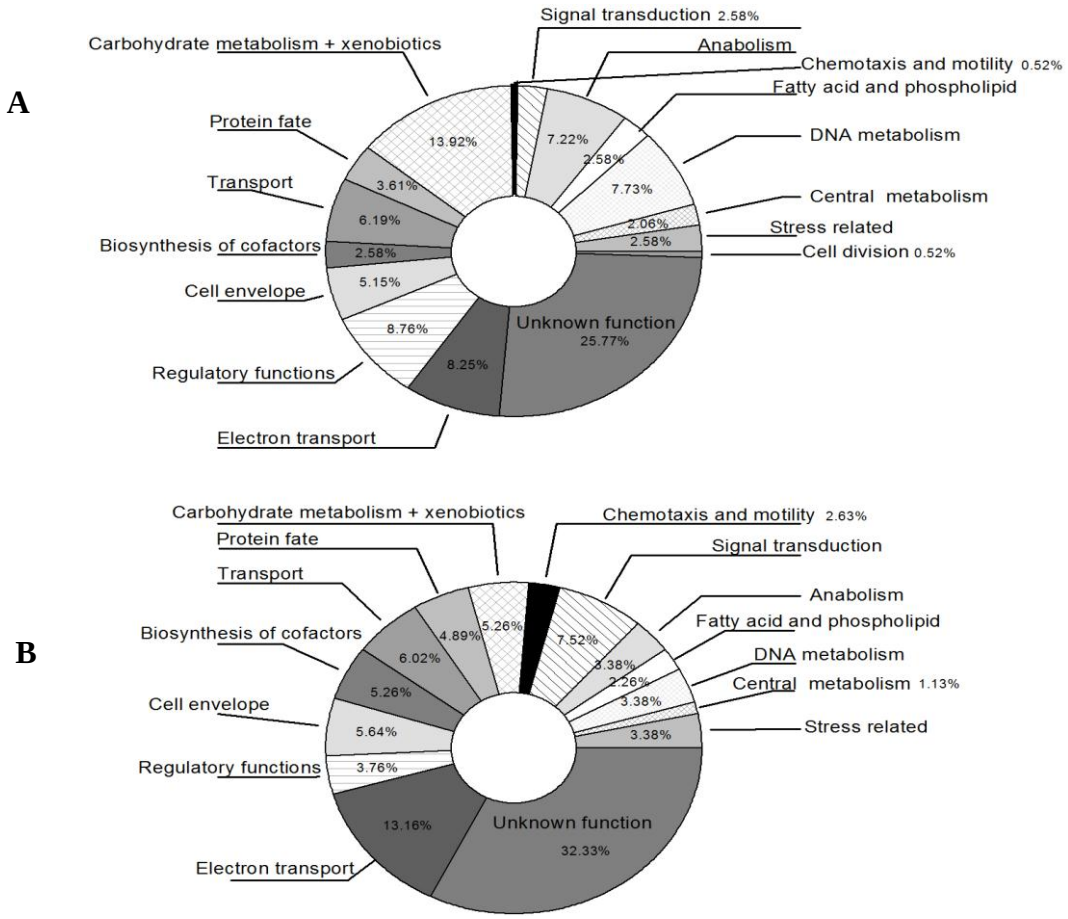

Figure 3-11 Qualitative functional distribution of proteins detected only at high growth rate during exponential phase in batch (A) or only at low growth rate in retentostats (B). Proteins detected at least in one condition or sampling point were considered as expressed at corresponding growth rate. For further details see Additional material, Table S7.

3.2.7 Catabolic pathways at low vs. high growth rates

Low growth rates increased abundances or induced formation of various catabolic proteins, related to peripheral catabolic pathways such as degradation of alcohols, aliphatic acids

(acetate, pyruvate, butyrate), aromatic hydrocarbons (*p*-cresol and *p*-hydroxybutyrate, benzoate) and fatty acids (Figure 3-12). The general feature in expression of significantly abundant catabolic proteins can be noticed: several proteins of the upstream reactions of peripheral catabolic pathways were newly formed or more abundant at low growth rates while the proteins from downstream reactions had decreased abundances at low growth rates in the retentostats or were only detected at exponential growth phase in batch (Figure 3-12). However, it is important to mention that the proteins involved in degradation of toluene were detected at high growth rates only (Figure 3-12).

The peripheral proteins of such catabolic pathways as ethanol, butyrate, and aromatic compounds degradation (except toluene) were abundant at low growth rates despite the absence of respective substrates in the medium. The highest fold change (up to 1468,8) at low relative to high growth rates was observed for two proteins of alcohol degradation such as the iron-containing putative ethanol dehydrogenase (Gmet_1046) and the tungsten-containing aldehyde ferredoxin oxidoreductase (AorA) (Table 3-3). Another two alcohol dehydrogenases (iron- (Gmet_1053) and zinc-containing (Gmet_0231)) were found at low growth rates only. Phosphate butyryltransferase (Ptb) which carries out the phosphorylation of butanoyl-CoA had also significantly increased abundance on acetate at low growth rates (28.3 fold change at t_1 relative to exponential growth phase). However, the acyl-CoA--carboxylate coenzyme A transferase (Gmet_1709 and Gmet_1708) which carries out downstream reaction in butyrate metabolism was detected at high growth rates only.

Moreover, enzymes of redundant reactions of acetate and pyruvate metabolism in *Geobactereaceae* (Segura et al., 2008; Sun et al., 2009) changed their abundances in the response to low growth rates. Among them are proteins of first step of acetate degradation. Thus, the acetate kinase (AckA) had significantly increased abundances at low growth rates in acetate-limiting chemostats relative to batch and ATP-consuming acetate--coenzyme A ligase (AcsA) was detected only in the retentostats (Additional material, Table S7). Three enzymes of the first steps of pyruvate degradation also were found to be low growth rates-specific: PEP-forming phosphoenolpyruvate synthase (PpsA) and acetyl-CoA-synthesizing E1 component of pyruvate dehydrogenase (BkdB) were detected at low growth rates only (Additional material, Table S7), while ATP-consuming pyruvate carboxylase Pyc had significantly increased abundances on the acetate and acetate plus benzoate-limiting conditions relative to batch (Table 3-3). It is important to mention that pyruvate ferredoxin oxidoreductase (Por) was also found to be more abundant during low growth rates relative to

batch in the acetate-limited retentostats (Additional material, Table S8). However, its false discovery rate (FDR=3.1) was slightly higher than the accepted threshold of FDR = 2.

As expected, during growth in retentostats with acetate plus benzoate, *G. metallireducens* expressed proteins of benzoate degradation pathway. Most of them did not exhibit differential expression relative to batch, except for significantly decreased abundances of the IclR family regulating protein (Gmet_2064) and the ABC transporter (LolD-2). Moreover, out of two proteins expected to be involved in the benzoate activation, the benzoate-CoA ligase (BamY) and the succinyl:benzoate coenzyme A transferase (Gmet_2054) (Oberender et al., 2012), only the Gmet_2054 which is an ATP-independent enzyme in contrast to BamY was detected in retentostats with acetate plus benzoate. As has been mentioned in the chapter 3.1 "Physiology of *G. metallireducens* at high substrate concentrations in batch", BamY was detected in batch experiments with benzoate, however, its expression was not significant relative to other carbon sources tested in batch. Notably, during cultivation on single substrate acetate, one protein from upstream reaction of benzoate degradation, subunit of benzoyl-CoA reductase (BamB-2) had increased abundances at t_1 and t_2 relative to batch. Several proteins which are involved in degradation of *p*-cresol and *p*-hydroxybenzoate degradation (Gmet_2141, PcmQ), and phenol degradation (Gmet_2102) were detected at low growth rates only in retentostats with acetate plus benzoate (Additional material, Table S7). Moreover, two proteins from the downstream reactions of fatty acids, butyrate, and benzoate degradation (3-hydroxyacyl-CoA dehydrogenase (Gmet_1717), thiolase (Gmet_0144)), were detected at low growth rates only (Additional material, Table S7) while the methylmalonyl-CoA epimerase (MceE) involved in succinyl-CoA formation from odd fatty acids had significantly high abundance on acetate plus benzoate in the retentostats relative to batch (Table 7-6). Meanwhile, proteins annotated to toluene degradation were not detected at low growth rates.

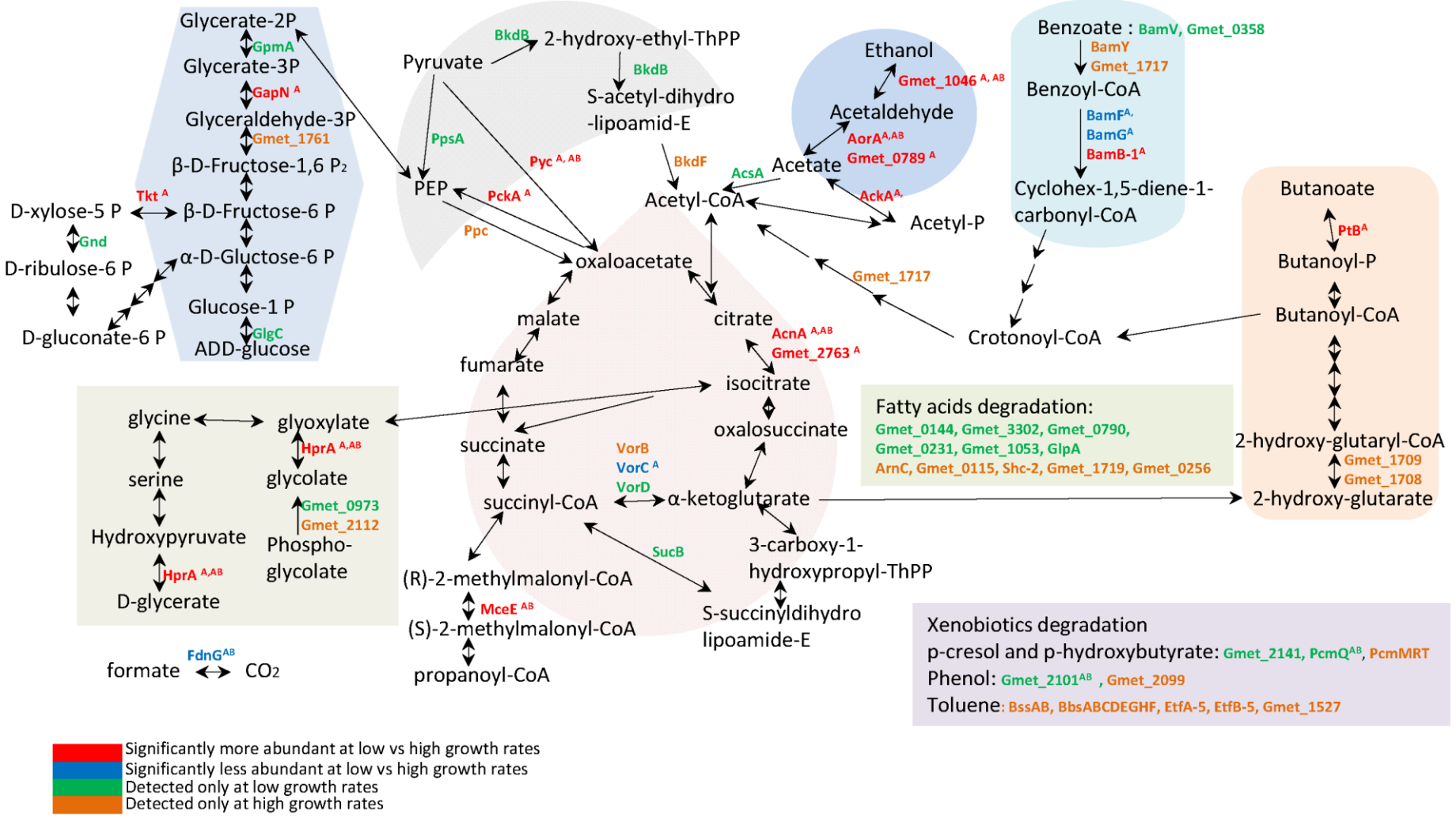

Figure 3-12. Selected catabolic proteins with differential abundances at low vs. high growth rates. Selected proteins are catabolic proteins identified by ANOVA as differentially expressed with FDR < 2 % (marked with *) and proteins detected only at low growth rates. Batch – proteins expressed at high growth rates during exponential phase in batch; R – proteins expressed at low growth rates in retentostat. A – acetate condition, AB – acetate plus benzoate condition. t_0, t_1, t_2, t_3 – time points of sampling at appropriate conditions, see Figure 3-7 and Figure 3-9.

3.2.8 Proteins of central metabolism

Eventually, all catabolic pathways coincide at the level of acetyl-CoA which enters the tricarboxylic (TCA) cycle. Few proteins from the TCA cycle had increased abundances or were detected at low growth rates only (two homologous aconitate hydratases (AcnA and Gmet_2763), enzyme 2 of 2-oxoglutorate dehydrogenase complex (SucB) and subunit D of 2-oxoglutarate ferredoxin oxidoreducatse (VorD)) (Figure 3-12). Other two subunits of 2-oxoglutarate dehydrogenase (VorB and VorC) were found at exponential phase only or had decreased abundances at low growth rates (Figure 3-12).

Two proteins of anapleurotic reactions, that provide TCA cycle with oxaloacetate, such as the already mentioned pyruvate carboxylase (Pyc) and the phosphoenolpyruvate carboxylase (Ppc) had different behaviour in response to low growth rates: Pyc increased its abundance at low growth rates, while Ppc was detected at high growth rates only (Figure 3-12).

Although, glyoxylate shunt was found not to be present in *G. metallireducens* (Tang et al., 2007). For example, the hydroxypuryvate reductase (HprA) which can be involved in both glyoxylate reduction and glycerate dehydrogenation had significantly increased abundances in the acetate- and acetate plus benzoate-limited retentostats (Figure 3-12; Table 3-3).

G. metallireducens is not able to use sugars; therefore it encodes gluconeogenesis in order to synthesize metabolites required for cell wall compounds as well as for nucleic acids biosynthesis. Several proteins of gluconeogenesis increased their abundances in response to slow growth rates or were detected only in the retentostats (e.g., PckA, GmpA, GapN) (Figure 3-6).

3.2.9 Change in abundances of other functional groups of enzymes in response to low growth rates

Besides catabolic proteins, the most distinguished response to low growth rates was observed for enzymes related to such functions as chemotaxis and motility, electron transfer, signal transduction and regulation, transport, and stress response.

The functional group of chemotaxis and motility was more abundant at low growth rates than at high growth rates (Figure 3-11). The proteins of this group are methyl-accepting chemotaxis proteins (e.g., Mcp40H-4, Mcp40H-6, Mcp64H-2), flagella- (e.g., FliL and FliC) and pili-associated (e.g., PilT-2).

The number of proteins involved in energy metabolism was also increased at low growth rates (Figure 3-11). The electron transferring proteins which were detected at low growth rates only or had increased abundances at low growth rates relative to batch were the nitrate reductases (e.g,, NarG-2 and NarH-2), dehydrogenases (Gmet_1728), nickel-dependent hydrogenases (HyaL and HyaB), and various cytochromes (e.g., CccA, OmcN, OmcP, OmcO, CydA) (Additional material, Table S7). Glu/Leu/Phe/Val dehydrogenase (Gmet_1728) is predicted to carry out ammonium assimilation via NADH and 2-oxoglutarate. It is worth to mention that HyaL had increased abundance in batch on toluene (see chapter 3.1) while HyaB was suggested to be involved in protection against oxidative stress (Tremblay and Lovley, 2012). Cytochrome CydA might be also involved in response to oxidative stress and is annotated to be related to aerobic respiration (Muller and Webster, 1997). The other electron transferring proteins related to oxynogenic conditions were three aerobic-type carbon monoxide dehydrogenases (Gmet_3490, Gmet_0838, and Gmet_0837), rubredoxin reductase selenocysteine-containing protein (Gmet_1148), protein with putative peroxidase activity, methylamine utilization protein (MauG), and thioredoxin protein (Trx-2). Electron transferring proteins with decreased abundances in retentostats relative to batch or absent at low growth rates are related to nitrogen fixation (e.g., nitrogenases (NifK and NifH), electron flavotransfer proteins, alpha and beta subunits (EtfA-7, EtfB-7**,** EtfB-2)), nitrate reduction (delta subunit of nitrate reductase chaperone (NarJ) and putative nitroreductase (Gmet_3446), and NADH-quinone oxidoreductase subunit C (NuoC)).

The majority of signal transduction proteins detected at low growth rates only belong to histidine kinases with HATPase_c domain, response receivers with REC domain, or hybrid histidine kinases containing both HATPase_c and REC domains. The encoding genes of these proteins are located in the distinct regions on the chromosome and their role should be elucidated. Two proteins that might be related to production of messenger molecule cyclic-di-GMP which plays a role in biofilm formation (Liu et al., 2012) as well as cell adhesion to Fe(III) oxide associate protein (Gmet_0556) (Smith et al., 2012) were also detected at low growth rates only (Additional material, Table S7). In contrast, two other proteins of signal transduction containing PAS domain (Gmet_1917 and Gmet_0009) had decreased abundances in retentostats relative to batch (Table 3-3).

Most of the regulating proteins that were detected at low growth rates only are related to transcription. Nitrogen regulatory protein P-II (GlnK), a modulator of glutamine synthase (Jiang et al., 1998) which scavenges ammonium under ammonium-limiting conditions

(Senior, 1975) was detected at low growth rates only and had significantly higher abundances at t_1 and t_3 relative to t_0 in retentostats with acetate plus benzoate (Table 7-6). The decreased abundances in retentostats relative to exponential growth phase were observed for the biosynthesis-related enzyme GreA1 at two growth conditions (Table 3-3) and for the PTS-related protein HPrNtr (ptsH) in the acetate-limited retentostats (Table 7-5) while in the batch with acetate plus benzoate this protein was not detected. Another important regulating protein, GTPase (ObgE), which is an essential growth regulator (Patel et al., 2009) was significantly higher in abundance in the acetate-limited retentostat at t_2 relative to batch (Table 7-5).

Some transporting efflux proteins were significantly more abundant at low growth rates, such as Cu(I)/Ag(I) efflux proteins (CusB and CusA) and probable macrolide-specific efflux proteins (MacA and two homologous MacB) (Table 7-5 and Table 7-6) which have 45.1% and 64%, 48% similarity to antibiotic-resistant enzymes MacA and MacB of *E. coli* K-12. The transporting proteins detected at low growth rates only are related to the transport of metals (e.g, transport of Mg/Co/Ni (CorA-2), Mn(II)/Zinc(II), (ZurA), Fe/Zn/Ni/Co/Cd (FieF)), ammonium (AmtB), amino acids, peptides, and carbohydrates (LivG, Gmet_1234, YibQ), cations and iron carrying compounds (Gmet_3258 and Gmet_1314) as well as to the transport of unknown compounds (ABC transporters (Gmet_1552, Gmet_2479, and Gmet_1553)) (Additional material, Table S7). In contrast, transporting proteins detected at high growth rates only belong to a transport of different compounds: phosphate (e.g., PstS, PstB, PhoU), vitamin B12 (Gmet_2735), potassium (Gmet_0063), lipids (MsbA).

Several proteins associated with stress conditions were found to be low growth rates-specific (universal stress protein (Usp), putative antibiotic biosynthesis protein (Gmet_1011), toxin production protein (Gmet_A3569), antitoxin proteins (Gmet_2534, Gmet_0678, Gmet_1321), and carbon starvation protein (CstA-2) (Table 7-5, Table 7-6 and Additional material, Table S7). It is important to mention that, although RelA protein related to stringent response under nutrient deprivation in *G. sulfurreducens* which has 95.8% similarity to *G. metallireducens* was not detected with our approach, the general behaviour of *G. metallireducens* at low growth rates was similar to the predicted behaviour of *G. sulfurreducens* during stringent response (DiDonato et al., 2006).

3.3 Cultivation of *G. metallireducens* in the indoor aquifer (mesocosm experiment)

The aim of the mesocosm experiment was to investigate physiology of *G. metallireducens* under natural conditions and compare it to its physiological behaviour exhibited at low growth rates in retentostats and during exponential growth phase in batch.

The oxygen concentrations were monitored in order to examine establishment of anoxic conditions in the cartridges (Figure 2-1). Oxygen concentration was high (above 4 mg/l) in the upper part of cartridges A and B (at height of 40 cm) during the whole incubation time (Figure 3-13 and Figure 3-14). In all other sampling points (below 40 cm height), the oxygen concentration started to decrease after 5 days of incubation and at 31 days reached low levels (below 0.01 mg/l) (Figure 3-13 and Figure 3-14) except for the sampling point at 20 cm height in cartridge B (Figure 3-13), where oxygen concentration was decreasing slower and reached low level 5 days later. Therefore, anoxic conditions were maintained in both cartridges at height of 30, 20, and 10 cm after 31 days of incubation. However, the oxygen concentration started to increase in the cartridge A after 53 days of incubation at the height of 10 cm (Figure 3-12). Thus, the experiment was stopped after 77 days of incubation in order to prevent further distribution of oxygen to the upper parts of cartridge A. Toluene was sampled 31, 47, and 76 days after the beginning of the experiment (Figure 3-15). The plume of toluene was stable in the cartridge A with the highest concentration (about 2.4 mM) at 25 cm height. In contrast, the cartridge B exhibited a shift of the toluene plume over time. Thus, the highest toluene concentration at 31 days of incubation was at 25 cm height, while at 47 and 76 days of incubation it was at 20 cm height. Therefore, the cartridge A exhibited more stable toluene concentration along the length when compared to the cartridge B. However, toluene concentrations were slightly increasing with time in the cartridge A at 10, 20, 25, and 30 cm (Figure 3-15A).

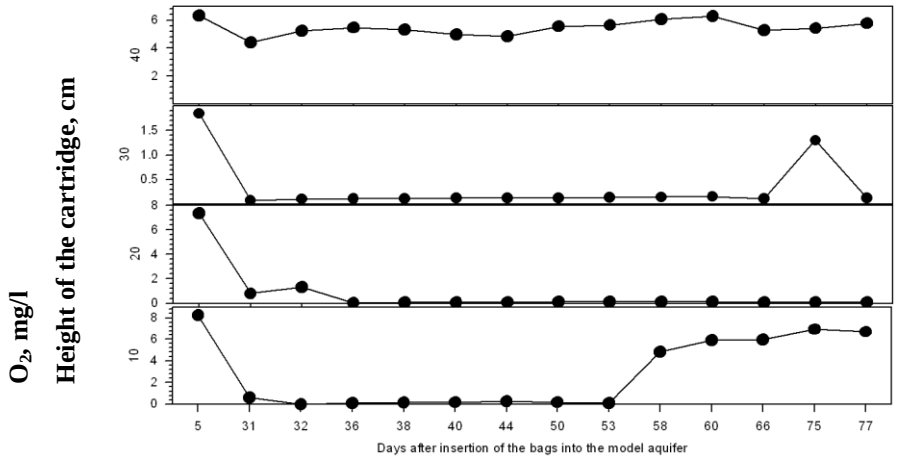

Figure 3-13 Concentrations of O_2 in the cartridge A during incubation of the dialysis bags in the indoor aquifer.

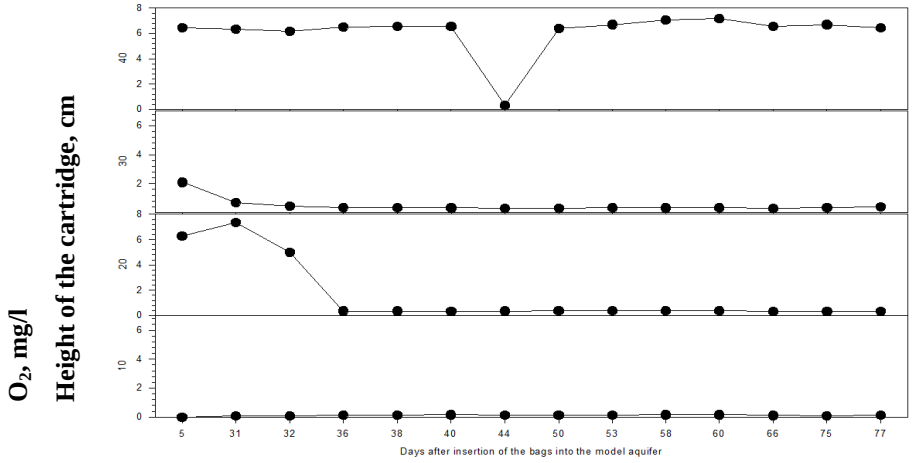

Figure 3-14 Concentrations of O_2 in the cartridge B during incubation of the dialysis bags in the indoor aquifer.

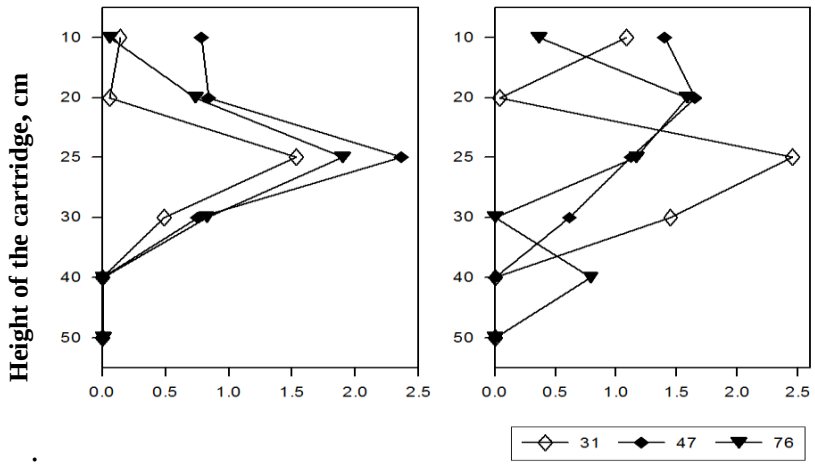

A. Toluene [mM] in cartridge A **B. Toluene [mM] in cartridge B**

Figure 3-15 Toluene concentrations in the cartridges A and B at 31, 47, and 76 days of incubation in the indoor aquifer.

The cartridges were removed from the indoor aquifer after 77 days of incubation. In order to check if the inoculation of dialysis bags went successfully, bacterial cells were extracted from the sediments and counted using flow cytometry. Bacterial cells were detected in all dialysis bags, even containing un-inoculated sterilized sediment (Figure 3-17). The highest number of cells was observed for two bags (bags 1 and 4) which were placed in cartridge A at 10 and 25 cm height (Figure 3-16) where toluene concentration was 0.06 and 0.7 mM, respectively, and for dialysis bags 5 and 6 placed in the cartridge B at 10 and 30 cm height (Figure 3-17), where toluene concentration was 0.36 and 0.8 mM, respectively.

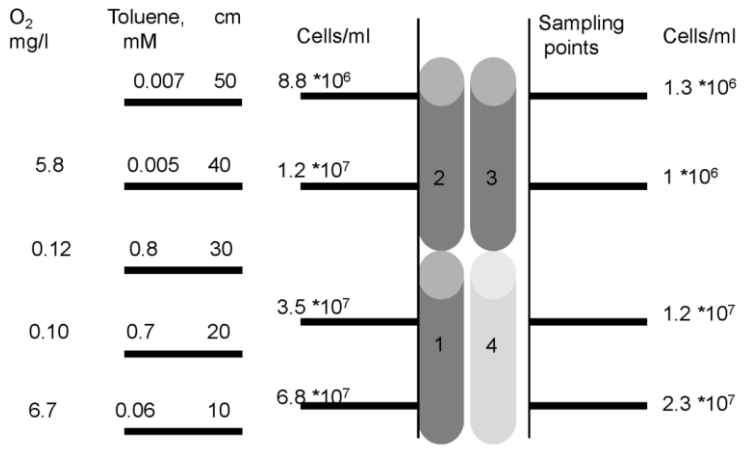

Figure 3-16 Concentrations of oxygen, toluene, and cells along the length of cartridge A after 77 days of incubation. Bags 1,2,3 were sterilized before inoculation with *G. metallireducens*, and bag 4 was not sterilized before inoculation.

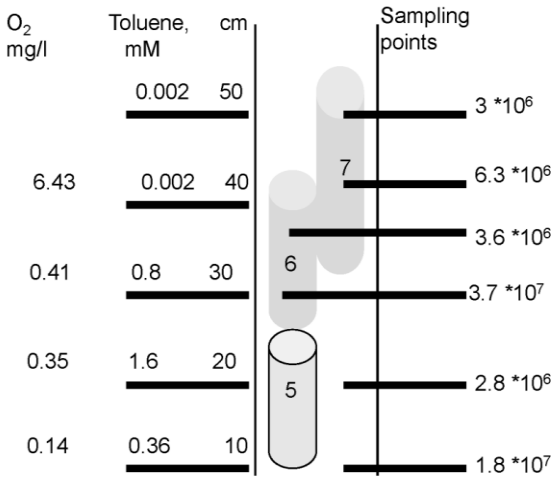

Figure 3-17 Concentrations of oxygen, toluene, and cell numbers in the cartridge B after 77 days of incubation. Bag 5 - was not sterilized before inoculation, bags 6,7 – were sterilized but not inoculated.

The previously sterile sediments inoculated with *G. metallireducens* were expected to be mainly composed of *G. metallireducens* as the dialysis bags with a pore size of 0.2 µm were supposed to prevent contamination from the outside sediments. Not sterile sediments but inoculated with *G. metallireducens* were used as controls to examine capabilities of *G. metallireducens* to compete with natural bacterial communities in the sediment, while uninoculated sterilized sediments were used as controls for barrier capabilities of dialysis bags. The presence of bacterial cells in the un-inoculated bags (bags 6 and 7) in cartridge B (Figure 3-17) suggests that the dialysis bags did not prevent the sediments from contamination by natural community inhabiting the indoor aquifer.

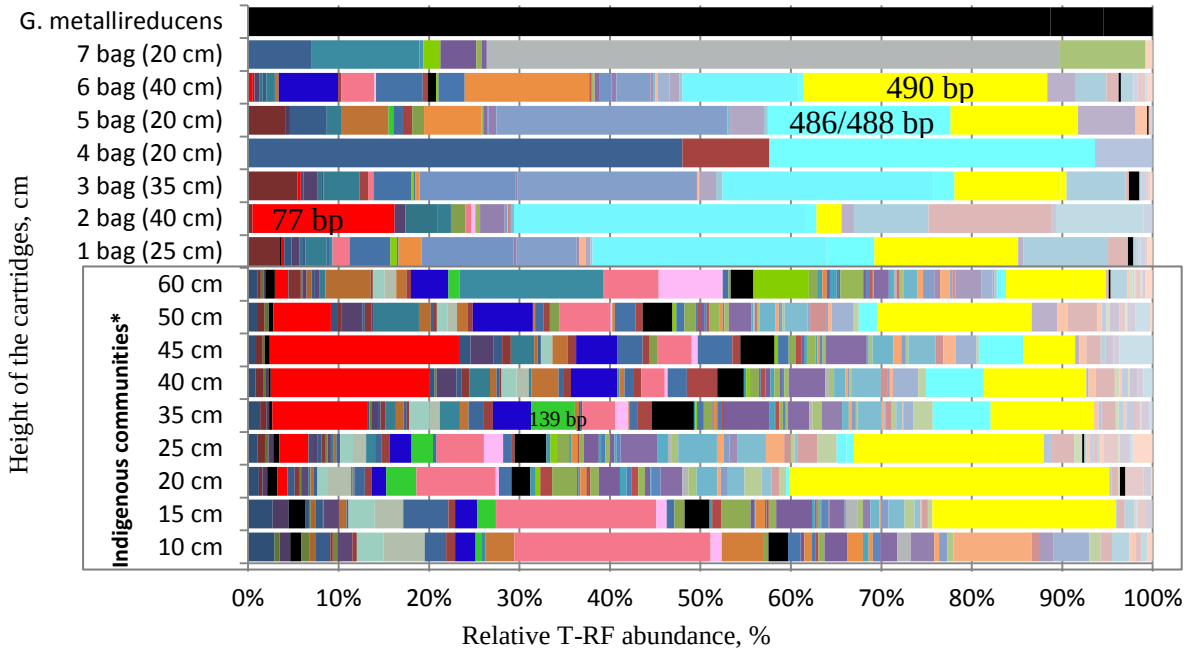

Figure 3-18 Bacterial 16S rRNA gene T-RFLP fingerprints of pure culture of *G. metallireducens*, communities in dialysis bags and indigenous communities of the sediment across height of the sediment core. *Data of T-RFLP fingerprints of the indigenous communities was kindly provided by Dr. A. Herzyk (Herzyk, 2012). The sampling of the sediment for analysis of indigenous communities was carried out prior to insertion of dialysis bags into the indoor aquifer by Dr. A. Herzyk. The fingerprints identified with application of pyrosyquencing (Herzyk, 2012) are indicated: 77 bp, 139 bp, 486/488 bp, 490 bp are fingerprints of *Azoarcus* sp., *Actinobacteria*, *Comamonadaceae*, *Pseudomonadaceae*, respectively. Fingerprints of *G. metallireducens* are indicated in black and are comprised of three typical fingerprints: 74 bd, 159 bp, and 505 bp. Data used for construction of the figure is given in Appendix, **Table 6**.

Further, T-RFLP analysis proved that contamination of the bags took place. T-RFLP fingerprints, characteristic for *G. metallireducens* (Figure 3-18), were found in low abundances or were not detected in sediments incubated in both cartridges (Figure 3-18). T-RFLP analysis showed that dialysis bags were inhabited by various microbial communities.

After 77 days of incubation in the indoor aquifer, sterile dialysis bags (bags 1, 2, and 3) which were inoculated with *G. metallireducens* prior to insertion into the cartridges, contained only minor fraction of putative fingerprints of *G. metallireducens* (Figure 3-18). Comparison between fingerprints of microbial communities of dialysis bags and fingerprints of indigenous communities from the sediment next to the cartridges indicate that *G. metallireducens* was outcompeted by members of the indigenous communities (Figure 3-18). The most abundant species in all dialysis bags except for dialysis bag 7 were *Pseudomonadaceae* and *Comamonadaceae*. *Azoarcus* sp., abundant in the indigenous communities, was also found in the dialysis bag 2 at 40 cm height, where toluene concentration was very low (0.05 mM).

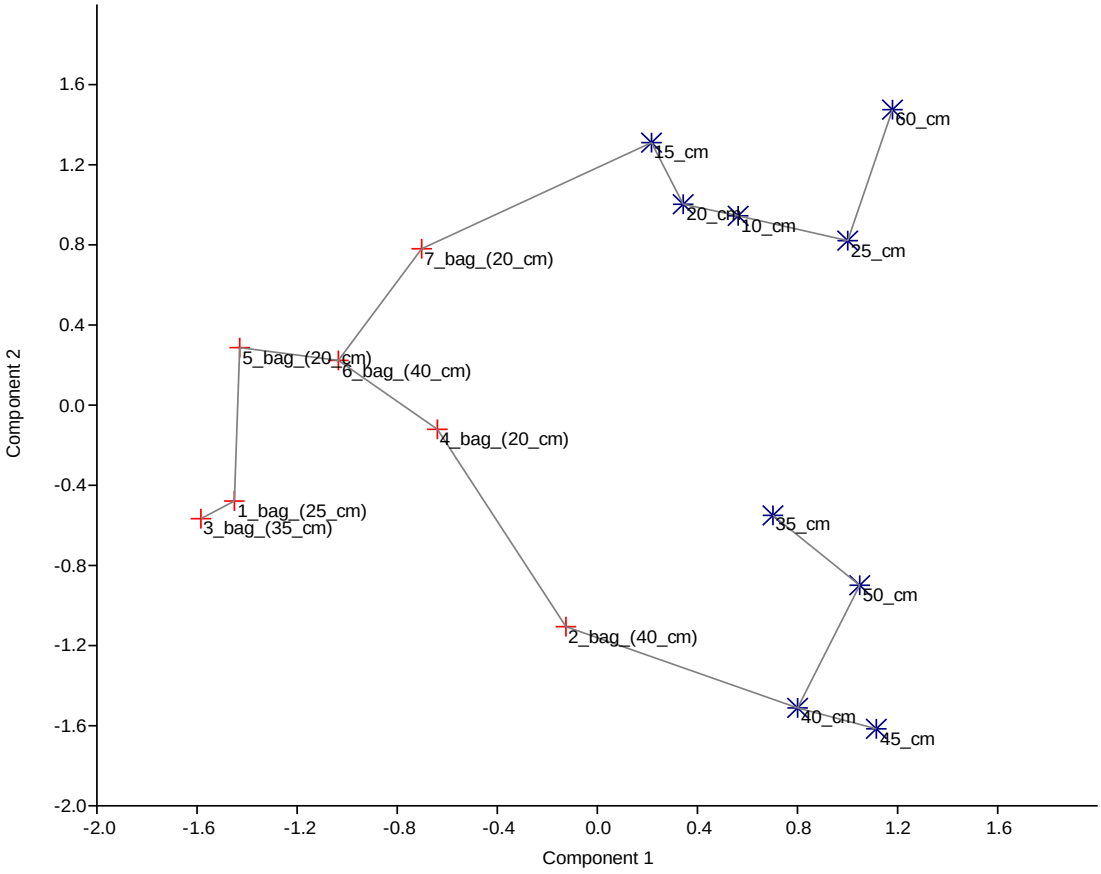

Figure 3-19 PCA plot with minimum span tree of normalized relative abundances of microbial communities in dialysis bags and in the sediment next to dialysis bags. The first two components with the highest eigen values have 88.9% of data variance, where component 1 explains 50.9% and component 2 explains 38% of data variability. "Red crosses" – dialysis bags, "blue stars" – sediment next to cartridges with dialysis bags. Data presented in Appendix, Table 6 was normalized via transfer into natural logarithm and used for construction of the PCA plot.

Principal component analysis (PCA) (Figure 3-19) shows that dialysis bags 2 and 7 reflect indigenous community at the same height of the sediment. Microbial communities in the dialysis bag 2 at height 40 cm are close to indigenous communities in the sediment outside cartridges at the height of 35-50 cm, while dialysis bag 7 (height 20 cm) is close to indigenous communities in the sediment at height 15-25 cm. Microbial communities in dialysis bags within one cartridge are similar to each other (Figure 3-19).

Thus, due to contamination of the dialysis bags, further proteomic analysis of proteins expressed by *G. metallireducens* during cultivation in the model groundwater mesocosm was not possible.

3.4 Physiology of *D. hafniense* Y51 under various nutrient limiting conditions in chemostats

3.4.1 Growth of *D. hafniense* Y51 on L-lactate and fumarate in batch and limited continuous cultures

The maximum growth rate (μ_{max}) of *D. hafniense* Y51 in batch cultures on 20 mM L-lactate in the presence of 30 mM fumarate was 0.075±0.01 h^{-1} (doubling time of 9.3 hours). During cultivation in batch and in chemostats lactate oxidation to acetate was coupled to the reduction of fumarate to succinate. No other organic acids or alcohols were detected during lactate utilization.

During cultivation in batch, the stoichiometry of lactate oxidation was in accordance to the theoretical stoichiometry (Equation 2-16) (Table 3-4). However, in chemostats, the stoichiometry of oxidation-reduction did not follow the theoretical. The ratios of consumed lactate to fumarate were approximately equal to the respective ratios in the inflow (Table 3-4). The residual concentrations of substrates supplied in excess were much lower than expected. Under lactate limitation (chemostats L1 and L2), expected residual 20 mM fumarate was completely reduced to succinate (Table 3-4). In two fumarate-limited chemostats (F2 and F4) with ratios of fumarate to lactate in the inflow above 1.3, *D. hafniense* Y51 utilized all 5 mM of excessive lactate almost completely. In the other two fumarate limiting chemostats, F1 and F3, with ratios of fumarate to lactate in the inflow lower than 1, only 50-60% of residual lactate was oxidized. Under ammonium limitation, *D. hafniense* Y51 showed different behavior in two replicated chemostats A1 and A2. Similarly to the fumarate-limited chemostat

F4, A1 was characterized by complete consumption of both lactate and fumarate. In contrast, despite fumarate limitation, 26% of fumarate was observed in the outflow in chemostat A2. The fumarate limiting chemostat F4, the lactate limiting chemostat L2 and the fumarate plus ammonium limited chemostat A1 were characterized by complete utilization of lactate and fumarate, leading to double limiting conditions.

Estimation of carbon and electron recoveries (*Crec%* and *erec%*, respectively) took into account the following assumptions: complete incorporation of yeast extract into the biomass (Equation 2-19); fermentation of lactate under fumarate limiting conditions (Equation 2-20) and disproportionation of fumarate under lactate limiting conditions (Equation 2-21 and Equation 2-22). As a result, *Crec%* and *erec%* were estimated to be close to 100% almost in all chemostats (Table 3-4). As an exception, chemostats under ammonium plus fumarate limiting conditions had low electron recoveries (65-88%).

Lactate-limited chemostats had the highest growth yields per mol of lactate (18.5 and 22.75 g biomass mol lactate^{-1}). The growth yields under fumarate- (chemostats F1, F2, and F3) and ammonium plus fumarate limitation (chemostats A1 and A2) were about 2-5 times lower. The yields per mole of fumarate were comparable for both lactate- and fumarate-limiting chemostats (4.6 to 6.2 g biomass mol fumarate^{-1}), while lower values were obtained under ammonium plus fumarate limitation (Table 3-4). An exception was the fumarate-limited chemostat F4, where both yields per mole of lactate and per mole of fumarate were higher than those obtained in the other three replicates under fumarate limitation (Table 3-4).

Table 3-4

Analysis of eight chemostat cultures of *D. hafniense* Y51 in steady state, grown under three different limiting conditions[a] and two replicates in batch culture

		Limitation							
		Lactate		**Fumarate**				**Ammonium-Fumarate**	
		L1	**L2**	**F1**	**F3**	**F2**	**F4**	**A1**	**A2**
Inflow ratio	Fumarate:lactate	3.2	3.8	0.6	0.9	1.3	1.5	1.7	1.9
Observed consumption ratio	Fumarate:lactate	3.3	3.8	0.8	1.2	1.4	1.5	1.7	2.2
Substrate/Product	Lactate:acetate	1.0	1.0	0.9	0.7	1.0	1.0	1.1	0.9
	Fumarate:succinate	1.1	1.0	0.9	1.2	0.9	1.2	1.2	1.1
Residual fumarate [mM]	Expected	22.6	21	0	0	0	0	0	0
	Observed	0.3	0	0.18	0	0	0	0	18.2
Residual lactate [mM]	Expected	0	0	19.2	20	5.9	5.6	6.7	2.3
	Observed	0	0	6.4	9.3	0.5	0	0	13.6
Biomass, [dry weight mg l^{-1}]		345	273	112	158	124	332	162	181
Carbon recovery,[% [b]]		98.9	100.6	112.8	132.5	100.5	99.2	92.3	109.6
e- recovery,[% [c]]		93.9	116.4	108.9	97.9	103.9	90.12	88.3	65.9
Yield [d][g dry weight substrate mol^{-1}]	Lactate	18.5	22.7	5.1	5.7	7.1	15.9	4.2	7.9
	Fumarate	5.8	6.1	6.2	4.6	5.2	10.9	2.5	3.6

[a] Dilution rate (D) of steady state limited chemostats was 0.02 h^{-1}
[b] and [c] were calculated as described in Analytical measurements.
[d] Expressed in gram of biomass formed per mol of substrate consumed (g mol^{-1})
ND, Not determined

3.4.2 ICPL labelled proteins detected with LC-MS/MS

Comparison between the number of proteins detected with LC-MS/MS analysis and the number of protein ratios generated by Proteome Discoverer revealed that 82% of detected proteins were isotope-code labelled. Further, 369 proteins were detected to be significantly expressed at least in one measurement. Investigation of the sources of variability (Table 7-7 and Figure 7-2 in Supplementary material) showed that most of the variability was due to the conduction of labelling campaigns separately or due to the variability within the biological replicates. Due to the high number of proteins with coefficients of variance within biological replicates below 30% (Table 7-7), biological replicates were not averaged.

Analysis of cellular distribution of ICPL-labelled proteins is well in accordance with theoretical distribution (Figure 3-20) suggesting that an appropriate fraction of extracellular and membrane proteins was extracted and labelled successfully.

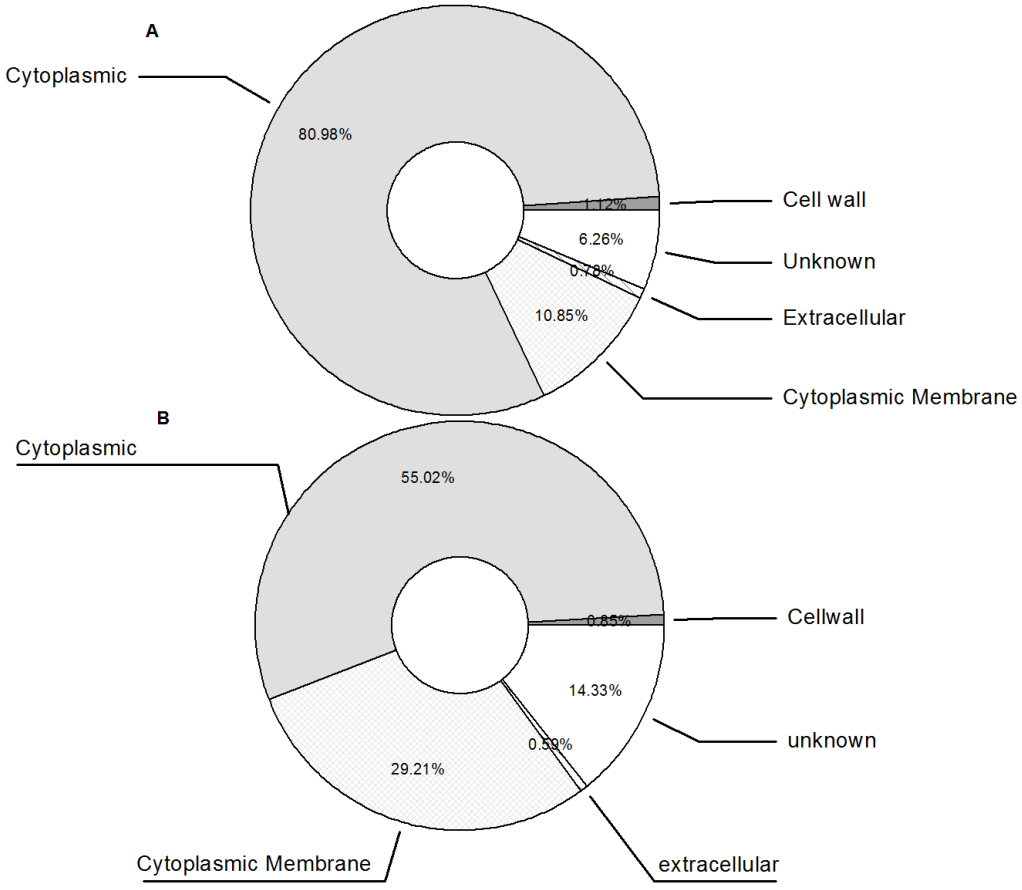

Figure 3-20 Cellular localization of ICPL-labelled proteins (**A**) vs. theoretical cell distribution (**B**) predicted by Psort database. Annotated localization of the detected and predicted proteins is given in Additional material, **Table S9.**

In order to visualize similarities/dissimilarities between the replicates analysed, principal component analysis (PCA) of relative protein abundances (proteins expressed in chemostats relative to batch) was conducted (Figure 3-21). PCA grouped chemostats into two main groups: 1) chemostats with residual lactate detected in the outflow (fumarate limiting chemostats F1 and F3); 2) and chemostats with complete lactate utilization (fumarate- (F2 and F4), lactate- (L1), and ammonium plus fumarate- (A1) limited chemostats). Technical replicates of the ammonium plus fumarate-limited chemostat A1 where lactate was also utilized completely were clustered together, and close to fumarate-limited chemostats F2 and F4. Another biological replicate of ammonium plus fumarate limitation A2 was located further from A1 technical replicates. The position of the lactate-limited chemostat L2 suggests that it might have different pattern of protein expression relative to other chemostats examined (Figure 3-21).

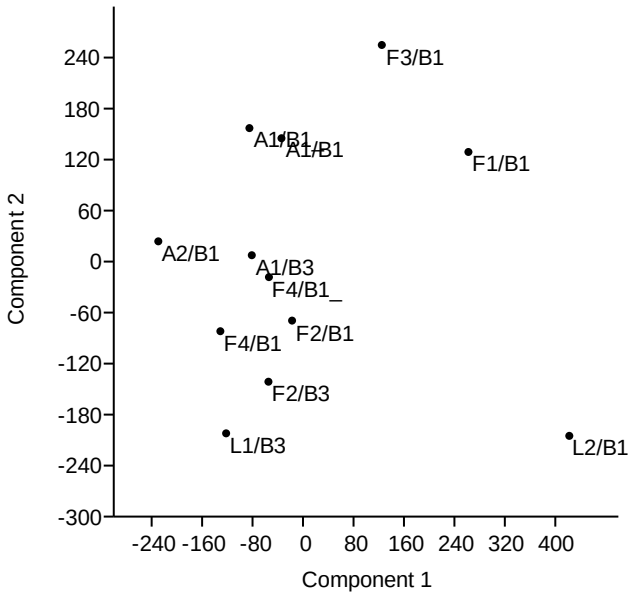

Figure 3-21 PCA plot of ratios of proteins expressed at different limiting conditions in chemostats relative to exponential growth phase in batch. 316 protein ratios detected to be significant at least in one measurement are presented. The first two components with the highest eigen values have 93 % of data variance, where component 1 explains 56 % and component 2 explain 37 % of data variability. A- ammonium-, L – lactate-, and F-fumarate-limited chemostats, B-batch. Data used for PCA is given in Additional material, **Table S10**.

3.4.3 Overview of expressed pathways

Proteins detected in the current study were assigned to 20 major functions (Figure 3-22). Proteins with unknown function had the highest fraction out of all detected (16.1%) followed by enzymes related to protein synthesis and amino acids metabolism (10.4 and 9.9%, respectively) (Figure 3-22).

The analysis of median values of relative protein abundances of metabolic pathways (Figure 3-22) showed that amino acids metabolism, biosynthesis of cofactors, regulation, signalling and cell division did not show major changes under limiting conditions relative to batch. However, pathways related to anabolism, e.g., protein synthesis, DNA metabolism, nucleotide metabolism as well as protein degradation decreased in abundance in chemostats relative to batch (median values < 0.8) (Figure 3-22, Table 4). Wood–Ljungdahl pathway (W-L pathway) increased in abundance in all chemostats relative to batch (median values > 1.8) (Figure 3-22). Sporulation, sulphur- and stress-related pathways were found to be more abundant almost under all limiting conditions relative to batch (Figure 3-22).

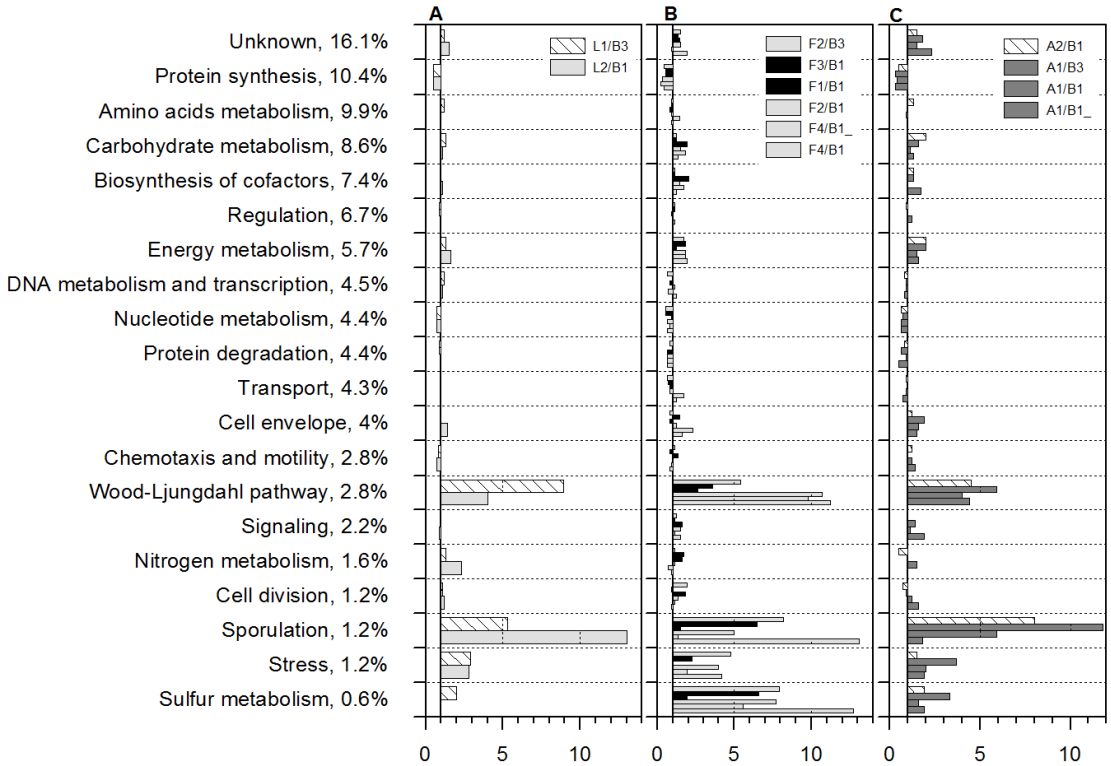

Figure 3-22. Metabolic pathways detected under all conditions. Medians of relative protein abundances assigned to given metabolic pathways are presented. **A**- lactate limitation (chemostats L1 and L2); **B** – fumarate limiting condition (chemostats F1 and F3 are in black colour, chemostats F2 and F2 are in grey colour); **C** – ammonium plus fumarate limitation (technical replicates of chemostats A1 are in grey colour). Assignment of

proteins to metabolic pathways was done via KEGG and JCVI databases. The data used for constructions the graph is given in Appendix, **Table 7**.

Further, catabolic pathways which are involved into carbon metabolism were subgrouped into 23 functions (Figure 3-23). The number of proteins detected within each pathway was similar among all limiting conditions. Analysis of the relative abundance of the pathways (median of the ratios of proteins expressed under limiting conditions relative to batch) shows that such pathways as lactate and xenobiotics degradation, W-L pathway, glyoxylate and dicarboxylate metabolism increased at least in one chemostat under all limiting conditions (median values > 2). Further, tricarboxylic acids (TCA) cycle, gluconeogenesis, fructose and mannose metabolism were increased under fumarate and/or ammonium-fumarate limiting conditions relative to batch (median values > 2) (Figure 3-23).

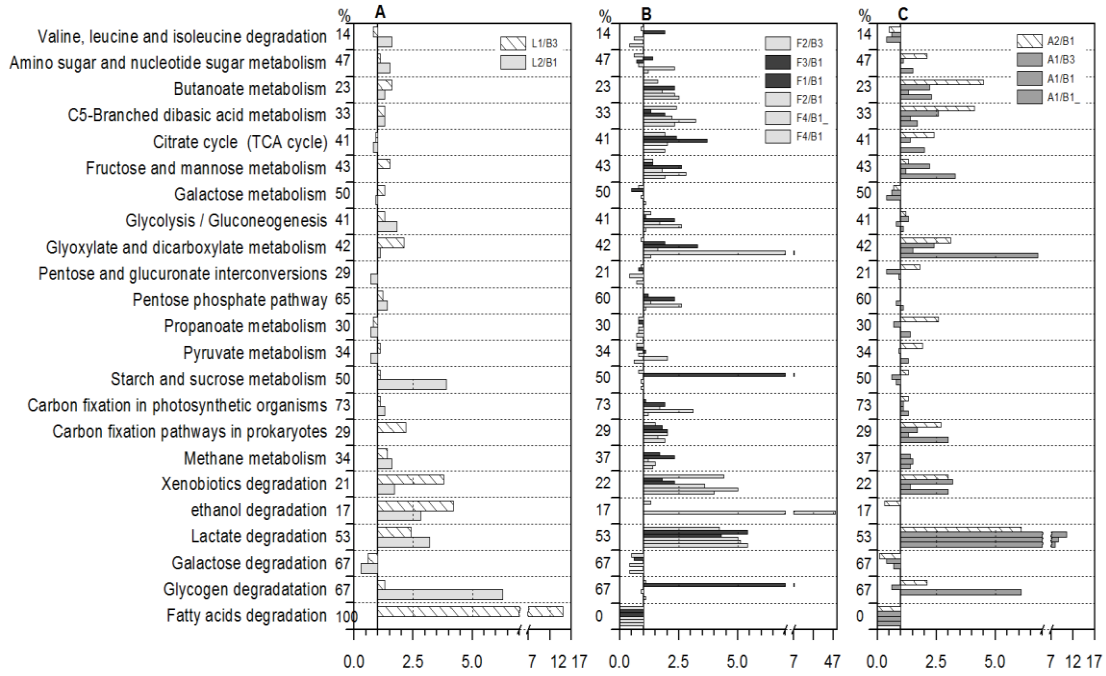

Figure 3-23 Comparison between the numbers of labelled proteins in chemostats and predicted proteins of selected catabolic pathways. Assignment of proteins to the functions was done via KEGG database. Pathways marked with * are not completely represented in the genome of *D. hafniense* Y51 or not fully expressed under conditions examined. **A**- lactate limitation (chemostats L1 and L2); **B** – fumarate limiting condition (chemostats F1 and F3 are in black colour, chemostats F2 and F2 are in grey colour); **C** – ammonium plus fumarate limitation (technical replicates of chemostats A1 are in grey colour).

The differences in physiology of *D. hafniense* Y51 cultivated under different limiting conditions can be observed in expression patterns of some metabolic pathways or proteins (Figure 3-24). For example, separate grouping within fumarate limiting chemostats depicted by PCA (Figure 3-21) can be explained by high expression of W-L pathway, fumarate, dimethylsulfoxid (DMSO), and sulphite reductases and some carbohydrate metabolism-related proteins in F2 and F4 chemostats relative to F1 and F3 chemostats (Figure 3-24,Table 7-8). F1 and F3 chemostats which were characterized by the detection of residual lactate in the outflow had higher expression of gluconeogenesis-related proteins and lactate degrading enzymes, superoxide dismutase (DSY4123), arylsulfotransferase (DSY0226), and sporulation-related proteins. The differences between lactate-limited chemostats are, probably, caused by higher abundances of some sporulation-related enzymes, enzymes of the carbonyl branch of the W-L pathway and the superoxide dismutase (DSY4123) (Figure 3-24). Differences between two biological replicates of ammonium plus fumarate limitation were reflected mainly in higher abundances of sporulation-related enzymes in chemostat A1 (Figure 3-24).

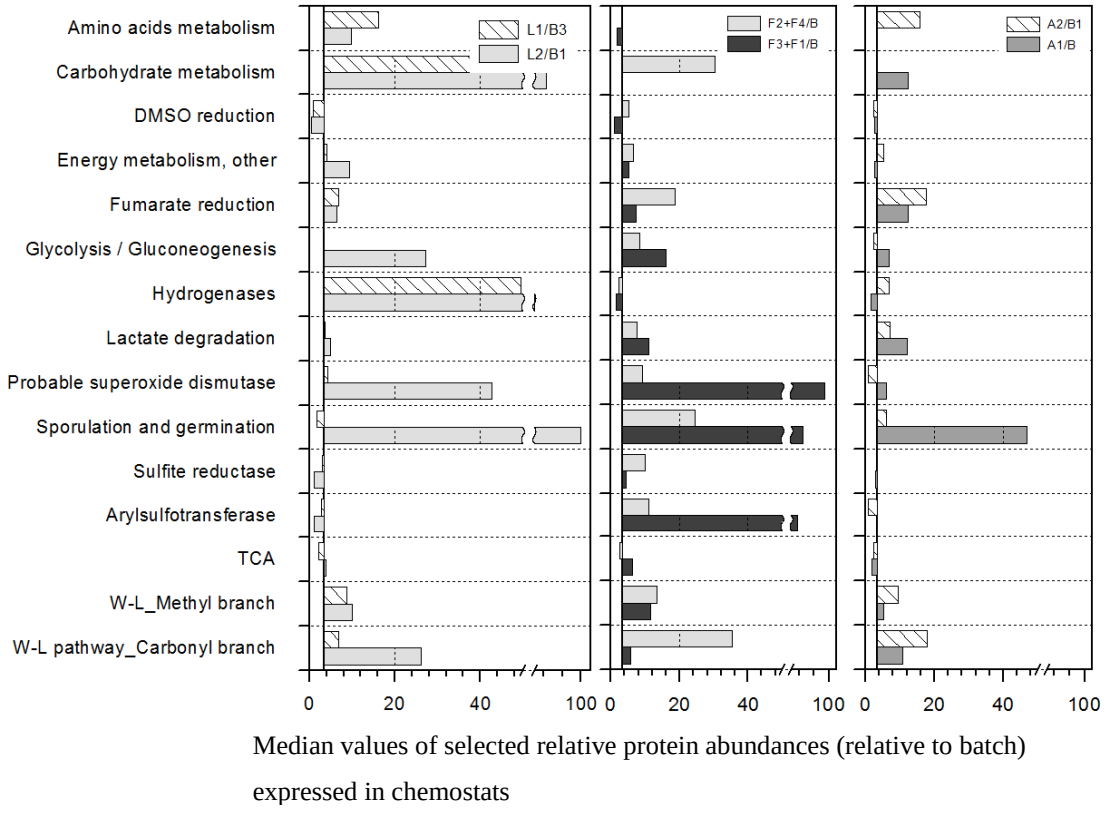

Figure 3-24 Differences between limiting conditions reflected in relative protein abundances. List of selected proteins used to estimate median values can be found in supplementary material. Relative protein ratios were averaged for fumarate limiting chemostats F2 and F4 and F3 and F1, and technical replicates of the ammonium plus fumarate limited chemostat A1.

Important catabolic pathways of carbon metabolism expressed by *D. hafniense* Y51 under limiting conditions were lactate utilization with subsequent acetate excretion, TCA cycle and CO_2 fixation (Figure 3-25).

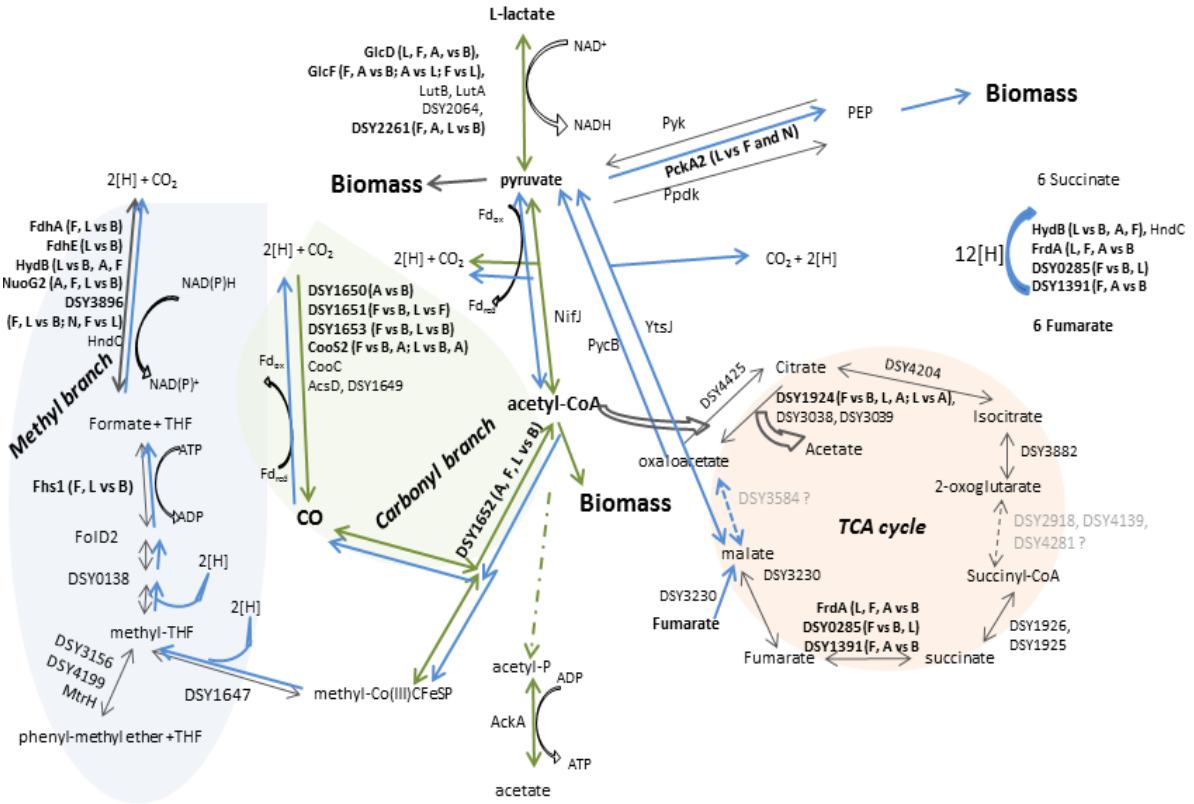

Figure 3-25 Proposed catabolic pathways expressed by *D. hafniense* Y51 under limiting conditions in chemostats. The pathways were constructed based on the following publications: (Kim et al., 2012), (Nonaka et al., 2006), (Peng et al., 2012) and the KEGG database. Proteins detected in the current study are presented. Proteins in bold exhibit significant relative abundance in chemostats relative to batch or under limiting conditions to each other. Indicated in brackets: A – ammonium limitation, F – fumarate limitation, L – lactate limitation, B - batch. Reactions for which proteins were not detected in the current study are presented with dashed arrows. Suggested reactions for utilization of expected residual substrates are given in colour: blue – fumarate disproportionation under lactate limitation, green – lactate fermentation coupled to CO_2 reduction under fumarate limitation. Annotation and expression of presented proteins is given in Table 3-5.

Lactate degradation

The genome of *D. hafniense* Y51 encodes putative lactate dehydrogenases (two homologues lutB (DSY1921 and DSY2092) and lutA (DSY2091 and DSY2064)) which have at least 50% similarity to the FeS cluster-containing L- and D-lactate dehydrogenases of *Shewanella oneidensis* MR-1 (Pinchuk et al., 2009). Moreover, it also encodes putative D-lactate/gluconate dehydrogenases (GlcF (DSY3218) and two homologues GlcD (DSY3357 and DSY3216), which are similar to D-lactate dehydrogenase of *Geobacter sulfurreducens* PCA. All putative lactate dehydrogenases were detected under all conditions tested. However,

only subunits of D-lactate/gluconate dehydrogenase together with one L-lactate permease (DSY2261) were found to be significantly abundant in some chemostats under all limiting conditions (Table 3-5). Lactate dehydrogenases transfer lactate into pyruvate. Further, pyruvate is converted to acetyl-CoA by flavodoxin/ferredoxin oxidoreductase (NifJ (DSY0115)). Subsequently, acetyl-CoA can be directly converted to acetate via the acetyl-CoA ligase (AcsA (DSY0515)) or acetyl-CoA hydrolase/transferase (DSY1711 and DSY3366) or via the phosphate acetyltransferase-acetate kinase pathways. Detection of only acetate kinase (AckA (DSY2668)) under all conditions suggests that the latter mechanism is preferred by *D. hafniense* Y51 for acetate excretion.

TCA cycle

In order to grow, microorganisms require the synthesis of building material. TCA cycle, pyruvate metabolism, glycolysis/gluconeogenesis, and pentose-phosphate pathways are important pathways for biomass synthesis. At least 40% of the proteins assigned to these pathways have been detected and labelled in the current study (Figure 3-22). Most of the enzymes required for TCA cycle functioning were detected (Figure 3-25, Table 3-5). However, according to the current KEGG annotation, the TCA cycle seems to be incomplete in *D. hafniense* Y51. The full enzyme complex of α-ketoglutarate dehydrogenase is missing. Only three putative genes of dihydrolipoamide dehydrogenase (DSY2918, DSY4139, DSY4281) which belong to the α-ketoglutarate dehydrogenase complex, are encoded in the genome of *D. hafniense* Y51. None of their gene products were detected in the current study.

CO_2 fixation

The W-L pathway is characterized by synthesis of CO from one CO_2 molecule via carbonyl branch and synthesis of a CH_3-group from another CO_2 molecule via methyl branch. Further, the produced CO and CH_3-group are used to form acetyl-CoA (Ragsdale and Pierce, 2008). All proteins of the W-L pathway were detected to be expressed under all conditions applied. Overall, all limiting conditions led to the increased abundance of the W-L pathway relative to the exponential growth phase (Figure 3-22). Lactate-limited chemostats L1 and fumarate-limited chemostas F2 and F4 had the highest number of significantly increased proteins of W-L pathway while fumarate-limited chemostats F1 and F3 and lactate-limited chemostat L2 were characterised by the lowest (Figure 3-24, Table 3-5). Additionally, periplasmic [NiFe] hydrogenase large subunit (HydB) was found to be significantly abundant only in lactate-limited chemostats (L1 and L2) relative to exponential growth phase

3.4.4 Increase in abundance of enzymes utilizing alternative electron donors

Single proteins from pathways which might be involved in the utilization of electron donors not present in the medium such as formate (formate dehydrogenase (DSY3969) and formate--tetrahydrofolate ligase 1 (DSY0205)), butyrate (3-hydroxybutyryl-CoA dehydrogenase (DSY1717)), citrate (citrate lyase, CitE (DSY1924)), aldehyde (aldehyde oxidoreductase, Mop (DSY1987)), and hydrogen (periplasmic [NiFe] hydrogenase large subunit of hydrogen uptake type, HydB (DSY1598) and hydrogenase (DSY4326)) significantly increased their abundances under some limiting conditions relative to batch (Table 3-5). For example, 3-hydroxybutyryl-CoA dehydrogenase was detected to be significantly abundant in the fumarate-limited chemostat F2 and the lactate-limited chemostat L1 while subunit beta of the citrate lyase (DSY1924) had significant increase only during fumarate limitation (chemostats F1 and F3). Aldehyde oxidoreductase and formate dehydrogenase were found to be significantly expressed at least in one chemostat under all limiting conditions relative to batch (Table 3-5). Ammonium plus fumarate limitation was characterized by low induction of carbohydrate metabolism-related proteins relative to lactate- and fumarate-limitation (Table 3-6).

3.4.5 Expression of proteins involved in utilization of alternative electron acceptors

Three analogous fumarate reductase flavoprotein subunits, FrdA (DSY3139, DSY0285, and DSY1391) were detected and found to have significantly higher abundances at least in one chemostat under all limiting conditions (Table 3-5 and Table 3-6). Encoding genes of these subunits are localized in different parts of the genome.

Several proteins related to sulphate metabolism such as sulphite reductase (DsrA (DSY0309) and DsrB (DSY0310)), dimethyl sulfoxide reductase (DmsA (DSY3410)), and aryl sylfonyltransferase (DSY0226) had increased abundances under fumarate limitation relative to batch (Table 3-6). The latter protein is involved in the transfer of a sulphate group from phenolic sulphate esters to phenolic and non-phenolic alcohol acceptor molecules (van der Horst et al., 2012) and might be related to utilization of alternative electron donors.

3.4.6 Response to ammonium limitation

Amino acid biosynthesis-related proteins with possible involvement into nitrogen metabolism exhibited changed abundances during ammonium limitation. 2-isopropylmalate synthase 2,

NifV (DSY4262) was significantly and exclusively expressed under ammonium limitation, showing higher abundances relative to batch (Table 3-6). This enzyme is involved in the production of homocitrate from acetyl-CoA for lysine biosynthesis as well as in the assembly of the nitrogenase FeMo complex by providing homocitrate to this complex (Rubio and Ludden, 2008). Furthermore, the protein related to nitrogen fixation (alpha subunit of nitrogenase (NifD (DSY4270)) was significantly abundant in the fumarate plus ammonium-limited chemostat A1 relative to batch (Table 3-6).

When compared to fumarate limitation, the response to ammonium limitation was reflected in the high abundance of the ammonium scavenging glutamine synthase GlnA3 (DSY4406) (Moat et al., 2002) and in increased abundances of two proteins which provide glutamate for glutamine synthesis: ferredoxin-dependent glutamate synthase 1, GltB (DSY4385) and carbamoyl-phosphate synthase large chain, CarB (DSY2042). Moreover, the low ammonium affinity glutamate dehydrogenase Gdh (DSY4953) decreased its abundance during ammonium limitation relative to batch (Table 3-6).

3.4.7 Stress-related proteins

All limiting conditions were characterized by the high induction of sporulation response relative to batch with representation of enzymes from four sporulation stages (Kim et al., 2012): sporulation initiation (Spo0A (DSY1866)), septum formation (SigF (DSY2304) and SpoIIAA (DSY2302)), and cortex formation (SpoIVA (DSY2248)) (Table 3-6). Moreover, formation of spores was supported by microscopic analysis in ammonium plus fumarate and lactate-limited chemostats (data not shown).

Besides sporulation, there was increase in abundance of two oxidative stress proteins (probable superoxide dismutase (DSY4123) and peroxiredoxin (DSY0524)) in some chemostats (Table 3-6). These proteins might be involved in the protection against free radicals produced during slowed growth in chemostats. The ppGpp synthase (DSY2451) did not increase its abundance (Table 3-6) as it is suggested to be increased in abundance in response to starvation (English et al., 2011), suggesting that applied conditions in chemostat did not lead to starvation.

Table 3-5 Function and ratios of proteins presented in **Figure 3-25**. Protein ratios are given for chemostats relative to batch. Protein ratios in bold are significantly different ratios.

Gene name	Annotation	Ammonium+fumarate limitation				Fumarate limitation						Lactate limitation	
		A2/B1	A1/B3	A1/B1	A1/B1_	F2/B3	F3/B1	F1/B1	F2/B1	F4/B1_	F4/B1	L1/B3	L2/B1
Lactate utilization													
lutB	L-Lactate utilization protein B	3.5	3.7	2.3	2.1	1.5	2.3	2.3	2.2	2.3	3.1	1.2	1.6
lutB	L-Lactate utilization protein B	4.9	4.5	3.3		2.6	3.0		3.2		3.7	1.3	3.3
lutA	L-Lactate utilization protein A			4.4			6.4						8.6
DSY2064	D-lactate dehydrogenase	15.2	7.6	3.1	4.6	3.3	3.1	1.9	4.0	4.0	6.5	3.5	2.5
glcD	D-lactate dehydrogenase/Glycolate oxidase subunit	17.4	**21.7**	**15.0**	**19.3**	5.2	4.5	4.3	6.0	5.1	4.2	1.2	1.1
glcD	D-lactate dehydrogenase/Glycolate oxidase subunit	3.1	13.4	**14.2**	9.6	**10.6**	**21.1**	**11.5**	11.5	9.7	7.3	4.6	**12.3**
glcF	D-lactate dehydrogenase/Glycolate oxidase FeS subunit	7.2	18.2	**12.8**	7.9	8.3	**14.1**	**11.6**	9.9	6.1	10.6	4.9	3.1
DSY2261	L-lactate permease			**16.2**			**43.7**						**36.4**
Pyruvate to acetate conversion													
nifJ	Pyruvate flavodoxin/ferredoxin oxidoreductase	6.5	3.4	1.3	1.4	1.4	1.2	0.9	2.7	1.0	2.6	2.8	0.7
ackA	Acetate kinase	2.6	1.8	1.1	1.4	0.6	0.8	1.0	0.8	0.8	1.3	1.6	0.3
Acetyl-CoA synthesis from CO and methyl group													
acsD	CO dehydrogenase/acetyl-CoA synthase delta subunit	2.9	5.9	4.6	5.8	4.4	6.8	2.8	7.5	8.3	10.5	6.4	4.6
DSY1649	Cobyrinic acid ac-diamide synthase	2.5	2.6	2.8	1.5	4.2	3.0	1.7	3.1	1.7	1.8	2.3	1.7
DSY1650	CO dehydrogenase/acetyl-CoA synthase ferredoxin-like	11.0	**26.6**	4.2	5.2	3.4	4.4	2.4	17.5	9.5	15.9	9.1	3.5
DSY1651	CO dehydrogenase/acetyl-CoA synthase gamma subunit		8.2	5.0	7.5	6.9	5.1	4.3	**22.4**	15.4	11.2		4.1
DSY1652	CO dehydrogenase/acetyl-CoA synthase subunit alpha	**44.8**	**48.2**	**10.2**	9.9	**16.8**	9.7	3.8	**51.8**	**23.2**	**100.0**	**47.7**	10.8
DSY1653	CO dehydrogenase/acetyl-CoA synthase subunit beta	12.5	18.5	8.9	10.1	**15.4**	10.1	4.5	17.9	**18.2**	**27.4**	**16.1**	9.0
cooC	Cobyrinic acid ac-diamide synthase	6.1	3.6	3.8	3.4	6.2	3.4	2.6	4.8	2.1	2.4	4.5	1.8
cooS2	CO dehydrogenase 2	3.2		0.4		**83.2**	2.3					**39.2**	1.7
Hydrogen production/utilization													
hydB	Periplasmic [NiFe] hydrogenase large subunit	11.5	3.1	3.6		8.2	3.0		3.6		2.0	**49.4**	**100.0**
hndC	NADP-reducing hydrogenase subunit HndC	2.6	5.6	3.7		2.7	3.7		11.3		11.6	8.9	9.9
formate production/utilization													
fdhA	Formate dehydrogenase subunit alpha	8.4	13.2	5.0	3.9	7.4	5.2	2.4	10.7	14.0	**31.8**	**30.7**	10.6
nuoG2	Formate dehydrogenase	**55.7**	16.7	4.4	7.3	**70.7**	3.6	3.7	**20.9**	**32.7**	**31.5**	**27.1**	8.9
fdhE	Formate dehydrogenase formation protein												**69.8**
DSY3896	Formate dehydrogenase	0.5	15.2	7.1		0.9	**12.7**		**28.0**		**50.2**	**0.03**	
methyl group formation from formate													
fhs1	Formate--tetrahydrofolate ligase 1	6.4	12.6	4.5	4.4	4.6	5.2	1.8	16.1	7.9	**18.4**	**20.4**	**11.2**

Gene name	Annotation	Ammonium+fumarate limitation				Fumarate limitation						Lactate limitation	
		A2/B1	A1/B3	A1/B1	A1/B1_	F2/B3	F3/B1	F1/B1	F2/B1	F4/B1_	F4/B1	L1/B3	L2/B1
folD2	Methylenetetrahydrofolate dehydrogenase (NADP(+))	1.3	2.6	3.1	2.9	1.5	2.6	1.5	2.2	10.0	3.5	3.0	7.2
DSY0138	Methylenetetrahydrofolate reductase	1.0	0.6	2.1		1.0	1.0		0.5		1.5	2.9	3.4
DSY1647	Dihydropteroate synthase DHPS	4.5	5.6	5.7	3.3	7.2	7.4	2.3	5.9	3.9	7.7	5.8	3.9
DSY3156	Trimethylamine methyltransferase			2.7			1.4						0.8
DSY4199	Uroporphyrinogen-III decarboxylase-like protein			3.1			2.8						0.4
mtrH	Tetrahydromethanopterin S-methyltransferase subunit H	**0.04**	1.1		1.6	0.6		**67.3**	0.4		0.8	0.6	
Pyruvate/PEP interconvertions													
pyk	Pyruvate kinase	1.9	1.6	1.2	1.9	1.7	1.1	1.9	1.8	3.2	1.0	1.0	1.0
pckA2	Phosphoenolpyruvate carboxykinase [ATP] 2	0.2	0.9	0.7		**0.1**	0.3		0.5		0.4	1.1	0.8
ppdK	Pyruvate, phosphate dikinase	10.4	2.5	1.4	1.3	1.0	1.5	1.2	2.1	4.1	4.9	6.0	3.2
Fumarate to pyruvate													
DSY3230	Fumarate hydratase subunit alpha, putative	3.0	1.4	0.9		2.6	2.6		2.1		2.0	4.9	4.3
ytsJ	Probable NAD-dependent malic enzyme 4 (malate oxydoreductase)	10.2	1.3	1.0	1.1	3.0	2.0	**0.1**	2.4	0.7	1.5	1.1	0.5
DSY3584	malate dehydrogenase	not detected											
pycB	Pyruvate carboxylase subunit B	9.2	1.8	1.0		0.6	0.7		1.1		1.0	1.4	0.8
Fumarate to succinate													
FrdA	Fumarate reductase flavoprotein subunit	**33.7**	**40.7**	**11.2**	8.1	**34.9**	8.3	5.1	**34.8**	1.8	7.6	**16.8**	9.3
DSY0285	Fumarate reductase flavoprotein subunit, putative	1.7	8.1	6.8		**12.5**	**12.7**		9.4		11.4	2.2	3.4
DSY1391	Fumarate reductase flavoprotein		**21.2**	4.7	4.6		2.3	1.6	8.5	**25.5**	**40.3**		2.0
TCA cycle													
DSY1924	Citrate lyase subunit beta	3.4	1.7	2.5	3.1	5.8	**22.2**	**8.1**	4.6	1.5	2.6	3.7	10.2
DSY1925	Succinyl-CoA ligase [ADP-forming] subunit alpha	2.9	3.2	2.0		2.4	2.8		4.6		2.1	0.7	0.4
DSY1926	Succinate--CoA ligase (ADP-forming)	4.1	1.3	1.4		2.4	2.4		2.0		1.9	0.8	0.9
DSY3038	Citrate lyase, alpha subunit	0.5				0.7						0.2	
DSY3039	Citrate lyase subunit beta	0.9	2.3			1.4			0.9		0.7	0.5	
DSY3139	Fumarate reductase flavoprotein subunit	**33.7**	**40.7**	**11.2**	8.1	**34.9**	8.3	5.1	**34.8**	1.8	7.6	**16.8**	9.3
DSY3230	Fumarate hydratase subunit alpha, putative	3.0	1.4	0.9		2.6	2.6		2.1		2.0	4.9	4.3
DSY3882	isocitrate dehydrogenase, NADP-dependent	0.5	0.6	0.5	0.7	0.8	1.3	2.3	0.9	0.4	0.7	0.7	0.6
DSY4203	Phosphoenolpyruvate carboxykinase [ATP] 2	0.2	0.9	0.7		**0.1**	0.3		0.5		0.4	1.1	0.8
DSY4204	Aconitase A	2.0	1.1	0.6	0.8	0.3	0.4	1.4	0.6	0.4	0.8	1.4	0.5
DSY4425	Citrate synthase			1.0			2.0						0.6

Proteins significantly different from batch are given in bold. **Av**: average of two technical replicates, **SD**: standard deviation of two technical replicates; ***** represents ratio significant only in one technical replicate; ****** represents ratio which was detected only in one technical replicate and was identified as significant.

Table 3-6 Ratios of significantly expressed proteins in at least two biological replicates in the nutrient limiting chemostats relative to batch and some other proteins mentioned in the study. A: ammonium and fumarate limitation, F: fumarate limitation, L: lactate limitation.

			A/Batch			F/Batch					L/Batch	
			A1		A2	F1	F2		F3	F4	L1	L2
Uniprot ID	Protein annotation	Gene	Av	SD			Av	SD				
Amino acids metabolism												
DSY4778	Aspartate aminotransferase	AspC	3.2	0.4	4.12		2.5	2.1	3.2	5.3	**19.1**	**16.8**
DSY4262	2-isopropylmalate synthase 2	NifV	**100****		**27.15**							
DSY4953	NADP-specific glutamate dehydrogenase	Gdh	**0.25***	0.32	0.24	2.69	1.39	0.03	3.55	0.92	1.23	1.88
Biosynthesis of cofactors												
DSY2114	Nicotinate-hosphoribosyltransferase	CobT	**16.8***	12.3	**33.83**	**6.6**	8.3	5.4	0.8	15.4	2.3	1.7
DSY1402	Hydroxyethylthiazole kinase	ThiM	**33.9****		**27.56**		2.9	0.5		5.2	2.1	0.5
DSY0520	1,4-Dihydroxy-2-naphthoyl-CoA synthase	MenB	**0.07****		**0.07**		0.2	0.1		0.2	**0.1**	
Carbohydrate metabolism												
DSY3218	D-lactate/gluconate dehydrogenase, subunit	GlcF	**15.5***	3.8	7.21	**11.6**	9.1	1.1	**14.1**	10.6	4.9	3.1
DSY3216	D-lactate/gluconate dehydrogenase, subunit	GlcD	**13.8***	0.5	3.09	**11.5**	**11.0***	0.7	**21.1**	7.3	4.6	**12.3**
DSY3357	D-lactate/gluconate dehydrogenase, subunit	GlcD	**18.3**	4.8	17.39	4.3	5.6	0.6	4.5	4.2	1.2	1.1
DSY4167	Hydroxypyruvate isomerase	Hyi	1.9		0.33		**17.1****		**48.0**		9.2	**66.6**
DSY1924	Citrate lyase subunit beta	CitE	2.1	0.5	3.40	**8.1**	5.2	0.8	**22.2**	2.6	3.7	10.2
DSY3896	Putative anaerobic formate dehydrogenase	DSY3896	11.1	5.7	0.55		**14.5***	19.2	**12.7**	**50.2**	**0.03**	
DSY1987	Aldehyde oxidoreductase	Mop	**12.5***	0.5	1.25		**58.5**	0.4		**27.2**	**14.2**	**63.3**
DSY1717	3-hydroxybutyryl-CoA dehydrogenase	DSY1717	8.47				**16.861**				**100**	
Chemotaxis and motility												
DSY3001	Flagellar hook-associated protein 2	FliD	0.5	0.2	1.10		0.5	0.1	0.2	0.2	**0.2**	**0.1**
DSY3355	Sensory transducer protein YfmS, putative	YfmS	**47.9****		18.64		**32.9****		**20.7**		7.9	3.9
DNA metabolism/replication and repair												
DSY3180	UPF0758 protein Dhaf_4352	DSY3180	**17.2***	1.0	5.92		**10.1***	0.9	**16.1**	5.8	4.3	6.2
DSY1318	Insertion element IS600	DSY1318	**0.1**	0.04	**0.05**		**0.4***	0.5	**0.03**	**0.1**	**0.1**	3.2
Energy metabolism												
DSY1598	Periplasmic [NiFe] hydrogenase large subunit	HydB	3.4	0.3	11.53		5.9	3.2	3.0	2.0	**49.4**	**100.0**
DSY4326	Hydrogenase large subunit domain protein	DSY4326	**0.1****		2.21		**0.2****		**0.04**		**0.1**	**0.1**
DSY1147	Rubrerythrin	Rbr	4.3	0.9	0.87		**24.2**	4.2	1.9	1.5	1.5	0.8
DSY3139	Fumarate reductase flavoprotein subunit	DSY3139	**25.9**	20.9	**33.67**	5.1	**34.9**	0.1	8.3	7.6	**16.8**	9.3
DSY0285	Fumarate reductase flavoprotein subunit	DSY0285	7.5	0.9	1.66		**11.0***	2.2	**12.7**	11.4	2.2	3.4
DSY1391	Fumarate reductase flavoprotein subunit	DSY1391	**12.9***	11.6		1.6	8.5		2.3	**40.3**		2.0

			A/Batch			F/Batch					L/Batch	
			A1		A2	F1	F2		F3	F4	L1	L2
Uniprot ID	**Protein annotation**	**Gene**	Av	SD			Av	SD				
DSY0309	Sulfite reductase, subunit alpha	DsrA	3.0	0.3	5.5	1.9	5.9	0.3	7.8	**18.9**	4.0	0.9
DSY0310	Sulfite reductase, subunit beta	DsrB	2.6	0.8	1.0	2.1	9.2	0.8	6.6	5.0	1.2	1.7
DSY0187	Putative anaerobic DMSO reductase, subunit	DmsB	0.8	0.3	1.8	0.9	2.3	2.4		1.0	0.9	
DSY3409	Putative anaerobic DMSO reductase, subunit	DmsB	2.5	0.8	1.1	0.7	1.3	0.1	1.5	5.0	0.3	0.7
DSY3410	Putative anaerobic DMSO reductase, subunit	DmsA	3.6	1.1	3.2	1.0	2.2	1.3	2.1	11.8	0.6	0.7
DSY4270	Nitrogenase molybdenum-iron protein alpha chain	NifD	**28.7***									
Wood-Ljungdal pathway												
DSY0205	Formate--tetrahydrofolate ligase 1	Fhs1	8.5	5.7	6.35	1.8	10.3	8.1	5.2	**18.4**	**20.4**	**11.2**
DSY3969	Formate dehydrogenase	NuoG2	10.5	8.7	**55.65**	3.7	**45.8**	35.2	3.6	**31.5**	**27.1**	8.9
DSY1652	CO dehydrogenase, subunit alpha	DSY1652	**29.2**	26.9	**44.76**	3.8	**34.3**	24.8	9.7	**100.0**	**47.7**	10.8
DSY1653	CO dehydrogenase, subunit beta	DSY1653	13.7	6.8	12.46	4.5	**16.6***	1.8	10.1	**27.4**	**16.1**	9.0
Nucleotide Metabolism												
DSY3929	AIR synthetase	PurM	**0.2**	0.1	**0.12**		**0.2***	0.1	**0.05**	**0.1**	**0.2**	**0.1**
DSY3931	SAICAR synthetase	PurC	**0.1***	0.005	**0.09**	**0.1**	0.2	0.02	**0.1**	**0.1**	**0.1**	**0.1**
DSY3930	Amidophosphoribosyltransferase	PurF	**0.1***	0.02	**0.05**		**0.2***	0.1	**0.1**	**0.1**	**0.1**	**0.1**
DSY3927	Bifunctional purine biosynthesis protein	PurH	0.2	0.02	0.14		0.2	0.01	**0.1**	**0.1**	**0.2**	**0.2**
Protein synthesis												
DSY1584	GTP-binding protein TypA/BipA homolog	TypA	**0.1***	0.01	**0.04**		**0.04**	0.002	**0.05**	0.2	0.7	**0.1**
DSY0488	30S ribosomal protein S5	RpsE	0.3	0.1	0.46	0.5	**0.2***	0.2	**0.1**	0.3	**0.2**	0.4
DSY0489	50S ribosomal protein L30	RpmD	**0.1**	0.04	0.13		**0.2***	0.1	**0.1**	0.2	**0.1**	**0.1**
DSY0500	50S ribosomal protein L17	RplQ	**0.1***	0.01	0.25		**0.2***	0.2	**0.1**	0.3	**0.1**	0.2
Salvage of nucleosides and nucleotides												
DSY1980	Xanthine dehydrogenase accessory factor	DSY1980	8.5	1.7	0.86	**1.8**	**24.0**	8.6	**27.8**	**18.4**	6.8	6.9
Sporulation and stress related												
DSY1866	Stage 0 sporulation protein A homolog	Spo0A	**19.0**	2.5	**30.80**		**40.1**	7.2	**34.7**	**43.4**	2.8	**48.3**
DSY2302	Anti-sigma F factor antagonist	SpoIIAA	**31.9****		**77.01**		**52.7****		**44.0**		**55.2**	**92.3**
DSY2304	RNA polymerase sigma-F factor	SigF	**36.1**	18.6	5.99		**23.4***	20.2	**87.8**	**26.3**	1.8	**100.0**
DSY2248	mraW RNA	SpoIVA	**51.0****		**100.00**		6.1	1.5		**71.5**	**10.0**	
DSY1861	Oligopeptide-binding protein oppA	OppA	0.4		1.68	**0.2**	0.6		**0.1**		1.9	**0.2**
DSY4123	Probable superoxide dismutase [Fe]	SodF	6.1	0.1	0.9		8.8	0.1	**93.8**	9.5	4.2	**42.6**
DSY0524	Peroxiredoxin	AhpC			2		5.2				6	
DSY2451	(p)ppGpp synthetase I, SpoT/RelA	RelA	0.6						0.4			0.6
Sulfur metabolism												
DSY0226	Arylsulfotransferase	DSY0226	3.3	2.3	0.95		**10.8***	0.4	**57.9**	11.0	2.8	1.0

Uniprot ID	Protein annotation	Gene	A/Batch			F/Batch					L/Batch	
			A1		A2	F1	F2		F3	F4	L1	L2
			Av	SD			Av	SD				
Unknown function												
DSY3352	Putative protein	DSY3352	**84.4**	22.0	**100.0**		**17.8**	4.2	**100.0**	**33.1**	4.7	
DSY4433	Putative protein, SAM dependent domain	DSY4433	**11.2***	13.2	**47.20**		3.4	2.5	1.0	**18.6**	3.8	4.0
DSY2525	Putative protein	DSY2525			**76.28**		**18.5***	25.5		**25.6**	5.0	
DSY2133	Uncharacterized protein	YuaG	**18.8***	15.3	**27.73**	1.8	**14.3***	3.8	4.9	**17.9**	**46.5**	3.2
DSY4209	UPF0210 protein Dred_1672	DSY4209	**0.1**	0.1	**0.08**		**0.2***	0.0	0.4	0.2	**0.1**	0.4
DSY3487	Putative protein, transposase domain	DSY3487	**99.6**		**31.08**		**68.2**	42.0		**47.6**	**9.7**	
DSY1284	Putative protein	DSY1284	17.2		14.66		**22.1**	7.1		10.6	**15.7**	

Proteins significantly different from batch are given in bold. **Av**: average of two technical replicates, **SD**: standard deviation of two technical replicates; * represents ratio significant only in one technical replicate; ** represents ratio which was detected only in one technical replicate and was identified as significant.

Table 3-7 Ratios of proteins expressed under one limiting condition relative to another in chemostats. Significantly expressed proteins in at least two biological replicates are presented. A: ammonium and fumarate limitation, F: fumarate limitation, L: lactate limitation.

Uniprot ID	Protein annotation	Gene	A/F				A/L		L/F	
			A2/F2	A1/F3	A1/F2	A1/F1	A2/L1	A1/L2	L1/F2	L2/F3
Amino acids metabolism										
DSY4385	Ferredoxin-dependent glutamate synthase 1	GltB	**7.6**	**8.9**				**10.4**		**0.3**
DSY4953	NADP-specific glutamate dehydrogenase	Gdh	**0.2**	**0.01**	**0.1**	0.2	0.3	**0.02**	0.7	0.6
DSY0760	N-acetyl-gamma-glutamyl-phosphate reductase	ArgC	**11.3**	**2.4**			1.9	1.3	**6.2**	1.7
DSY4406	Type-3 glutamine synthetase	GlnA3	**99.0**		**84.5**		**100.0**			
DSY4778	Aspartate aminotransferase	AspC	2.8	0.8	0.7		0.4	**0.2**	**10.7**	**4.5**
DSY2042	Carbamoyl-phosphate synthase large chain	CarB	**19.4**	**3.2**		1.7	0.8	1.8	**25.5**	1.7
Bacterial motility										
DSY3001	Flagellar hook-associated protein 2	FliD	2.1	**3.2**	1.2		**8.0**	**5.1**	0.3	0.6
Biosynthesis of cofactors										
DSY2114	Nicotinate-hosphoribosyltransferase	CobT	**7.6**	**9.9**	1.8	1.0	**13.2**	**5.4**	0.6	1.8
DSY4246	Pyridoxal biosynthesis lyase PdxS	PdxS	**51.6**		**10.7**	0.4	1.9		**52.2**	

Uniprot ID	Protein annotation	Gene	A/F				A/L		L/F	
			A2/F2	A1/F3	A1/F2	A1/F1	A2/L1	A1/L2	L1/F2	L2/F3
DSY1402	Hydroxyethylthiazole kinase	ThiM	**6.8**		**37.9**		**10.5**		0.6	
Biosynthesis of secondary metabolites										
DSY0517	Menaquinone-specific isochorismate synthase	MenF	**81.2**	1.0	**11.6**		**9.9**	3.0	**8.8**	**0.3**
Carbohydrate metabolism										
DSY0565	Alcohol dehydrogenase 2	AdhB	**0.2**	**0.1**	**0.03**		**0.1**		2.2	2.3
DSY4167	Hydroxypyruvate isomerase	Hyi	**0.02**	**0.04**			**0.04**	**0.03**	0.5	0.7
DSY3357	d-lactate/gluconate dehydrogenase, subunit	GlcD	3.2	**3.4**	**3.3**	**4.5**	**10.7**	**6.7**	0.2	0.4
DSY1924	Citrate lyase subunit beta	CitE	0.6	**0.1**	**0.3**	**0.5**	1.0	0.2	0.9	**0.5**
DSY1717	3-hydroxybutyryl-CoA dehydrogenase	DSY1717	0.5				**0.1**		**7.0**	**10.9**
DSY4838	Enolase 2	Eno2	0.4	**0.2**	0.5	**0.2**	0.6	**0.2**	0.9	0.9
DSY4203	Phosphoenolpyruvate carboxykinase [ATP] 2	pckA2	0.8	2.3	2.0		**0.2**	0.9	**6.9**	2.9
Cell envelope										
DSY3411	Component of anaerobic dehydrogenase	DSY3411	0.3	1.2	1.1		1.4	**4.1**	**0.2**	**0.3**
DSY4431	UDP-glucose/GDP-mannose dehydrogenase	DSY4431	**23.4**	1.2	**6.5**		**9.3**	0.5	3.2	**4.0**
Central intermediary metabolism, Other										
DSY2601	5-methylthioadenosine deaminase	MtaD	**0.1**	**0.1**	0.9					
DNA metabolism/replication and repair										
DSY1318	Insertion element IS600 uncharacterized	DSY1318	**0.1**	**5.8**	1.1		0.8	**0.02**	**0.1**	**76.4**
Energy metabolism										
DSY4617	Tetrathionate reductase subunit B	TtrB	**0.1**		**0.05**		**0.1**		0.6	
DSY1598	Periplasmic [NiFe] hydrogenase large subunit	HydB	1.3	1.2	0.5		0.2	**0.03**	**6.4**	**34.8**
DSY4326	Hydrogenase large subunit domain protein	DSY4326	**13.2**	**3.1**			**15.9**	2.7	0.9	1.1
DSY1147	Rubrerythrin	Rbr	**0.03**	1.7	**0.2**		0.9	**4.7**	**0.03**	0.4
DSY1987	Aldehyde oxidoreductase	Mop	**0.02**	**0.1**	**0.2**	0.3	**0.1**	0.3	0.2	**0.1**
DSY3410	Dimethyl sulfoxide reductase DmsA	DmsA	1.9	1.2	1.6	2.6	**5.6**	**3.8**	0.4	0.3
DSY0310	Sulfite reductase, dissimilatory-type subunit	DsrB	**0.1**	0.4	0.4	0.9	0.8	1.5	**0.2**	**0.2**
Wood-Ljungdal pathway										
DSY3157	Tetrahydromethanopterin S-methyltransferase	MtrH	**0.1**		2.5	**0.05**	**0.1**		1.0	
DSY4442	Carbon monoxide dehydrogenase 2	CooS2	**0.1**	**0.2**	0.4		**0.1**	0.3	0.5	0.6
Oxidative stress										
DSY4123	Probable superoxide dismutase [Fe]	SodF	**0.1**	**0.1**	0.8		**0.2**	**0.2**	0.4	0.4
Protein synthesis and fate										
DSY1584	GTP-binding protein TypA/BipA homolog	TypA	0.9	**3.7**	**2.7**		**0.1**	1.5	**14.9**	2.3
DSY2463	Queuine tRNA-ribosyltransferase	Tgt	**0.2**	**0.2**			**0.2**	0.3	0.8	0.8
DSY1747	UPF0365 protein Dhaf_2899	DSY1747	**10.3**	**3.2**	1.7		1.6	1.0	**7.0**	2.4

Uniprot ID	Protein annotation	Gene	A/F				A/L		L/F	
			A2/F2	A1/F3	A1/F2	A1/F1	A2/L1	A1/L2	L1/F2	L2/F3
DSY1891	Oligoendopeptidase F homolog	YjbG	0.4	**0.3**	**0.3**		0.4	0.6	1.0	0.5
Regulatory functions										
DSY3163	GTPase obg	Obg	0.6	**6.1**	**6.0**		0.3	3.1	1.9	2.0
Salvage of nucleosides and nucleotides										
DSY1980	Xanthine dehydrogenase accessory factor	DSY1980	0.2	**0.3**	**0.3**	3.4	0.3	1.1	0.4	**0.2**
Sporulation and germination										
DSY2248	mraW RNA	SpoIVA	**38.0**	1.5	**3.9**	2.0	**21.0**	0.5	1.5	2.8
DSY1780	Peptidoglycan-binding domain 1 protein	CwIH	**17.8**	0.8		**4.1**		0.3		2.7
Sulfur metabolism										
DSY0226	Aryl sulfotransferase	DSY0226	**0.1**	**0.1**	0.4		0.3	1.7	0.3	**0.02**
Transcription										
DSY3222	Ribonuclease PH	Rph	0.4	**0.2**	0.9	**0.1**	0.5	0.4	0.8	0.5
Transporters										
DSY4278	Glutamine transport ATP-binding protein	GlnQ	**0.2**	0.8	1.0		**0.2**	**0.2**	1.1	**3.1**
Unknown function										
DSY3324	Putative protein	DSY3324	**8.3**	**3.4**	**3.7**		**8.3**	**4.7**	1.2	0.7
DSY1389	Putative protein	DSY1389	**61.0**	**4.0**	**10.9**		**35.7**	2.4		
DSY1674	Putative protein	DSY1674	**0.1**	**0.1**	0.7		0.4	0.2	0.4	0.5
DSY4433	Putative protein	DSY4433	**28.0**	1.8	**3.9**		**11.9**	0.5	2.5	**3.4**
DSY2525	Putative protein	DSY2525	**18.0**	1.7	**4.1**	2.5	**14.9**	0.8	2.0	0.7
DSY4860	Putative protein	DSY4860	**25.8**		**4.4**					
DSY3134	Bacterial group 1 Ig-like protein	DSY3134		**7.0**	**0.1**			**0.1**		**28.8**
DSY3352	Putative protein	DSY3352	4.3	0.9	1.4	1.0	**25.2**	0.3	**0.2**	**3.3**

4 Discussion

4.1 Physiology of *G. metallireducens* at high vs. low growth rates

4.1.1 Preference of easily degradable substrates over aromatic compounds in batch

The presence and the extent of carbon catabolite repression (CCR) in the strictly anaerobic aromatic hydrocarbon-degrading microorganism *G. metallireducens* via growth experiments were analysed. *G. metallireducens* showed a preferential consumption of acetate over benzoate and toluene. While ethanol revealed repression not only of benzoate degradation but also of acetate consumption, the fatty acid butyrate was consumed simultaneously with benzoate. This diauxic behaviour suggests a catabolite repression by acetate and ethanol. It is consistent with the fact that acetate and ethanol support higher maximum specific growth rates ([μ_{max}]) relative to aromatic compounds (Supplementary material, Table 7-2 A).

Acetate utilization is preferred over aromatic compounds by the environmentally relevant aerobic (*Acinetobacter baylyi* (Zimmermann et al., 2009)) and facultative anaerobic microorganisms (*Azoarcus* sp. strain CIB (Barragan et al., 2004), *Pseudomonas putida* (Morales et al., 2004), and *Pseudomonas stutzeri* A1501 (Li et al., 2010)). Preferential utilization of ethanol has been reported for BTEX degraders in aerobic and anaerobic microcosm experiments (Ruiz-Aguilar et al., 2002; Da Silva et al., 2005). Although preferential utilization of benzoate associated with relatively low μ_{max} has been observed (Mazzoli et al., 2007; Trautwein et al., 2011), the CCR of aromatic degradation by acetate and ethanol seems to prevail in a wide range of organisms.

4.2 Aromatic hydrocarbon degradation is not subjected to strong CCR at the molecular level

While the growth experiments demonstrated CCR of aromatic hydrocarbon degradation, proteomic analysis of *G. metallireducens* growing on acetate plus benzoate revealed that the some enzymes involved in the benzoate degradation pathway were not strictly repressed during consumption of acetate (Figure 3-1). Background expression of toluene-degrading proteins was also observed in the absence of toluene. This observation suggests that aromatic degrading-pathways are subjected to probably an incomplete CCR.

It has been suggested that aromatic inducers such as benzoate, phenol, and *p*-cresol are required for the activation of the benzoyl-CoA pathway in *G. metallireducens* (Juarez et al., 2010). Their role is to initiate transcription of *bamY* which encodes the benzoate-CoA ligase (Juarez et al., 2010). It has been shown for *G. bemidjiensis* that the produced benzoyl-CoA

binds and thus inactivates the BgeR repressor, enabling the transcription of other benzoate-degrading genes (Ueki, 2011). In the current study, the gene product of *bamA* 6-oxocyclohex-1-ene-1-carbonyl-CoA hydrolase (Q39TV7) which is regulated by the BgeR repressor in *G. bemidjiensis* (Ueki, 2011), was highly abundant not only with benzoate or toluene but also with butyrate or acetate plus benzoate in the late exponential growth phase relative to acetate or ethanol only. The significant expression of the benzoyl-CoA-degrading pathway on acetate plus benzoate suggests that in the presence of acetate, transport of benzoate is not entirely repressed and benzoate molecules can still enter the cell and induce the expression of the benzoyl-CoA pathway. The significant expression on butyrate (Figure 3-5) suggests that butyrate-derived metabolic intermediates can also participate in the induction of the benzoyl-CoA-degrading pathway leading to the simultaneous consumption of benzoate and butyrate (Figure 3-2 D).

However, it is important to mention that the protein involved in the first step of benzoate degradation, succinyl:benzoate coenzyme A transferase (Q39TZ1) (Oberender et al., 2012), was significantly abundant only on benzoate in contrast to benzoyl-CoA ligase BamY (Q39TQ2) which was not significantly expressed at any of the conditions tested. The averaged abundance of succinyl:benzoate coenzyme A transferase was 57 times higher than the one of BamY (Q39TQ2) on benzoate (Additional material, Table S11) suggesting that the CoA transferase reaction is preferred over ligation of CoA to benzoate as it is less energy demanding (Oberender et al., 2012). Since the abundance of this protein is the highest on benzoate (18 fold more abundant relative to acetate plus benzoate) and acetate plus benzoate during late exponential phase (approximately, 5 fold higher relative to the other four conditions), it is clear that its expression is related to the presence of benzoate in the medium. Although the benzoyl-CoA pathway is found to be under weak CCR control, the significant expression of the proteins involved in the first step of benzoate degradation depends only on the presence of the respective substrate.

There are contrasting reports on the repression of benzoate degradation in other aromatics-degrading microorganisms. A strong repression of the benzoyl-CoA pathway occurred in the absence of benzoate in *Azoarcus* sp. strain CIB (Barragan et al., 2004), but not in *Th. aromatica* K172 (Heider et al., 1998) or in *A. aromaticum* EbN1 (Trautwein et al., 2011).

While at the molecular level aromatic degradation pathways are not strictly repressed, a significant substrate dependent induction of substrate-activating enzymes is observed.

4.2.1 Co-expression of catabolic pathways in *G. metallireducens*

The coordinated expression of peripheral catabolic proteins described in the results section can be partially explained by the co-localization of their genes within the genome (Figure 3-5, and Table 7-4 in Supplementary material) (Rocha, 2008). Genes coding for the toluene (1.72-1.74 Mb), butyrate (1.83-1.94 Mb) and benzoate degradation (2.0-2.4 Mb) pathways occupy contiguous sections on the chromosome. Indeed, the availability of the respective substrates induces the strongest expression of proteins derived from the substrate specific cluster.

Proteins of central metabolism co-expressed during growth on butyrate, such as proteins related to valine, leucine and isoleucine-, and geraniol-metabolism, also have their encoding genes located in proximity to butyrate degradation genes. For example, the gene coding for acyl-CoA dehydrogenase *Gmet_1710* of the geraniol-degrading pathway is located next to glutaconate CoA-transferase subunit A *Gmet_1709* of butyrate metabolism. The gene coding for methylmalonyl-CoA mutase-like *Gmet_1722* of leucine and isoleucine degradation and propionate metabolism is located close to 3-hydroxyacyl-CoA dehydrogenase HbdA *Gmet_1717* of butyrate metabolism (Table 7-4 in Supplementary material). However, two proteins of the TCA cycle which were also predicted to be involved in propionate degradation Ach1 (Q39WL) and Cit1 (Q39WL2) (Aklujkar et al., 2009) were highly abundant on butyrate. They are encoded by genes which are 0.6 Mb distinct from the butyrate cluster (Table 7-4 in Supplementary material). Ach1 is predicted to transfer succinyl-CoA to propionate, while Cit1 to synthesize 2-methylcitrate from propionate and oxaloacetate (Aklujkar et al., 2009). The high abundance of these proteins on butyrate could suggest that they also take part in the activation of butyrate even if their genes are not located in the butyrate cluster.

Co-metabolism of aromatic compounds is wide-spread in different microorganisms (Foght, 2008). For example, co-expression of several degradation pathways in batch cultures with single substrates was also reported for other xenobiotic-degrading bacteria such as *P. putida* CB55 co-expressing distinct degradation pathways for theophylline and caffeine (Yu et al., 2009). *Mycobacterium aromativorans* JS19b1 co-expressed proteins involved in degradation of contaminants such as polyaromatic hydrocarbons, biphenyl, dibenzothiophene with phenanthrene and phthalate (Seo et al., 2011). The ethylbenzene degradation pathway was found to be induced when *A. aromaticum* EbN1 was cultivated on toluene only (Kuhner et al., 2005). Co-expression of other aromatic-degrading proteins (involved in *p*-cresol and phenol)

on benzoate has been shown earlier for *G. metallireducens* (Peters et al., 2007; Schleinitz et al., 2009).

Chromosomal proximity, thus, provides a partial but not full explanation of protein co-expression, for instance, suggesting that the co-expression of the aromatic pathways is mainly due to their metabolic routes overlapping with each other in *G. metallireducens*.

4.2.2 Role of PTS-like proteins

G. metallireducens is incapable of using sugars and has a rudimental enteric Gram-negative bacteria-like PTS-system. In *Geobacteraceae,* Hpr kinase (homologue of Hpr kinase of Gram-positive bacteria) is co-localized with *pts*-like genes in one operon (Boel et al., 2003). It has been suggested that the PTS proteins and Hpr kinase might be mostly involved in regulation of transcription and carbon sensing in the majority of bacteria (Cases et al., 2007). The homologue of EIIA in *P. putida*, IIA^{Ntr} was found to be involved in global regulation function rather than in control of expression of catabolic proteins (Cases et al., 2001b).

The current study aimed to gain insights into possible differential expressions of PTS-like proteins in *G. metallireducens* grown on different single substrates as well as on a mixture of acetate plus benzoate. However, the proteomic approach did not reveal differences in protein abundances of PTS-like proteins expressed on different conditions. The only observed difference was an absence of HPr^{Ntr} and EIIA on acetate plus benzoate. Previous studies on *P. putida* bearing plasmid pWW0 showed that in a *ptsO* mutant, containing a deletion of the gene coding for HPr^{Ntr}, the *Pu* promoter of an operon upstream of the toluene degradation pathway was inhibited (Cases et al., 2001a). Similarly, in our case, expression of HPr^{Ntr} was below the detection limits on acetate plus benzoate and its absence could lead to accumulation of the phosphorylated form of IIA^{Ntr} and subsequent partial CCR of the benzoyl-CoA pathway. However, it is a speculation only and this statement needs further investigation.

4.2.3 Metabolic regulation of central pathways in batch

Even though background expression of catabolic proteins in the absence of respective substrates was observed, proteins of the upper degradation pathways involved in toluene, ethanol and butyrate degradation had significantly high abundances with their respective substrates only. This suggests that peripheral pathways are regulated by changes in the enzyme concentrations of substrate-degrading proteins.

In contrast to the peripheral pathways, changes in flux through central metabolism with different substrates does not depend on enzyme concentrations. All substrates used in this

study eventually are channelled into the TCA cycle of *G. metallireducens*. The applied hierarchical regulation analysis revealed that changes in the flux of carbon through the central TCA cycle of *G. metallireducens* were primarily regulated at the metabolic level via changes in concentrations of metabolites, rather than by changes in gene expression. The advantage of metabolic regulation of the TCA cycle for *G. metallireducens* is a reduction in energetic costs as protein synthesis requires a lot of ATP (Stouthamer, 1973), and provision of plasticity in the physiological response to environmental changes.

4.2.4 Regulation of catabolic pathways in *G. metallireducens* in batch

The results of the current study suggest that *G. metallireducens* does not exhibit strong hierarchical global carbon control (that is, control by changes in protein levels) because it is adapted to habitats where conditions change only slowly, if at all, and where it lives on a mixture of carbon sources. Thus, gene regulation of *G. metallireducens* probably differs strongly from the typical r-strategists like *Enterobactereaceae* which are adapted to fast growth during sudden high substrate supply.

In conclusion, a model for regulation of catabolic pathways by *G. metallireducens* at high substrate concentrations is proposed (Figure 4-1). Due to CCR, acetate and ethanol are preferred over aromatic compounds. Although aromatic compounds contain more energy per molecule than short chain fatty acids and alcohols, for *G. metallireducens* it is more advantageous to use acetate or ethanol as they are degraded faster than aromatic compounds. Therefore, CCR controls preferential utilization of these substrates in *G. metallireducens.* Another level of regulation is the overlapping metabolism regulation (Figure 4-1). The catabolic pathways of aromatics degradation such as toluene, benzoate, phenol, and *p*-cresol coincide on the level of benzoyl-CoA. The benzoyl-CoA degradation pathway coincides with butyrate degradation pathway on the level of the fatty acid β-oxidation steps and as a result the co-expression of catabolic pathways involved in the degradation of the substrates mentioned above occurs. Central metabolic pathways, such as the TCA cycle, are characterized by regulation through changes in metabolite concentration (acetyl-CoA) rather than in gene expression (chapter 3.7.1).

Therefore, the proposed model suggests an optimized consumption of carbon sources by *G. metallireducens* in the environment: the preference for easily degradable substrates such as acetate and ethanol gives an opportunity to quickly gain energy in the presence of various substrates; a simultaneous consumption of different aromatic compounds with short fatty acid butyrate as an inducer of benzoyl-CoA pathway reflects an adaptation to multi-substrate

contaminated habitats; a metabolite-regulated central metabolism represents an energy-saving strategy.

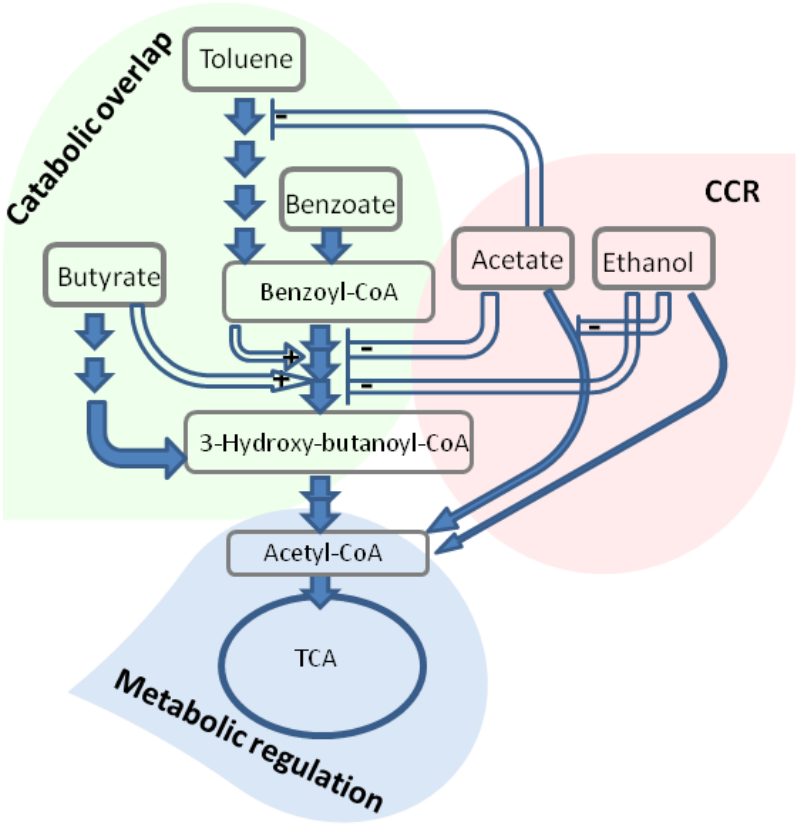

Figure 4-1 Schematic representation of proposed regulation of catabolic pathways in *G. metallireducens* at high substrate concentrations in batch cultures. Thick blue arrows represent simplified degradation pathways. Open arrows indicate positive (+) or negative (-) effect on expression of degradation pathways by a corresponding substrate.

4.2.5 Distinguishing physiological response to carbon limitation from a response to low growth rates

Carbon limitation causes slower growth rates relative to excess of carbon where microorganisms exhibit exponential growth. However, other types of limitations such as ammonium limitation, electron acceptor limitations, etc. induce a slowing down of the physiological processes as well. Therefore, under carbon limitation two general physiological responses can be distinguished: response to carbon limitation itself and response to low growth rates. As discussed in the introduction, the first response is expected to be characterized by the relief from carbon catabolite repression, search for alternative carbon substrates, and increase in abundance of enzymes transporting the limiting substrates. These

changes are specific to the type of limitation. However, the response to the low growth rates is more general and expected to be independent from the source of limitation. Changes such as decrease in protein and DNA synthesis, cell envelope modifications, and increase in signal transduction might be similar in all limiting conditions under a certain range of the growth rates. These two major physiological responses exhibited by *G. metallireducens* that was cultivated in retentostats at carbon limitation under extremely low growth rates are discussed below.

4.2.6 Carbon limitation specific physiology

i) Relief from carbon catabolite repression

In *G. metallireducens*, the degradation of acetate and benzoate proceeds through distinct peripheral metabolic pathways. Acetate can be activated via three enzymes yielding acetyl-CoA which then directly enters the TCA cycle (Aklujkar et al., 2009), while benzoate has to be subjected to much more degradation steps: activation, dearomatization, modified β-oxidation until it is converted into three molecules of acetyl-CoA and one CO_2 (Butler et al., 2007; Carmona et al., 2009). The free energy values under standard conditions for acetate and benzoate degradation are -819 kJ mol^{-1} and -3,070 kJ mol^{-1} (Eq. 6 and 7), respectively, suggesting that benzoate degradation provides more energy per acetyl-CoA produced. However, as shown in chapter 3.1, during exponential growth phase the easily degradable carbon source acetate represses the utilization of benzoate via carbon catabolite repression (CCR). The current study shows that such a repression is eliminated at low growth rates where *G. metallireducens* can utilize acetate and benzoate simultaneously.

Simultaneous consumption of aromatic compounds in carbon-limited chemostats at growth rates lower than exponential has been reported for other aromatic-degrading microorganisms: benzene was consumed together with succinate in *Ralstonia picketii* PKO1 (Bucheli-Witschel et al., 2009); *Pseudomonas putida* F1 utilized toluene and/or benzene simultaneously with succinate (Rueegg et al., 2007); *Pseudomonas putida* (pWWO) co-metabolized *o*-xylene and succinate (Duetz et al., 1994). Therefore, at carbon limitation, the presence of an easily utilizable carbon source does not block the utilization of aromatics suggesting that such a strategy can be advantageous in carbon-limited environments.

ii) Search for alternative carbon substrates

Previous investigations of proteomic and/or transcriptomic profiles expressed by various microorganisms cultivated under carbon limitation have shown presence of alternative

catabolic pathways involved in the degradation of substrates absent from the growth medium. For example, such a phenomenon has been observed for the facultative anaerobes "*Aromatoleum aromaticum*" EnN1(Trautwein et al., 2012), *E. coli* (Wick et al., 2001; Ihssen and Egli, 2005), the mixed consortia of *Pseudomonas reinekei* MT1 and *Achromobacter xylosoxidans* MT3 (Bobadilla Fazzini et al., 2009), *Lactobacillus plantarum* (Goffin et al., 2010) and the obligate aerobe *Mycobacterium smegmatis* (Berney and Cook, 2010). Ihssen and Egli (2005) suggested that under carbon limitation microorganisms relieve catabolic pathways from carbon catabolite repression in order to be able to react fast to the changing conditions in carbon-limited environments. The baseline expression of many pathways would make the organism ready to utilize all substrates which are present simultaneously. Furthermore, it would prepare the organism for utilization of other substrates that might appear but not yet present in their environment.

In the current study, during carbon-limited cultivation in retentostat the strict anaerobe *G. metallireducens* also expressed several proteins related to consumption of alternative substrates which were not present in the medium, such as butyrate and benzoate in the acetate-limited retentostat and phenol, *p*-cresol and *p*-hydroxybenzoate under acetate plus benzoate limitation. Extremely high abundances were observed for proteins involved in the first two steps of ethanol degradation for all types of carbon limitation at low growth rates in the retentostat (Table 3-3). Overexpression of alcohol dehydrogenases and aldehyde dehydrogenases was observed previously for *A. aromaticum* EbN1 (Trautwein et al., 2011) and *Mycobacterium smegmatis* (Berney and Cook, 2010) cultivated in carbon-limited chemostats. Moreover, high expression of ethanol dehydrogenase and AorA was observed for *G. metallireducens* grown in nitrate-limited chemostats compared to Fe(III) limitation (Ahrendt et al., 2007). In *E. coli*, alcohol dehydrogenase was shown to be a protector against oxidative stress (Echave et al., 2003). Induction of ethanol-degrading proteins at carbon limitation seems to be a wide spread phenomenon among various microorganisms and might be not only due to derepression of catabolic pathways but also due to oxidative stress. However, the fact that ethanol exhibits strong catabolic repression of acetate and benzoate in batch indicates its role as a preferred substrate and observation of expression of alcohol dehydrogenase together with acetate and benzoate degrading proteins during carbon-limitation indicates clearly that *G. metallireducens* relieves carbon repression at low growth rates.

However, the nitrite metabolic assay carried out on the cells harvested after 100 h of cultivation in acetate-limited retentostat contradicts the proteomic data because production of NO_2^- on ethanol or aromatic compounds has not been significant enough to conclude that consumption of these substrates took place. There is a possibility that sampling for nitrite production was done too late when nitrite was already reduced to N_2O in ethanol amended serum tubes as concentration of alcohol dehydrogenase should be extremely high as indicated by proteomic data. Meanwhile, high concentration of nitrite in acetate and butyrate containing tubes suggests that proteins, responsible for utilization of these substrates were active.

From the first glance, it seems that *G. metallireducens* expressed fewer alternative catabolic pathways in response to low growth rates relative to catabolic pathways exhibited by *E. coli* cultivated in chemostats with low growth rates. However, being a copiotroph, *E. coli* utilizes many carbon sources and as a consequence needs many enzymes for their degradation. Notably, *G. metallireducens* is able to utilize 20 carbon substrates (Lovley et al., 2011), 10 of which are aromatic compounds. Enzymes which might be involved in the peripheral catabolic pathways of four aromatic compounds benzoate, phenol, *p*-cresol and *p*-hydroxybutyrate were detected at low growth rates only. The number of easily degradable carbon substrates that might be utilized by *G. metallireducens* simultaneously at low growth rates was five (acetate, butanol, butyrate, ethanol, and pyruvate). Therefore, it is suggested that carbon limiting conditions in retentostat prepared *G. metallireducens* to utilize nearly 50 % from the carbon sources it is able to utilize. The expected general derepression of all pathways was not observed under the conditions applied.

It is important to mention that most of the chemostat experiments that have been performed until now were run at growth rates far above growth rates which are characteristic for microorganisms in the environments ($> 0.02\ h^{-1}$). The extremely low growth rates applied in the current study ($0.003\ h^{-1}$ and below) might put *G. metallireducens* in an energy-saving mode and prevent the derepression of the costly enzymes of such alternative pathways, as, for example, toluene degradation. Taking into consideration the spectrum of catabolic enzymes expressed at low growth rates during carbon limitation; *G. metallireducens* seems to perform an adaptation to habitats where aromatics and fermentation products dominate as substrates. This would be the typical anoxic habitats where primary fermenters deplete sugars, cellulose or proteins. Consequently, only few catabolic proteins from peripheral pathways were induced at low growth rates relative to previous reports (Ihssen and Egli, 2005), suggesting that at

extremely low growth rates *G. metallireducens* does not derepress all possible catabolic pathways probably due to high energy costs under extremely low growth rates.

iii) **Increase in abundance of high affinity proteins**

One of the expected physiological behaviours of microorganisms under limitation is the increase of the proteins involved in the first steps of degradation of a limiting substrate (Harder and Dijkhuizen, 1983a). In *G. metallireducens*, acetate can be activated via three different ways (Aklujkar et al., 2009): two reversible activations of acetate via succinyl:acetate coenzyme A transferases Ato-1 and Ato-2, acetate phosphorylation by acetate kinase AckA, and one irreversible activation via acetate-coenzyme A ligase AcsA. The detection of the last protein at low growth rates only together with increased abundances of AckA suggests that *G. metallireducens* applies more effective utilization of acetate when its concentration is limited in the environment. In contrast, the proteomic study of response of *Geobacteraceae* to acetate amendments in uranium contaminated site, succinyl:acetate coenzyme A transferase was suggested to be a key protein in the activation of acetate (Wilkins et al., 2009). However, the acetate concentrations during sampling for proteomic analysis were in the range of 0.6-2.5 mM. Therefore, the increase in abundance of high affinity proteins for acetate utilization was not necessary in such conditions.

Moreover, absence of benzoyl-CoA ligase at low growth rates suggests that *G. metallireducens* prefers ATP-independent activation of benzoate at conditions close to natural.

iv) **Changes in the enzymes of central catabolism**

Carbon limitation impacts not only the peripheral carbon metabolism but also the rates of central metabolism as limited flux of metabolites of a limiting substrate might decrease the expression of central catabolic pathways. Thus, it has been shown that the benzoate degrading pathway together with the TCA cycle decreased their fluxes in *Aromatoleum aromaticum* when it was cultivated in chemostats during benzoate limitation (Trautwein et al., 2012). Moreover, similar observations were done for *Geobacteraceae*. For example, previous studies on *Geobacter* sp. showed that the level of acetate limitation was reflected in the level of expression of citrate synthase gene *gltA* where the decrease in acetate concentrations were accompanied by a decrease in expression of citrate synthase transcripts (Holmes et al., 2005). Citrate synthase is the first enzyme of the TCA cycle which condensates acetyl-CoA and oxaloacetate to citrate. This enzyme was suggested to have a control over the flux to the TCA cycle and reflects a physiological state of *Geobacter* species (Bond et al., 2005). The decrease

in abundance of both citrate synthases, acetyl-CoA- (GltA) and propionyl-CoA-dependent (Gmet_1124) has been also observed in the current study during acetate limitation relative to exponential growth phase. However, due to the variability of the data in the replicates, the differences were not found to be significant. Another protein of the TCA cycle, 2-oxoglutarate ferredoxin oxidoreductase, also exhibited decrease in abundance in retentostat with its gamma subunit significantly decreased during acetate limitation relative to acetate excess in batch. However, 4Fe-4S-containing subunit delta of this protein was detected at low growth rates only. In contrast to the decrease in abundance of citrate synthase and 2-oxoglutarate ferredoxin oxidoreductase, the abundance of the second enzyme of the TCA cycle, aconitate hydratase (4Fe-4S domain-containing AcnA and Gmet_2763), which isomerizes citrate to isocitrate, was significantly increased during acetate and acetate plus benzoate limitations. Earlier, Matin et al. (1976) observed an increase in the activity of aconitate hydratase in response to a decrease in the growth rates when *Pseudomonas* sp. was cultivated in chemostats under lactate, succinate, ammonium or phosphorus limitations. Therefore, increase in abundance of aconitate hydratase in *G. metallireducens* cultivated in retentostats might be explained by the general response to low growth rates and not by the carbon limitation. Relief from the carbon catabolite control, as suggested by Matin et al (1976) cannot be responsible for increase in abundance of aconitase in *G. metallireducens*, as all other enzymes of the TCA cycle which are dependent on the same regulator would increase their abundances as well. A possible explanation for increase in the abundance of this enzyme as well as in detection of delta subunit of 2-oxoglutarate ferredoxin oxidoreductase is that 4Fe-4S domain-containing proteins are sensitive to oxidative stress (Rouault and Klausner, 1996). Proteomic data suggests that *G. metallireducens* experienced oxidative stress to some extent (see chapter 3.2). Therefore, overexpression of important 4Fe-4S domain-containing proteins might be a strategy to save their activity.

In *G. metallireducens* pyruvate can be used for refilling the TCA cycle metabolites via four different enzyme systems:

- direct oxaloacetate synthesis from pyruvate via pyruvate carboxylase (Pyc);

- oxaloacetate synthesis from pyruvate through phosphoenol-pyruvate (PEP) synthesis (PpdK, PpsA, Gmet_2100, Gmet_2101, Ppc);

- acetyl-CoA synthesis via pyruvate dehydrogenase complex (BkdA, BkdB, PdhB, PdhA, BkdF, AceF, LpdA-2, LpdA-1);

- finally, malate can be synthesized from pyruvate via malate synthase MaeB.

Increase in abundance as well as new formation of several enzymes from the first three anapleurotic reactions (Pyc, PpsA, BkdB) in retentostats might suggest a requirement in refilling of the TCA cycle with oxaloacetate and acetyl-CoA as well as an increased readiness to utilize pyruvate during carbon limitations.

Meanwhile, it has been shown for *G. sulfurreducens* that during exponential growth phase in batch, pyruvate-ferredoxin oxidoreductase (Por) is the only enzyme which reversibly produces acetyl-CoA from pyruvate (Segura et al., 2008). Segura et al. (2008) suggested that the redundant pathway of pyruvate dehydrogenase was not functional under the conditions tested. However, the current study shows that this alternative pathway for production of acetyl-CoA from pyruvate is present under low growth rates in *G. metallireducens*. Similar behaviour has been observed for *Corynebacterium glutamicum* in glucose-limited chemostats where pyruvate kinase activity was increased at low growth rates (Cocaign-Bousquet et al., 1996). Apparently, under low growth rates *G. metallireducens* increases abundances of anapleurotic enzymes involved in refilling reactions of the TCA cycle. Moreover, increase in the abundance of some gluconeogenesis-related proteins (e.g., Pyc, GapN) suggests that *G. metallireducens* might imply a strategy for carbon storage under carbon limiting conditions. However, previous studies on *Geobacteraceae* have shown increase in the abundances of phosphopyruvate hydratase which connects gluconeogenesis with PEP (Wilkins et al., 2009) in response to acetate amendments to uranium contaminated environments as well as increased abundances of irreversible PEP-forming enzymes at faster growth on Fe(III) citrate relative to Fe(III) oxide (Ding et al., 2006). These observations suggest that gluconeogenesis is overexpressed during active metabolism. The current study displays that also extreme carbon limitations favour investments of energy into gluconeogenesis as an approach to prepare for future starvation.

4.2.7 Growth rate specific physiology

Growth rate specific physiology of *G. metallireducens* is characterised by a general response that might be a programmed strategy of survival in its natural habitat where this bacterium is also exposed to energy limitation, heavy metals, oxidative stress, predators and competitors. Under such conditions, *G. metallireducens* might increase abundance of enzymes searching for alternative electron acceptors, as well as proteins involved in signal transduction, protection against oxidative stress, pathogens and competitors.

i) Search for alternative electron acceptors

Geobacteraceae are found to be predominant in many environments rich with Fe(III) (Snoeyenbos-West et al., 2000; Röling et al., 2001; Anderson et al., 2003; Cummings et al., 2003), where Fe(III) is presented in the insoluble form rather than in the solution. During the course of evolution, *Geobacteraceae* have developed strategies for an optimized reduction of insoluble Fe(III): its genome encodes large amounts of c type cytochromes (over 90) (Aklujkar et al., 2009) which are required for anaerobic respiration; it can use external electron shuttles (Lovley et al., 1998) and "nano wires"(Tremblay et al., 2012) to transfer electrons to external electron acceptors. Moreover, a chemotactic response is produced when the bacteria are exposed to insoluble electron acceptors (Childers et al., 2002). Physiological response of *G. metallireducens* to low growth rates was characterized by the expression of strategies listed above.

Although *G. metallireducens* was cultivated in retentostat in excess of soluble electron acceptor Fe(III) citrate, it induced the expression of many enzymes for alternative electron acceptors such as nitrate, oxides of Fe(III), Mn(IV), and humic acids. Increased abundance of nitrate reductases was unexpected as it has been shown earlier that *G. metallireducens* grown in batch with soluble Fe(III) citrate does not reduce nitrate (Gorby and Lovley, 1991). However, it has been shown earlier by Lin et al., (Lin et al., 2009) that cells of *G. metallireducens* cultivated in retentostat under acetate limitation were able to reduce various electron acceptors, including nitrate. The current study showed that, the cells of *G. metallireducens* taken after 300 h of cultivation in acetate-limited retentostat were able to reduce nitrate even in the absence of electron donor (Figure 3-8B). The reduction of nitrate in the absence of electron donor can be supported by the carbon storage strategy described above. Transcriptomic analysis of *G. sulfurreducens* (Aklujkar et al., 2013) and *G. uraniireducens* (Holmes et al., 2009) cultivated with insoluble Fe(III) oxides showed increased expression of *nrfA* and *nrfH* genes, coding for nitrite reductase. It has been pointed out by Aklujkar et al. (2013) that expression of these genes was connected previously to nitrogen limitation. Therefore, expression of nitrate reductase (NarG-2 and NarH-2) in the current study by *G. metallireducens* might also indicate that low growth rates trigger this bacterium to prepare for nutrient limitation.

Changes in abundances of cytochromes at low growth rates indicate that *G. metallireducens* might prepare to reduce not only soluble (Fe(III) citrate and nitrate) but also insoluble electron acceptors. Thus, several proteins of energy metabolism which were found to be growth rate-specific in the current study were recently suggested to be important for Fe(III)

oxide reduction in *G. metallireducens* (OmcN, OmcP, OmcO, CbcX, Gmet_0155) (Smith et al., 2012). Another two homologues proteins, which were related to current production (OmcZ) (Nevin et al., 2009), Fe(III) and Mn(IV) oxides (OmcB) (Aklujkar et al., 2013), humic acids and anthraquinone-2,6-disulfonate reduction (OmcZ and OmcB) (Voordeckers et al., 2010) in *G. sulffureducens,* increased their abundances in *G. metallireducens* cultivated at low growth rates in retentostat relative to batch. However, these increased abundances under low growth rates relative to batch were not found to be significantly expressed in the current study. A similar response of upregulation of many energy-related genes has been observed on transcriptomic level for a close relative of *G. metallireducens, G. uraniireducens* when it was cultivated in Fe(III) oxide-containing natural sediments taken from uranium contaminated site (Holmes et al., 2009). Therefore, the physiology of *G. metallireducens* at extremely low growth rates in retentostats might resemble its metabolic state in its natural environments.

Newly formed or increased in abundances flagella- (FliC and FliL) and pilus biogenesis-related (PilQ, PilY1-2, PilT-2, PilV-2, PilC) proteins at low growth rates indicate that *G. metallireducens* increased its motility and electron conductivity in order to reduce effectively insoluble electron acceptors typical for the natural habitats of this bacterium. For example, in *G. sulfurreducens,* transcripts of *pilY1-2, pilV-2,* and *pilC* were found to be upregulated on Fe(III) oxide relative to Fe(III) citrate (Aklujkar et al., 2013). Moreover, deletion of the *fliC* gene, responsible for expression of flagelin protein from *G. metallireducens* prevented formation of flagella and, therefore, decreased reduction of Fe(III) oxide relative to wild type (Tremblay et al., 2012).

ii) Protection against oxidative stress

Phenomena of induction of oxidative stress response has been observed for *Geobacter* species in various experiments: when *G. sulfurreducens* was cultivated with oxides of Fe(III) and Mn(IV) in batch (Aklujkar et al., 2013) and with Fe(III) citrate in chemostat (Methe et al., 2005), or when *G. uraniireducens* was cultivated in natural sediments containing Fe(III) oxide (Holmes et al., 2009) and in chemostat with Fe(III) citrate with or without oxygen exposure (Mouser et al., 2009a). Notably, soluble Fe(III) citrate was used as a reference electron acceptor in the first study and fumarate in all other studies. All cultivations were carried out under strictly anaerobic conditions with an exception for the last investigation where *G. uraniireducens* was also exposed to various concentrations of oxygen. Therefore, it seems obvious that expression of oxidative stress in *Geobacter* sp. is not related to the presence of oxygen itself but rather connected to the usage of Fe-containing electron acceptors.

The current study also revealed strong oxidative stress response by *G. metallireducens* when cultivated with soluble Fe(III) citrate in retentostat relative to the exponential growth phase in batch. This response was similar to the physiological changes expressed by *G. uraniireducens* on transcriptomic level when it was exposed to 5% of oxygen in the presence of fumarate as an electron acceptor (Mouser et al., 2009a). 11 homologues genes were found to be differentially expressed in both studies. For example, at low growth rates *G. metallireducens* newly formed cytochromes *c* (Gmet_0115) and *bd* (CydA), ferredoxin (Frx-4), and decreased abundance of NADH-quinone oxidoreductase (NuoC and NuoE-1). The first three proteins might be related in radical detoxification (Mouser et al., 2009a), while NADH oxidoreductases might be down regulated in order to avoid reaction with hydrogen peroxide which releases radicals (Imlay and Linn, 1988). Periplasmic diheme cytochrome *c* catalase (CccA) which was detected at low growth rates only in the current study, was also upregulated in *G. sulfurreducens* cultivated with Fe(III) and Mn(IV) oxides as opposed to Fe(III)-citrate (Aklujkar et al., 2013). The expression of catalase indicates the presence of hydrogen peroxide in the cells. Hydrogen peroxide can be formed from oxidation of Fe(II) by traces of molecular oxygen according to the Haber-Weiss reaction (Equation 4-1 and Equation 4-2) (Hug and Leupin, 2003).

$$Fe(II) + O_2 \rightarrow O_2^{\cdot -} + Fe(III) \qquad \text{Equation 4-1}$$

$$Fe(II) + O_2^{\cdot -} + 2H^+ \rightarrow H_2O_2 + Fe(III) \qquad \text{Equation 4-2}$$

The possible explanation for a strong induction of protection against oxidative stress is that hydrogen peroxide might react with Fe(II) via the Fenton reaction (Touati, 2000) and produce hydroxyl radicals. Apparently, *Geobacter* sp. cells require protection from radicals at any time when they grow with Fe(III) citrate (current study; (Mouser et al., 2009a)) but this requirement increases as cells are exposed to metal oxides or grow with Fe(III) citrate at low growth rates. Therefore, expression of many metal efflux proteins at low growth rates seems to be logical in order to reduce amount of Fe in the cell to decrease the rate of Fenton reaction. Moreover, efflux of soft metals such as Ag and Cu at low growth rates might be a mechanism for protection of many Fe-S cluster containing enzymes which were highly abundant at low growth rates (Xu and Imlay, 2012).

Moreover, response to reactive oxygen species is also reflected in expression of many other enzymes (Imlay, 2008). For example, enzymes which were suggested to play a role in the protection against oxidative stress (Imlay, 2008) and were detected with changed abundances

at low growth rates in the current study are the following: oxidant-resistant aconitase (AcnA), catalase for hydrogen peroxide scavenging, and thioredoxin for disulphide reduction.

iii) Increase in motility and signal transduction

The aim of the signalling proteins is to sense environmental and internal stimuli. The more complex the natural habitat of microorganisms is, the more signalling proteins bacteria encode (Galperin, 2005). *Geobacter* species are considered to possess the highest number of encoded signal transduction proteins among microorganisms with completely sequenced genomes (Galperin, 2005). The reason for such high bacterial regulation is that versatile *Geobacter* species are able to utilize many electron acceptors in the environment (Galperin, 2005). Additionally, being environmental microorganisms they are exposed to various changes in physicochemical gradients (Alexandre et al., 2004). Thus, the genome of *G. metallireducens* encodes 83 putative sensor histidine kinases and 94 proteins with response receiver domains (Aklujkar et al., 2009). Moreover, *G. metallireducens* encodes seven chemotaxis-like clusters which are involved into signal transduction while *E. coli* encodes only one (Tran et al., 2008). Histidine kinases and response receivers belong to the same two-component signal transduction system which is in the centre of signalling mechanisms in bacteria (Koretke et al., 2000). This system regulates many responses to changing environments, such as chemotaxis, biofilm formation, osmoregulation, sporulation, etc. (Koretke et al., 2000; Nowak and Tyski, 2012; Wu et al., 2012).

For *G. metallireducens,* the majority of signalling proteins which were newly formed in response to low growth rate are related to chemotaxis. As mentioned earlier, *G. metallireducens* produces flagella when exposed to insoluble electron acceptors (Childers et al., 2002). Increase and *de novo* formation of chemotaxis and flagella related proteins at low growth rates suggest that *G. metallireducens* becomes more mobile under these conditions. Detection of various other proteins related to two-component signal transduction at low growth rates only suggests that *G. metallireducens* increases expression of its sensing machinery. Taking into consideration that the same soluble electron acceptor, Fe(III)citrate was applied for cultivation of *G. metallireducens* in batch and retentostat, we suggest that extremely low growth rates "remind" *G. metallireducens* of its natural environments rich in insoluble electron acceptors.

4.2.8 Indication of other types of limitation at low growth rates

Various proteins which have been shown earlier to be indicators for nutrient limitations in the environments had contradicting patterns of expression at low and high growth rates. The

AmtB protein which is involved in ammonium transport and was suggested to be an indicator for ammonium limitation (Mouser et al., 2009b), was found at low growth rates only. However, ammonium was applied in excess during retentostat cultivation. Detection of AmtB at low growth rates only in retentostat with excess of ammonium might suggest that care should be taken when AmtB is used as a biomarker for nitrogen limitation in the environment.

The iron/manganese-dependent transcriptional regulator IdeR which regulates Fe(II) uptake in *Geobacteraceae* was detected at high growth rates only. Previously, it has been shown that expression of the IdeR regulator depends on Fe(II) concentrations in the environment (O'Neil et al., 2008). It's concentration below detection limits in retentostats with high Fe(II) concentrations is in consistency with previous observations (O'Neil et al., 2008) confirming that its expression is related to low concentrations of Fe(II). Meanwhile, proteins involved in phosphate transport (PhoU, PstB, and PstS) were detected at high growth rates only. PhoU and PstB were shown previously to be upregulated during phosphorus limitation in *Geobacteraceae* (N'Guessan et al., 2010). Detection of these proteins in batch experiments suggests higher demand for phosphorus during exponential growth phase.

Expression of the transcripts of the putative acetate transporters (AplA, AplB, and AplC) was shown to be growth rate dependent and increased in response to acetate limitation (Risso et al., 2008). The current study also showed elevated levels of AplA during retentostat cultivation with acetate plus benzoate relative to batch (FDR = 4.8) indicating that acetate transporters might increase their abundances in response to acetate limitation on enzymatic level as well.

In conclusion, retentostat cultivation allows mimicking natural environments to a great extent. Carbon limitation at extremely low growth rates makes *G. metallireducens* "remember" its natural habitat with a mixture of carbon sources such as fermentation products (acetate, ethanol, butyrate), aromatic compounds and fatty acids, and a mixture of soluble (nitrate, humic acids) and insoluble (Fe(III) and Mn(IV) oxides) electron acceptors. Moreover, these environments might be exposed to occasional influx of oxygenated surface water and various microbial predators. Apparently, low growth rates trigger various stress programmes in *G. metallireducens* in order to prepare it for future stress conditions (future provision model) (Dukan and Nystrom, 1999). These programmes are reflected in resistance to oxidation, heavy metals, and toxins. Moreover, *G. metallireducens* increases its motility capabilities in order to search for new environments.

4.3 Survival of *G. metallireducens* in groundwater aquifer contaminated with toluene

Microorganisms which are known to be the key degraders of targeted contaminants can be introduced into natural habitats in order to increase the rates of degradation. Those microbes are pre-grown on the compounds of interest and introduced in concentrated amounts into the aquifers. Such strategy is called bioaugmentation and is an alternative approach to natural attenuation where indigenous communities are the main players in the purification of the ecosystem. Bioaugmentation has been successfully applied with help of environmentally relevant microorganisms such as *Mycobacterium* sp. CHXY119 and *Pseudomonas* sp. YATO41 (in BTEX-contaminated groundwaters) (Xin et al., 2013), *Dehalococcoides* containing cultures (in chlorinated ethene contaminated groundwaters) (Schaefer et al., 2010a), *Desulfitobacterium dichloroeliminans* strain DCA1 (1,2-DCA-contaminated groundwater) (Maes et al., 2006), etc. However, there are many examples when bacteria which degrade pollutants under laboratory conditions were not able to fulfil this function under natural conditions due to inability to survive under extreme environmental conditions (Tyagi et al., 2011). Such stress conditions as pH, oxygen, toxic compounds, and predators can decrease the activity of bacteria introduced into environment. Therefore, special care should be taken when laboratory cultured microorganisms are used for bioaugmentation. It means that the existing environmental conditions should be tested to be compatible with survival of the introduced microorganisms.

The current study aimed to investigate the physiology of *G. metallireducen*s in "natural" environments in order to give insights of its response to an *in situ* contamination. The achieved data have shown that after 2.5 months of incubation in the indoor aquifer with constant injection of toluene, *G. metallireducens* was not maintained in the sediments. There are few reasons that could explain the obtained results. First of all, the dialysis bags did not prevent the sediments from outside contamination. It is possible, that the PVDF membrane was sheared by sharp sediment particles during packing or perhaps the sealed parts of the dialysis bags were disattached during the sterilization process. The choice of material and/or the construction of dialysis bags should be improved for further experiments. Additionally, *G. metallireducens* could have been outcompeted by the indigenous community. Although the dialysis bags might allow contact with natural environment, it was expected that *G. metallireducens* would be able to survive as *Geobacteraceae* are known to be the predominant species in the natural subsurface sediments containing Fe oxides (Lovley et al., 2011). In

contrast to the dialysis bags, the sediment of the indoor aquifer did not contain extensive quantities of Fe(III) hydroxide to select for Fe reducing microorganisms. Therefore, the direct competitors of *G. metallireducens* were not expected to be present in the indoor aquifer. However, T-RFLP analysis of the sediments from dialysis bags did not show fingerprints characteristic for *G. metallireducens*. Some amounts of nitrate present in the aquifer (data not shown) suggest that nitrate-reducing microorganisms, e.g., *Azoarcus* sp. and *Thauera* sp. could compete with *G. metallireducens* for toluene degradation. This suggestion is supported by the fact that indigenous communities were rich with *Azoarcus* sp. Indeed, dialysis bags were inhabited by the microbial communities from the groundwater mesocosm (Figure **3-18**). Another possibility could be that due to the apparent leakiness of constructed dialysis bags *G. metallireducens* was simply washed out from the sediments with groundwater flow or it was subjected to grazing by predators. Moreover, high concentrations of oxygen in the beginning of the experiment could have killed the oxygen-sensitive *G. metallireducens*, although a close relative, *G. uraniireducens*, has been shown to be oxygen resistant over short period of time (Mouser et al., 2009a). Additionally, high initial concentrations of toluene could be toxic for *G. metallireducens*.

Therefore, further experiments on induction of *G. metallireducens* into the natural environments should be conducted under strictly anaerobic conditions. Immobilization with chitosan or gel-based beads could be used to prevent washing out of the culture (Tyagi et al., 2011). Moreover, special attention should be given to the pre-growing conditions of inoculum of the bacteria of interest. In the current study, *G. metallireducens* was pre-grown on acetate in batch and then harvested for inoculation of the sediments. However, pre-growth on toluene which was used as a model contaminant in the indoor aquifer would have been a better strategy. Microorganisms would be already adapted to the carbon source of interest before inoculation. Additionally, the inflow concentration of toluene in the model aquifer should be lowered to represent real-life scenario. Furthermore, usage of an inoculum taken from a culture cultivated in retentostat under carbon limitation can be a promising approach. As shown in this study, *G. metallireducens* expressed several alternative catabolic pathways together with cell protecting mechanisms under carbon limitation in retentostats. There is a relief from carbon catabolite repression when *G. metallireducens* grows at low growth rates. Hence, it is expected that carbon limited cells, when introduced into the environment, will be able to utilize multiple carbon substrates simultaneously, including contaminants. Therefore, cultivation in retentostat prepares microorganisms to natural conditions to probably make them more competitive. Additionally, it provides concentrated biomass for inoculation.

4.4 Physiology of *D. hafniense* Y51 under nutrient limitations

4.4.1 Utilization of residual electron donors and acceptors under limiting conditions

Under lactate and fumarate limiting conditions, physiology of *D. hafniense* Y51 was characterized by complete or nearly complete utilization of the excessive substrates. Therefore, in the chemostats, electron donor and acceptor were not utilized according to the stoichiometric reaction (Equation 2-16). Possible scenarios of utilization of excessive substrates under lactate and fumarate limitations are given below.

The presence of alternative electron donors or partial utilization of fumarate itself as electron donor might attribute to the excessive consumption of fumarate under lactate limitation. Although the yeast extract supplied in the medium (0.01%) could provide 16 electrons and, therefore, reduce 8 mM of fumarate, the observed residual fumarate was much lower than expected (Table 3-4). Besides, the yeast extract was expected to be a preferred source of carbon for biomass formation in *D. hafniense* Y51 because lactate was almost completely excreted in the form of acetate. Therefore, the role of yeast extract in fumarate reduction under lactate limitation may be of minor contribution.

The most plausible explanation for the absence of residual fumarate in the outflow under lactate limitation is fumarate disproportionation (Equation 2-21 and Equation 2-22). The consumption of 3 to 4 mM of fumarate may yield 18 to 24 mM of H_2, enough to reduce residual fumarate (> 20 mM). The approximate 1:1 ratio between fumarate consumed and succinate produced (Table 3-4) supports this hypothesis.

The fumarate disproportionation has been described earlier for *Proteus rettgeri* (Kroger, 1974), *Syntrophobacter fumaroxidans* MPOB (Plugge et al., 1993; Plugge et al., 2012), *Desulfovibrio vulgari*s (Zaunmueller et al., 2006), and recently for *Geobacter bemidjiensis* (Aklujkar et al., 2010). In the latter two microorganisms, fumarate is partly used as an electron donor and hydrated via the fumarate hydratase with subsequent production of malate. However, further steps of malate oxidation might differ. In *G. bemidjiensis,* malate is suggested to be converted to oxaloacetate with subsequent oxidation to pyruvate via the malate dehydrogenase and the oxaloacetate decarboxylase. In contrast, in *D. vulgaris*, malate is oxidized directly to pyruvate via the malate oxidoreductase with production of CO_2 and NAD(P)H (Aklujkar et al. 2010). Further, the produced pyruvate is expected to be used for biomass production in *G. bemidjiensis* and for acetate excretion in *D. vulgaris.* However, it was shown by Plugge et al. (1993), that in *Syntrophobacter fumaroxidans* MPOB, acetyl-CoA

produced from fumarate oxidation is split via acetyl-CoA cleavage pathway into 2 mol of CO_2 and 8 mol of [H]. Notably, CO dehydrogenase/acetyl-CoA synthase subunit alpha (DSY1652) of *D. hafniense* Y51 has 44% identity to bifunctional acetyl-CoA decarbonylase/synthase complex subunit alpha/beta (Sfum_2565) of *Syntrophobacter fumaroxidans* MPOB. Therefore, similarly to *Syntrophobacter fumaroxidans* MPOB, this enzyme can be involved into splitting acetyl-CoA into [CO] and [CH_3] groups with subsequent formation of CO_2 and [H] via carbonyl- and methyl-branches of the Wood-Ljungdahl (W-L)pathway (Figure 3-25).

The genome of *D. hafniense* Y51 encodes all the possible enzymes which might be involved into the first steps of utilization of fumarate as a source of electrons: fumarate hydratase (DSY3230), malate dehydrogenase (DSY3584), pyruvate carboxylase (oxaloacetate dehydrogenase (PycB (DSY2367)), and malate oxidoreductase (YtsJ (DSY1923)). Proteomic analysis did not reveal expression of the malate dehydrogenase (DSY3584), suggesting that fumarate oxidation might proceed similarly to *D. vulgaris* via the malate oxidoreductase pathway (Figure 3-25). However, unlike *D. vulgaris, D. hafniense* Y51 does not produce acetate from fumarate oxidation because acetate production corresponded to the lactate consumption (1:1) and no additional acetate was detected under lactate limitation. Therefore, either acetyl-CoA was directed into biomass as might be suggested by significantly increasing phosphoenolpyruvate carboxykinase (PckA2 (DSY4203)) under lactate limitation relative to ammonium or fumarate limitation (Table 3-7) or it was split by the reverse W-L pathway.

Under fumarate limitation, the fermentation of residual lactate with production of CO_2 and H_2 according to Equation 2-20 is a thermodynamically favourable reaction ($\Delta G^{0'}$ = - 26.3 kJ/mol). In the absence of the required amount of fumarate, lactate fermentation is the most possible explanation due to the observed 1:1 ratio between consumed lactate and produced acetate. Furthermore, CO_2 and H_2 produced can be utilized by enzymes of the W-L pathway according to Equation 4-3 and the produced acetate might contribute to the biomass formation (Figure 3-25).

$$4H_2 + 2CO_2 \rightarrow C_2H_4O_2 + H^+ 2H_2O \qquad \text{Equation 4-3}$$

$$\Delta G^{0'} = -95 \text{ kJ/mol}$$

Previous studies have shown a discrepancy between theoretical and experimental stoichiometries in *D. hafniense* TCE-1 (Gerritse et al., 1999). In the presence of PCE, this strain exhibited higher consumption of lactate and H_2 than predicted by electron balances. One of the suggestions for this observation was a transfer of electrons to CO_2 as a possible alternative electron acceptor (Gerritse et al., 1999). Therefore, the current study provides

further support to the fact that *Desulfitobacterium* species have a flexible metabolism and are able to change the way they utilize substrates, especially, how they shuffle their electron pool, depending on the conditions they are exposed to.

4.4.2 Expression of CO_2 fixation under limiting conditions in chemostats

The increased expression of the W-L pathway under all limiting conditions relative to batch suggests that it might play an important role in the physiology of *D. hafniense* Y51. As various limitations occur in the environment, the expression of the W-L pathway might help to cope with unfavourable conditions. For example, it is known that the methyl-branch of W-L is involved into *O*-demethylation of phenyl ethers abundant in forest soils (Peng et al., 2012). Moreover, Prat et al. (2011) found that in *D. hafniense* TCE-1 cultivated in batch, some proteins from the carbonyl- (subunits of CO dehydrogenase/acetyl-CoA synthase (DSY1651 and DSY1653) and CO-dehydrogenase maturation factor (DSY1654)) and methyl-branch (proteins involved in addition of H_2 to methenyl-THF (DSY2356) and to methylene-THF (DSY0138)) of the W-L pathway were more abundant on H_2/PCE than on H_2/fumarate. The mentioned enzymes were not identified either on lactate/PCE, lactate/fumarate or H_2/fumarate. Therefore, it can be suggested that a mixture of PCE and hydrogen might trigger the expression of CO_2 fixation in *Desulfitobacterium* sp. Earlier, it has been shown that some acetogenic bacteria are able to dechlorinate PCE. The level of dechlorination depends on the activity of cobalt-containing enzymes of the W-L pathway (Terzenbach and Blaut, 1994) (Wildeman, 2003). Although, the W-L pathway was not expressed by *Desulfitobacterium* sp. in the presence of chlorinated ethenes in batch (Prat et al., 2011; Peng et al., 2012), its increased expression under limiting conditions in chemostats as has been shown in the current study for *D. hafniense* Y51 might indicate its potential for xenobiotics detoxification.

Additionally, induction of CO dehydrogenases and hydrogenases from the W-L pathway under lactate limitation could be related to an increase in hydrogen production from fumarate disproportionation. Acetyl-CoA produced could be incorporated into biomass completely, leading to the highest biomass obtained in the lactate-limited chemostat.

4.4.3 Do proteins expressed under limiting conditions reflect physiological differences?

Due to the utilization of expected residual electron donors or acceptors under respective limiting conditions, the true difference between the limitations was difficult to see. For example, fumarate and lactate degrading enzymes were overexpressed under all types of limitations. However, Figure 3-21 suggested that the differences between limiting conditions

do exist and might be observed in the protein expression pattern. Differences in the level of expression between some pathways might be reflected in the bacterial physiology. Thus, the high increase of the W-L pathway in lactate- and fumarate-limited chemostats (F2 and F4) can be explained by complete or nearly complete consumption of lactate and a requirement to search for alternative sources of electrons or by split of produced acetyl-CoA from pyruvate via acetyl-CoA cleavage pathway as suggested for *Syntrophobacter fumaroxidans* MPOB (Plugge et al., 1993). The increase of energy-related enzymes in fumarate-limited chemostats and in fumarate plus ammonium-limited chemostat A1 and the slight increase in the lactate-limited chemostat L2 can be explained by the nearly complete utilization of fumarate in these chemostats. The difference in physiology within fumarate-limited chemostats might be related to the different ratios of fumarate to lactate in the inflow (1.5-2 times lower in F1 and F3 than in chemostats F2 and F4). Apparently, the ratio of electron donor to electron acceptor in the environment might be an important factor for induction of catabolic pathways in *D. hafniense* Y51.

The expected response to limitations (Harder and Dijkhuizen, 1983b) was observed under ammonium limitation which is the increase in abundance of proteins involved into the ammonium scavenging (glutamine synthase). Additionally, nitrogen fixation could be also switched on. The genome of *D. hafniense* Y51 encodes all proteins required for nitrogen fixation. Due to the presence of yeast extract in the medium which might provide 0.014 g of nitrogen, the ammonium limitation was not characterized by a strong induction of nitrogen scavenging proteins. However, the biomass obtained in ammonium-limited chemostat was higher than the theoretical biomass which can be formed from nitrogen present in the yeast extract (>0.14 g). Therefore, although only two proteins related to nitrogen fixation increased their abundances under ammonium limitation, nitrogen fixation might occur.

Moreover, no differential expression of global regulators, which might play a role in carbon catabolite repression (CCR) between limiting conditions and exponential growth phase, was observed. Nevertheless, the induction of the W-L pathway as well as several proteins related to the utilization of some alternative electron donors (formate, butyrate, aldehyde, citrate, hydrogen) and acceptors (sulphate, sulphite) by *D. hafniense* Y51 under nutrient limiting conditions might suggest that relief from carbon catabolite repression (CCR) took place. In overall, the examination of differentially expressed proteins suggests that carbon sources such as CO_2, formate, CO, methylated compounds, lactate, acetate, and butyrate could be used by

D. hafniense Y51 under carbon limiting conditions and sulphate/sulphite under fumarate limiting conditions.

4.4.4 Stress response to limiting conditions in chemostat

Limiting conditions are well known to be strong stress factors for bacteria. The protective mechanisms against stress are sporulation, increase in motility, biofilm formation, toxin production, and induction of various efflux pumps (Rangel, 2011). The response of *D. hafniense* to limitations applied in the current study was characterized by spore formation, which was also reflected on the proteomic level. The ability of several *Desulfitobacterium* strains to sporulate was described previously (Villemur et al., 2006; Kim et al., 2012). It is well known that spore formation is the most dramatic response to nutrient limitations that can be triggered by a depletion of carbon, nitrogen or phosphorus sources from the environment (Moat et al., 2002). Moreover, sporulation is not simply a way to survive under the occasional stress. Spore forming organisms take advantage of their capabilities to populate a variety of inhospitable environments (Nicholson et al., 2000). Therefore, the ability of *D. hafniense* Y51 to form spores under limiting conditions in chemostat represents its strategy to look for more favourable environments.

In overall, applied limitations did not lead to induction of various strong stress responses in *D. hafniense* Y51, suggesting that sporulation is a preferred solution to escape conditions of electron donor, electron acceptor and ammonium limitations.

In order to survive, *D. hafniense* Y51 is able to adapt its physiology to limiting conditions. When exposed to carbon limitations at low growth rates, limiting conditions in chemostat might force *D. hafniense* Y51 to resemble its behaviour to natural habitats characterized by low amounts of various carbon substrates, electron donors and nitrogen sources. Thus, the W-L pathway expressed by *D. hafniense* Y51 might not only help to gain additional carbon from CO_2 but also assist in oxidizing compounds characteristic of their environments (e.g., products of lignin degradation, butyrate, formate, sulphate, etc.) or dechlorinated xenobiotic contaminants such as PCE. Furthermore, *D. hafniense* Y51 exhibits a highly flexible metabolism via switching between reduction-oxidation reactions and fermentation depending on the conditions applied. Thus, under fumarate limiting conditions, it ferments lactate while under lactate limiting conditions it might disproportionate fumarate. Moreover, formation of spores under limiting conditions shows that *D. hafniense* Y51 is able to cope with stress conditions. Additionally, cultivation of *D. hafniense* Y51 in carbon-limited chemostat prior to

its introduction into aquifers contaminated with chlorinated compounds might prepare *D. hafniense* Y51 for future environmental constraints. Therefore, such an approach can assist in a successful outcome of bioaugmentation strategies.

5 General conclusions and outlook

5.1 General conclusions

Investigation of *in situ* physiology of bacteria that are capable of degrading pollutants in groundwater is important for understanding how microorganisms survive under environmental conditions. Various batch experiments conducted in the laboratory gave information on the mineralization rates, degradation products formed, activation pathways, toxicity, etc. However, all this information can become ineffective when the microorganisms introduced into the ecosystems contaminated with pollutants of interest are not able to cope with the provided conditions. Therefore, physiological studies under natural or closely to natural conditions represent necessary steps towards development of successful bioremediation strategies. Moreover, insights into *in situ* physiology of bacteria exposed to xenobiotics gives important information on improvements in the field of bioremediation monitoring. For example, the identification of key genes, enzymes, or metabolites during degradation of pollutants can be used for construction of biomarkers specific to certain conditions. Correlation between physiology and *in situ* conditions can answer the questions on requirements of certain nutrients for better performance of biodegradation.

The current study addressed this aim by focusing on extending our knowledge on the physiology of two key anaerobic degraders in contaminated groundwater: the aromatic hydrocarbon-degrading *G. metallireducens* and the halogenated compounds-degrading *D. hafniense* Y51. The physiology of these model microorganisms under conditions of extremely low growth rates (in case of *G. metallireducens*) and various limitations (in case of *D. hafniense* Y51) has not been studied before.

The exploration of expressed proteomes showed that being environmentally relevant the examined microorganisms exhibit strong physiological flexibility. Thus, during carbon excess, *G. metallireducens* prefers the easily degradable substrates acetate and ethanol over aromatic compounds, while under carbon limitation it is able to degrade acetate and benzoate simultaneously. *D. hafniense* Y51, in turn, induces CO_2 and N_2 fixation as a response to electron donor/acceptor and ammonium limitations, respectively. Moreover, under energy or electron donor limitations, *D. hafniense* performs maximum use of available sources of energy and carbon. Such behaviour is in the line with the physiology of the copiotroph *E. coli* under carbon limitations. However, *E. coli* is not an environmentally relevant microorganism. Therefore, it seems that such a strategy to induce many catabolic pathways for alternative substrates under carbon and/or energy limitations is a universal microbial behaviour. Moreover, the absence of carbon catabolite control under carbon limiting conditions in the

environment might enable microorganisms such as *Geobacter* sp. and *Desulfitobacterium* sp. to utilize xenobiotics simultaneously with easily degradable substrates. Subsequently, application of *Geobacter* sp. and *Desulfitobacterium* sp. to purify groundwater containing traces of pollutants is an attractive approach.

Therefore, these two different microorganisms isolated from distinct habitats apply similar strategies to cope with limiting conditions. Both *G. metallireducens* GS-15 and *D. hafniense* Y51 increase expression of high affinity systems to consume limiting substrates or nutrients together with several catabolic pathways directed to consumption of alternative substrates. Proteome analysis suggests that both microorganisms might exhibit relief of alternative catabolic pathways from carbon catabolite repression during electron donor and/or acceptor limitations. The absence of regulation of catabolic pathways might be an efficient strategy under limiting conditions (Hoehler and Jorgensen, 2013). In such a way bacteria are able to express various degradation systems and perform mineralization of pollutants which are normally less preferred during conditions of carbon excess. Additionally, both bacteria investigated in the current study applied specific strategies to escape unfavourable environments via induction of chemotaxis- (*G. metallireducens*) and spore-related (D. *hafniense* Y51) enzymes.

Moreover, extremely low growth rates induced by carbon limitation led to a stimulation of various protective systems by *G. metallireducens*. In *D. hafniense* Y51, the general response to low growth rates during limitations is characterized by slowing down the metabolic rates and induction of spore formation processes. For *G. metallireducens*, the specific response to low growth rates was reflected in expression of proteins related to oxidative stress, metal efflux and various alternative electron acceptors. As mentioned in the discussion, the latter proteins have been found to be expressed by *G. metallireducens* in natural sediments. Habitats where *G. metallireducens* is usually found are characterized with high amounts of metals which might cause toxic and oxidative stress to bacteria. Hence, it seems that under low growth rates such as 0.003 h^{-1} and below, it switches on a general stress programme devoted to coping with all possible environmental constraints characteristic for a given environment.

Consequently, the pre-cultivation of microorganisms of interest at extremely low growth rates under laboratory conditions prior to their introduction into ecosystems containing persistently low amounts of contaminants might be a reasonable solution to achieve possible cleaning of the environment.

5.2 Future experiments based on proteomic studies of physiology of *G. metallireducens* at high vs. low growth rates

The outcome of the current study provides background for further investigations of the physiology of microorganisms of interest. Proteomic analysis is of descriptive nature as it only indicates that certain proteins or pathways might be important under specific growth conditions. But the confirmation of the processes suggested by proteomics should be done via application of metabolomics or enzyme activity assays. For example, expression of the benzoyl-CoA pathway in the presence of butyrate as a sole carbon source when *G. metallireducens* was cultivated in batch requires further support by enzyme and metabolite analyses. Two explanations exist for the expression of benzoyl-CoA pathway in the presence of butyrate: firstly, butyryl-CoA, an intermediate of butyrate degradation, could be involved in the induction of benzoyl-CoA pathway; secondly, similarly to what has been observed for the syntrophic microorganism *Syntrophus aciditrophicus* (Mouttaki et al., 2007) where cyclic molecules of cyclohexane and benzoate were produced from the fatty acid crotonate, crotonoyl-CoA, a common intermediate of benzoate and butyrate degradation, might trigger reductive direction of the benzoyl-CoA pathway. Confirmation of one of these hypotheses might suggest that the presence of butyrate-excreting microorganisms in the environment might be advantageous for degradation of aromatic compounds by *G. metallireducens*.

More detailed insights into CCR mechanisms in *G. metallireducens* can attribute to our understanding of the consumption of substrates by this bacterium in the environment with multiple carbon sources present. Thus, recently developed genetic system for *G. metallireducens* (Tremblay et al., 2012) can be applied to further elucidate the role of possible candidates for regulation of CCR in *Geobacter* sp. on molecular level. No studies have been done so far on investigation of CCR in this important species. The achieved proteomic studies suggested that proteins of PTS-system such as HPr^{Ntr} and EIIA might be involved in sensing carbon concentrations in the environment with subsequent triggering of appropriate response. Construction of knock-out mutants of the corresponding genes or analysis of phosphorylation of gene products of interest can confirm or falsify the suggested hypothesis. One possible metabolite which might play a role in the regulation of CCR in *G. metallireducens* is acetyl-CoA. Elevated levels of acetyl-CoA in the presence of preferred substrates (acetate or ethanol) might block the degradation of less preferred substrates such as aromatic compounds. The analysis of the concentration of this metabolite during the cultivation with two different

substrates in batch can give additional information on regulation of CCR on metabolic level in *Geobacter* sp.

Moreover, variations in consumption of the substrates acetate plus benzoate in replicated retentostats might suggest that the *G. metallireducens* population is divided into two subpopulations specialized on one carbon source each and that sizes of these populations might vary over time. Therefore, cultivation in the presence of ^{13}C labelled and unlabelled substrates might clarify whether this division in bacterial population exists and whether each population is specialized on one certain compound or whether single cells are able to utilize two compounds simultaneously. Incorporation of ^{13}C into the cells can be investigated by Raman microscopy (Huang et al., 2004), protein based stable isotope probing (protein-SIP) (Jehmlich et al., 2008a) or FISH-MAR (Wagner et al., 2006). Raman microscopy or FISH-MAR allow to distinguish the cells which utilized ^{13}C labelled carbon source from the unlabelled cell population which mineralized different substrate. Protein-SIP is an alternative approach to microscopy and may give help to identify pathways involved in the degradation of labelled substrate from unlabelled one. Moreover, for future experiments on cultivation of *G. metallireducens* in retentostat other soluble electron acceptors (for example humic acids, or nitrate) should be chosen instead of Fe(III) citrate. Although test experiments did not exhibit problems, later experiments conducted with Fe(III) citrate were characterized with Fe precipitation and blockage of the filter unit. Therefore, no appropriate estimation of biomass in the culture was possible.

Besides, transcriptomic analysis of genes expressed under low growth rates relative to high growth rates would be a good approach to confirm results obtained with proteomics and to give insights into correlation between transcription and translation under extremely low growth rates. Catabolomic approaches devoted to the investigation of functionality of expressed catabolic pathways might also be helpful. The nitrate assay used in this study failed to provide sufficient information on utilization patterns of substrates that were supposed to be utilized according to the proteomic analysis. Unfortunately, bacterial cells were reacting with nitrate even in the absence of substrates, suggesting that cell might have carbon storage or as has been suggested by the research group of D. Lovley, *Geobacteraceae* might store electrons in their cytochromes under electron acceptor-limiting conditions (Lovley et al., 2011). Thus, in case of *G. metallireducens*, analysis of degradation rates of the substrates of interest by cells taken from retentostat is a better approach instead of monitoring of reduction rates of electron acceptor. Similarly to the studies on *E. coli* which were conducted by the research

group of Th. Egli (Wick et al., 2001; Ihssen and Egli, 2005; Franchini and Egli, 2006), the conjunction of transcriptomic, proteomic and catabolomic analysis will close the current gaps in the obtained knowledge as well as provide a broad and deep picture on the physiology of *G. metallireducens* under growth rates close to natural conditions.

5.3 Future experiments based on proteomic study of *D. hafniense* cultivated under limiting conditions in chemostats

In order to prove the suggested mechanisms of utilization of residual electron donor and acceptor during limiting conditions in chemostats by *D. hafniense* Y51, several experiments should be conducted.

Firstly, *D. hafniense* Y51 should be cultivated in batch experiments where lactate or fumarate is used as a sole source of energy and carbon.

Secondly, the reduction of CO_2 should be monitored in fumarate-limited chemostats in order to demonstrate the role of the Wood-Ljungdahl pathway in coping with energy limitations. Moreover, a simple batch experiment with lactate as a carbon source and CO_2 in a form of ^{13}C labelled carbonate buffer could be done to determine the ability of *D. hafniense* Y51 to reduce CO_2.

In order to confirm proteomic results, microarray analysis has been run in parallel. However, the analysis has not been completed. Future comparison of the patterns of gene expression accompanied by proteomic analysis under different limiting conditions related to gene expression at maximum growth rates will help to elucidate the complete physiological response of *D. hafniense* Y51 to limitations in chemostat.

5.4 Future perspectives

Physiological responses of microorganisms to changing environment can be investigated on kinetic, metabolic and molecular level. In the light of recent technological developments the last approach becomes more and more attractive to the researchers. One only needs to have sequenced genomes available, good techniques for isolation of genes and/or proteins and bioinformatic tools in order to give detailed insights into adaptive physiology. The increasing accumulation of sequenced bacterial genomes together with continuous enhancement of analytical tools offers captivating opportunities for application of transcriptomic and proteomic analysis not only to pure cultures but also to mixed microbial communities.

To date, most of the physiological studies have been focused on gene expression and postgenomic translational modifications in pure cultures. Indeed, without detailed examination of simplified systems it is impossible to explain more complicated setups. Such an approach is a preparatory stage for investigation of bacterial behaviour in the natural environment.

However, extrapolation of laboratory results to the field is not always possible. For example, biomarkers, provided by investigation of a limiting condition in the laboratory, can have unexpected expression in the environment due to other limiting or stress conditions which were not taken into account in the laboratory (Elifantz et al., 2010). Therefore, confirmation of achieved results should be done in the systems resembling limiting conditions as close as possible. In this respect, the current study made an attempt to investigate the physiology of *G. metallireducens* under conditions close to natural: carbon limitation accompanied with extremely slow growth. The advantage of the current study was the possibility to accumulate large amounts of biomass for proteomic analysis. One might argue that cultivation in retentostat is still not a perfect representation of the natural conditions where microorganisms are present in communities and dense biomasses are usually not observed. Another important difference between retentostat and natural environments is that microorganisms are cultivated in the liquid medium in retentostat while they are attached to the sediments in their natural habitats. For that reason, investigation of microbial physiology in the sediment columns is of strong interest.

Additional physiological studies on consumption of multiple carbon and electron sources in retentostat, sediment columns or model aquifers are necessary. For example, varying the supply of different electron acceptors and donors into model aquifers containing microbial communities will give further answers whether observed relief from carbon catabolite repression under low growth rates is characteristic for many environmentally relevant microorganisms. Moreover, co-culturing of *G. metallireducens* with other microorganisms in retentostat may give further insights on its physiology within microbial communities.

Further investigations of *in situ* physiology in contaminated aquifers are required. Collection of metatranscriptomic and metaproteomic data from different ecosystems across gradients of various environmental factors might be a good approach to relate levels of gene or protein expression to the strength of the factors.

According to Konopka and Wilkins (2012), the investigation of bacterial physiology under laboratory conditions will still remain important in future years. It is related to the fact that

laboratory experiments provide solid ground for field investigations. Cultivation of other important degraders, for example, polyaromatic hydrocarbon-utilizing sulphate reducers or halogenated compounds-respiring bacteria under conditions close to natural with subsequent examination of expressed proteomes will give valuable insights into their physiologies during degradation of pollutants in the environments.

After accumulation of extensive knowledge on bacterial behaviour in pure cultures under laboratory conditions, researchers started to draw their attention to the environment. Thus, a lot of information has been collected on the response of *Geobacter* species to various but single environmental constraints such as phosphorus (N'Guessan et al., 2010), nitrogen (Holmes et al., 2004; Mouser et al., 2009b; Yun et al., 2011), iron (O'Neil et al., 2008) and acetate limitations (Elifantz et al., 2010), oxidative (Mouser et al., 2009a), and heavy metal stress (Holmes et al., 2009). All these studies investigated the abundances of transcripts and enzymes in the field or in the sediments taken from the field. The choice of biomarkers reflecting limiting conditions was based on the preliminary observations of laboratory conditions. The achieved knowledge gave a basis for identification of nutrient limitation biomarkers in the field. The advantage of such approaches is the fast screening of numerous environmental samples taken from bioremediated environments for indicators of *in situ* physiological status of key microorganisms.

However, in order to indicate more detailed information on the physiological status of bacteria in the field, "omic" approaches under natural conditions are required. To date, only a few relevant studies were conducted. For example, metaproteomic tools were applied to investigate snapshots of the protein-abundance levels in acid mine drainage biofilm communities (Ram et al., 2005); metabolic pathways in enhanced biological phosphorus removal (Wilmes et al., 2008); metaproteome of microbial communities in phosphate-depleted water of the Sargasso Sea (Sowell et al., 2009); expression of membrane proteins in South Atlantic surface waters along environmental gradients (Morris et al., 2010); or investigation of the metaproteome expressed during acetate amendments into aquifer contaminated with uranium (Wilkins et al., 2009; Callister et al., 2010). The studies mentioned above were carried out in the environments where collection of bacterial biomass was relatively easy, e.g., by collecting the biofilms (in case of acid mine drainage biofilm community) or pumping the environmental water (sea water or groundwater) with subsequent concentration of the cell biomass on the filter. However in groundwater, most of the bacteria are attached to the sediment which makes it difficult to extract significant amounts of biomass

for proteomic analysis. Therefore, development of effective techniques for extraction of proteins from subsurface sediments together with improvement of sensitivity of mass spectrometry used for identification of proteins in the environmental samples is necessary.

In conclusion, the current study gave insights into the "hidden physiology" of bacteria under extremely low growth rates. The obtained results proved adaptive capacities of microorganisms, such as increase in affinity to limiting substrates, derepression of several catabolic pathways, induction of redundancy in central metabolism, increase in motility. The expression of enzymes involved in the utilization of the substrates which are not present in the environment at the moment is energetically expensive. However, under carbon (energy)-limiting conditions, microorganisms choose this strategy in order to be able to react fast when the required substrates appear. Moreover, limiting factors leading to slowing down of growth rates made bacteria to resemble their natural habitats by increasing the abundance of alternative electron acceptors, metal efflux proteins and enzymes related to oxidative stress. *D. hafniense* Y51 which was cultivated in chemostat also exhibited strong adaptive response to limiting conditions. However, many questions remained unclear: Do other environmentally important species behave similar to *G. metallireducens* and *D. hafniense* under *in situ*-like limiting conditions? Which physiological characteristics enable microorganisms such as *Geobacter* sp. to compete with natural communities when introduced to a new environment? Which molecular mechanisms govern relief from carbon catabolite control under carbon or energy limiting conditions in the model anaerobic xenobiotic-degrading microorganisms such as *Geobacter* sp. and *Desulfitobacterium* sp.?

Future work is warranted to discover more fascinating facts in the physiology of anaerobic degraders of contaminants in polluted groundwater.

6 References

Ahrendt, A.J., Tollaksen, S.L., Lindberg, C., Zhu, W., Yates, J.R., III, Nevin, K.P. et al. (2007) Steady state protein levels in *Geobacter metallireducens* grown with iron (III) citrate or nitrate as terminal electron acceptor. *Proteomics* **7**: 4148-4157.

Aklujkar, M., Krushkal, J., DiBartolo, G., Lapidus, A., Land, M.L., and Lovley, D.R. (2009) The genome sequence of *Geobacter metallireducens*: features of metabolism, physiology and regulation common and dissimilar to *Geobacter sulfurreducens*. *BMC Microbiology* **9**: 109.

Aklujkar, M., Young, N.D., Holmes, D., Chavan, M., Risso, C., Kiss, H.E. et al. (2010) The genome of *Geobacter bemidjiensis*, exemplar for the subsurface clade of *Geobacter* species that predominate in Fe(III)-reducing subsurface environments. *BMC Genomics* **11**.

Aklujkar, M., Coppi, M.V., Leang, C., Kim, B.-C., Chavan, M.A., Perpetua, L.A. et al. (2013) Proteins involved in electron transfer to Fe(III) and Mn(IV) oxides by *Geobacter sulfurreducens* and *Geobacter uraniireducens*. *Microbiology* **doi:10.1099/mic.0.064089-0**.

Alexa, A., Rahnenfuehrer, J., and Lengauer, T. (2006) Improved scoring of functional groups from gene expression data by decorrelating GO graph structure. *Bioinformatics* **22**: 1600-1607.

Alexandre, G., Greer-Phillips, S., and Zhulin, I.B. (2004) Ecological role of energy taxis in microorganisms. *FEMS Microbiol Rev* **28**: 113-126.

Allison, C., and Macfarlane, G.T. (1990) Regulation of protease production in *Clostridium sporogenes*. *Appl Environ Microb* **56**: 3485-3490.

Ampe, F., and Lindley, N.D. (1995) Acetate utilization is inhibited by benzoate in *Alcaligenes eutrophus*: evidence for transcriptional control of the expression of acoE coding for acetyl coenzyme A synthetase. *J Bacteriol* **177**: 5826-5833.

Ampe, F., Leonard, D., and Lindley, N.D. (1998) Repression of phenol catabolism by organic acids in *Ralstonia eutropha*. *Appl Environ Microbiol* **64**: 1-6.

Anderson, R.T., Vrionis, H.A., Ortiz-Bernad, I., Resch, C.T., Long, P.E., Dayvault, R. et al. (2003) Stimulating the *in situ* activity of *Geobacter* species to remove uranium from the groundwater of a uranium-contaminated aquifer. *Appl Environ Microb* **69**: 5884-5891.

Anneser, B., Einsiedl, F., Meckenstock, R.U., Richters, L., Wisotzky, F., and Griebler, C. (2008) High-resolution monitoring of biogeochemical gradients in a tar oil-contaminated aquifer. *Appl Geochem* **23**: 1715-1730.

Aranda-Olmedo, I., Marin, P., Ramos, J.L., and Marques, S. (2006) Role of the *ptsN* gene product in catabolite repression of the *Pseudomonas putida* TOL toluene degradation pathway in chemostat cultures. *Appl Environ Microbiol* **72**: 7418-7421.

Arbige, M., and Chesbro, W. (1982) Very slow growth of *Bacillus polymyxa*: stringent response and maintenance energy. *Arch Microbiol* **132**: 338-344.

Arneth, J.D., Milde, G., Kerndorff, H., and Schlyer R (1989) Waste deposit influences on groundwater quality as a tool for waste type and site selection for final storage quality. In *The landfill-Lecture notes in earth sciences*. Baccini, P. (ed). Berlin: Springer Verlag.

Ayoubi, P.J., and Harker, A.R. (1998) Whole-cell kinetics of trichloroethylene degradation by phenol hydroxylase in a *Ralstonia eutropha* JMP134 derivative. *Appl Environ Microbiol* **64**: 4353-4356.

Barragan, M.J.L., Carmona, M., Zamarro, M.T., Thiele, B., Boll, M., Fuchs, G. et al. (2004) The *bzd* gene cluster, coding for anaerobic benzoate catabolism, in *Azoarcus* sp strain CIB. *J Bacteriol* **186**: 5762-5774.

Bartfeld, S., Engels, C., Bauer, B., Aurass, P., Flieger, A., Brueggemann, H., and Meyer, T.F. (2009) Temporal resolution of two-tracked NF-kappa B activation by *Legionella pneumophila*. *Cell Microbiol* **11**: 1638-1651.

Bastida, F., Rosell, M., Franchini, A.G., Seifert, J., Finsterbusch, S., Jehmlich, N. et al. (2010) Elucidating MTBE degradation in a mixed consortium using a multidisciplinary approach. *FEMS Microbiol Ecol* **73**: 370-384.

Baun, A., Reitzel, L.A., Ledin, A., Christensen, T.H., and Bjerg, P.L. (2003) Natural attenuation of xenobiotic organic compounds in a landfill leachate plume (Vejen, Denmark). *J Contam Hydrol* **65**: 269-291.

Bazylinski, D.A., Dean, A.J., Schuler, D., Phillips, E.J.P., and Lovley, D.R. (2000) N-2-dependent growth and nitrogenase activity in the metal-metabolizing bacteria, *Geobacter* and *Magnetospirillum species*. *Environ Microbiol* **2**: 266-273.

Berney, M., and Cook, G.M. (2010) Unique flexibility in energy metabolism allows mycobacteria to combat starvation and hypoxia. *Plos One* **5**.

Bhuyan, S.J., and Latin, M.R. (2012) BTEX Remediation under challenging site conditions using *In-situ* ozone injection and soil vapor extraction technologies: a case study. *Soil Sediment Contam* **21**: 545-556.

Biegert, T., Fuchs, G., and Heider, F. (1996) Evidence that anaerobic oxidation of toluene in the denitrifying bacterium *Thauera aromatica* is initiated by formation of benzylsuccinate from toluene and fumarate. *Eur J Biochem* **238**: 661-668.

Bleichrodt, F.S., Fischer, R., and Gerischer, U.C. (2010) The beta-ketoadipate pathway of *Acinetobacter baylyi* undergoes carbon catabolite repression, cross-regulation and vertical regulation, and is affected by Crc. *Microbiol-SGM* **156**: 1313-1322.

Blencke, H.M., Reif, I., Commichau, F.M., Detsch, C., Wacker, I., Ludwig, H., and Stulke, J. (2006) Regulation of citB expression in *Bacillus subtilis*: integration of multiple metabolic signals in the citrate pool and by the general nitrogen regulatory system. *Arch Microbiol* **185**: 136-146.

Bobadilla Fazzini, R.A., Bielecka, A., Quintas, A.K.P., Golyshin, P.N., Preto, M.J., Timmis, K.N., and dos Santos, V.A.P.M. (2009) Bacterial consortium proteomics under 4-chlorosalicylate carbon-limiting conditions. *Proteomics* **9**: 2273-2285.

Boel, G., Mijakovic, I., Maze, A., Poncet, S., Taha, M.K., Larribe, M. et al. (2003) Transcription regulators potentially controlled by HPr kinase/phosphorylase in gram-negative bacteria. *J Mol Microb Biotech* **5**: 206-215.

Bond, D.R., Mester, T., Nesbo, C.L., Izquierdo-Lopez, A.V., Collart, F.L., and Lovley, D.R. (2005) Characterization of citrate synthase from *Geobacter sulfurreducens* and evidence for a family of citrate synthases similar to those of eukaryotes throughout the *Geobacteraceae*. *Appl Environ Microb* **71**: 3858-3865.

Bradford, M.M. (1976) A rapid and sensitive method for the quantitation of microgram quantities of protein utilizing the principle of protein-dye binding. *Anal Biochem* **72**: 248-254.

Braunschweig, J., Bosch, J., Heister, K., Kuebeck, C., and Meckenstock, R.U. (2012) Reevaluation of colorimetric iron determination methods commonly used in geomicrobiology. *J Mirobiol Meth* **89**: 41-48.

Brosch, M., Yu, L., Hubbard, T., and Choudhary, J. (2009) Accurate and sensitive peptide identification with Mascot Percolator. *J Proteome Res* **8**: 3176-3181.

Bucheli-Witschel, M., Hafner, T., Ruegg, I., and Egli, T. (2009) Benzene degradation by *Ralstonia pickettii* PKO1 in the presence of the alternative substrate succinate. *Biodegradation* **20**: 419-431.

Butler, J.E., He, Q., Nevin, K.P., He, Z.L., Zhou, J.Z., and Lovley, D.R. (2007) Genomic and microarray analysis of aromatics degradation in *Geobacter metallireducens* and comparison to a *Geobacter* isolate from a contaminated field site. *BMC Genomics* **8**: 180.

Callister, S.J., Wilkins, M.J., Nicora, C.D., Williams, K.H., Banfield, J.F., VerBerkmoes, N.C. et al. (2010) Analysis of biostimulated microbial communities from two field experiments reveals temporal and spatial differences in proteome profiles. *Environ Sci Technol* **44**: 8897-8903.

Carmona, M., Teresa Zamarro, M., Blazquez, B., Durante-Rodriguez, G., Juarez, J.F., Valderrama, J.A. et al. (2009) Anaerobic catabolism of aromatic compounds: a genetic and genomic view. *Microbiol Mol Biol R* **73**: 71.

Cases, I., Perez-Martin, J., and de Lorenzo, V. (1999) The IIA(Ntr) (PtsN) protein of *Pseudomonas putida* mediates the C source inhibition of the sigma(54)-dependent *Pu* promoter of the TOL plasmid. *J Biol Chem* **274**: 15562-15568.

Cases, I., Velazquez, F., and de Lorenzo, V. (2001a) Role of *ptsO* in carbon-mediated inhibition of the *Pu* promoter belonging to the pWWO *Pseudomonas putida* plasmid. *J Bacteriol* **183**: 5128-5133.

Cases, I., Velazquez, F., and de Lorenzo, V. (2007) The ancestral role of the phosphoenolpyruvate-carbohydrate phosphotransferase system (PTS) as exposed by comparative genomics. *Res Microbiol* **158**: 666-670.

Cases, I., Lopez, J.A., Albar, J.P., and De Lorenzo, V. (2001b) Evidence of multiple regulatory functions for the PtsN (IIA(Ntr)) protein of *Pseudomonas putida*. *J Bacteriol* **183**: 1032-1037.

Chauvaux, S., Paulsen, I.T., and Saier, M.H. (1998) CcpB, a novel transcription factor implicated in catabolite repression in *Bacillus subtilis*. *J Bacteriol* **180**: 491-497.

Chen, Y.D., Barker, J.F., and Gui, L. (2008) A strategy for aromatic hydrocarbon bioremediation under anaerobic conditions and the impacts of ethanol: A microcosm study. *J Contam Hydrol* **96**: 17-31.

Chesbro, W., Evans, T., and Eifert, R. (1979) Very slow growth of *Escherichia coli*. *J Bacteriol* **139**: 625-638.

Childers, S.E., Ciufo, S., and Lovley, D.R. (2002) *Geobacter metallireducens* accesses insoluble Fe(III) oxide by chemotaxis. *Nature* **416**: 767-769.

Choi, K.Y., Zylstra, G.J., and Kim, E. (2007) Benzoate catabolite repression of the phthalate degradation pathway in *Rhodococcus* sp strain DK17. *Appl Environ Microbiol* **73**: 1370-1374.

Cocaign-Bousquet, M., Guyonvarch, A., and Lindley, N.D. (1996) Growth rate-dependent modulation of carbon flux through central metabolism and the kinetic consequences for glucose-limited chemostat cultures of *Corynebacterium glutamicum*. *Appl Environ Microbiol* **62**: 429-436.

Cowles, C.E., Nichols, N.N., and Harwood, C.S. (2000) BenR, a XylS homologue, regulates three different pathways of aromatic acid degradation in *Pseudomonas putida*. *J Bacteriol* **182**: 6339-6346.

Cox, J., and Mann, M. (2008) MaxQuant enables high peptide identification rates, individualized p.p.b.-range mass accuracies and proteome-wide protein quantification. *Nat Biotechnol* **26**: 1367-1372.

Cox, J., Neuhauser, N., Michalski, A., Scheltema, R.A., Olsen, J.V., and Mann, M. (2011) Andromeda: a peptide search engine integrated into the MaxQuant environment. *J Proteome Res* **10**: 1794-1805.

Cummings, D.E., Snoeyenbos-West, O.L., Newby, D.T., Niggemyer, A.M., Lovley, D.R., Achenbach, L.A., and Rosenzweig, R.F. (2003) Diversity of *Geobacteraceae* species inhabiting metal-polluted freshwater lake sediments ascertained by 16S rDNA analyses. *Microb Ecol* **46**: 257-269.

Da Silva, M.L.B., Ruiz-Aguilar, G.M.L., and Alvarez, P.J.J. (2005) Enhanced anaerobic biodegradation of BTEX-ethanol mixtures in aquifer columns amended with sulfate, chelated ferric iron or nitrate. *Biodegradation* **16**: 105-114.

Daniels, C., Godoy, P., Duque, E., Antonia Molina-Henares, M., de la Torre, J., Maria del Arco, J. et al. (2010) Global regulation of food supply by *Pseudomonas putida* DOT-T1E. *J Bacteriol* **192**: 2169-2181.

Davidson, M.M., Bisher, M.E., Pratt, L.M., Fong, J., Southam, G., Pfiffner, S.M. et al. (2009) Sulfur isotope enrichment during maintenance metabolism in the thermophilic sulfate-reducing bacterium *Desulfotomaculum putei*. *Appl Environ Microbiol* **75**: 5621-5630.

Deutscher, J. (2008) The mechanisms of carbon catabolite repression in bacteria. *Curr Opin Microbiol* **11**: 87-93.

DiDonato, L.N., Sullivan, S.A., Methe, B.A., Nevin, K.P., England, R., and Lovley, D.R. (2006) Role of Rel(Gsu) in stress response and Fe(III) reduction in *Geobacter sulfurreducen*s. *J Bacteriol* **188**: 8469-8478.

Ding, Y.-H.R., Hixson, K.K., Giometti, C.S., Stanley, A., Esteve-Nunez, A., Khare, T. et al. (2006) The proteome of dissimilatory metal-reducing microorganism *Geobacter sulfurreducens* under various growth conditions. *BBA-Proteins Proteom* **1764**: 1198-1206.

Dinkla, I.J., and Janssen, D.B. (2003) Simultaneous growth on citrate reduces the effects of iron limitation during toluene degradation in Pseudomonas. *Microb Ecol* **45**: 97-107.

Dispensa, M., Thomas, C.T., Kim, M.K., Perrotta, J.A., Gibson, J., and Harwood, C.S. (1992) Anaerobic growth of *Rhodopseudomonas palustris* on 4-hydroxybenzoate is dependent on AadR, a member of the cyclic AMP receptor protein family of transcriptional regulators. *J Bacteriol* **174**: 5803-5813.

Donoso, R.A., Perez-Pantoja, D., and Gonzalez, B. (2011) Strict and direct transcriptional repression of the *pobA* gene by benzoate avoids 4-hydroxybenzoate degradation in the pollutant degrader bacterium *Cupriavidus necator* JMP134. *Environ Microbiol* **13**: 1590-1600.

Duetz, W.A., Marques, S., de Jong, C., Ramos, J.L., and van Andel, J.G. (1994) Inducibility of the TOL catabolic pathway in *Pseudomonas putida* (pWW0) growing on succinate in

continuous culture: evidence of carbon catabolite repression control. *J Bacteriol* **176**: 2354-2361.

Dukan, S., and Nystrom, T. (1999) Oxidative stress defense and deterioration of growth-arrested *Escherichia coli* cells. *J Biol Chem* **274**: 26027-26032.

Durante-Rodriguez, G., Zamarro, M.T., Garcia, J.L., Diaz, E., and Carmona, M. (2008) New insights into the BzdR-mediated transcriptional regulation of the anaerobic catabolism of benzoate in *Azoarcus* sp CIB. *Microbiol-SGM* **154**: 306-316.

Echave, P., Tamarit, J., Cabiscol, E., and Ros, J. (2003) Novel antioxidant role of alcohol dehydrogenase E from *Escherichia coli*. *J Biol Chem* **278**: 30193-30198.

Egland, P.G., and Harwood, C.S. (2000) HbaR, a 4-hydroxybenzoate sensor and FNR-CRP superfamily member, regulates anaerobic 4-hydroxybenzoate degradation by *Rhodopseudomonas palustris*. *J Bacteriol* **182**: 100-106.

Egli, T. (2010) How to live at very low substrate concentration. *Water Res* **44**: 4826-4837.

Egli, T., Bosshard, C., and Hamer, G. (1986) Simultaneous utilization of methanol-glucose mixtures by *Hansenula polymorpha* in chemostat: Influence of dilution rate and mixture composition on utilization pattern. *Biotechnol Bioeng* **28**: 1735-1741.

Elifantz, H., N'Guessan, L.A., Mouser, P.J., Williams, K.H., Wilkins, M.J., Risso, C. et al. (2010) Expression of acetate permease-like (apl) genes in subsurface communities of *Geobacter* species under fluctuating acetate concentrations. *Fems Microbiol Ecol* **73**: 441-449.

Elser, J.J., Stabler, L.B., and Hassett, R.P. (1995) Nutrient limitation of bacterial growth and rates of bacterivory in lakes and oceans: a comparative study. *Aquat Microb Ecol* **9**: 105-110.

English, B.P., Hauryliuk, V., Sanamrad, A., Tankov, S., Dekker, N.H., and Elf, J. (2011) Single-molecule investigations of the stringent response machinery in living bacterial cells. *P Natl Acad Sci USA* **108**: E365-E373.

Falcon, S., and Gentleman, R. (2007) Using GOstats to test gene lists for GO term association. *Bioinformatics* **23**: 257-258.

Ferenci, T. (2001) Hungry bacteria - definition and properties of a nutritional state. *Environ Microbiol* **3**: 605-611.

Fischer, R., Bleichrodt, F.S., and Scher, U.C.G. (2008) Aromatic degradative pathways in *Acinetobacter baylyi* underlie carbon catabolite repression. *Microbiol-SGM* **154**: 3095-3103.

Foght, J. (2008) Anaerobic biodegradation of aromatic hydrocarbons: Pathways and prospects. *J Mol Microb Biotech* **15**: 93-120.

Fonseca, P., Moreno, R., and Rojo, F. (2012) *Pseudomonas putida* growing at low temperature shows increased levels of CrcZ and CrcY sRNAs, leading to reduced Crc-dependent catabolite repression. *Environ Microbiol* **doi:10.1111/j.1462-2920.2012.02708.x.**

Franchini, A.G., and Egli, T. (2006) Global gene expression in *Escherichia coli* K-12 during short-term and long-term adaptation to glucose-limited continuous culture conditions. *Microbiology-SGM* **152**: 2111-2127.

Frankena, J., Van Verseveld, H.W., and Stouthamer, A.H. (1988) Substrate and energy costs of the production of exocellular enzymes by Bacillus licheniformis. *Biotechnology and Bioengineering* **32**: 803-812.

Fredrickson, J.K., and Madylin, F. (2001) *Subsurface microbiology and biogeochemistry*. the USA: Wiley-Liss, Inc.

Fujita, Y. (2009) Carbon catabolite control of the metabolic network in *Bacillus subtilis*. *Biosci Biotech Bioch* **73**: 245-259.

Gabor, K., Verissimo, C.S., Cyran, B.C., ter Horst, P., Meijer, N.P., Smidt, H. et al. (2006) Characterization of CprK1, a CRP/FNR-type transcriptional regulator of halorespiration from *Desulfitobacterium hafniense*. *J Bacteriol* **188**: 2604-2613.

Gaines, G.L., Smith, L., and Neidle, E.L. (1996) Novel nuclear magnetic resonance spectroscopy methods demonstrate preferential carbon source utilization by *Acinetobacter calcoaceticus*. *J Bacteriol* **178**: 6833-6841.

Galperin, M.Y. (2005) A census of membrane-bound and intracellular signal transduction proteins in bacteria: Bacterial IQ, extroverts and introverts. *BMC Microbiol* **5**.

Gaupels, F., Sarioglu, H., Beckmann, M., Hause, B., Spannagl, M., Draper, J. et al. (2012) Deciphering systemic wound responses of the pumpkin extrafascicular phloem by metabolomics and stable isotope-coded protein labeling. *Plant Physiol* **160**: 2285-2299.

Gerdes, K., Christensen, S.K., and Lobner-Olesen, A. (2005) Prokaryotic toxin-antitoxin stress response loci. *Nat Rev Microbiol* **3**: 371-382.

Gerritse, J., Drzyzga, O., Kloetstra, G., Keijmel, M., Wiersum, L.P., Hutson, R. et al. (1999) Influence of different electron donors and acceptors on dehalorespiration of tetrachloroethene by *Desulfitobacterium frappieri* TCE1. *Appl Environ Microbiol* **65**: 5212-5221.

Goelzer, A., and Fromion, V. (2011) Bacterial growth rate reflects a bottleneck in resource allocation. *BBA-GEN Subjects* **1810**: 978-988.

Goffin, P., van de Bunt, B., Giovane, M., Leveau, J.H.J., Hoppener-Ogawa, S., Teusink, B., and Hugenholtz, J. (2010) Understanding the physiology of *Lactobacillus plantarum* at zero growth. *Mol Syst Biol* **6**: -.

Gorby, Y.A., and Lovley, D.R. (1991) Electron transport in the dissimilatory iron reducer, GS-15. *Appl Environ Microbiol* **57**: 867-870.

Gorke, B., and Stulke, J. (2008) Carbon catabolite repression in bacteria: many ways to make the most out of nutrients. *Nat Rev Microbiol* **6**: 613-624.

Gribble, G.W. (1994) The natural production of chlorinated compounds. *Environ Sci Technol* **28**: 310A-319A.

Grimmler, C., Held, C., Liebl, W., and Ehrenreich, A. (2010) Transcriptional analysis of catabolite repression in *Clostridium acetobutylicum* growing on mixtures of D-glucose and D-xylose. *J Bacteriol* **150**: 315-323.

Haest, P.J., Lookman, R., Van Keer, I., Patyn, J., Bronders, J., Joris, M. et al. (2010) Containment of groundwater pollution (methyl tertiary butyl ether and benzene) to protect a drinking-water production site in Belgium. *Hydrogeol J* **18**: 1917-1925.

Hammer, Ø., Harper, D.A.T., and Ryan, P.D. (2001) PAST: Paleontological statistics software package for education and data analysis. *Palaeontol Electron* **4 (1)**: 9 pp.

Harder, W., and Dijkhuizen, L. (1983a) Physiological responses to nutrient limitation. *Annual review of microbiology* **37**: 1-23.

Harder, W., and Dijkhuizen, L. (1983b) Physiological responses to nutrient limitation. *Annu rev microbiol* **37**: 1-23.

Hearn, E.M., Patel, D.R., and van den Berg, B. (2008) Outer-membrane transport of aromatic hydrocarbons as a first step in biodegradation. *Proc Natl Acad Sci USA* **105**: 8601-8606.

Heider, J., Boll, M., Breese, K., Breinig, S., Ebenau-Jehle, C., Feil, U. et al. (1998) Differential induction of enzymes involved in anaerobic metabolism of aromatic compounds in the denitrifying bacterium *Thauera aromatica*. *Arch Microbiol* **170**: 120-131.

Heintz, D., Gallien, S., Wischgoll, S., Ullmann, A.K., Schaeffer, C., Kretzschmar, A.K. et al. (2009) Differential membrane proteome analysis reveals novel proteins involved in the degradation of aromatic compounds in *Geobacter metallireducens*. *Mol Cell Proteomics* **8**: 2159-2169.

Hernández-Arranz, S., Moreno, R., and Rojo, F. (2012) The translational repressor Crc controls the *Pseudomonas putida* benzoate and alkane catabolic pathways using a multi-tier regulation strategy. *Environ Microbiol* **doi: 10.1111/j.1462-2920.2012.02863.x**.

Herzyk, A. (2012) Resilience and resistance of a pristine aquifer towards toluene contamination - impact assessment using microbes and elucidation of factors limiting natural attenuation. In *Fakultät Wissenschaftszentrum Weihenstephan für Ernährung, Landnutzung und Umwelt*. Munich: Technischen Universität München, p. 150.

Higa, F., and Edelstein, P.H. (2001) Potential virulence role of the *Legionella pneumophila* ptsP ortholog. *Infect Immun* **69**: 4782-4789.

Hirata, T., Nakasugi, O., Yoshida, M., and Sumi, K. (1992) Groundwater pollution by volatile organochlorines in Japan and related phenomena in the subsurface environment. *Wat Sci Technol* **25**: 9-16.

Hoehler, T.M., and Jorgensen, B.B. (2013) Microbial life under extreme energy limitation. *Nat Rev Microbiol* **11**: 83-94.

Holliger, C., Wohlfarth, G., and Diekert, G. (1998) Reductive dechlorination in the energy metabolism of anaerobic bacteria. *Fems Microbiol Rev* **22**: 383-398.

Holmes, D.E., Nevin, K.P., and Lovley, D.R. (2004) *In situ* expression of *nifD* in *Geobacteraceae* in subsurface sediments. *Appl Environ Microbiol* **70**: 7251-7259.

Holmes, D.E., Nevin, K.P., O'Neil, R.A., Ward, J.E., Adams, L.A., Woodard, T.L. et al. (2005) Potential for quantifying expression of the *Geobacteraceae* citrate synthase gene to assess the activity of *Geobacteraceae* in the subsurface and on current-harvesting electrodes. *Appl Environ Microbiol* **71**: 6870-6877.

Holmes, D.E., O'Neil, R.A., Chavan, M.A., N'Guessan, L.A., Vrionis, H.A., Perpetua, L.A. et al. (2009) Transcriptome of *Geobacter uraniireducens* growing in uranium-contaminated subsurface sediments. *ISME J* **3**: 216-230.

Hoskisson, P.A., and Hobbs, G. (2005) Continuous culture - making a comeback? *Microbiology-SGM* **151**: 3153-3159.

http://www-stat.stanford.edu/~tibs/SAM/sam.pdf In.

Huang, W.E., Griffiths, R.I., Thompson, I.P., Bailey, M.J., and Whiteley, A.S. (2004) Raman microscopic analysis of single microbial cells. *Anal Chem* **76**: 4452-4458.

Hug, S.J., and Leupin, O. (2003) Iron-catalyzed oxidation of arsenic(III) by oxygen and by hydrogen peroxide: pH-dependent formation of oxidants in the Fenton reaction. *Environ Sci Technol* **37**: 2734-2742.

Ihssen, J., and Egli, T. (2004) Specific growth rate and not cell density controls the general stress response in *Escherichia coli*. *Microbiology-SGM* **150**: 1637-1648.

Ihssen, J., and Egli, T. (2005) Global physiological analysis of carbon- and energy-limited growing *Escherichia coli* confirms a high degree of catabolic flexibility and preparedness for mixed substrate utilization. *Environ Microbiol* **7**: 1568-1581.

Ilin, A., and Raiko, T. (2010) Practical approaches to principal component analysis in the presence of missing values. *J Mach Learn Res* **11**: 1957-2000.

Ilyes, H., Fekete, E., Karaffa, L., Sandor, E., Szentirmai, A., and Kubicek, C.P. (2004) CreA-mediated carbon catabolite repression of beta-galactosidase formation in *Aspergillus nidulans* is growth rate dependent. *FEMS Microbiol Lett* **235**: 147-151.

Imlay, J.A. (2008) Cellular defenses against superoxide and hydrogen peroxide. In *Annu Rev Biochem*, pp. 755-776.

Imlay, J.A., and Linn, S. (1988) DNA damage and oxygen radical toxicity. *Science* **240**: 1302-1309.

Jannasch, H.W., and Egli, T. (1993) Microbial growth kinetics: a historical perspective. *Antonie Van Leeuwenhoek* **63**: 213-224.

Jehmlich, N., Schmidt, F., von Bergen, M., Richnow, H.-H., and Vogt, C. (2008a) Protein-based stable isotope probing (Protein-SIP) reveals active species within anoxic mixed cultures. *Isme J* **2**: 1122-1133.

Jehmlich, N., Schmidt, F., Hartwich, M., von Bergen, M., Richnow, H.-H., and Vogt, C. (2008b) Incorporation of carbon and nitrogen atoms into proteins measured by protein-based stable isotope probing (Protein-SIP). *Rapid Commun Mass SP* **22**: 2889-2897.

Jiang, P., Peliska, J.A., and Ninfa, A.J. (1998) Enzymological characterization of the signal-transducing uridylyltransferase/uridylyl-removing enzyme (EC 2.7.7.59) of *Escherichia coli* and its interaction with the PII protein. *Biochemistry* **37**: 12782-12794.

Johnson, S.J., Woolhouse, K.J., Prommer, H., Barry, D.A., and Christofi, N. (2003) Contribution of anaerobic microbial activity to natural attenuation of benzene in groundwater. *Eng Geol* **70**: 343-349.

Juarez, J.F., Teresa Zamarro, M., Barragan, M.J.L., Blazquez, B., Boll, M., Kuntze, K. et al. (2010) Identification of the *Geobacter metallireducens* BamVW two-component system, involved in transcriptional regulation of aromatic degradation. *Appl Environ Microbiol* **76**: 383-385.

Kemp, L.R., Dunstan, M.S., Fisher, K., Warwicker, J., and Leys, D. (2013) The transcriptional regulator CprK detects chlorination by combining direct and indirect readout mechanisms. *Philos T Roy Soc B* **368**: 20120323-20120323.

Kim, S.-H., Harzman, C., Davis, J.K., Hutcheson, R., Broderick, J.B., Marsh, T.L., and Tiedje, J.M. (2012) Genome sequence of *Desulfitobacterium hafniense* DCB-2, a Gram-positive anaerobe capable of dehalogenation and metal reduction. *Bmc Microbiology* **12**.

Kimbrough, R.D. (1972) Toxicity of chlorinated hydrocarbons and related compounds. A review including chlorinated dibenzodioxins and chlorinated dibenzofurans. *Arch environ health* **25**: 125-131.

Konopka, A. (2000) Microbial physiological state at low growth rate in natural and engineered ecosystems. *Curr Opin Microbiol* **3**: 244-247.

Konopka, A., and Wilkins, M.J. (2012) Application of meta-transcriptomics and -proteomics to analysis of in situ physiological state. *Front Microbiol* **3**: 184-184.

Konopka, A., Zakharova, T., Oliver, L., Paseuth, E., and Turco, R.F. (1998) Physiological state of a microbial community in a biomass recycle reactor. *J Ind Microbiol Biotechnol* **20**: 232-237.

Koretke, K.K., Lupas, A.N., Warren, P.V., Rosenberg, M., and Brown, J.R. (2000) Evolution of two-component signal transduction. *Mol Biol Evol* **17**: 1956-1970.

Kovarova-Kovar, K., and Egli, T. (1998) Growth kinetics of suspended microbial cells: From single-substrate-controlled growth to mixed-substrate kinetics. *Microbiol Mol Biol Rev* **62**: 646-666.

Kovarova, K., Kach, A., Zehnder, A.J.B., and Egli, T. (1997) Cultivation of *Escherichia coli* with mixtures of 3-phenylpropionic acid and glucose: Steady-state growth kinetics. *Appl Environ Microb* **63**: 2619-2624.

Kroger, A. (1974) Electron-transport phosphorylation coupled to fumarate reduction in anaerobically grown *Proteus rettgeri*. *Biochim Biophys Acta* **347**: 273-289.

Kuhn, T.K., Hamonts, K., Dijk, J.A., Kalka, H., Stichler, W., Springael, D. et al. (2009) Assessment of the Intrinsic Bioremediation Capacity of an Eutrophic River Sediment Polluted by Discharging Chlorinated Aliphatic Hydrocarbons: A Compound-Specific Isotope Approach. *Environ Sci Technol* **43**: 5263-5269.

Kuhner, S., Wohlbrand, L., Fritz, I., Wruck, W., Hultschig, C., Hufnagel, P. et al. (2005) Substrate-dependent regulation of anaerobic degradation pathways for toluene and ethylbenzene in a denitrifying bacterium, strain EbN1. *J Bacteriol* **187**: 1493-1503.

Kwakman, J.H., and Postma, P.W. (1994) Glucose kinase has a regulatory role in carbon catabolite repression in *Streptomyces coelicolor*. *J Bacteriol* **176**: 2694-2698.

Laemmli, U.K. (1970) Cleavage of structural proteins during the assembly of the head of bacteriophage T4. *Nature* **227**: 680-685.

Landmann, J.J., Werner, S., Hillen, W., Stuelke, J., and Goerke, B. (2011) Carbon source control of the phosphorylation state of the *Bacillus subtilis* carbon-flux regulator Crh *in vivo*. *FEMS Microbiol Lett* **327**: 47-53.

Langenhoff, A.A.M., Zehnder, A.J.B., and Schraa, G. (1996) Behaviour of toluene, benzene and naphthalene under anaerobic conditions in sediment columns. *Biodegradation* **7**: 267-274.

Langwaldt, J.H., Munster, U., and Puhakka, J.A. (2005) Characterization and microbial utilization of dissolved organic carbon in groundwater contaminated with chlorophenols. *Chemosphere* **59**: 983-996.

LaPat-Polasko, L.T., McCarty, P.L., and Zehnder, A.J. (1984) Secondary substrate utilization of methylene chloride by an isolated strain of *Pseudomonas* sp. *Appl Environ Microb* **47**: 825-830.

Lee, C.-R., Cho, S.-H., Yoon, M.-J., Peterkofsky, A., and Seok, Y.-J. (2007) *Escherichia coli* enzyme IIA(Ntr) regulates the K+ transporter TrkA. *Proc Natl Acad Sci USA* **104**: 4124-4129.

Lendenmann, U., and Egli, T. (1995) Is *Escherichia coli* growing in glucose-limited chemostat culture able to utilize other sugars without lag? *Microbiology* **141 (Pt 1)**: 71-78.

Lendenmann, U., and Egli, T. (1998) Kinetic models for the growth of *Escherichia coli* with mixtures of sugars under carbon-limited conditions. *Biotechnol Bioeng* **59**: 99-107.

Li, D.H., Yan, Y.L., Ping, S.Z., Chen, M., Zhang, W., Li, L. et al. (2010) Genome-wide investigation and functional characterization of the beta-ketoadipate pathway in the nitrogen-fixing and root-associated bacterium *Pseudomonas stutzeri* A1501. *BMC Microbiol* **10**: 36.

Lin, B., Westerhoff, H.V., and Roling, W.F.M. (2009) How *Geobacteraceae* may dominate subsurface biodegradation: physiology of *Geobacter metallireducens* in slow-growth habitat-simulating retentostats. *Environ Microbiol* **11**: 2425-2433.

Lisk, D.J. (1988) Environmental implications of incineration of municipal solid waste and ash disposal. *Sci Total Environ* **74**: 39-66.

Liu, N., Xu, Y., Hossain, S., Huang, N., Coursolle, D., Gralnick, J.A., and Boon, E.M. (2012) Nitric oxide regulation of cyclic di-GMP synthesis and hydrolysis in *Shewanella woodyi*. *Biochemistry* **51**: 2087-2099.

Liu, X.Q., and Ferenci, T. (1998) Regulation of porin-mediated outer membrane permeability by nutrient limitation in *Escherichia coli*. *J Bacteriol* **180**: 3917-3922.

Lovley, D.R. (1997) Microbial Fe(III) reduction in subsurface environments. *FEMS Microbiol Rev* **20**: 305-313.

Lovley, D.R., and Phillips, E.J. (1988) Novel mode of microbial energy metabolism: organic carbon oxidation coupled to dissimilatory reduction of iron or manganese. *Appl Environ Microb* **54**: 1472-1480.

Lovley, D.R., Holmes, D.E., and Nevin, K.P. (2004) Dissimilatory Fe(III) and Mn(IV) reduction. In *Advances in Microbial Physiology, Vol 49*. Poole, R.K. (ed), pp. 219-286.

Lovley, D.R., Fraga, J.L., Blunt-Harris, E.L., Hayes, L.A., Phillips, E.J.P., and Coates, J.D. (1998) Humic substances as a mediator for microbially catalyzed metal reduction. *Acta Hydroch Hydrob* **26**: 152-157.

Lovley, D.R., Giovannoni, S.J., White, D.C., Champine, J.E., Phillips, E.J., Gorby, Y.A., and Goodwin, S. (1993) *Geobacter metallireducens* gen. nov. sp. nov., a microorganism capable of coupling the complete oxidation of organic compounds to the reduction of iron and other metals. *Arch Microbiol* **159**: 336-344.

Lovley, D.R., Ueki, T., Zhang, T., Malvankar, N.S., Shrestha, P.M., Flanagan, K.A. et al. (2011) *Geobacter*: The microbe electric's physiology, ecology, and practical applications. In *Adv Microb Physiol*. Poole, R.K. (ed), pp. 1-100.

Maes, A., van Raemdonck, H., Smith, K., Ossieur, W., Lebbe, L., and Verstraete, W. (2006) Transport and activity of *Desulfitobacterium dichloroeliminans* strain DCA1 during bioaugmentation of 1,2-DCA-contaminated groundwater. *Environ Sci Technol* **40**: 5544-5552.

Matin, A., Grootjans, A., and Hogenhuis, H. (1976) Influence of dilution rate on enzymes of intermediary metabolism in two freshwater bacteria grown in continuous culture. *J Gen Microbiol* **94**: 323-332.

Matin, A., Veldhuis, C., Stegeman, V., and Veenhuis, M. (1979) Selective advantage of a *Spirillum* sp. in a carbon-limited environment. Accumulation of poly-beta-hydroxybutyric acid and its role in starvation. *J Gen Microbiol* **112**: 349-355.

Mazzoli, R., Pessione, E., Giuffrida, M.G., Fattori, P., Barello, C., Giunta, C., and Lindley, N.D. (2007) Degradation of aromatic compounds by *Acinetobacter radioresistens* S13: growth characteristics on single substrates and mixtures. *Arch Microbiol* **188**: 55-68.

McFall, S.M., Abraham, B., Narsolis, C.G., and Chakrabarty, A.M. (1997) A tricarboxylic acid cycle intermediate regulating transcription of a chloroaromatic biodegradative pathway: Fumarate-mediated repression of the clcABD operon. *J Bacteriol* **179**: 6729-6735.

McKinney, D.C., and Lin, M.D. (1996) Pump and treat ground-water remediation system optimization. *J Water Res PL-ASCE* **122**: 128-136.

Merl, J., Ueffing, M., Hauck, S.M., and von Toerne, C. (2012) Direct comparison of MS-based label-free and SILAC quantitative proteome profiling strategies in primary retinal Muller cells. *Proteomics* **12**: 1902-1911.

Methe, B.A., Webster, J., Nevin, K., Butler, J., and Lovley, D.R. (2005) DNA microarray analysis of nitrogen fixation and Fe(III) reduction in *Geobacter sulfurreducens*. *Appl Environ Microbiol* **71**: 2530-2538.

Moat, A.G., Foster, J.W., and Spector, M.P. (2002) *Microbial Physiology*. Hoboken, NJ, USA: John Wiley & Sons, Inc.

Monod, J. (1942) Recherches sur la croissance des cultures bacte´riennes. *Hermann et Cie, Paris, France*

Morales, G., Linares, J.F., Beloso, A., Albar, J.P., Martinez, J.L., and Rojo, F. (2004) The *Pseudomonas putida* Crc global regulator controls the expression of genes from several chromosomal catabolic pathways for aromatic compounds. *J Bacteriol* **186**: 1337-1344.

Moreno, R., Fonseca, P., and Rojo, F. (2012) Two small RNAs, CrcY and CrcZ, act in concert to sequester the Crc global regulator in *Pseudomonas putida*, modulating catabolite repression. *Mol Microbiol* **83**: 24-40.

Moreno, R., Marzi, S., Romby, P., and Rojo, F. (2009a) The Crc global regulator binds to an unpaired A-rich motif at the *Pseudomonas putida* alkS mRNA coding sequence and inhibits translation initiation. *Nucleic Acids Res* **37**: 7678-7690.

Moreno, R., Martinez-Gomariz, M., Yuste, L., Gil, C., and Rojo, F. (2009b) The *Pseudomonas putida* Crc global regulator controls the hierarchical assimilation of amino acids in a complete medium: Evidence from proteomic and genomic analyses. *Proteomics* **9**: 2910-2928.

Morita, R.Y. (1990) The starvation-survival state of microorganisms in nature and its relationship to the bioavailable energy. *Experientia* **46**: 813-817.

Morris, R.M., Nunn, B.L., Frazar, C., Goodlett, D.R., Ting, Y.S., and Rocap, G. (2010) Comparative metaproteomics reveals ocean-scale shifts in microbial nutrient utilization and energy transduction. *Isme J* **4**: 673-685.

Mouser, P.J., Holmes, D.E., Perpetua, L.A., DiDonato, R., Postier, B., Liu, A., and Lovley, D.R. (2009a) Quantifying expression of *Geobacter* spp. oxidative stress genes in pure culture and during *in situ* uranium bioremediation. *Isme J* **3**: 454-465.

Mouser, P.J., N'Guessan, A.L., Elifantz, H., Holmes, D.E., Williams, K.H., Wilkins, M.J. et al. (2009b) Influence of heterogeneous ammonium availability on bacterial community structure and the expression of nitrogen fixation and ammonium transporter genes during *in situ* bioremediation of uranium-contaminated groundwater. *Environ Sci Technol* **43**: 4386-4392.

Mouttaki, H., Nanny, M.A., and McInerney, M.J. (2007) Cyclohexane carboxylate and benzoate formation from crotonate in *Syntrophus aciditrophicus*. *Appl Environ Microb* **73**: 930-938.

Muller, C., Petruschka, L., Cuypers, H., Burchhardt, G., and Herrmann, H. (1996) Carbon catabolite repression of phenol degradation in *Pseudomonas putida* is mediated by the inhibition of the activator protein PhlR. *J Bacteriol* **178**: 2030-2036.

Muller, M.M., and Webster, R.E. (1997) Characterization of the *tol-pa*l and *cyd* region of *Escherichia coli* K-12: Transcript analysis and identification of two new proteins encoded by the cyd operon. *J Bacteriol* **179**: 2077-2080.

Muller, R.H., and Babel, W. (1996) Measurement of growth at very low rates (mu>=0), an approach to study the energy requirement for the survival of *Alcaligenes eutrophus* JMP 134. *Appl Environ Microbiol* **62**: 147-151.

Munster, U. (1993) Concentrations and fluxes of organic carbon substrates in the aquatic environment. *Antonie van Leeuwenhoek* **63**: 243-274.

N'Guessan, A.L., Elifantz, H., Nevin, K.P., Mouser, P.J., Methe, B., Lwoodard, T. et al. (2010) Molecular analysis of phosphate limitation in *Geobacteraceae* during the bioremediation of a uranium-contaminated aquifer. *ISME J* **4**: 253-266.

Nebe-von-Caron, G., Stephens, P.J., Hewitt, C.J., Powell, J.R., and Badley, R.A. (2000) Analysis of bacterial function by multi-colour fluorescence flow cytometry and single cell sorting. *J Microbiol Meth* **42**: 97-114.

Nevin, K.P., Kim, B.-C., Glaven, R.H., Johnson, J.P., Woodard, T.L., Methe, B.A. et al. (2009) Anode biofilm transcriptomics reveals outer surface components essential for high density current production in *Geobacter sulfurreducens* fuel cells. *Plos One* **4**.

Nguyen, T.N., Borges, K.M., Romano, A.H., and Noll, K.M. (2001) Differential gene expression in *Thermotoga neapolitana* in response to growth substrate. *FEMS Microbiol Lett* **195**: 79-83.

Nicholson, W.L., Munakata, N., Horneck, G., Melosh, H.J., and Setlow, P. (2000) Resistance of *Bacillus* endospores to extreme terrestrial and extraterrestrial environments. *Microbiol Mol Biol R* **64**: 548.

Nonaka, H., Keresztes, G., Shinoda, Y., Ikenaga, Y., Abe, M., Naito, K. et al. (2006) Complete genome sequence of the dehalorespiring bacterium *Desulfitobacterium hafniense* Y51 and comparison with *Dehalococcoides ethenogenes* 195. *J Bacteriol* **188**: 2262-2274.

Nowak, A., and Tyski, S. (2012) The role of two-component regulatory systems of Gram-positive cocci in biofilm formation. *Postep Mikrobiol* **51**: 265-276.

O'Leary, N.D., Duetz, W.A., Dobson, A.D.W., and O'Connor, K.E. (2002) Induction and repression of the *sty* operon in *Pseudomonas putida* CA-3 during growth on phenylacetic acid under organic and inorganic nutrient-limiting continuous culture conditions. *FEMS Microbiol Lett* **208**: 263-268.

O'Neil, R.A., Holmes, D.E., Coppi, M.V., Adams, L.A., Larrahondo, M.J., Ward, J.E. et al. (2008) Gene transcript analysis of assimilatory iron limitation in *Geobacteraceae* during groundwater bioremediation. *Environ Microbiol* **10**: 1218-1230.

Oberender, J., Kung, J.W., Seifert, J., von Bergen, M., and Boll, M. (2012) Identification and characterization of a succinyl-coenzyme A (CoA):benzoate CoA transferase in *Geobacter metallireducens*. *J Bacteriol* **194**: 2501-2508.

Ohtsubo, Y., Goto, H., Nagata, Y., Kudo, T., and Tsuda, M. (2006) Identification of a response regulator gene for catabolite control from a PCB-degrading beta-proteobacteria, *Acidovorax* sp KKS102. *Mol Microbiol* **60**: 1563-1575.

Patel, B.A., Moreau, M., Widom, J., Chen, H., Yin, L.F., Hua, Y.J., and Crane, B.R. (2009) Endogenous nitric oxide regulates the recovery of the radiation-resistant bacterium *Deinococcus radiodurans* from exposure to UV light. *P Natl Acad Sci USA* **106**: 18183-18188.

Paustian, M.L., May, B.J., Cao, D.W., Boley, D., and Kapur, V. (2002) Transcriptional response of *Pasteurella multocida* to defined iron sources. *J Bacteriol* **184**: 6714-6720.

Peng, X., Yamamoto, S., Vertes, A.A., Keresztes, G., Inatomi, K.-i., Inui, M., and Yukawa, H. (2012) Global transcriptome analysis of the tetrachloroethene-dechlorinating bacterium *Desulfitobacterium hafniense* Y51 in the presence of various electron donors and terminal electron acceptors. *J Ind Microbiol Biot* **39**: 255-268.

Perelo, L.W. (2010) Review: *In situ* and bioremediation of organic pollutants in aquatic sediments. *J hazard mater* **177**: 81-89.

Peters, F., Heintz, D., Johannes, J., van Dorsselaer, A., and Boll, M. (2007) Genes, enzymes, and regulation of para-Cresol metabolism in *Geobacter metallireducens*. *J Bacteriol* **189**: 4729-4738.

Pflueger-Grau, K., Chavarria, M., and de Lorenzo, V. (2011) The interplay of the EIIA(Ntr) component of the nitrogen-related phosphotransferase system (PTS(Ntr)) of *Pseudomonas putida* with pyruvate dehydrogenase. *BBA-GEN Subjects* **1810**: 995-1005.

Pieper, R., Huang, S.-T., Clark, D.J., Robinson, J.M., Parmar, P.P., Alami, H. et al. (2008) Characterizing the dynamic nature of the *Yersinia pestis* periplasmic proteome in response to nutrient exhaustion and temperature change. *Proteomics* **8**: 1442-1458.

Pilloni, G., von Netzer, F., Engel, M., and Lueders, T. (2011) Electron acceptor-dependent identification of key anaerobic toluene degraders at a tar-oil-contaminated aquifer by Pyro-SIP. *FEMS Microbiol Ecol* **78**: 165-175.

Pinchuk, G.E., Rodionov, D.A., Yang, C., Li, X., Osterman, A.L., Dervyn, E. et al. (2009) Genomic reconstruction of *Shewanella oneidensis* MR-1 metabolism reveals a previously uncharacterized machinery for lactate utilization. *P Natl Acad Sci USA* **106**: 2874-2879.

Pirt, S.J. (1965) The maintenance energy of bacteria in growing cultures. *P R Soc London* **163**: 224-231.

Plugge, C.M., Dijkema, C., and Stams, A.J.M. (1993) Acetyl-CoA cleavage pathway in a syntrophic propionate oxidizing bacterium growing on fumarate in the absence of methanogens. *FEMS Microbiol Lett* **110**: 71-76.

Plugge, C.M., Henstra, A.M., Worm, P., Swarts, D.C., Paulitsch-Fuchs, A.H., Scholten, J.C.M. et al. (2012) Complete genome sequence of *Syntrophobacter fumaroxidans* strain (MPOBT). *SIGS* **7**: 91-106.

Poblete-Castro, I., Escapa, I.F., Jaeger, C., Puchalka, J., Lam, C.M.C., Schomburg, D. et al. (2012) The metabolic response of *P. putida* KT2442 producing high levels of polyhydroxyalkanoate under single- and multiple-nutrient-limited growth: Highlights from a multi-level omics approach. *Microb Cell Fact* **11**.

Pop, S.M., Kolarik, R.J., and Ragsdale, S.W. (2004) Regulation of anaerobic dehalorespiration by the transcriptional activator CprK. *J Biol Chem* **279**: 49910-49918.

Potrykus, K., Murphy, H., Philippe, N., and Cashel, M. (2011) ppGpp is the major source of growth rate control in *E. coli*. *Environ Microbiol* **13**: 563-575.

Prat, L., Maillard, J., Grimaud, R., and Holliger, C. (2011) Physiological adaptation of *Desulfitobacterium hafniense* strain TCE1 to tetrachloroethene respiration. *Appl Environ Microb* **77**: 3853-3859.

Putrins, M., Ainelo, A., Ilves, H., and Horak, R. (2011) The ColRS system is essential for the hunger response of glucose-growing *Pseudomonas putida*. *BMC Microbiol* **11**.

Ragsdale, S.W., and Pierce, E. (2008) Acetogenesis and the Wood-Ljungdahl pathway of CO_2 fixation. *BBA-Proteins Proteom* **1784**: 1873-1898.

Raimann, E., Schmid, B., Stephan, R., and Tasara, T. (2009) The alternative sigma factor sigma(L) of *L. monocytogenes* promotes growth under diverse environmental stresses. *Foodborne Pathog Dis* **6**: 583-591.

Rakoczy, J., Schleinitz, K.M., Mueller, N., Richnow, H.H., and Vogt, C. (2011) Effects of hydrogen and acetate on benzene mineralisation under sulphate-reducing conditions. *FEMS Microbiol Ecol* **77**: 238-247.

Ram, R.J., VerBerkmoes, N.C., Thelen, M.P., Tyson, G.W., Baker, B.J., Blake, R.C. et al. (2005) Community proteomics of a natural microbial biofilm. *Science* **308**: 1915-1920.

Rangel, D.E.N. (2011) Stress induced cross-protection against environmental challenges on prokaryotic and eukaryotic microbes. *World J Microb Biot* **27**: 1281-1296.

Risso, C., Methe, B.A., Elifantz, H., Holmes, D.E., and Lovley, D.R. (2008) Highly conserved genes in *Geobacter* species with expression patterns indicative of acetate limitation. *Microbiology-Sgm* **154**: 2589-2599.

Rocha, E.P.C. (2008) The organization of the bacterial genome. In *Annu Rev Genet*, pp. 211-233.

Roels, J.A. (1983) *Energetics and kinetics in biotechnology*: Elsevier Biomedical Press: Amsterdam, Netherlands; New York, N.Y., USA. Illus.

Rojo, F. (2010) Carbon catabolite repression in *Pseudomonas*: optimizing metabolic versatility and interactions with the environment. *FEMS Microbiol Rev* **34**: 658-684.

Röling, W., and van Verseveld, H. (2002) Natural attenuation: What does the subsurface have in store? *Biodegradation* **13**: 53-54.

Roling, W.F.M., van Breukelen, B.M., Braster, M., Lin, B., and van Verseveld, H.W. (2001) Relationships between microbial community structure and hydrochemistry in a landfill leachate-polluted aquifer. *Applied and Environmental Microbiology* **67**: 4619-4629.

Röling, W.F.M., van Breukelen, B.M., Braster, M., Lin, B., and van Verseveld, H.W. (2001) Relationships between microbial community structure and hydrochemistry in a landfill leachate-polluted aquifer. *Appl Environ Microb* **67**: 4619-4629.

Rooney-Varga, J.N., Anderson, R.T., Fraga, J.L., Ringelberg, D., and Lovley, D.R. (1999) Microbial communities associated with anaerobic benzene degradation in a petroleum-contaminated aquifer. *Appl Environ Microb* **65**: 3056-3063.

Rossell, S., van der Weijden, C.C., Kruckeberg, A.L., Bakker, B.M., and Westerhoff, H.V. (2005) Hierarchical and metabolic regulation of glucose influx in starved *Saccharomyces cerevisiae*. *FEMS Yeast Res* **5**: 611-619.

Rouault, T.A., and Klausner, R.D. (1996) Iron-sulfur clusters as biosensors of oxidants and iron. *Trends Biochem Sci* **21**: 174-177.

Rubio, L.M., and Ludden, P.W. (2008) Biosynthesis of the iron-molybdenum cofactor of nitrogenase. In *Ann Rev Microbiol*, pp. 93-111.

Rueegg, I., Hafner, T., Bucheli-Witschel, M., and Egli, T. (2007) Dynamics of benzene and toluene degradation in *Pseudomonas putida* F1 in the presence of the alternative substrate succinate. *Eng Life Sci* **7**: 331-342.

Ruiz-Aguilar, G.M.L., Fernandez-Sanchez, J.M., Kane, S.R., Kim, D., and Alvarez, P.J.J. (2002) Effect of ethanol and methyl-tert-butyl ether on monoaromatic hydrocarbon biodegradation: Response variability for different aquifer materials under various electron-accepting conditions. *Environ Toxicol Chem* **21**: 2631-2639.

Schaefer, C.E., Lippincott, D.R., and Steffan, R.J. (2010a) Field-scale evaluation of bioaugmentation dosage for treating chlorinated ethenes. *Ground Water Monit R* **30**: 113-124.

Schaefer, C.E., Yang, X., Pelz, O., Tsao, D.T., Streger, S.H., and Steffan, R.J. (2010b) Aerobic biodegradation of *iso*-butanol and ethanol and their relative effects on BTEX biodegradation in aquifer materials. *Chemosphere* **81**: 1104-1110.

Schleinitz, K.M., Schmeling, S., Jehmlich, N., von Bergen, M., Harms, H., Kleinsteuber, S. et al. (2009) Phenol degradation in the strictly anaerobic iron-reducing bacterium *Geobacter metallireducens* GS-15. *Appl Environ Microb* **75**: 3912-3919.

Schrickx, J.M., Raedts, M.J., Stouthamer, A.H., and van Verseveld, H.W. (1995) Organic acid production by *Aspergillus niger* in recycling culture analyzed by capillary electrophoresis. *Anal Biochem* **231**: 175-181.

Scow, K.M., and Hicks, K.A. (2005) Natural attenuation and enhanced bioremediation of organic contaminants in groundwater. *Curr Opin Biotech* **16**: 246-253.

Segura, D., Mahadevan, R., Juarez, K., and Lovley, D.R. (2008) Computational and experimental analysis of redundancy in the central metabolism of *Geobacter sulfurreducens*. *Plos Comput Biol* **4**.

Senior, P.J. (1975) Regulation of nitrogen metabolism in *Escherichia coli* and *Klebsiella aerogenes*: studies with the continuous-culture technique. *J Bacteriol* **123**: 407-418.

Seo, J.S., Keum, Y.S., and Li, Q.X. (2011) Comparative protein and metabolite profiling revealed a metabolic network in response to multiple environmental contaminants in *Mycobacterium aromativorans* JS19b1(T). *J Agric Food Chem* **59**: 2876-2882.

Sepers, A.J.B. (1984) The uptake capacity for organic compounds of two heterotrophic strains at carbon limited growth. *Zeitschr Allg Mikrobiol* **24**: 261-267.

Servant, P., Le Coq, D., and Aymerich, S. (2005) CcpN (YqzB), a novel regulator for CcpA-independent catabolite repression of *Bacillus subtilis* gluconeogenic genes. *Mol Microbiol* **55**: 1435-1451.

Silver, R.S., and Mateles, R.I. (1969) Control of mixed-substrate utilization in continuous cultures of *Escherichia coli*. *J Bacteriol* **97**: 535-543.

Smith, J.A., Lovley, D.R., and Tremblay, P.-L. (2012) Outer cell surface components essential for Fe(III) oxide reduction by *Geobacter metallireducens*. *Appl Environ Microb* **79**: 901-907.

Snoeyenbos-West, O.L., Nevin, K.P., Anderson, R.T., and Lovley, D.R. (2000) Enrichment of *Geobacter* species in response to stimulation of Fe(III) reduction in sandy aquifer sediments. *Microb Ecol* **39**: 153-167.

Sonenshein, A.L. (2005) CodY, a global regulator of stationary phase and virulence in Gram-positive bacteria. *Curr Opin Microbiol* **8**: 203-207.

Sonnleitner, E., Abdou, L., and Haas, D. (2009) Small RNA as global regulator of carbon catabolite repression in *Pseudomonas aeruginosa*. *P Natl Acad Sci USA* **106**: 21866-21871.

Sonnleitner, E., Valentini, M., Wenner, N., Haichar, F.e.Z., Haas, D., and Lapouge, K. (2012) Novel targets of the CbrAB/Crc carbon catabolite control system revealed by transcript abundance in *Pseudomonas aeruginosa*. *PLoS One* **7**.

Sowell, S.M., Wilhelm, L.J., Norbeck, A.D., Lipton, M.S., Nicora, C.D., Barofsky, D.F. et al. (2009) Transport functions dominate the SAR11 metaproteome at low-nutrient extremes in the Sargasso Sea. *Isme J* **3**: 93-105.

Stouthamer, A.H. (1973) A theoretical study on the amount of ATP required for synthesis of microbial cell material. *Antonie van Leeuwenhoek* **39**: 545-565.

Sun, J., Sayyar, B., Butler, J.E., Pharkya, P., Fahland, T.R., Famili, I. et al. (2009) Genome-scale constraint-based modeling of *Geobacter metallireducens*. *BMC Syst Biol* **3**: 174.

Suyama, A., Iwakiri, R., Kai, K., Tokunaga, T., Sera, N., and Furukawa, K. (2001) Isolation and characterization of *Desulfitobacterium* sp strain Y51 capable of efficient dehalogenation of tetrachloroethene and polychloroethanes. *Biosci Biotech Bioch* **65**: 1474-1481.

Tancsics, A., Szabo, I., Baka, E., Szoboszlay, S., Kukolya, J., Kriszt, B., and Marialigeti, K. (2010) Investigation of catechol 2,3-dioxygenase and 16S rRNA gene diversity in hypoxic, petroleum hydrocarbon contaminated groundwater. *Syst Appl Microbiol* **33**: 398-406.

Tang, Y.J., Chakraborty, R., Martin, H.G., Chu, J., Hazen, T.C., and Keasling, J.D. (2007) Flux analysis of central metabolic pathways in *Geobacter metallireducens* during reduction of soluble Fe(III)-nitrilotriacetic acid. *Appl Environ Microbiol* **73**: 3859-3864.

Tappe, W., Tomaschewski, C., Rittershaus, S., and Groeneweg, J. (1996) Cultivation of nitrifying bacteria in the retentostat, a simple fermenter with internal biomass retention. *FEMS Microbiol Ecol* **19**: 47-52.

Tappe, W., Laverman, A., Bohland, M., Braster, M., Rittershaus, S., Groeneweg, J., and van Verseveld, H.W. (1999) Maintenance energy demand and starvation recovery dynamics of *Nitrosomonas europaea* and *Nitrobacter winogradskyi* cultivated in a retentostat with complete biomass retention. *Appl Environ Microbiol* **65**: 2471-2477.

ter Kuile, B.H., and Westerhoff, H.V. (2001) Transcriptome meets metabolome: hierarchical and metabolic regulation of the glycolytic pathway. *FEBS Lett* **500**: 169-171.

Terzenbach, D.P., and Blaut, M. (1994) Transformation of tetrachloroethylene to trichloroethylene by homoacetogenic bacteria. *FEMS Microbiol Lett* **123**: 213-218.

Thauer, R.K., Jungermann, K., and Decker, K. (1977) Energy conservation in chemotrophic anaerobic bacteria. *Bacteriol rev* **41**: 100-180.

Tomas-Gallardo, L., Santero, E., and Floriano, B. (2012) Involvement of a putative cyclic AMP receptor protein (CRP)-like binding sequence and a CRP-like protein in glucose-mediated catabolite repression of *thn* genes in *Rhodococcus* sp strain TFB. *Appl Environ Microbiol* **78**: 5460-5462.

Touati, D. (2000) Iron and oxidative stress in bacteria. *Arch Biochem Biophys* **373**: 1-6.

Tran, H.T., Krushkal, J., Antommattei, F.M., Lovley, D.R., and Weis, R.M. (2008) Comparative genomics of *Geobacter* chemotaxis genes reveals diverse signaling function. *BMC Genomics* **9**.

Trautwein, K., Grundmann, O., Woehlbrand, L., Eberlein, C., Boll, M., and Rabus, R. (2011) Benzoate mediates repression of C(4)-dicarboxylate utilization in "*Aromatoleum aromaticum*" EbN1. *J Bacteriol* **194**: 518-528.

Trautwein, K., Lahme, S., Woehlbrand, L., Feenders, C., Mangelsdorf, K., Harder, J. et al. (2012) Physiological and proteomic adaptation of *"Aromatoleum aromaticum"* EbN1 to low growth rates in benzoate-limited, anoxic chemostats. *J Bacteriol* **194**: 2165-2180.

Tremblay, P.-L., and Lovley, D.R. (2012) Role of the NiFe hydrogenase *Hya* in oxidative stress defense in *Geobacter sulfurreducens*. *J Bacteriol* **194**: 2248-2253.

Tremblay, P.-L., Aklujkar, M., Leang, C., Nevin, K.P., and Lovley, D. (2012) A genetic system for *Geobacter metallireducens*: role of the flagellin and pilin in the reduction of Fe(III) oxide. *Environ Microbiol Reports* **4**: 82-88.

Tusher, V.G., Tibshirani, R., and Chu, G. (2001) Significance analysis of microarrays applied to the ionizing radiation response. *Proc Natl Acad Sci USA* **98**: 5116–5121.

Tyagi, M., da Fonseca, M.M.R., and de Carvalho, C.C.C.R. (2011) Bioaugmentation and biostimulation strategies to improve the effectiveness of bioremediation processes. *Biodegradation* **22**: 231-241.

Ueki, T. (2011) Identification of a transcriptional repressor involved in benzoate metabolism in *Geobacter bemidjiensis*. *Appl Environ Microb* **77**: 7058-7062.

US-EPA (1998) Carcinogenic effects of benzene: an update. In *National Center for Environmental Assessment, Office of Reserach and Development, US Environmental Protection Agency*. Washington, DC, pp. 1-45.

van der Horst, M.A., van Lieshout, J.F.T., Bury, A., Hartog, A.F., and Wever, R. (2012) Sulfation of various alcoholic groups by an arylsulfate sulfotransferase from *Desulfitobacterium hafniense* and synthesis of estradiol sulfate. *Ad Synth Catal* **354**: 3501-3508.

van Verseveld, H.W., Chesbro, W.R., Braster, M., and Stouthamer, A.H. (1984) Eubacteria have 3 growth modes keyed to nutrient flow - consequences for the concept of maintenance and maximal growth-yield. *Arch Microbiol* **137**: 176-184.

van Verseveld, H.W., de Hollander, J.A., Frankena, J., Braster, M., Leeuwerik, F.J., and Stouthamer, A.H. (1986) Modeling of microbial substrate conversion, growth and product formation in a recycling fermentor. *Antonie van Leeuwenhoek* **52**: 325-342.

Vargas, M., and Noll, K.M. (1996) Catabolite repression in the hyperthermophilic bacterium *Thermotoga neapolitana* is independent of cAMP. *Microbiology UK* **142**: 139-144.

Velazquez, F., di Bartolo, I., and de Lorenzo, V. (2004) Genetic evidence that catabolites of the entner-doudoroff pathway signal C source repression of the sigma(54) *Pu* promoter of *Pseudomonas putida*. *J Bacteriol* **186**: 8267-8275.

Velazquez, F., Pfluger, K., Cases, I., De Eugenio, L.I., and de Lorenzo, V. (2007) The phosphotransferase system formed by PtsP, PtsO, and PtsN proteins controls production of polyhydroxyalkanoates in *Pseudomonas putida*. *J Bacteriol* **189**: 4529-4533.

Villemur, R., Lanthier, M., Beaudet, R., and Lepine, F. (2006) The *Desulfitobacterium* genus. *FEMS Microbiol Rev* **30**: 706-733.

Vinuselvi, P., Kim, M.K., Lee, S.K., and Ghim, C.-M. (2012) Rewiring carbon catabolite repression for microbial cell factory. *BMP Rep* **45**: 59-70.

Voordeckers, J.W., Kim, B.-C., Izallalen, M., and Lovley, D.R. (2010) Role of *Geobacter sulfurreducens* outer surface c-Type cytochromes in reduction of soil humic acid and anthraquinone-2,6-disulfonate. *Appl Environ Microb* **76**: 2371-2375.

Wagner, M., Nielsen, P.H., Loy, A., Nielsen, J.L., and Daims, H. (2006) Linking microbial community structure with function: fluorescence in situ hybridization-microautoradiography and isotope arrays. *Curr Opin Biotech* **17**: 83-91.

Wang, Y., Rawlings, M., Gibson, D.T., Labbe, D., Bergeron, H., Brousseau, R., and Lau, P.C. (1995) Identification of a membrane protein and a truncated LysR-type regulator associated with the toluene degradation pathway in *Pseudomonas putida* F1. *Mol Gen Genet* **246**: 570-579.

Wanner, U., and Egli, T. (1990) Dynamics of microbial growth and cell composition in batch culture. *FEMS Microbiol Rev* **6**: 19-43.

Warner, J.B., and Lolkema, J.S. (2003) CcpA-dependent carbon catabolite repression in bacteria. *Microbiol Mol Biol R* **67**: 476.

Wick, L.M., and Egli, T. (2004) Molecular components of physiological stress responses in *Escherichia coli*. *Adv Bioch Eng Biot* **89**: 1-45.

Wick, L.M., Quadroni, M., and Egli, T. (2001) Short- and long-term changes in proteome composition and kinetic properties in a culture of *Escherichia coli* during transition from glucose-excess to glucose-limited growth conditions in continuous culture and vice versa. *Environ Microbiol* **3**: 588-599.

Widdel, F., and Rabus, R. (2001) Anaerobic biodegradation of saturated and aromatic hydrocarbons. *Curr Opin Biotech* **12**: 259-276.

Wiegeshoff, F., Beckering, C.L., Debarbouille, M., and Marahiel, M.A. (2006) Sigma L is important for cold shock adaptation of *Bacillus subtilis*. *J Bacteriol* **188**: 3130-3133.

Wiersma, M., and Harder, W. (1978) A continuous culture study of the regulation of extracellular protease production in *Vibrio* SA1. *Antonie van Leeuwenhoek* **44**: 141-155.

Wilkins, M.J., VerBerkmoes, N.C., Williams, K.H., Callister, S.J., Mouser, P.J., Elifantz, H. et al. (2009) Proteogenomic monitoring of *Geobacter* physiology during stimulated uranium bioremediation. *Appl Environ Microb* **75**: 6591-6599.

Wilmes, P., Wexler, M., and Bond, P.L. (2008) Metaproteomics Provides Functional Insight into Activated Sludge Wastewater Treatment. *Plos One* **3**.

Wischgoll, S., Heintz, D., Peters, F., Erxleben, A., Sarnighausen, E., Reski, R. et al. (2005) Gene clusters involved in anaerobic benzoate degradation of *Geobacter metallireducens*. *Mol Microbiol* **58**: 1238-1252.

Wu, Y., Wang, J., Xu, T., Liu, J., Yu, W., Lou, Q. et al. (2012) The two-component signal transduction system ArlRS regulates *Staphylococcus epidermidis* biofilm formation in an ica-dependent manner. *Plos One* **7**.

Xin, B.-P., Wu, C.-H., Wu, C.-H., and Lin, C.-W. (2013) Bioaugmented remediation of high concentration BTEX-contaminated groundwater by permeable reactive barrier with immobilized bead. *J hazard mater* **244-245**: 765-772.

Xu, F.F., and Imlay, J.A. (2012) Silver(I), Mercury(II), Cadmium(II), and Zinc(II) target exposed enzymic Iron-Sulfur clusters when they toxify *Escherichia coli*. *Appl Environ Microbiol* **78**: 3614-3621.

Yu, C.L., Louie, T.M., Summers, R., Kale, Y., Gopishetty, S., and Subramanian, M. (2009) Two distinct pathways for metabolism of theophylline and caffeine are coexpressed in *Pseudomonas putida* CBB5. *J Bacteriol* **191**: 4624-4632.

Yun, J., Ueki, T., Miletto, M., and Lovley, D.R. (2011) Monitoring the metabolic status of *Geobacter* species in contaminated groundwater by quantifying key metabolic proteins with *Geobacter*-specific antibodies. *Appl Environ Microbiol* **77**: 4597-4602.

Zaunmueller, T., Kelly, D.J., Gloeckner, F.O., and Unden, G. (2006) Succinate dehydrogenase functioning by a reverse redox loop mechanism and fumarate reductase in sulphate-reducing bacteria. *Microbiol-SGM* **152**: 2443-2453.

Zehnder, A.J.B. (1989) *Biology of anaerobic microorganisms*. New York, USA: John Wiley and Sons.

Zhan, Y., Yu, H., Yan, Y., Ping, S., Lu, W., Zhang, W. et al. (2009) Benzoate catabolite repression of the phenol degradation in *Acinetobacter calcoaceticus* PHEA-2. *Curr Microbiol* **59**: 368-373.

Zhang, B., VerBerkmoes, N.C., Langston, M.A., Uberbacher, E., Hettich, R.L., and Samatova, N.F. (2006) Detecting differential and correlated protein expression in label-free shotgun proteomics. *J Proteome Res* **5**: 2909-2918.

Zhang, T., Bain, T.S., Nevin, K.P., Barlett, M.A., and Lovley, D.R. (2012) Anaerobic benzene oxidation by *Geobacter* species. *Appl Environ Microbiol* **78**: 8304-8310.

Zimmermann, T., Sorg, T., Siehler, S.Y., and Gerischer, U. (2009) Role of *Acinetobacter baylyi* Crc in catabolite repression of enzymes for aromatic compound catabolism. *J Bacteriol* **191**: 2834-2842.

Zollars, R.L. (2010) Chemical process principles and calculations. In: Washington state university, Voiland school of chemical engineering and bioengineering.

7 Supplementary material

Table 7-1 Calculation of free energy change at pH 7 ($\Delta G^{0'}$) for oxidation of acetate and benzoate in the presence of Fe(III)

According to (Thauer et al., 1977), $\Delta G^{0'} = \Delta G^{0} + m\Delta Gf'(H^{+})$, where ΔG^{0} is free energy of a reaction at standard conditions (T=25 C°, pressure of 1atm, and pH 0), m – is net number of protons in the reaction, $\Delta Gf'(H^{+})$ is the free energy of formation of proton at pH 7.
$\Delta Gf'(H^{+}) = 2.3*RT \log 10^{-7}$, where R is the gas constant (1.987 cal/mol/T) and T is absolute temperature.
Taking into consideration that retentostat experiments were run at pH 7 and temperature 30 C°, $\Delta Gf'(H^{+})$ was calculated as -40.58 (kJ/mol).

$\Delta G^{0'}$ for acetate consumption with Fe(III)		
	ΔGf^{0},kJ/mol (Thauer et al., 1977	Coefficient in reaction
Acetate	-369.41	1
Fe(II)	-78.87	8
Fe(III)	-4.6	8
H_2O	-237.178	3
HCO_3^-	-586.85	1
CO_2	-394.359	1
H^+ at pH 7, t 30C°	-40.58	8
	$\sum\Delta f^{0}$, kJ	
Products	-1936.809	
Substrates	-1117.744	
$\Delta G^{0'}$	**-819.07**	

$\Delta G^{0'}$ for benzoate consumption with Fe(III)		
	ΔGf^{0},kJ (Thauer et al., 1977	Coefficient in reaction
Benzoate	-245.6	1
Fe(II)	-78.87	30
Fe(III)	-4.6	30
H_2O	-237.178	13
CO_2	-394.359	6
HCO_3^-	-586.85	1
H^+ at pH 7, t 30C°	-40.58	30
	$\sum\Delta f^{0}$, kJ	
Products	-6536.504	
Substrates	-3466.914	
$\Delta G^{0'}$	**-3069.59**	

Table 7-2. Data used for hierarchical regulation analysis of flux through TCA cycle in *G. metallireducens* cultivated under high carbon substrate concentrations in batch.

(A) Measured maximum specific growth rate and growth rates at sampling for proteomics.

Growth condition	Acetyl-CoA produced from 1mole of substrate (theor.)	Substrate consumed (stat.), mM	Fe(II) (stat.), mM	Flux (mmol acetyl-coA/cell/h)	Maximum specific growth rate[a], [μ_{max}] [1/h]
Butyrate	2	2.5	46	$4.21*10^{-15}$	0.05
Acetate	1	5	35.7	$5.88*10^{-15}$	0.16
Ethanol	1	5	33	$2.41*10^{-14}$	0.22
Benzoate	3	1	26.7	$1.17*10^{-14}$	0.11
Toluene	3	1	33.7	$2.62*10^{-15}$	0.07
Acetate plus benzoate	1 plus 3	0.63+1.93	38.1[b]	$2.13*10^{-14}$	0.24

[a]Growth rates are calculated from the averaged values of produced Fe(II) from three replicated experiments, according to the following formula $\mu=(Fe(II)_{t+1}-Fe(II)_{t1})/(t_{+1}-t_1)*t_0^{-1}$

[b]calculated theoretically

(B) Ln of averaged protein abundances of TCA enzymes expressed on different growth conditions.

TCA proteins	Acetate plus benzoate	Acetate	Benzoate	Butyrate	Ethanol	Toluene
Citrate synthase	20.4	19.9	17.6	19.6	18.5	19.1
Aconitase 1	12.0	14.0	12.7	12.7	12.0	12.7
Aconitase 2	10.8	12.2	10.6	12.0	9.4	11.9
Aconitate hydratase 2	19.0	17.9	19.4	19.4	18.5	18.0
Isocitrate dehydrogenase [NADP]	19.5	19.9	19.8	19.6	19.3	18.7
2-oxoglutarate dehydrogenase E1 component	9.6	9.8	10.3	10.6	7.6	10.5
2-oxoglutarate ferredoxin oxidoreductase, alpha subunit	20.0	20.0	20.3	19.4	20.0	19.6
2-oxoglutarate ferredoxin oxidoreductase, beta subunit	18.5	19.6	18.2	18.2	18.5	18.9
2-oxoglutarate ferredoxin oxidoreductase, gamma subunit	18.2	19.3	18.5	18.6	17.3	18.0
Succinyl-CoA ligase [ADP-forming] subunit alpha	16.2	13.3	19.0	16.5	12.5	18.1
Succinyl-CoA ligase [ADP-forming] subunit alpha	13.2	13.6	11.6	12.8	12.5	12.5
Succinyl-CoA ligase [ADP-forming] subunit beta 1	12.6	14.2	12.5	12.6	13.0	13.0
Succinate dehydrogenase subunit C	15.0	16.3	16.3	16.2	15.1	16.3
Succinate dehydrogenase subunit A	18.0	18.6	18.6	19.1	18.1	18.9
Succinate dehydrogenase subunit B	18.6	18.2	19.1	18.8	18.0	19.2
Fumarase	18.2	17.5	17.9	18.6	17.6	18.0
Malate dehydrogenase	20.2	20.4	20.4	20.3	20.3	17.1

7.1 Simultaneous consumption of two substrates in batch in terms of Monod kinetics

According to Monod kinetics, the substrate degradation rate can be expressed as follows:

$$\frac{dS}{dt} = -\frac{X_t}{Y}\frac{\mu * S}{S + K_s} \qquad \text{Equation 7-1}$$

where S – substrate [mol], X – biomass [g/l], Y – yield coefficient [gdw of bacteria produced per mol of substrate], $\boldsymbol{K_s}$ – half-saturation constant [mg/l], μ - specific growth rate [h^{-1}].

During exponential growth in batch, $S >> K_s$, therefore

$$\frac{dS}{dt} = -\frac{X_t}{Y}\frac{\mu * S}{S + K_s} \qquad \text{Equation 7-2}$$

In the case of simultaneous growth on two substrates, these substrates are degraded by the same biomass X_t:

$$\frac{dS_1}{dt} = -X_t * \frac{\mu_{max1}}{Y_1}$$

and

$$\frac{dS_2}{dt} = -X_t * \frac{\mu_{max2}}{Y_2} \qquad \text{Equation 7-3}$$

Therefore, if two substrates are consumed simultaneously, the ratio of their consumption rates should be equal to the ratio of the growth rates related to the yield coefficients and can be expressed as following:

$$\frac{dS_1}{dt} \Big/ \frac{dS_2}{dt} = \frac{\mu_{max1}}{Y_1} \Big/ \frac{\mu_{max2}}{Y_2} \qquad \text{Equation 7-4}$$

Calculated ratios for conditions of acetate plus benzoate, acetate plus toluene and benzoate plus toluene are presented in Table 7-3.

Table 7-3.

Table 7-3. Comparison between the ratios of substrate consumption rate during growth on mixed substrates to the ratio of maximum specific growth rate with the individual substrates for that particular growth condition.

Conditions	**S**	$\frac{dS}{dt}$ **mol substrate/h**	$\frac{dS_1/dt}{dS_2/dt}$ **mol substrate$_1$/h/mol substrate$_2$/h**	**Y[a], gdw/mol of substrate**	$\frac{\mu_{max1}}{Y_1} / \frac{\mu_{max2}}{Y_2}$
Acetate plus benzoate	Acetate, S1	0.11	17.2	7	6.4
	Benzoate, S2	0.01		27.5	
Benzoate plus toluene	Benzoate, S1	0.01	1.1	27.5	1.4
	Toluene, S2	0.01		31	
Acetate plus toluene	Acetate, S1	0.12	587.5	7	9
	Toluene, S2	0.0002		27.5	

[a] Yield coefficients were taken from (Sun et al., 2009).

Therefore,

$\frac{dS_1}{dt} / \frac{dS_2}{dt} = \frac{\mu_{max1}}{Y_1} / \frac{\mu_{max2}}{Y_2}$ for benzoate plus toluene is 1.1~1.4, clearly supporting simultaneous consumption of these two aromatics, while for conditions of acetate plus benzoate and acetate plus toluene the relationship is the following: 17.2>6.4, and 587.5>>9, respectively, suggesting that two latter condition did not exhibit simultaneous consumption of the substrates.

Table 7-4. Pairwise comparisons of protein abundances between different growth conditions. FDRs<5% are presented.

			Gene coordinates				Acetate plus benzoate[c]				Acetate				Benzoate					Butyrate					Ethanol					Toluene				
Clusters	Pathway	ID	start[a]	end[b]	Name	Annotation	Ace[d]	But	Eth	Tol	AB	Benz	But	Eth	Tol	AB	Ace	But	Eth	Tol	AB	Ace	Benz	Eth	Tol	AB	Ace	Benz	But	Tol	AB	Ace	Benz	But	Eth
Benzoate	Acetate	Q39TZ1	2306453	2307779	Gmet_2054	Succinyl:benzoate coenzyme A transferase										0.4	0.1	0.1	0.1	0.1															
	Benzoate	Q39TP3	2422547	2423456	BamP	Electron transfer flavoprotein, alpha subunit	0.2		0.2								0.2		0.2			0.1		0.1								0.1			0.1
		Q39TP4	2421275	2422349	BamQ	6-hydroxycyclohex-1-ene-1-carbonyl-CoA dehydrogenase	1.5		4.2								0.2		0.3			0.1		0.5								0.2			0.5
		Q39TP5	2420425	2421196	BamR	Cyclohexa-1,5-dienecarbonyl-CoA hydratase											0.1	0.8	0.1			0.1		0.1								0.1		0.6	0.1
		Q39TP6	2419307	2420207	BamS	Lipoprotein, putative											0.1	0.6	0.1			0.1		0.1								0.1		0.4	0.1
		Q39TP8	2416877	2417738	BamU	Metal-dependent hydrolase, putative											0.2		0.8			0.2		1.6								0.8			
		Q39TV7	2349628	2350774	BamA	6-oxocyclohex-1-ene-1-carbonyl-CoA hydratase											0.1	3.3	0.1			0.1		0.1								0.1			0.1
		Q39TV8	2347468	2349430	BamB-1	Benzoyl-CoA reductase, putative											0.1	0.1	0.1			0.1		0.1								0.1		0.2	0.1
		Q39TV9	2346880	2347420	BamC-1	Benzoyl-CoA reductase ,putative											0.1	2.2	0.7			0.1		1.4								0.1		0.3	0.4
		Q39TW0	2345702	2346866	BamD	Benzoyl-CoA reductase ,putative											0.1	0.3	0.1			0.1		0.3								0.3			0.4
		Q39TW2	2341788	2342427	BamF	Benzoyl-CoA reductase ,putative											0.1	0.3	0.1			0.1		0.2								0.1		0.4	0.1
		Q39TW5	2339230	2341138	BamH	Benzoyl-CoA reductase ,putative											0.1	0.1	0.1			0.2		0.1								0.1		0.4	0.1
		Q39TX3	2331095	2331941	HbdA	3-hydroxyacyl-CoA dehydrogenase			4.3								0.2	4.1	0.1			0.2		0.1								0.2			0.1
		Q39TX8	2324929	2325742	EtfB-2	Electron transfer flavoprotein, beta subunit	3.9		4.3							0.6	0.1	0.3	0.1			0.2		0.1							1.3	0.1		0.2	0.1
		Q39TY0	2321546	2323523	Gmet_2065	Iron-sulfur cluster-binding oxidoreductase											0.1	2.5	0.1			1.8		0.7								0.2			0.1
		Q39UP2	2019007	2019544	BamC-2	Benzoyl-CoA reductase, putative																2		1								0.6			0.6
		Q39UP3	2017050	2019021	BamB-2	Benzoyl-CoA reductase, putative											1.4		1.4			0.1		0.1								0.2			0.2
		Q39ZG7	134614	135493	Gmet_0108	ATPase, AAA_5 family											0.4	0.2	0.3	4.2		2		1.5								0.7		2.5	0.5
	Cell envelope	Q39U15	2271771	2272620	Gmet_2030	Periplasmic polysaccharide biosynthesis/export protein					2.4	1.8														0.6		0.6			0.5		0.4	3.4	
		Q39ZH2	128527	129958	GlmU	Glucosamine-1-phosphate N-acetyltransferase																3.5			1.5					3.6					
	Cellular processes	Q39U17	2269312	2270164	YveL	Protein tyrosine kinase, putative		2.2					1.4																0.5			2.8	1.1	0.4	
	Energy metabolism, Electron transport	Q39TX5	2328261	2330253	Gmet_2070	Iron-sulfur cluster-binding oxidoreductase											0.2	4.5	0.2			0.4		0.5								0.1		1.3	0.1
		Q39TX9	2323562	2324909	EtfA-2	Electron transfer flavoprotein, alpha subunit										4.7	0.1	0.1	0.1			0.2		0.2								0.2		2.3	0.1
	Fatty acid and phospholipids	Q39TX0	2334413	2335592	BamM	Glutaryl-CoA dehydrogenase	2.8		3.3								0.1		0.1			0.1		0.1								0.1			0.1
		Q39TX1	2333225	2334401	BamN	Thiolase	1.9		2.3								0.1		0.1			0.1		0.1								0.1			0.1
		Q39TX4	2330298	2331081	FadB1	Enoyl-CoA hydratase/isomerase											0.1	2.8	0.2			0.1		0.3								0.1		4.1	0.1
		Q39TY6	2313440	2314184	Adh	Oxidoreductase, short-chain dehydrogenase/reductase	0.2		0.1								0.1		0.1			0.1		0.1								0.1			0.1
		Q39TY7	2312206	2313406	Act	Thiolase			0.7								0.9		0.2			3.4		0.2								1.8			0.2
		Q39TY8	2311304	2312141	Ech	Enoyl-CoA hydratase/isomerase											2.3																			
	Folate biosynthesis	Q39TW1	2342606	2345651	BamE	Benzoyl-CoA reductase, putative											0.1	0.8	0.1			1.6		1.5								0.2		1.8	0.2
	Phenol	Q39TP2	2423465	2424242	BamO	Electron transfer flavoprotein, beta subunit	0.2		0.2								0.1		0.1			0.1		0.1								0.1			0.1
		Q39TW6	2338562	2339219	BamI	Iron-sulfur cluster-binding protein, putative											0.1	0.3	0.1			0.1		0.1								0.1		0.4	0.1
	Regulatory functions	Q39TZ0	2308427	2310230	YqiR	Sigma-54-dependent sensor transcriptional regulator											3.8	4														4.8			
	TCA	Q39TX6	2326777	2327941	SucC2	Succinyl-CoA ligase [ADP-forming] subunit beta 2	3.8		3								0.1	4.4	0.1			0.1		0.1								0.2			0.2
		Q39TX7	2325873	2326764	SucD-2	Succinyl-CoA ligase [ADP-forming] subunit alpha	1		0.9								0.2		0.2			0.2		0.2								0.2			0.2
	Uknown function	Q39TP7	2417867	2419211	Gmet_2148	Uncharacterized protein											0.1		0.4			0.1		0.5								0.1			0.8
Butyrate	Amino acid biosynth.;Butanoate	Q39V49	1845015	1846668	Gmet_1644	Pyridoxal-5'-phosphate-dependent decarboxylase							3.2				2.5		0.3			2.2		0.2								1.4			0.3
	Benzoate	Q39UX6	1930131	1930977	HbdA	3-hydroxyacyl-CoA dehydrogenase															0.9	0.1	0.2	0.1	0.1										
	Biosynthesis of cofactors	Q39V51	1843293	1844097	PanB	3-methyl-2-oxobutanoate hydroxymethyltransferase													0.8					0.7							1.2	1.8			0.2
	Butyrate	Q39UX7	1929188	1929971	Crt	Enoyl-CoA hydratase/isomerase															0.1	0.1	0.1	0.1	0.1										
		Q39UY4	1921137	1922103	GctA	Glutaconate CoA-transferase subunit A															0.3	0.3	0.3	0.2	0.2										
		Q39UY5	1920314	1921136	GctB	Glutaconate CoA-transferase subunit B															0.1	0.1	0.1	0.2	0.1										
	Energy metabolism, Electron transport	Q39UX9	1925956	1927972	Gmet_1714	Iron-sulfur cluster-binding oxidoreductase																		4.4	3.8										
		Q39UY0	1925069	1925846	EtfB-7	Electron transfer flavoprotein, beta subunit															0.1	0.1	0.1	0.1	0.1										
		Q39UY1	1924141	1925056	EtfA-7	Electron transfer flavoprotein, alpha subunit															0.1	0.1	0.1	0.1	0.1										
	Fatty acid and phospholipid	Q39UX4	1932263	1933439	ThlA	Thiolase															0.1	0.1	0.2	0.1	0.1										
		Q39UX8	1928020	1929160	Gmet_1715	Short-chain acyl-CoA dehydrogenase															0.2	0.2	0.2	0.2	0.2										
	Geraniol degradation	Q39UY3	1922127	1923288	Gmet_1710	Short-chain acyl-CoA dehydrogenase															0.1	0.1	0.1	0.1	0.2										
	Protein fate,Degradation	Q39UX3	1933769	1934939	Gmet_1720	Aminopeptidase, putative															0.2	0.4	0.3	0.3	0.3										
	Uknown function	Q39UX0	1939519	1940095	Gmet_1723	Uncharacterized protein															0.1	0.1	0.1	0.2	0.1										
		Q39UX2	1934970	1936014	Gmet_1721	Acyl-CoA thioesterase															0.5	1.6	0.6	0.4	1.1										
		Q39UY2	1923272	1924118	Gmet_1711	Acyl-CoA--carboxylate coenzyme A transferase, family III															0.2	0.1	0.1	2.4	0.1										
	Valine, leucine and isoleucine degr.	Q39UX1	1936254	1939503	Mmcm-1	Cobalamin-binding protein kinase (ArgK)															0.1	0.1	0.1	0.1	0.1										
Other	ABC transporters	Q39WU3	1155471	1156281	TupA	Tungstate ABC transporter	0.3										0.4					0.4										1.3			
	Acetate	Q39R65	3431740	3433336	Ato-1	Succinyl:acetate coenzyme A transferase																		3.5											3.4
	Amino acid biosynthesis	Q39VH8	1712791	1713688	Gmet_1512	Glyoxylase-related zinc-dependent hydrolase																2.5	1.8		1.1										
		Q39XT4	765465	766641	MetC-1	Cystathionine gamma-synthase/beta-lyase				3.7																				3.6					
		Q39YS0	405317	406052	Gmet_0361	Oxidoreductase, short-chain dehydrogenase/reductase																0.9	1.5	1.2	0.9										
		Q39YT5	384596	385616	AroG-2	3-deoxy-D-arabino-heptulosonate 7-phosphate synthase		3.7																				1.3	0.9	0.4				3.2	
	antioxidant activity	Q39SB0	2995682	2996213	Gmet_2646	Carboxymuconolactone decarboxylase family protein					2.6		1	4.8	2.9																				

Continue Table 7-4

	Benzoate	Q39XP3	813504	815259	AplA	Sodium/solute symporter family protein				0.8	0.1				3.6	0.1				0.2						2.6		0.4	0.1	0.1		
	Cell envelope	Q39PX0	3929492	3930077	Pal	Peptidoglycan-binding outer membrane lipoprotein								3.5				0.7			0.5											
		Q39W61	1438749	1439568	KdsA	2-dehydro-3-deoxyphosphooctonate aldolase																	1.4	0.9	3.2	0.7						
		Q39WG7	1292646	1293672	Gmet_1169	Uncharacterized protein	4.9	4.1																								
		Q39X08	1082249	1082798	PilP	Type IV pilus assembly lipoprotein PilP												0.8		1.1	0.6											
		Q39XE3	924606	925224	Gmet_0839	Lipoprotein, putative				1.8			2.2																			
		Q39XG8	897119	897893	Gmet_0814	Flotillin band_7_stomatin-like domain protein				0.3	0.4	4.5	1.6					0.8		1.4							1.2		1.9		4.3	
		Q39XS7	775049	776099	Gmet_0705	Membrane protein, putative												0.8	0.8	0.1	0.2	0.1										
	Cellular processes	Q39Q44	3833192	3833684	MglB	Cell polarity determinant GTPase-activating protein MglB				1.5		0.2				1.9																
	Energy metabolism, Electron transport	Q39PV0	3952524	3953298	CbcT-1	Menaquinol oxidoreductase complex Cbc4						0.5																		1.5		
		Q39PV1	3952049	3952532	CbcS-1	Menaquinol oxidoreductase complex Cbc4						1.1															0.6		3.8	0.2	1.2	
		Q39QD0	3744463	3746164	HyaL	[NiFe]-hydrogenase, large subunit							0.1				0.3				0.1							0.6	0.2	0.1	0.1	
		Q39UU0	1968094	1969216	Gmet_1753	NADPH-dependent glutamate synthase,																	4.9	1.6		1						
		Q39WZ7	1093190	1093589	GcvH1	Glycine cleavage system H protein 1																		1.7								
	Glycerophospholipids	Q39ZR6	12342	13350	GpsA	Glycerol-3-phosphate dehydrogenase [NAD(P)+]																		3.5		1.4						
	Glycolysis/gluconeogenesis	Q39WT8	1161194	1162358	Gmet_1046	Ethanol dehydrogenase, putative						2.8											0.1	0.1	0.1	0.1	0.1					
		Q39WT9	1159180	1160911	AorA	Aldehyde:ferredoxin oxidoreductase, tungsten-containing																	0.1	0.1	0.2	0.1	0.1					
	Mob. and extrachrom. Functions	Q39WR7	1189035	1189890	Csd2	CRISPR-associated protein Csd2			1.5				0.6				1				2.8					0.4						
	Nitrogen metabolism	Q39XX0	724757	725627	NifH	Nitrogenase reductase																		2.8								
	Propinoate metabolism	Q39WL1	1245849	1247445	Gmet_1125	Succinyl:acetate coenzyme A transferase		3.2										2.9	4	3.8	0.6	1										
		Q39WL2	1244475	1245792	Gmet_1124	Citrate synthase												0.5	1.4	2.4	0.9	0.8										
	Protein fate,Degradation	Q39RQ5	3228779	3231374	ClpB	ATP-dependent chaperone ClpB	2.7					0.5	1.5																3.7		
		Q39SZ0	2724288	2724792	Gmet_2409	Intracellular protease, PfpI family, putative				0.9	4		2.2														3.2					
	Protein synthesis	Q39Z86	222075	223659	PrfC	Peptide chain release factor 3 (RF-3)	0.6					0.4				0.7																
		Q39ZJ9	93141	93429	GatC	Aspartyl/glutamyl-tRNA(Asn/Gln) amidotransferase				2.6		3		1.4		1																
	Purine ribonucl. Biosynth.	Q39TA7	2597751	2599314	GuaA	GMP synthase [glutamine-hydrolyzing]	3.1		0.8																4.6	3.7					
	Regulatory functions	Q39QU7	3562228	3563176	Gmet_3164	Helix-turn-helix XRE domain protein								0.6	1.5	0.1	0.8														
		Q39XM0	835270	836008	Gmet_0762	Response receiver				0.2	1.1							0.8									4.1					
		Q39XP1	815944	816712	Gmet_0741	Helix-turn-helix transcriptional regulator, IclR family					0.4		0.9																			
		Q39Z96	210641	212915	Tex	S1 RNA-binding domain-containing transcriptional protein	0.3		0.5			1.4	3.8			1.8	4.8															
	Transport and binding proteins,Porins	Q39WU2	1156443	1157688	Gmet_1042	Phosphate-selective outer membrane channel	1.4								0.4				0.4					2.8				4.1				
	Uknown function	Q39RR9	3216591	3217302	Gmet_2837	Cytidylate kinase-like domain protein				2.7	1.6		0.4	4.5																		
		Q39TA8	2597140	2597626	Gmet_2291	Ferritin-like domain protein				0.1		4.5	0.4					4.3														
		Q39YM7	445790	446732	RsmH	Ribosomal RNA small subunit methyltransferase H	1.4									3.7													2.8			
		Q39Z93	214612	215779	Gmet_0185	Uncharacterized protein	0.6					0.2	2.5			2.4									0.2	1						
		Q39ZN0	57519	58038	Gmet_0044	Uncharacterized protein				3.1		1.3	0.2	2.3																		
		Q39ZP4	36668	38729	PrkA	Protein serine/threonine kinase PrkA					2		2.5																			3.8
	Unknown function	Q39RC2	3373648	3374491	Gmet_2987	Adenosine nucleotide alpha-hydrolase superfamily protein																		3.5	1.4	1.6	0.6					
		Q39SD3	2966567	2967026	Gmet_2622	Uncharacterized protein				3.5	0.9		0.2								0.6										1.2	
		Q39SI4	2919542	2920436	Gmet_2571	ATPase DUF815, putative									3.4		1.6											3.8			2.6	
Toluene	Protein fate, folding	Q39VF3	1741121	1742006	Gmet_1537	Aromatic hydrocarbon degradation ATPase																						1.5	0.3	1.6	2.4	
	Toluene	Q39VF1	1742441	1745030	BssA	(R)-benzylsuccinate synthase, alpha subunit																					0.1	0.1	0.1	0.1	0.1	
		Q39VF9	1734052	1734802	BbsD	Succinyl-CoA dehydrogenase subunit																					0.1	0.1	0.1	0.1	0.1	
		Q39VG0	1733277	1734024	BbsC	Succinyl-CoA dehydrogenase subunit																					0.1	0.1	0.1	0.1	0.1	
		Q39VG1	1732057	1733230	BbsB	Benzoylsuccinyl-CoA thiolase subunit																					0.1	0.1	0.1	0.1	0.1	
		Q39VG3	1729575	1731540	Gmet_1527	Iron-sulfur cluster-binding oxidoreductase																					0.2	0.3	0.2	0.1	0.2	
		Q39VG4	1728686	1729574	EtfA-5	Electron transfer flavoprotein, alpha subunit																					0.1	0.2	0.3	0.1	0.2	
		Q39VG5	1727934	1728690	EtfB-5	Electron transfer flavoprotein, beta subunit																					0.1	0.3	0.2	0.1	0.1	
		Q39VG6	1727153	1727924	BbsH	(E)-2-benzylidenesuccinyl-CoA hydratase																					0.1	0.1	0.1	0.1	0.1	
		Q39VG7	1725876	1727109	BbsG	(R)-benzylsuccinyl-CoA dehydrogenase																					0.1	0.1	0.1	0.1	0.1	
		Q39VG8	1724613	1725843	BbsF	Succinyl:(R)-benzylsuccinate CoA transferase subunit																						0.3	0.4	0.8	0.9	
		Q39VG9	1723391	1724630	BbsE	Succinyl:(R)-benzylsuccinate CoA transferase subunit																					0.2	0.2	0.2	0.2	0.2	
	Transport and binding proteins,Unknown substrate	Q39VF5	1737983	1739345	Gmet_1535	Aromatic hydrocarbon degradation membrane protein																					0.1	0.1	0.2	0.2	0.2	

[a] - start of the encoding gene on the genome

[b] - end of the encoding gene on the genome

[c] - first condition of comparison

[d] - second condition of comparison, where" Ace" - acetate, "But" - butyrate, "Eth" - ethanol, "Tol" - toluene, "AB" - acetate plus benzoate

FDRs are showed for differentially expressed proteins (FDRs<5%)

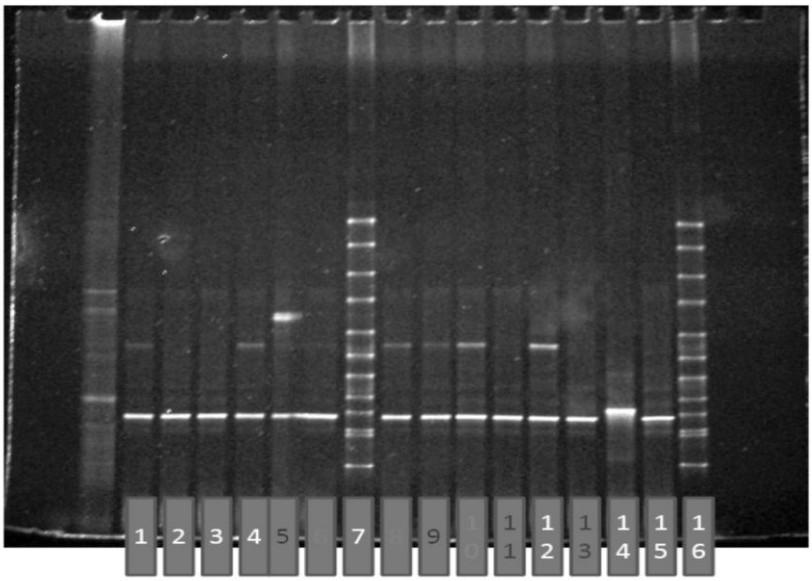

Figure 7-1. DGGE profile of 16S rRNA extracted from cells cultivated in different retentostats at different sampling points. "A3 t18" and "A3 final" – acetate limited retentostat, run 1, at the beginning and the end of cultivation; "a5 t6" - acetate limited retentostat, run 2, t_0; "Ab1 t14" and "Ab1 final" – acetate and benzoate limited retentostat, run 1, at the beginning and the end of cultivation; "ab3 t5" and "ab3 final" - acetate and benzoate limited retentostat, run 2, at the beginning and the end of cultivation.

Table 7-5. Relative fold changes in abundances of proteins identified as differentially expressed in acetate-limited retentostats relative to batch.

Protein abundances in retentostat were compared to protein abundances in exponential growth phase (μ_{max}). Proteins which were not detected in batch are labelled with * and were related to t0 in retentostat. Proteins with FDRs < 2% were considered as significantly expressed and were further used for pairwise comparisons. Significantly expressed proteins with FDRs <5% for pairwise comparison are highlighted with colour. t0, t1, t2 indicate the sampling points for proteomic analysis, see Fig.1. [AB]Proteins differentially expressed on condition acetate plus benzoate as well (see Table S3).

	Annotation	Gene name	FDR	$^{A}t_0/{}^{A}batch$	$^{A}t_1/{}^{A}batch$	$^{A}t_2/{}^{A}batch$	$^{A}t_0/{}^{A}t_1$	$^{A}t_0/{}^{A}t_2$	$^{A}t_1/{}^{A}t_2$
Amino acid biosynthesis									
Q39QR3	Glutamate 5-kinase	proB	0.1	5.5	8.1	79.4	0.7	0.1	0.1
Q39UT7	NADPH-dependent glutamate synthase, Fe-S cluster-binding	Gmet_1756	0.1	0.4	0	0		26.3	0.0
Q39VD2	Cysteine synthase	cysK-2	0.4	12	81.8	43.1	0.1	0.3	1.9
Q39QL2	Biotin-dependent acyl-CoA carboxylase, subunit	Gmet_3249	0.4	14.3	10.9	12.7	1.3	1.1	0.9
Q39WN5	Alanine dehydrogenase	ald	0.5	3.6	11.6	11.5	0.3	0.3	1.0
Q39X26	Valine--tRNA ligase	valS	0.5	6.7	6.8	8.6	1.0	0.8	0.8
Q39V41[AB]	Efflux pump, RND family, inner membrane protein	Gmet_1652	0.2	5.4	12.1	18.6	0.4	0.3	0.7
Q39SS2	Tryptophan synthase alpha chain	trpA	0.2	2.3	3.8	5.7	0.6	0.4	0.7
Q39YP3	Phosphoribosylformimino-5-aminoimidazole carboxamide isomerase	hisA	0.3	0.5	0.2	0.1	2.4	5.3	2.2
Q39W69	Isopropylmalate/citramalate isomerase, small subunit	leuD	0.7	0.3	0.1	0.1	2.2	3.3	1.5
Q39YT0	Isoleucine--tRNA ligase	ileS	1.2	16.2	9.1	13.5	1.8	1.2	0.7
Q39YP8	ATP phosphoribosyltransferase	hisG	1.2	1.3	0.3	0.3	4.1	4.4	1.1
Q39UM0	Phenylacetate--coenzyme A ligase	paaK-2	1.6	3.2	5.8	4.1	0.6	0.8	1.4
Q39YM4	Meso-diaminopimelate-adding enzyme	murE	1.8	3.7	6	6.4	0.6	0.6	0.9
Q39Y27	Aspartate-semialdehyde dehydrogenase 2	asd2	2	3.6	3	5.6	1.2	0.6	0.5
Q39RJ5*[AB]	Oxidoreductase, flavin-binding protein	Gmet_2911	0.6		17.93	1.35	0.1	0.7	13.3
Bacterial secretion system									
Q39X31	Protein translocase subunit SecA	secA	0.3	8.6	6.6	16.4	1.3	0.5	0.4
Biosynth. and degradation of polysacchar.									
Q39XE9[AB]	Alpha-amylase family protein	Gmet_0833	0.1	3.5	35.6	32.7	0.1	0.1	1.1
Q39QV2[AB]	Alpha-glucan phosphorylase	Gmet_3159	0.2	4.3	17.2	10.8	0.3	0.4	1.6
Biosynthesis of cofactors									
Q39YF0	Cobalt-precorrin-6B C5,C15-methyltransferase and C12-decarboxylase	cbiET	0.8	4.7	6.8	9.7	0.7	0.5	0.7
Q39RX2[AB]	BioD and DRTGG domain protein	Gmet_2784	1.2	9.1	26.9	39.7	0.3	0.2	0.7
Q39QM8	Glutamyl-tRNA reductase	hemA	1.8	3	5.3	10.2	0.6	0.3	0.5
Carbohydrate metabolism									
i) Benzoate degradation									
Q39TW4	Benzoyl-CoA reductase electron transfer protein, putative	bamG	0.5	0	0	0			
Q39ZG7	ATPase, AAA_5 family	Gmet_0108	0.6	0	0.1	0	0.0		
Q39TV8	Benzoyl-CoA reductase, putative	bamB-1	0.9	11.8	14.4	14	0.8	0.8	1.0
Q39TW2	Benzoyl-CoA reductase, selenocysteine-containing	bamF	1.3	0.3	0.1	0.1	4.5	3.2	0.7
ii) Aliphatic acids metabolism									
Q39WV0	Acetate kinase	ackA	0.7	3.5	6.6	9.5	0.5	0.4	0.7
Q39S61[AB]	Hydroxypyruvate reductase, putative	hprA	0.8	2.4	18	19.5	0.1	0.1	0.9
Q39ZA0	Transketolase	tkt	1.1	3.4	5.4	3.3	0.6	1.0	1.6
Q39QU2	Phosphoenolpyruvate carboxykinase	pckA	1.2	4.7	9.9	6.4	0.5	0.7	1.5
Q39TU7	Phosphotransbutyrylase	ptb	1.2	9.5	28.3	27.4	0.3	0.3	1.0
iii) Citrate cycle (TCA cycle)									
Q39XG6[AB]	Pyruvate carboxylase	pyc	0.1	36	22.3	23.4	1.6	1.5	1.0
Q39RZ3	Aconitate hydratase, putative	Gmet_2763	0.1	9.2	22.6	8.8	0.4	1.1	2.6

	Annotation	Gene name	FDR	$^{A}t_0/^{A}batch$	$^{A}t_1/^{A}batch$	$^{A}t_2/^{A}batch$	$^{A}t_0/^{A}t_1$	$^{A}t_0/^{A}t_2$	$^{A}t_1/^{A}t_2$
Q39WW6[AB]	Aconitate hydratase 1	acnA	0.3	33	95.3	52.7	0.3	0.6	1.8
Q39W29	2-oxoacid:ferredoxin oxidoreductase, gamma subunit	vorC	1	0.5	0.2	0.2	2.3	2.6	1.1
iv) Alcohols degradation									
Q39WT9[AB]	Aldehyde:ferredoxin oxidoreductase, tungsten-containing	aorA	0	125.8	455.9	367.5	0.3	0.3	1.2
Q39WT8[AB]	Ethanol dehydrogenase, putative	Gmet_1046	0.1	1672	1180	629.6	1.4	2.7	1.9
Q39XJ3	Aldehyde dehydrogenase family 11 protein	GapN	1.9	4.5	9.9	3.2	0.5	1.4	3.1
Cell envelope									
Q39X72[AB]	Lipoprotein cytochrome c	Gmet_0910	0.3	12.4	32.1	23.2	0.4	0.5	1.4
Q39SC7	Lipoprotein, putative	Gmet_2628	0.5	7	8.6	6	0.8	1.2	1.4
Q39WY7	VacJ family lipoprotein fusion protein	Gmet_0995	0.7	0	0	0	0.5	0.7	1.5
Q39ZH8[AB]	Uncharacterized protein	Gmet_0097	1.1	0	0	0		0.0	0.0
Q39UF9	Phosphoglucosamine mutase	glmM	1.1	2.3	3.7	5.1	0.6	0.4	0.7
Q39U17	Protein tyrosine kinase, putative	Gmet_2028	1.5	1.2	2.7	8.7	0.5	0.1	0.3
Q39PY3[AB]	Lipoprotein, putative	Gmet_3486	1.5	0	0	0.1		0.0	0.0
Q39PU7	Outer membrane protein, putative	Gmet_3522	1.6	0.2	0.1	0.1	3.2	3.2	1.0
Central intermediary metabolism									
Q39X36[AB]	N-acetylglutamate synthase	argA	1.5	0	0	0	44.1	10.1	0.2
Chemotaxis and motility									
Q39SS1[AB]	Methyl-accepting chemotaxis sensory transducer, class 40+24H	mcp64H-2	0	8.6	11.6	30.3	0.7	0.3	0.4
Q39Q44	Cell polarity determinant GTPase-activating protein MglB	mglB	0	0	0	0	0.0		
Q39RG8	Methyl-accepting chemotaxis sensory transducer, class 40+24H	mcp64H-1	1.1	3.6	5.8	12.6	0.6	0.3	0.5
Q39U12*	Uncharacterized protein	Gmet_2033	0.9		1.96	7.19	0.5	0.1	0.3
Detoxification									
Q39XJ8[AB]	Organic solvent tolerance ABC transporter	Gmet_0784	0.8	0.7	0.2	0.1	4.2	11.2	2.7
Electron transport									
Q39Z19[AB]	Twitching motility pilus retraction ATPase	pilT-2	0.8	4.5	5.7	5.2	0.8	0.9	1.1
Q39X15	Type IV pilus assembly protein PilY1	pilY1-2	1.7	12.2	14.4	18.4	0.8	0.7	0.8
Q39TX8	Electron transfer flavoprotein, beta subunit	etfB-2	0.1	0	0	0	4.4	0.7	0.2
Q39WP0	Periplasmic diheme cytochrome *c* catalase	cccA	0.3	10.6	16.3	1.7	0.6	6.2	9.6
Q39UY1[AB]	Electron transfer flavoprotein, alpha subunit	etfA-7	0.3	0	0	0		4.7	0.0
Q39QD0	[NiFe]-hydrogenase, large subunit	hyaL	0.4	4.8	31.3	42.4	0.2	0.1	0.7
Q39XM1	Iron-sulfur cluster-binding oxidoreductase	Gmet_0761	0.7	3.6	4.6	3.8	0.8	1.0	1.2
Q39ZH5	Cytochrome c/b	cbcY	0.7	11.9	9.8	9.5	1.2	1.2	1.0
Q39QA9	NADH-quinone oxidoreductase subunit C	nuoC	1.3	0.3	0.2	0.1	1.8	2.3	1.3
Q39RH8*	Menaquinol oxidoreductase complex Cbc5, cytochrome c subunit	cbcA	1.4					4.8	0.0
Q39XE5	Aerobic-type carbon monoxide dehydrogenase, large subunit	Gmet_0837	0.4	4.3	9.3	4.3	0.5	1.0	2.2
Q39WI8*	Rubredoxin reductase, selenocysteine-containing	Gmet_1148	1.5				0.3	0.3	1.0
Q39QA3[AB]	ATP synthase subunit a	atpB	0.4	0	0	0.2	0.0	0.0	0.0
Q39QB7	NADH-quinone oxidoreductase subunit K 2	nuoK2	0.7	0.2	0.1	0.1	1.9	2.4	1.3
Q39QB1	NADH dehydrogenase I, E subunit	nuoE-1	0.8	0.2	0.1	0	2.6	8.8	3.4
Q39QW7[AB]	NAD-dependent nucleoside diphosphate-sugar epimerase/dehydratase	Gmet_3144	1.2	3.8	8.9	6.2	0.4	0.6	1.4
Mobile and extrachrom. element functions									
Q39SF2	Toxin, MazF family	Gmet_2603	0.1	0.1	0.1	0	1.0	1.9	1.8
Nitrogen metabolism									
Q39R30	Thioredoxin/NifU-like domain protein	Gmet_3080	0	0	0	0	0.3	1.1	3.2
Q39UW5	Glu/Leu/Phe/Val dehydrogenase superfamily protein	Gmet_1728	1.3	22.2	14.5	10.6	1.5	2.1	1.4
Nucleotide biosynthesis									
Q39UH0[AB]	Non-canonical purine NTP pyrophosphatase	rdgB	0.2	0	0	0	1.1	0.4	0.3
Q39UA7	Orotate phosphoribosyltransferase	pyrE	0.7	0.3	0.1	0	5.1	14.5	2.8
Q39UA4	Phosphoribosylformylglycinamidine synthase 2	purL	1.2	12.4	8.4	7.6	1.5	1.6	1.1

	Annotation	Gene name	FDR	$^{A}t_0/^{A}batch$	$^{A}t_1/^{A}batch$	$^{A}t_2/^{A}batch$	$^{A}t_0/^{A}t_1$	$^{A}t_0/^{A}t_2$	$^{A}t_1/^{A}t_2$
Q39XX1	Carbamoyl-phosphate synthase large chain 1	carB-2	1.8	26.7	12.2	9.3	2.2	2.9	1.3
Protein and peptide secretion and trafficking									
Q39ST3	Peptidoglycan-binding ATPase, putative	exeA	0.1	0	0	0	1.1	1.0	0.9
Q39XY6	Protein translocase subunit SecY	secY	1.2	5.9	6.1	9	1.0	0.7	0.7
Protein folding and stabilization									
Q39UM8[AB]	Peptidylprolyl cis-trans isomerase, PpiC-type	Gmet_1817	0.7	0	0	0	1.3	1.6	1.2
Q39Z20	Peptidyl-prolyl cis-trans isomerase	Gmet_0259	0.8	0.1	0	0	3.6	6.2	1.7
Q39SQ3	Chaperone protein HtpG	htpG	1.6	0.7	0.2	0.1	3.1	10.5	3.4
Protein synthesis									
Q39Y25	50S ribosomal protein L13	rplM	0.1	0.2	0.2	0.2	1.0	0.7	0.7
Q39VS4	Phenylalanine--tRNA ligase beta subunit	pheT	0.5	5.6	4.5	14.6	1.3	0.4	0.3
Q39VS9[AB]	Threonine--tRNA ligase	thrS	0.7	3.8	5.9	10.2	0.6	0.4	0.6
Q39Y20	50S ribosomal protein L33	rpmG	0.8	0	0	0		0.0	0.0
Q39VA6	Translation initiation factor IF-2	infB	0.8	8.3	6.9	19.4	1.2	0.4	0.4
Q39U60[AB]	Elongation factor G 2	fusA-1	1.2	4.7	10.3	5.6	0.5	0.8	1.8
Q39Z77	Alanine--tRNA ligase	alaS	1.3	7.7	5	3.4	1.5	2.3	1.5
Q39UK8[AB]	Translation initiation factor IF-1	infA	1.6	0	0.1	0	0.6	1.4	2.4
Q39UK7	Elongation factor P 2	efp2	1.8	0.5	0.3	0.5	2.0	1.1	0.5
Regulatory functions									
Q39W50	Phosphocarrier protein HPr	ptsH	0	0.1	0	0.1	1.1	0.7	0.7
Q39QR4	GTPase obg (GTP-binding protein obg)	obg	0.2	7.2	3.1	21.8	2.3	0.3	0.1
Q39WF6	Ribonuclease Y	rny	1.2	3.1	3.1	10.2	1.0	0.3	0.3
Q39WN1[AB]	Transcription elongation factor GreA 1	greA1	1.5	0	0	0	0.0	0.0	0.5
RNA degradation									
Q39SK9	Ribonuclease, Rne/Rng family	Gmet_2546	0.8	13.2	9.2	13	1.4	1.0	0.7
Signal transduction									
Q39UC8	Response receiver sensor diguanylate cyclase, PAS domain-containing	Gmet_1917	0.1	0	0	0	0.0		
Q39ZR5[AB]	Sensor histidine kinase, HAMP and PAS domain-containing	Gmet_0009	0.2	0	0	0	0.4	1.2	3.1
Transcription									
Q39Y13[AB]	DNA-directed RNA polymerase subunit beta	rpoB	1.1	21.5	6.7	8.2	3.2	2.6	0.8
Q39Y12[AB]	DNA-directed RNA polymerase subunit beta	rpoC	1.2	21.2	8.3	9.7	2.6	2.2	0.9
Q39VR9	RNA polymerase sigma factor	rpoS	1.2	0.4	0	0	7.5	15.0	2.0
Transport and binding proteins									
Q39R73[AB]	ABC transporter, membrane protein	macB	0.3	8.6	35.9	49.2	0.2	0.2	0.7
Q39VE2[AB]	Metal ion efflux pump, RND family, membrane fusion protein	cusB	0.8	7.4	25.1	21.7	0.3	0.3	1.2
Q39WX0	Uncharacterized protein	Gmet_1012	1.3	7.3	16.1	8	0.5	0.9	2.0
Q39VE3[AB]	Metal ion efflux pump, RND family, inner membrane protein	cusA	1.5	5.8	11.7	13	0.5	0.4	0.9
Q39VD4*	Heavy metal transport/detoxification domain protein	Gmet_1556	1.1		8.94	7.70	0.1	0.1	1.2
Q39ST4*	Membrane protein, major facilitator superfamily	Gmet_2465	0.6		1.16	23.00	0.9	0.0	0.1
Unknown function									
Q39U13	TPR domain lipoprotein	Gmet_2032	0.7	8.5	25.6	145.8	0.3	0.1	0.2
Q39WC8[AB]	Peptidase, putative	Gmet_1209	0.1	3.9	5.6	3.1	0.7	1.3	1.8
Q39ZP4[AB]	Protein serine/threonine kinase PrkA	prkA	0.1	5	13.4	6.4	0.4	0.8	2.1
Q39QI8	Uncharacterized protein	Gmet_3273	0.2	0.1	0.1	0	1.3	1.5	1.2
Q39T38[AB]	Uncharacterized protein	Gmet_2361	0.2	0.3	0.1	0	4.3	10.0	2.3
Q39V97	tRNA (N6-threonylcarbamyl-A37) modification ATPase	yrdC	0.3	1.9	1.9	41	1.0	0.0	0.0
Q39WV2	Uncharacterized protein	Gmet_1032	0.3	8.9	8	12.5	1.1	0.7	0.6
Q39T93	HEAT-like repeat-containing protein	Gmet_2306	0.6	15.5	18.5	8.5	0.8	1.8	2.2
Q39XS8[AB]	Uncharacterized protein	Gmet_0704	0.7	0	0	0	0.0		
Q39RB8	Uncharacterized protein	Gmet_2991	0.8	0	0	0	0.9	0.4	0.4

	Annotation	Gene name	FDR	$^{A}t_0/^{A}batch$	$^{A}t_1/^{A}batch$	$^{A}t_2/^{A}batch$	$^{A}t_0/^{A}t_1$	$^{A}t_0/^{A}t_2$	$^{A}t_1/^{A}t_2$
Q39QD3	Glyoxalase/bleomycin resistance protein	Gmet_3328	1.1	0.1	0.1	0.1	1.0	1.5	1.5
Q39S01	Uncharacterized protein	Gmet_2755	1.1	0.3	0.7	0.1	0.4	1.8	5.0
Q39YN1	Uncharacterized protein	Gmet_0400	1.1	0.3	0.2	0.2	1.9	1.6	0.9
Q39X68[AB]	Uncharacterized protein	Gmet_0914	1.2	0.1	0.1	0	0.8	3.0	3.7
Q39Q16[AB]	Periplasmic protein YceI	Gmet_3449	1.2	0.5	0	0.1	14.9	8.9	0.6
Q39XT9	Uncharacterized protein	Gmet_0693	1.5	1	0.1	3.8	12.8	0.3	0.0
Q39XF1	Uncharacterized protein	Gmet_0831	1.5	11.7	16	11.9	0.7	1.0	1.3
Q39RC8	Uncharacterized protein	Gmet_2981	1.5	17.5	17.4	12.5	1.0	1.4	1.4
Q39UR7	Uncharacterized protein	Gmet_1776	1.6	0.3	0	1.1	36.5	0.3	0.0
Q39RS7[AB]	DUF748 repeat protein	Gmet_2829	1.7	20.7	24.2	33.6	0.9	0.6	0.7
Q39V18*	Uncharacterized protein	Gmet_1675	1.1		1.22	4.46	0.8	0.2	0.3
Q39QY8*	Rhodanese homology domain superfamily protein	Gmet_3122	1.2		1.22	7.39	0.8	0.1	0.2
Q39T12*	Uncharacterized protein	Gmet_2387	0		0.03	0.07	38.2	13.4	0.4

Table 7-6. Relative fold changes in abundances of proteins identified as differentially expressed in acetate plus benzoate-limited retentostats relative to batch. Protein abundances in retentostat were compared to protein abundances in exponential growth phase (μ_{max}). Proteins which were not detected in batch are labeled with * and were related to t0 in retentostat. Proteins with FDRs < 2% were considered as significantly expressed and were further used for pairwise comparisons. Significantly expressed proteins with FDRs <5% for pairwise comparison are highlighted with colour. t0, t1, t2 indicate the sampling points for proteomic analysis, see Fig.1. [AB]Proteins differentially expressed on condition acetate plus benzoate as well (see Table S3).

ID	Name	Gene name	FDR	$^{AB}t_0/^{AB}batch$	$^{AB}t_1/^{AB}batch$	$^{AB}t_2/^{AB}batch$	$^{AB}t_3/^{AB}batch$	$^{AB}t_0/^{AB}t_1$	$^{AB}t_0/^{AB}t_2$	$^{AB}t_0/^{AB}t_3$	$^{AB}t_1/^{AB}t_2$	$^{AB}t_1/^{AB}t_3$	$^{AB}t_2/^{AB}t_3$
Q39S60	Carbon starvation protein CstA	cstA-2	1	14.6	104.9	160.1	80	0.1	0.1	0.2	0.7	1.3	2
Amino acid biosynthesis													
Q39YP5	Imidazoleglycerol-phosphate dehydratase	hisB	0.5	1.2	1.2	0.1	0.6	1	11.3	1.9	11	1.9	0.2
Q39VH8	Glyoxylase-related hydrolase	Gmet_1512	0.9	0.2	0.1	0	0.1	1.6	4	2.5	2.5	1.6	0.6
Q39Y82	5-methyltetrahydrofolate S-methyltransferase	metH	1.1	3.9	6.1	7.1	6.8	0.6	0.5	0.6	0.9	0.9	1
Q39V41[A]	Efflux pump, RND family	Gmet_1652	1.1	12.3	21.6	47.8	23.7	0.6	0.3	0.5	0.5	0.9	2
Q39Q67	4-oxobutanoate dehydrogenase	gabD	1.8	0.1	0.1	0	0	0.9					
Q39RJ5*[A]	Oxidoreductase, flavin-binding protein	Gmet_2911	1.9		69063.6013	72492.188	222586				1	0.3	0.3
Biosynthethis and degradation of polysaccharides													
Q39XE9[A]	Alpha-amylase family protein	Gmet_0833	0.1	5.3	33.2	46.3	36	0.2	0.1	0.1	0.7	0.9	1.3
Q39QV2[A]	Alpha-glucan phosphorylase	Gmet_3159	1.5	3.2	6	7.3	3.9	0.5	0.4	0.8	0.8	1.5	1.9
Biosynthesis of cofactors													
Q39XB6	4-hydroxy-3-methylbut-2-enyl reductase	ispH	1.6	0	0	0	0	5.3	5.8	4	1.1	0.8	0.7
Q39RX2[A]	BioD and DRTGG domain protein	Gmet_2784	1.7	2	12.8	29.5	14.5	0.2	0.1	0.1	0.4	0.9	2
Q39WW9	Rhodanese homology domain	Gmet_1013	1.7	0.2	0.4	0.4	0.1	0.5	0.5	2.6	1.1	5.5	4.9
Q39RJ7	Hydroxymethylpyrimidine kinase	thiD	1.8	0.5	1.1	1.8	3.7	0.5	0.3	0.1	0.6	0.3	0.5
Q39UD6*	Pyridoxamine-5'-phosphate oxidase-related	Gmet_1909	0.2		3.64	1.08	80.60	0.3	0.9	0	3.4	0	0
Carbohydrate metabolism													
i) Benzoate degradation													
Q39TY1	Helix-turn-helix transcr. regulator, IclR	Gmet_2064	0.2	0	0.2	0	0					22.5	
Q39VH2	Lipoprotein release ABC transporter	lolD-2	1.1	0	0.1	0.1	0.1	0.2	0.1	0.2	0.5	1	2.1
ii) Aliphatic acids metabolism													
Q39QK8	Methylmalonyl-CoA epimerase	mceE	0.2	212.2	325.8	47.1	49.7	0.7	4.5	4.3	6.9	6.6	0.9
Q39S61[A]	Hydroxypyruvate reductase, putative	hprA	0.4	3.5	12.2	17.3	13.3	0.3	0.2	0.3	0.7	0.9	1.3

ID	Name	Gene name	FDR	$^{AB}t_0$/ ^{AB}batch	$^{AB}t_1$/ ^{AB}batch	$^{AB}t_2$/ ^{AB}batch	$^{AB}t_3$/ ^{AB}batch	$^{AB}t_0$/ $^{AB}t_1$	$^{AB}t_0$/ $^{AB}t_2$	$^{AB}t_0$/ $^{AB}t_3$	$^{AB}t_1$/ $^{AB}t_2$	$^{AB}t_1$/ $^{AB}t_3$	$^{AB}t_2$/ $^{AB}t_3$
Q39WS5	Formate dehydrogenase, major subunit,	fdnG	1.6	0	0.2	0	0	0					
Q39X45*	HAD superfamily hydrolase	Gmet_0937	1.7		1352.52364	0	3521.74					0.4	
iii) Citrate cycle (TCA cycle)													
Q39XG6[A]	Pyruvate carboxylase	pyc	0.4	10.5	7.3	10.9	11.5	1.4	1	0.9	0.7	0.6	0.9
Q39WW6[A]	Aconitate hydratase 1	acnA	1.7	10.6	44.6	87.8	389	0.2	0.1	0	0.5	0.1	0.2
Q39Z08*	Lipoprotein, putative	Gmet_0271	0.4		0.59	0.83	0.08	1.7	1.2	12.4	0.7	7.3	10.3
iv) Alcohols degradation													
Q39WT9[A]	Aldehyde:ferredoxin oxidoreductase	aorA	0.4	1326.7	1441.2	1468.8	1517.7	0.9	0.9	0.9	1	0.9	1
Q39WT8[A]	Ethanol dehydrogenase, putative	Gmet_1046	1.7	5288.1	774.3	427.5	262.8	6.8	12.4	20.1	1.8	2.9	1.6
v) Xenobiotics degradation													
Q39TU3*	Phenylphosphate carboxylase, beta subunit	Gmet_2102	1.4		16.10	0.70	0.58	0.1	1.4	1.7	22.8	27.7	1.2
Cell division													
Q39X87	Maf-like protein	Gmet_0895	1.9	0.9	1.7	0	1	0.6	23.5	0.9	42.6	1.6	0
Cell envelope													
Q39WG7	Uncharacterized protein	Gmet_1169	0.3	0.1	0	0	0	12.9					
Q39PY3[A]	Lipoprotein, putative	Gmet_3486	0.4	0	0	0	0.1	0.2		0		0.1	
Q39U15	Periplasmic polysacch. biosynthesis/export	Gmet_2030	0.4	2.8	2.7	6	21.9	1	0.5	0.1	0.4	0.1	0.3
Q39XG8	Flotillin band_7_stomatin-like	Gmet_0814	0.4	6.8	6.5	5.7	6.6	1	1.2	1	1.1	1	0.9
Q39V14	Peptidoglycan-binding domain 1 protein	Gmet_1679	0.5	7.7	4.9	5.4	3.7	1.6	1.4	2	0.9	1.3	1.4
Q39VR1	Outer membrane lipoprotein, Slp family	Gmet_1429	0.5	38.4	25.5	28.1	51.5	1.5	1.4	0.7	0.9	0.5	0.5
Q39VE5	Germane superfamily lipoprotein, putative	Gmet_1545	0.8	1.3	97.2	407.1	129	0	0	0	0.2	0.8	3.2
Q39ZH8[A]	Uncharacterized protein	Gmet_0097	1	0.4	0	0.3	0.3	11.6	1.2	1.2	0.1	0.1	1
Q39Y54	Uncharacterized protein	Gmet_0577	1	3.7	1.8	0.2	0.5	2.1	22.2	7.8	10.8	3.8	0.4
Q39V42	Efflux pump, RND family,fusion lipoprotein	Gmet_1651	1.2	3.4	21.8	36.5	20.6	0.2	0.1	0.2	0.6	1.1	1.8
Q39R95	Outer membrane protein assembly factor	yfiO	1.4	1.3	1.2	0.2	0.4	1	7.6	2.9	7.5	2.8	0.4
Q39X72[A]	Lipoprotein cytochrome c	Gmet_0910	1.4	8.9	78.3	232.8	280.8	0.1	0	0	0.3	0.3	0.8
Q39Q84	Outer membrane lipoprotein LolB, putative	Gmet_3378	1.7	1.5	0.3	0	0.2	4.5		6.5		1.4	
Q39Z08*	Lipoprotein, putative	Gmet_0271	0.4		0.59	0.83	0.08	1.7	1.2	12.4	0.7	7.3	10.3
Central intermediary metabolism													
Q39X36[A]	N-acetylglutamate synthase	argA	0.5	0	0	0	0	0					
Q39VV8	Arylsulfotransferase	Gmet_1382	0.8	0.1	0.3	0	0	0.3					
Chemotaxis and motility													
Q39XK2	Glutamate methylesterase	cheBR	1.5	5.5	4.1	5.8	2.4	1.3	0.9	2.3	0.7	1.7	2.4
Q39SS1[A]	Methyl-accepting chemotaxis	mcp64H-2	0	8.1	12.1	16.1	18.8	0.7	0.5	0.4	0.8	0.6	0.9
Q39V52	GAF sensor methyl-accepting chemotaxis	mcp40H-1	1.4	4.2	8.1	9.3	7.1	0.5	0.4	0.6	0.9	1.1	1.3
Degradation of proteins													
Q39SZ0	Intracellular protease, PfpI family	Gmet_2409	0.5	15.8	26.9	42.9	46.3	0.6	0.4	0.3	0.6	0.6	0.9
Q39UH3	ATP-dependent Clp protease ATP-binding	clpX	1.1	0	0	0	0.1	1.7	3.8	0.9	2.3	0.6	0.2
Detoxification													
Q39XJ8[A]	Organic solvent tolerance ABC transporter	Gmet_0784	1.4	0.9	0.2	0.1	0.1	4	15.9	7	3.9	1.7	0.4
DNA metabolism													
Q39XB4	Integration host factor, beta subunit	ihfB-2	0.4	0.3	0.2	0.1	0.2	1.6	2.2	1.6	1.4	1	0.7
Mobile and extrachromosomal functions													
Q39XV5*	Toxin, RelE family	Gmet_0677	0.4		0.61	0.93	0.30	1.6	1.1	3.3	0.7	2	3.1
Transcription													
Q39Y12[A]	DNA-directed RNA polymerase subunit beta	rpoC	2	12.3	4.4	5.9	4.5	2.8	2.1	2.7	0.8	1	1.3
Q39Y13[A]	DNA-directed RNA polymerase subunit beta	rpoB	2	13	4.6	5.9	4.1	2.8	2.2	3.1	0.8	1.1	1.4
Electron transport													

ID	Name	Gene name	FDR	$^{AB}t_0$/ ^{AB}batch	$^{AB}t_1$/ ^{AB}batch	$^{AB}t_2$/ ^{AB}batch	$^{AB}t_3$/ ^{AB}batch	$^{AB}t_0$/ $^{AB}t_1$	$^{AB}t_0$/ $^{AB}t_2$	$^{AB}t_0$/ $^{AB}t_3$	$^{AB}t_1$/ $^{AB}t_2$	$^{AB}t_1$/ $^{AB}t_3$	$^{AB}t_2$/ $^{AB}t_3$
Q39Z19[A]	Twitching motility pilus retraction ATPase	pilT-2	1.9	3	4.5	8.3	4.3	0.7	0.4	0.7	0.5	1	1.9
Q39X07	Type IV pilus secretin lipoprotein PilQ	pilQ	0.3	4.4	8.9	13.3	8.1	0.5	0.3	0.5	0.7	1.1	1.6
Q39UY0	Electron transfer flavoprotein, beta subunit	etfB-7	0.1	0	0	0	0	0.7					
Q39Y50	Lipoprotein cytochrome c	omcN	0.1	7.8	23.8	41.2	20.1	0.3	0.2	0.4	0.6	1.2	2
Q39SW7	Cytochrome c	Gmet_2432	0.2	0.2	0.4	0	0.1	0.5	25.1	1.8	52.6	3.9	0.1
Q39UY1[A]	Electron transfer flavoprotein, subunit	etfA-7	0.2	0	0	0	0					1.3	
Q39Y74	Cytochrome c	omcP	1.7	1	9.9	7.7	4	0.1	0.1	0.2	1.3	2.5	1.9
Q39W96	Carbonic anhydrase (EC 4.2.1.1)	Gmet_1242	0.2	0.2	0	0	0	21.7	58.1	17.8	2.7	0.8	0.3
Q39PV2*	Carbonic anhydrase, beta-family, clade B	can	0.6		51910.9347	0	5139.87					10.1	
Q39QA3[A]	ATP synthase subunit a	atpB	1.6	0.1	0	0	0.2			0.4			
Q39QA7	NADH-quinone oxidoreductase subunit A 2	nuoA2	1.8	0.1	0.1	0	0	1.3	5.4	1.6	4.2	1.3	0.3
Q39QW7[A]	NAD-dependent epimerase	Gmet_3144	1.9	5.4	8.9	12.6	6.2	0.6	0.4	0.9	0.7	1.5	2
Lipopolysaccharide biosynthesis													
Q39T58	ADP-heptose--lipopolysacch. heptosyltransf.	Gmet_2341	0.3	0	0.1	0.4	0				0.2	4.8	19.4
Nucleotide biosynthesis													
Q39UH0[A]	Purine NTP pyrophosphatase	rdgB	0.1	0	0	0	0	1.1		0.6		0.5	
Q39QT3	Mannose-1-P guanylyltransferase	Gmet_3178	0.6	11.4	5	6.5	2.9	2.3	1.7	4	0.8	1.8	2.3
Pathogenesis													
Q39W66	ABC transporter	Gmet_1272	0.5	0.4	0.1	0.5	0.2	3.3	0.9	2	0.3	0.6	2.3
Q39YZ9	Type VI secretion system needle	tssD	1.7	5.9	0.2	0.1	0.7	24.3	116	8.4	4.8	0.3	0.1
Protein folding and stabilization													
Q39UM8[A]	Peptidylprolyl cis-trans isomerase	Gmet_1817	0.3	36.1	14.5	13.9	5.4	2.5	2.6	6.7	1	2.7	2.6
Q39PT6	Protein GrpE (HSP-70 cofactor)	grpE	1.1	0.8	0.3	0.2	0.3	2.9	4.9	2.8	1.7	1	0.6
Protein synthesis													
Q39UK8[A]	Translation initiation factor IF-1	infA	0.3	0.1	0	0.1	0	2	0.9	4.8	0.5	2.4	5.1
Q39VS9[A]	Threonine--tRNA ligase	thrS	0.9	2.3	8.4	7.1	6.7	0.3	0.3	0.3	1.2	1.2	1
Q39U60[A]	Elongation factor G 2	fusA-1	1	5.8	28.3	33.2	14.7	0.2	0.2	0.4	0.9	1.9	2.3
Regulatory functions													
Q39WN1[A]	Transcription elongation factor GreA 1	greA1	1.7	0	0.1	0	0.1	0.1		0.2		1.1	
Q39XT8*	Nitrogen regulatory protein P-II	glnK	0.1					0		0		4	
Signal transduction													
Q39W47	Winged-helix transcriptional regulator	Gmet_1291	1.5	0.1	0.4	0	0.3	0.3	6.2	0.5	19	1.5	0.1
Q39Z76	Motility response receiver histidine kinase	Gmet_0202	0.9	3.1	3.4	5	3	0.9	0.6	1	0.7	1.1	1.7
Q39ZR5[A]	Sensor histidine kinase	Gmet_0009	0	0	0	0	0	1					
Q39WT0*	Sensor histidine kinase, with GAF domain	Gmet_1054	0.2					1.3	1.2	22.9	0.9	17.1	18.5
Q39UU6*	Response receiver-related	Gmet_1747	0.2					1.7	1.5	11.5	0.9	6.8	7.6
Q39XA4*	Protein phosphohistidine phosphatase	sixA	0.4		0.91	2.80	0.14	1.1	0.4	7	0.3	6.4	19.7
Transport and binding proteins													
Q39R73[A]	ABC transporter, membrane protein	macB	0	9.9	87.4	184.2	98.3	0.1	0.1	0.1	0.5	0.9	1.9
Q39VD8*	ABC transporter, ATP-binding protein	Gmet_1552	1.3		9.77	5.70	4.22	0.1	0.2	0.2	1.7	2.3	1.4
Q39R72	ABC transporter, ATP-binding protein	Gmet_3037	0	6.2	33.4	43.4	36.5	0.2	0.1	0.2	0.8	0.9	1.2
Q39VE2[A]	Metal ion efflux pump, RND family	cusB	0.1	5.7	85.5	101.3	52.2	0.1	0.1	0.1	0.8	1.6	1.9
Q39VE3[A]	Metal ion efflux pump, RND family	cusA	0.3	3.5	21.8	35.9	23.4	0.2	0.1	0.1	0.6	0.9	1.5
Q39QA2	ATP synthase subunit c	atpE	0.4	0.3	0.6	0.1	13.7	0.5	5.3	0	10.3	0	0
Q39V43	Efflux pump, RND family	Gmet_1650	0.5	6.5	33.7	47.1	51.3	0.2	0.1	0.1	0.7	0.7	0.9
Q39R71	Efflux pump, RND family	macA	1.1	1.9	11	16.7	11.2	0.2	0.1	0.2	0.7	1	1.5
Q39VD7*	ABC transporter, membrane protein	Gmet_1553	0.3		343.47	647.00	241.38	0	0	0	0.5	1.4	2.7
Unknown function													

ID	Name	Gene name	FDR	$^{AB}t_0$/ ^{AB}batch	$^{AB}t_1$/ ^{AB}batch	$^{AB}t_2$/ ^{AB}batch	$^{AB}t_3$/ ^{AB}batch	$^{AB}t_0$/ $^{AB}t_1$	$^{AB}t_0$/ $^{AB}t_2$	$^{AB}t_0$/ $^{AB}t_3$	$^{AB}t_1$/ $^{AB}t_2$	$^{AB}t_1$/ $^{AB}t_3$	$^{AB}t_2$/ $^{AB}t_3$
Q39T60	Acyl carrier protein	acpP-4	0	56.9	32.5	83.5	31.4	1.7	0.7	1.8	0.4	1	2.7
Q39U94	Uncharacterized protein	Gmet_1951	0	0	0	0	0	0.7	16.4		23.5		
Q39T38[A]	Uncharacterized protein	Gmet_2361	0.1	0.5	0.1	0	0.5	3.7	320	0.9	85.9	0.3	0
Q39RS7[A]	DUF748 repeat protein	Gmet_2829	0.2	9.8	9	11.7	18.3	1.1	0.8	0.5	0.8	0.5	0.6
Q39VD6	Uncharacterized protein	Gmet_1554	0.3	3.4	277.6	173.6	111.1	0	0	0	1.6	2.5	1.6
Q39XS8[A]	Uncharacterized protein	Gmet_0704	0.3	0.3	14.9	0	14.5	0		0		1	
Q39PP3	Uncharacterized protein	Gmet_A3576	0.3	0.1	0	0	0	1.7	13.2	3.6	7.7	2.1	0.3
Q39UV2	Uncharacterized protein	Gmet_1741	0.3	0.1	0.1	0	0.1	1.4	1.7	0.9	1.2	0.7	0.5
Q39ZP4[A]	Protein serine/threonine kinase PrkA	prkA	0.4	7.5	27.4	77.4	33	0.3	0.1	0.2	0.4	0.8	2.3
Q39UI4	Type II secretion system protein	pulO	0.6	7.6	2.9	3	5.4	2.6	2.5	1.4	1	0.5	0.6
Q39WC8[A]	Peptidase, putative	Gmet_1209	1	11	6.9	8.2	5.3	1.6	1.4	2.1	0.8	1.3	1.6
Q39Q16[A]	Periplasmic protein YceI	Gmet_3449	1	0.2	0	0	0	6.9	12	14.8	1.7	2.1	1.2
Q39X68[A]	Uncharacterized protein	Gmet_0914	1.7	0	0	0	0	0.4	1.1	1.5	2.4	3.4	1.4
Q39WP9	Selenium metabolism protein	yedF	1.7	1.2	1	0.1	0.3	1.2	20.9	3.6	16.8	2.9	0.2
Q39X02	GTPase-activating protein, putative	Gmet_0980	1.8	0.1	0.3	0	0.1	0.3	2.8	0.9	9.8	3.1	0.3
Q39RR9	Cytidylate kinase-like domain protein	Gmet_2837	1.8	10.9	4.1	2.5	1.8	2.7	4.3	5.9	1.6	2.2	1.4
Q39Z17	UPF0502 protein Gmet_0262	Gmet_0262	1.8	0.8	0.9	0.1	0.2	0.9	6.1	4.4	6.6	4.8	0.7
Q39UY9	[lipopolysaccharide]-lipid A	Gmet_1704	1.9	1.9	0.5	0.1	0	3.4	36.7		10.9		
Q39PV3*	Peroxiredoxin-like 2 family protein	Gmet_3516	0		1.29	0.00	0.01	0.8		90.2		116	
Q39VQ7*	Uncharacterized protein	Gmet_1433	0.1		1.51	18.75	1.67	0.7	0.1	0.6	0.1	0.9	11.2
Q39XU1*	Cupin superfamily barrel domain protein	Gmet_0691	0.2		0.20	0.40	0.04	5	2.5	23.8	0.5	4.8	9.5
Q39UJ8*	Uncharacterized protein	Gmet_1847	0.3		0.81	0.01	0.17	1.2	161	5.7	130.4	4.7	0
Q39PR7*	Uncharacterized protein	Gmet_3552	0.8		10.87	0.02	99.75	0.1	48.3	0	524.4	0.1	0
Q39V45*	Uncharacterized protein	Gmet_1648	0.9		0.46	0.12	0.04	2.2	8.3	25.2	3.9	11.7	3
Q39ZD6*	Uncharacterized protein	Gmet_0139	1.5		0.00	0.26	11.13		3.8	0.1			0
Q39X90*	Uncharacterized protein	Gmet_0892	1.7		6.39	0.13	0.00	0.2	8		51		

7.2 Investigation of reproducibility of technical and biological replicates used in ICPL analysis

In order to investigate the possible causes of technical and biological variability in the data, a correlation in a number of detected proteins and coefficients of variance were carried out for some technical and biological replicates (Table 7-7). Technical replicates were introduced for analysis of proteins extracted from chemostats F2 (labeled individually but separated together) and A1 (labelled and separated individually). Moreover, two biological replicates F2 and F4 were combined in one run in order to distinguish possible reasons for data variation.

Table 7-7. **Analysis of variation within technical and biological replicates of ICPL analysis** where CV is a coefficient of variance in %. Correlation plots are presented in Figure 7-2

	Technical replicates		Biological replicates	
Chemostats	**F2**	**A1**	**F2 vs F4**	**F2 vs F4**
Label (run codes)	ICPL-4 (4944_A2 run) ICPL-6 (4944_A3 run)	ICPL-10 (4944_A3 vs 5120 runs)	ICPL-4 (4944_A2 vs 4944_A3 runs)	ICPL-6 (4944_A3 run) ICPL-4 (4944_A3)
Total # of proteins detected	625	748	625	508
# of proteins detected in both replicates	459	431	455	499
% with CV <30%	60	61	51	69
% with CV <50%	83	80	75	87
Correlation coefficient (R^2)	0.49	0.55	0.26	0.50

Analysis of variation between replicates (Table 7-7) suggests that although two technical replicates from chemostat F2 were subjected to simultaneous extraction, separation and LC-MS/MS analysis, the correlation coefficient between them was lower (R^2 = 0.49) than expected for technical replicates (Zhang et al., 2006). The possible cause of variation could be the use of two different labels ICPL-4 and ICPL-6. In contrast, two biological replicates F2 and F4 which were also labelled with different labels (ICPL-4 and ICPL-6) but in the same labelling campaign (4944_A3), had the highest percentage of similarity in terms of a number of detected proteins (98.2%) among selected replicates (Table 7-7). However, the percentage

of proteins with coefficients of variance (CV) below 30% and 50% was similar to the technical replicates from chemostats F2 and A1 and was in the range of 51-69% and 75-87%, respectively (Table 7-7). Due to the highest number of commonly detected proteins in replicates which were extracted, separated and analysed simultaneously, it is recommended to carry out simultaneous extraction, labelling, separation and LC-MS/MS analysis for all samples. Due to the low percentage of proteins with CV below 30 % (lower than expected 70%), the protein ratios detected in biological replicates were not averaged.

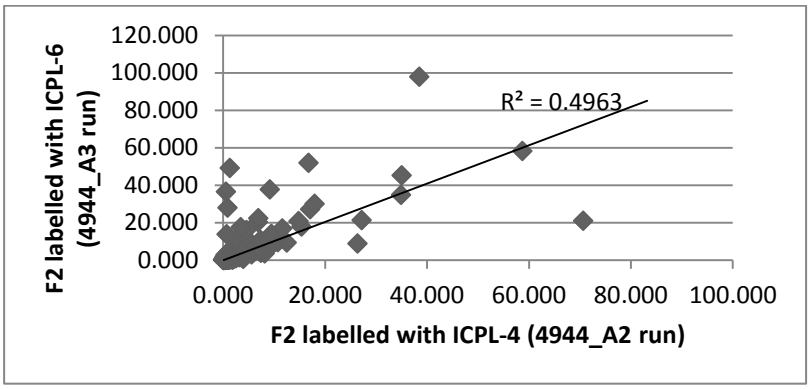

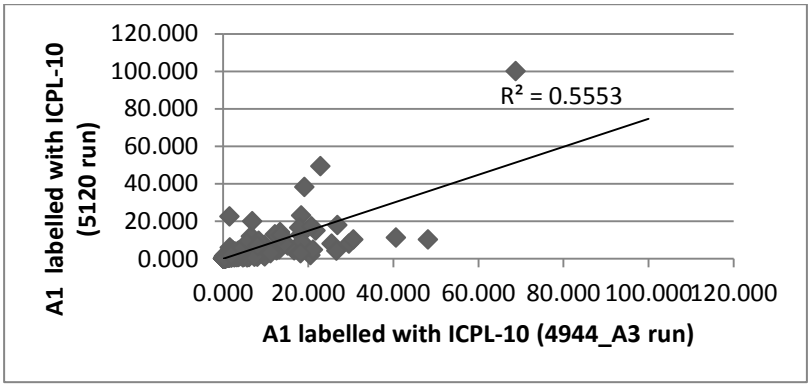

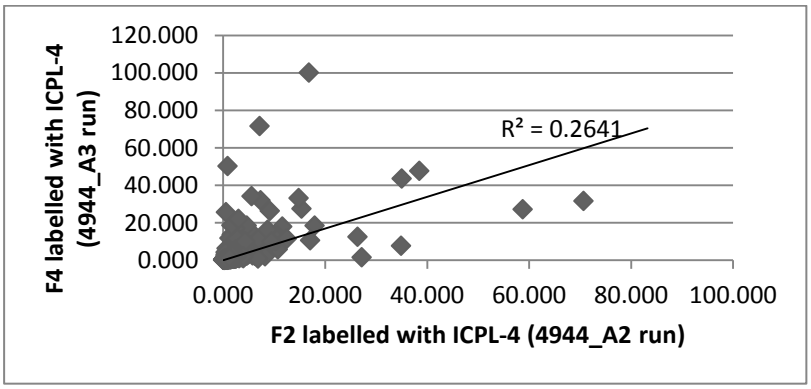

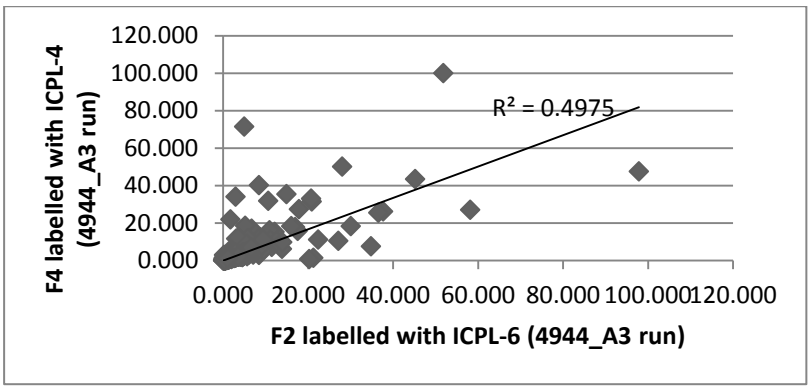

Figure 7-2. Correlation plots for some technical and biological replicates used in ICPL analysis

Table 7-8. Relative abundances of proteins which might contribute to differences between chemostats depicted in Figure 3-24. *indicates that average values of two biological replicates are presented.

		A2/B1	A1 vs B	F2+F4 vs B	F3+F1 vs B	L1/B3	L2/B1
Amino acids metabolism							
DSY0398	Carbamoyl-phosphate synthase large chain	4.55	0.46	0.46	0.30	4.32	0.30
DSY2042	Carbamoyl-phosphate synthase large chain	11.66	0.76	0.70	0.34	**14.45**	0.41
DSY2882	Isoleucine--tRNA ligase	12.18	3.47	4.85	0.96	**11.62**	0.64
DSY3239	Uncharacterized HTH-type regulator		1.71		3.69		**30.28**
DSY4189	O-acetylserine sulfhydrylase	**46.85**	10.45	7.04		**30.89**	
DSY4778	Aspartate aminotransferase	4.12	3.15	3.45	3.16	**19.10**	**16.84**
Carbohydrate metabolism							
DSY1717	3-hydroxybutyryl-CoA dehydrogenase	8.47		16.86		**100.00**	
DSY0565	Alcohol dehydrogenase 2	0.31		25.27		4.22	
DSY1987	Aldehyde oxidoreductase	1.25	12.55	48.03		**14.22**	**63.27**
DMSO reductase							
DSY3409	Anaerobic dimethyl sulfoxide reductase	1.12	2.45	2.49	1.12	0.71	0.32
DSY3410	Dimethyl sulfoxide reductase DmsA	3.16	3.57	5.12	1.41	0.96	0.58
DSY0186	Dimethyl sulfoxide reductase DmsA	2.82	1.68	7.91	0.48	1.01	0.50
Energy metabolism, other							
DSY0431	Rubrerythrin		2.74	4.53	20.58		**28.53**
DSY0676	Putative uncharacterized protein	9.54	1.12	1.66	1.18	**11.37**	1.04
DSY1147	Rubrerythrin	0.87	4.28	16.64	1.39		1.45
DSY1468	Iron-sulfur flavoprotein MJ1083		1.18	1.68	3.40		4.00
DSY3407	Reverse rubrerythrin-1	3.45	3.65	8.62	4.06	1.65	6.66
DSY4916	ATP synthase subunit b	9.52	2.37	3.82	0.69	0.57	**14.74**
DSY1146	Rubredoxin	2.77	3.49	9.33		2.64	
Fumarate reduction							
DSY1391	Fumarate reductase flavoprotein		10.14	24.77	2.13	1.60	
DSY0285	Fumarate reductase flavoprotein subunit, putative	1.66	7.48	11.12	12.69	2.19	3.38
DSY3139	Fumarate reductase flavoprotein subunit	**33.67**	19.97	19.80	6.70	**16.84**	9.33
Glycolysis / Gluconeogenesis							
DSY1839	6-phosphofructokinase		0.23	0.17	0.47		0.91
DSY4167	Hydroxypyruvate isomerase	0.33	1.88	17.15	48.02	9.25	**66.61**
DSY4430	NAD-dependent epimerase/dehydratase		22.36	25.21	16.12		**52.97**
DSY1609	Glyceraldehyde-3-phosphate dehydrogenase	4.25	4.11	5.20	4.92	1.26	3.76
DSY2038	Glucose-1-phosphate adenylyltransferase	3.74	12.03	0.84	23.93	1.07	**35.57**
DSY4838	Enolase 2	0.76	0.59	1.37	2.95	1.32	2.57
Hydrogenase							
DSY1598	Periplasmic [NiFe] hydrogenase, subunit	11.53	3.36	4.62	2.96	**49.36**	**100.00**
DSY4326	Hydrogenase large subunit domain protein	2.21	0.13	0.16	0.05		**0.14**

		A2/B1	A1 vs B	F2+F4 vs B	F3+F1 vs B	L1/B3	L2/B1
Amino acids metabolism							
Lactate degradation							
DSY3216	Glycolate oxidase subunit glcD	3.09	12.41	9.78	16.28	4.55	**12.30**
DSY3217	FAD-linked oxidase	3.02	13.15	11.09	20.45	3.70	3.98
DSY3218	Probable glycolate oxidase, FeS subunit	7.21	12.94	8.73	12.83	4.85	3.08
DSY3357	Glycolate oxidase subunit glcD	17.39	18.68	5.11	2.81	4.28	1.17
DSY2092	Lactate utilization protein B	4.93	3.88	3.17	2.99	1.31	3.35
Oxidative stress							
DSY4123	Probable superoxide dismutase [Fe]	0.86	6.13	9.06	93.82	4.22	**42.56**
Sporulation and germination							
DSY2304	RNA polymerase sigma-F factor	5.99	36.08	24.38	87.79	1.76	**100.00**
DSY4887	Stage III sporulation protein D		57.47		42.06		**100.00**
Sulfite reductase							
DSY0309	Sulfite reductase, dissimilatory-type subunit alpha	5.53	2.96	10.99	4.87	3.97	0.93
DSY0310	Sulfite reductase, dissimilatory-type subunit beta	1.00	2.58	8.90	4.17	2.13	1.16
Sulfur metabolism							
DSY0226	Arylsulfotransferase	0.95	3.27	10.89	57.86	2.75	0.99
TCA							
DSY3882	isocitrate dehydrogenase, NADP-dependent	0.53	0.63	0.70	1.76	0.68	0.64
DSY1925	Succinyl-CoA ligase [ADP-forming] subunit alpha	2.86	2.58	3.03	1.58		0.73
DSY1924	Citrate lyase subunit beta	3.40	2.45	3.62	15.15	3.73	10.18
Wood-Ljungdahl pathway/Methyl branch							
DSY2356	Methylenetetrahydrofolate dehydrogenase (NADP(+))	1.35	2.85	4.31	2.04	2.96	7.16
DSY4199	uroporphyrinogen-III decarboxylase-like protein		3.10		2.82		0.41
DSY0138	Methylenetetrahydrofolate reductase	1.01	1.36	0.98	0.95	2.95	3.38
DSY0205	Formate--tetrahydrofolate ligase 1	6.35	7.14	11.76	3.48	**20.38**	**11.18**
DSY3157	Tetrahydromethanopterin S-methyltransferase subunit H	**0.04**	1.33	0.61	67.33	0.63	
DSY3968	Formate dehydrogenase subunit alpha	8.37	7.36	15.97	3.82	**30.72**	10.57
DSY3969	Formate dehydrogenase	**55.65**	9.44	38.94	6.22	3.72	**27.11**
DSY3970	NADP-reducing hydrogenase subunit HndC	2.60	4.61	8.54	3.66	8.88	9.90
DSY3896	Formate dehydrogenase	0.55	11.12	26.36	12.69	**0.03**	
Wood-Ljungdal pathway/Carbonyl branch							
DSY1650	CO dehydrogenase/acetyl-CoA synthase	11.03	12.02	11.59	3.93	2.41	9.09
DSY1651	CO dehydrogenase/acetyl-CoA synthase gamma subunit		6.92	13.96	4.61	4.33	
DSY1652	CO dehydrogenase/acetyl-CoA synthase subunit α	**44.76**	22.75	47.97	10.25	3.82	**47.70**
DSY1653	CO dehydrogenase/acetyl-CoA synthase subunit beta	12.46	12.51	19.70	7.32	**16.08**	9.00
DSY4442	CO dehydrogenase 2	3.20	0.44	83.21	2.00		**39.19**

8 Clarifications

Chapter 3.1: "Physiology of *G. metallireducens* at high substrate concentrations in batch"

The concept of the experiment was developed by Prof. Dr. Rainer Meckenstock and the PhD candidate. The experimental design was done by Prof. Dr. Rainer Meckenstock, Dr. Jana Seifert and the PhD candidate. The cultivation of bacteria in batch, cell counting, analytical measurements and sampling for proteomics was done by the PhD candidate. Extraction of proteins and their separations on SDS gels was done by Kathleen Eismann and Christine Schumann (Helmholtz Zentrum for Environmental research). Proteins identification with UPLC-LTQ Orbitrap-MS/MS was done by Dr. Jana Seifert (Helmholtz Zentrum for Environmental research). Statistical analysis of detected proteins (one way ANOVA and hypergeometric test) was performed by Dr. Robert Küffner (LMU, Munich). Correspondence analysis was conducted by the PhD candidate. The application of hierarchical regulation analysis of TCA cycle was suggested and performed by Dr. Wilfred Röling (VU University Amsterdam). The evaluation of proteomic data and annotation of significantly expressed proteins to a function was done independently by the PhD candidate. Prof. Dr. Rainer Meckenstock, Dr. Wilfred Röling and the PhD candidate interpreted and discussed results together. The draft on the manuscript was written by the PhD candidate independently and the comments of Prof. Dr. Rainer Meckenstock, Dr. Wilfred Röling, Dr. Jana Serfert, Dr. Robert Küffner and Dr. Martin von Bergen were added afterwards. The manuscript was submitted by the corresponding author Prof. Dr. Rainer Meckenstock to the Journal *Systematic and applied microbiology* on 2.09.2013.

Chapter 3.2: "Physiology of *G. metallireducens* during carbon limitation in retentostats"

The concept of the experiment was developed by Prof. Dr. Rainer Meckenstock, and the PhD candidate. The experimental design was done by Dr. Wilfred Röling, Dr. Jana Seifert and the PhD candidate. The cultivation of bacteria in retentostats, cell counting, analytical measurements and sampling for proteomics was done by the PhD candidate. Denaturing gradient gel electrophoresis (DGGE) analysis was performed by Martin Braster (VU University Amsterdam). Extraction of proteins and their separations on SDS gels was done by Kathleen Eismann and Christine Schumann. Proteins identification with UPLC-LTQ Orbitrap-MS/MS was done by Dr. Jana Seifert. Statistical analysis of detected proteins (one way ANOVA) was performed by Dr. Robert Küffner. Experiments on control of readiness to use alternative carbon substrates were performed by the PhD candidate. The evaluation of proteomic data and annotation of significantly expressed proteins to a function was done

independently by the PhD candidate. Prof. Dr. Rainer Meckenstock, Dr. Wilfred Röling and the PhD candidate interpreted and discussed results together. The draft on the manuscript was written by the PhD candidate independently and the comments of Prof. Dr. Rainer Meckenstock, Dr. Wilfred Röling, Dr. Jana Serfert, Dr. Robert Küffner and Dr. Martin von Bergen were added afterwards. The manuscript was submitted by the corresponding author Prof. Dr. Rainer Meckenstock to the Journal *Systematic and applied microbiology* on 2.09.2013.

Chapter 3.3: "Cultivation of *G. metallireducens* in the indoor aquifer (mesocosm experiment)"

The concept of the experiment was developed by Prof. Dr. Rainer Meckenstock, and the PhD candidate. The experimental design was done by Dr. Marko Hünniger (Helmholtz Zentrum München) and the PhD candidate. The construction of dialysis bags, their inoculation with bacteria was done by Dr. Housna Mouttaki. The insertion of inoculated dialyses bags into the indoor aquifer was done by Dr. Housna Mouttaki (Helmholtz Zentrum München) and Dr. Marko Hünniger. The construction of indoor aquifer was carried out by Dr. Marko Hünniger and Dr. Susanne Smidt (Helmholtz Zentrum München). Regular monitoring of oxygen concentration in the aquifer was done by Sigrid Kaschuba (Helmholtz Zentrum München) and the PhD candidate. Toluene sampling and toluene measurements were done by Shiran Qiu (Helmholtz Zentrum München). Sampling of dialysis bags was done by Dr. Marko Hünniger, Agnieszka Herzyk (Helmholtz Zentrum München) and the PhD candidate. The evaluation of obtained data was done independently by the PhD candidate. The draft was written by the PhD candidate independently and the comments of Dr. Housna Mouttaki were added afterwards.

Chapter 3.4: "Physiology of *D. hafniense* Y51 under various nutrient limiting conditions in chemostats"

The concept of the experiment was developed by Dr. Wilfred Röling and Raquel Vargas. The experimental design was done by Dr. Wilfred Röling and Raquel Vargas (VU University Amsterdam). The cultivation of *D. hafniense* Y51 in batch was carried out by Raquel Vargas. The cultivation of *D. hafniense* Y51 in chemostats was carried out by Martin Braster. The sampling for proteomic analysis was done by Raquel Vargas and Martin Braster. The extraction of proteins, ICPL labelling and separation by SDS-PAGE was done by the PhD candidate. LC-MS/MS analysis was performed my Dr. Juliane Merl (Helmholtz Zentrum München). Statistical analysis was done by the PhD candidate. KEGG pathway annotation was done by Thomas Weinmaier (Wien University). Evaluation of proteomic data was done

by the PhD candidate independently. Kinetic calculations were done by Raquel Vargas. The results were discussed by Raquel Vargas and the PhD candidate together. The results and discussion on proteomic outcomes was first written by the PhD candidate and then comments from Raquel Vargas were added. Results and discussion of kinetics was written by Raquel Vargas. Proof reading was done by Raquel Vargas and the PhD candidate. The presented results and discussion will be later combined with microarray data and published as one paper.

9 Acknowledgments

First of all, I would like to thank my supervisor Prof. Dr. Rainer Meckenstock for his supervision during my phD, for his help in developing the main concept of this study, for his numerous ideas to solve upcoming problems and relentless optimism, for his patient guidance and timeous pressure during the last months of writing of this dissertation. Additionally, I am thankful to him for giving me the opportunity to get a financial support after completion of the Marie Curie project.

I am also highly grateful to Dr. Housna Mouttaki. Housna, thank you so much for your endless help in the lab, for teaching the various techniques, numerous suggestions and advices, for taking your time in constructing the dialysis bags during my absence, for interesting scientific discussions, for reading my manuscripts, for correcting them, for being a great friend and support in the hard moments in the lab and outside, and, of course, for having fun during all these years!

I am also highly grateful to Prof. Dr. Wilfred Röling for his immediate answers to my e-mails, valuable and thoughtful comments to my manuscripts, for his brilliant suggestions to complicated issues, for letting me run retentostat experiments in his lab twice!

Next, I would like to thank my collaborators, Dr. Jana Seifert and Dr. Robert Küffner for providing their expertise and teaching me important aspects of their work.

I am also highly grateful to Alexander Shaeffer for his time, help, and advices with the ICPL data analysis.

I would like to thank Raquel Vargas for her help in the lab, fruitful discussions and great fun we had during my stay in Amsterdam.

I would like to thank Martin Braster for his help with retentostat experiments, optimism and support.

I am thankful to Dr. Julian Bosch and Juliane Braunschweig. Julian, thank you for being such a nice peaceful and positive energy irradiating office-mate, thank you for help and advices; Juliane, thank you for your tips on some bureaucracy issues, support and valuable comments to my last chapter.

I would like to thank Dr. Kerstin Nicolaisen, Dr. Julian Bosch and Janina Kölschbach for their time and effort in translating my abstracts and CV into German.

Next, I am very grateful to my friends at IGOE, Agnieszhka Herzyk, Michael Larentis, Housna and Armin. Thank you for your support, advices, help in the lab and, of course, for sharing lunch!

I would like to acknowledge the financial support by the Marie Curie ITN "Goodwater" and all Goodwater fellows for them being who they are: brilliant, helpful and wonderful people; and for having a great time during three years of the Goodwater project.

Moreover, I would like to thank my wonderful friends who I do not see often anymore as we live in different cities and different countries: Alexey Kolodkin, Elizaveta Mirgorodskaya, Frida Kupper, Merrin Upchurch, Raquel Vargas, Hanneke Hoogendoorn, Konstantina Christodoulou, Nasja Barka, Ioannis Vouldis, Tatjana Konoplijanik, Maria Muntian, Ilja Konovalov and many others for their support and invaluable friendship.

Finally, I am grateful to my family for their patience and caring, for their support and love. Without them I would not be where I am now.

This work was founded by the EU within the FP7 Marie Curie Initial Training Network (ITN) "GOODWATER", grant agreement number 212683.

10 Curriculum Vitae

Born in 1983, Gomel, Belarus

Education

09/1990-05/2001	Basic school and Gymnasium (School № 71), Gomel, Belarus
2001-2006	Diploma of Biologist, teacher of biology and chemistry, Belarusian State University, Minsk, Republic of Belarus
2005-2006	Diploma thesis: "Genetic monitoring of diseases of Liquidators of Chernobyl Disaster consequences", supervised by Prof. Dr. Sergej Borisovich Melnov, Republican scientific center of radiation medicine and human ecology, Gomel, Republic of Belarus
2007-2009	MSc Ecolgy, Vrije Universiteit, Amsterdam, the Netherlands
2009	Master thesis: "Role of vegetation in methane emissions from wetlands", supervised by Dr. Peter van Bodegom, Department of Systems Ecology, Faculty of Earth and Life Sciences, Vrije Universiteit, Amsterdam, the Netherlands

Internship

2008	Minor master internship "Determining nutrient status in the field using molecular techniques", supervised by Prof. Dr. Wilfred Röling, Department of molecular cell physiology, Faculty of Earth and Life Sciences, Vrije Universiteit, Amsterdam, the Netherlands
2009	Major master internship: "Role of secondary metabolites in interactions between plant *Plantago lanceolata* and arbuscular mycorrhizal fungi *Glomus* sp.", Department of Animal ecology, Faculty of Earth and Life Sciences, Vrije Universiteit, Amsterdam, the Netherlands

Work experience

2007	Ecologist, Belarusian Scientific Centre "Ecology", the department of accompaniment to UNFCCC and Kyoto Protocol, Minsk, Republic of Belarus
08/2009-05/2013	Doctoral candidate at the Institute of Groundwater Ecology, Helmholtz Zentrum München. EU project, GOODWATER ITN, WP: 1 „Insights into the microbial physiology of bacteria capable of degrading pollutants in contaminated groundwater ecosystems", supervised by Prof. Dr. R. U. Meckenstock

11 Appendix

Table 1

A. Acetate, benzoate and Fe(II) concentrations for Figure 3-1A

	Benzoate, mM		Acetate, mM		Fe(II), mM	
Time,h	Mean*	SD*	Mean	SD	Mean	SD
0	0.6	0.0	1.9	0.3	4.8	0.1
8	0.6	0.0	1.5	0.1	8.1	1.1
12	0.6	0.1	0.8	0.2	13.8	2.1
16	0.5	0.1	0.2	0.3	17.6	3.3
20	0.3	0.2	0.0	0.0	27.4	3.9
23	0.0	0.0	0.0	0.0	33.6	3.3
26	0.0	0.0	0.0	0.0	34.7	3.1
34	0.0	0.0	0.0	0.0	36.4	2.2
38	0.0	0.0	0.0	0.0	36.6	2.9

B. Toluene, acetate and Fe(II) concentrations for Figure 3-1B

	Toluene, mM		Acetate, mM		Fe(II), mM	
Time, h	Mean	SD	Mean	SD	Mean	SD
0	0.44	0.10	2.46	0.09	0.93	0.11
7	0.42	0.08	1.82	0.47	1.22	0.10
12	0.43	0.09	0.99	0.86	1.39	0.11
20	0.40	0.09	0.08	0.07	21.44	0.88
27	0.41	0.09	0.00	0.00	22.15	0.72
33	0.36	0.07	0.00	0.00	24.06	0.25
45	0.11	0.11	0.00	0.00	29.05	5.69
53	0.03	0.03	0.00	0.00	29.46	1.41
59	0.01	0.01	0.00	0.00	35.39	5.34
72	0.00	0.00	0.00	0.00	37.97	2.61
80	0.00	0.00	0.00	0.00	35.48	5.39

C. Toluene, benzoate and Fe(II) concentrations for Figure 3-1C

	Toluene, mM		Benzoate, mM		Fe(II), mM	
Time, h	Mean	SD	Mean	SD	Mean	SD
0	0.47	0.03	0.28	0.08	0.60	0.13
7	0.41	0.02	0.26	0.09	1.32	0.74
12	0.38	0.07	0.18	0.08	1.09	0.21
20	0.27	0.04	0.00	0.00	22.54	1.08
27	0.00	0.00	0.00	0.00	24.61	0.45
33	0.00	0.00	0.00	0.00	24.64	0.88

*Mean - mean of three biological replicates; SD – standard deviation

Table 2.

A. Acetate, butyrate and Fe (II) concentrations for Figure 3-2A

	Acetate, mM		Butyrate, mM		Fe (II), mM	
Time, h	Mean*	SD*	Mean	SD	Mean	SD
0	1.75	0.05	3.08	0.12	5.08	0.03
5	1.98	0.09	3.02	0.04	4.01	0.13
10	1.12	0.36	2.17	0.00	4.98	0.17
28	1.29	0.26	2.99	0.11	8.29	0.42
37.5	1.08	0.24	2.88	0.01	11.31	1.76
47	0.74	0.34	3.08	0.09	11.70	0.67
50	0.64	0.90	3.45	0.16	11.29	1.86
58	0.95	0.18	3.42	0.03	13.33	2.33
74	0.31	0.06	3.25	0.12	17.69	4.08
78	0.41	0.26	3.10	0.33	26.66	0.55
82	0.12	0.20	3.15	0.29	27.70	0.04
146	0.11	0.20	2.65	0.04	37.13	1.36
154	0.20	0.35	2.63	0.16	38.34	0.06
171	0.12	0.21	2.74	0.06	38.90	0.05
179	0.02	0.03	2.53	0.27	39.58	0.00
194	0.06	0.06	2.36	0.39	39.49	0.46
201	0.09	0.13	2.52	0.03	39.24	0.27
219	0.06	0.09	2.51	0.03	39.90	0.49
226	0.04	0.06	2.39	0.21	39.68	0.02

B. Acetate, ethanol and Fe (II) concentrations for Figure 3-2B

	Acetate, mM		Ethanol, mM		Fe (II), mM	
Time, h	Mean	SD	Mean	SD	Mean	SD
0.0	2.45	0.18	0.12	41.38	4.79	0.07
5.0	2.62	0.25	0.12	-0.10	4.47	0.27
10.0	2.79	0.23	0.19	1.74	5.21	0.24
28.0	3.17	0.23	0.09	9.48	8.94	0.73
37.5	2.49	0.29	0.18	19.89	11.61	1.93
47.0	1.74	0.18	0.09	26.53	14.59	1.10
50.0	1.35	0.28	0.62	25.24	15.66	0.77
58.0	0.38	0.38	0.50	31.35	15.48	1.59
74.0	0.00	0.00	0.52	33.86	21.85	1.29
78.0	0.00	0.00	0.51	34.58	35.28	0.42
82.0	0.00	0.00	0.00	41.00	35.07	1.19
146.0	0.00	0.00	0.57	36.33	37.19	0.82
154.0	0.00	0.00	0.73	35.91	36.21	1.66
171.0	0.00	0.00	0.00	41.00	37.04	0.87
179.0	0.00	0.00	0.00	41.00	37.30	0.68

C. Butyrate, ethanol and Fe (II) concentrations for Figure 3-2C

	Butyrate, mM		Ethanol, mM		Fe (II), mM	
Time, h	Mean	SD	Mean	SD	Mean	SD

0	3.97	0.16	1.70	0.07	5.05	0.06
5	3.81	0.11	1.83	0.11	3.57	0.34
10	4.09	0.08	1.57	0.11	4.79	0.06
28	3.77	0.16	1.70	0.60	7.25	0.54
37.5	3.59	0.38	0.41	0.05	10.86	0.35
47	3.19	0.23	0.27	0.13	12.06	0.53
50	3.49	0.24	0.38	0.07	11.06	0.51
58	3.57	0.18	0.35	0.01	12.71	1.06
74	3.21	0.12	0.35	0.02	17.82	1.14
78	3.18	0.11	0.37	0.04	32.49	0.65
82	3.17	0.08	0.27	0.06	32.91	0.27
146	3.35	0.08	0.00	0.00	39.54	0.51
154	3.18	0.31	0.00	0.00	39.94	0.23
171	3.35	0.13	0.00	0.00	40.21	0.93
179	3.30	0.11	0.00	0.00	41.83	0.27
194	2.88	0.30	0.00	0.00	40.95	0.64
201	3.28	0.06	0.00	0.00	40.42	1.42
219	3.10	0.24	0.00	0.00	43.05	0.53
226	3.18	0.23	0.00	0.00	41.78	0.80
242	2.81	0.20	0.00	0.00	42.01	0.79
291	2.92	0.05	0.00	0.00	43.70	0.33

D. Butyrate, benzoate and Fe (II) concentrations for Figure 3-2D

	Benzoate, mM		Butyrate, mM		Fe (II), mM	
Time, h	Mean	SD	Mean	SD	Mean	SD
0.0	0.46	0.09	4.51	0.09	4.84	0.17
5.0	0.47	0.09	4.49	0.06	3.81	0.05
10.0	0.43	0.09	4.60	0.35	4.14	0.07
28.0	0.42	0.09	4.03	0.29	6.21	0.07
37.5	0.39	0.07	4.22	0.19	7.83	0.38
50.0	0.40	0.09	3.81	0.10	9.89	0.23
58.0	0.38	0.08	3.26	0.69	11.39	0.65
74.0	0.24	0.05	3.23	0.36	16.49	1.43
82.0	0.10	0.04	3.04	0.07	32.69	0.42
146.0	0.00	0.00	2.88	0.14	37.11	1.00
154.0	0.00	0.00	2.82	0.09	38.15	0.33
179.0	0.00	0.00	2.08	0.80	37.52	0.54
194.0	0.00	0.00	2.63	0.15	37.83	0.20
201	0.00	0.00	2.74	0.09	36.33	0.50
219	0.00	0.00	2.66	0.07	38.78	1.31
226	0.00	0.00	2.75	0.14	38.19	0.41
242	0.00	0.00	2.60	0.08	36.98	0.46
291	0.00	0.00	2.67	0.14	37.84	1.96
315	0.00	0.00	2.29	0.16	36.81	0.60

E. Butyrate, benzoate and Fe (II) concentrations for Figure 3-2E

	Ethanol, mM		Benzoate, mM		Fe (II), mM	
Time, h	Mean	SD	Mean	SD	Mean	SD
0	1.20	1.00	0.65	0.07	2.07	0.44
16.5	1.17	0.97	0.62	0.10	4.01	0.06
40.5	1.22	1.05	0.63	0.09	4.15	0.05
50.5	1.18	1.05	0.65	0.17	3.79	0.10
66.5	1.25	1.01	0.62	0.07	4.24	0.12
88.5	1.13	0.97	0.62	0.10	4.17	0.22
159.5	1.04	0.75	0.57	0.05	6.08	2.81
170.5	0.85	0.55	0.57	0.09	8.12	5.71
185.5	0.62	0.30	0.51	0.18	11.63	11.65
206.5	0.00	0.00	0.31	0.21	18.49	15.65
252.5	0.00	0.00	0.20	0.25	32.74	1.11
322.5	0.00	0.00	0.15	0.07	35.48	0.83
346.5	0.00	0.00	0.08	0.05	36.66	0.69
395.5	0.00	0.00	0.11	0.11	36.61	0.51
415.5	0.00	0.00	0.12	0.06	36.76	0.77
440.5	0.00	0.00	0.05	0.04	37.45	0.67
462.5	0.00	0.00	0.14	0.08	35.50	1.30
484.5	0.00	0.00	0.15	0.10	38.13	0.09

*Mean - mean of three biological replicates; SD – standard deviation

Table 3. Z-scores of catabolic pathways comparisons generated by hypergeometric test depicted in **Figure 3-6**

	Column Labels									
Row Labels	**Acetate**	**Geraniol degradation**	**Glycolysis+ gluconeogenesis**	**Glyoxylate +dicarboxylate**	**Fatty acid+phospholipid**	**Phenol**	**Butanoate**	**Propinoate**	**Toluene**	**Benzoate**
AB>Ace	0	0	0	0	**4.71**	2.891	0	0	0	**6.50**
AB>Benz	0	0	0	0	0	0	0	0	0	3.45
AB>Eth	0	0	0	0	**6.78**	2.891	0	3.61	0	**6.50**
AB>Tol	0	0	0	0	0.10	0	0	0	0	1.53
Benz>AB	2.57	0	0	0	0	0	0	0	0	0.88
Benz>Ace	0.77	0	0	0	**5.45**	**4.79**	0	0	0	**17.42**
Benz>But	0.85	0	0	0	-0.25	1.49	0	0	0	**13.69**
Benz>Eth	3.32	0	0	0	**4.52**	**4.99**	0	0	0	**18.11**
But>AB	0	3.14	0	0	1.15	0	**5.82**	**6.78**	0	-0.20
But>Ace	0	2.18	0	0	**4.99**	3.77	3.95	**4.77**	0	**14.68**
But>Benz	0	3.14	0	0	1.15	0	**5.82**	**6.78**	0	-0.20
But>Eth	0.46	2.21	0	0	**5.10**	3.84	**4.02**	**4.85**	0	**15.85**
But>Tol	0	2.80	0	0	2.04	0	**5.17**	**6.07**	0	-0.35
Eth>AB	0	0	3.91	0	0	0	0	0	0	0
Eth>Ace	0	0	1.86	0	0	0	0	0	0	0
Eth>Benz	0	0	2.73	0	0	0	0	0	0	0
Eth>But	0	0	2.43	0	0	0	0	0	0	0
Eth>Tol	0	0	1.32	**4.29**	0.97	0	0	0	0	0
Tol>AB	0	0	0	0	0	0	0	0	**19.72**	1.47
Tol>Ace	0	0	0	0	3.65	**4.22**	0	0	**14.64**	**15.39**
Tol>Benz	0	0	0	0	0	0	0	0	**23.89**	0.15
Tol>But	0	0	0	0	-0.38	1.31	0.58	0	**15.75**	**9.15**
Tol>Eth	0.51	0	0	0	3.36	3.98	0.40	0	**13.84**	**14.52**

Z-scores > 4 are in bold.

Table 4. Biomass production rate $r_{x(substrates)}$, fitted biomass production rate $r_x(t)_{fit}$ growth rate μ, fitted biomass x(t)fit, measured cell numbers, and substrate concentrations in acetate-limited retentostats for **Figure 3-7**

Run 1

Time, h	r_x(substrates) [mmol C h^{-1}]	r_x(t) fit [mmol C h^{-1}]	μ [h^{-1}]	Fitted biomass, x(t)fit total	Cells measured, total	acetate [mM]	Fe II [mM]
20.8	0.333	0.024	0.006	2.20E+11	2.34E+11	0.413	22.6
26.8	0.344	0.024	0.006	2.28E+11		0.264	17.6
33.8	0.366	0.024	0.006	2.38E+11		0	12.1
46.2	0.359	0.024	0.006	2.55E+11	4.02E+11	0	4.6
49.5	0.357	0.024	0.005	2.60E+11		0	5.9
55.8	0.353	0.025	0.005	2.69E+11		0	7.4
69.5	0.345	0.025	0.005	2.89E+11	4.75E+11	0	15.9
74	0.342	0.025	0.005	2.95E+11		0	20.4
78.5	0.34	0.025	0.005	3.02E+11		0	20.3
87.2	0.334	0.025	0.005	3.14E+11	5.96E+11	0	21.1
111.75	0.32	0.026	0.004	3.51E+11	6.13E+11	0	0.4
132.5	0.307	0.026	0.004	3.82E+11	6.41E+11	0	9.8
136.75	0.305	0.026	0.004	3.89E+11		0	10.7
139.5	0.303	0.026	0.004	3.93E+11		0	16.7
142.5	0.301	0.026	0.004	3.97E+11		0	19.6
156.5	0.293	0.027	0.004	4.19E+11	7.26E+11	0	13
160.5	0.291	0.027	0.004	4.25E+11		0	23.3
164	0.289	0.027	0.004	4.31E+11	7.10E+11	0	16.6
166.5	0.287	0.027	0.004	4.35E+11		0	4.4
179.5	0.279	0.027	0.003	4.55E+11	9.46E+11	0	21.7
186.67	0.275	0.027	0.003	4.67E+11		0	23.3

Time, h	r_x(substrates) [mmol C h^{-1}]	r_x(t) fit [mmol C h^{-1}]	μ [h^{-1}]	Fitted biomass, x(t)fit total	Cells measured, total	acetate [mM]	Fe II [mM]
190.5	0.273	0.028	0.003	4.73E+11		0	25.1
203.5	0.265	0.028	0.003	4.94E+11	6.71E+11	0	24.1
208	0.262	0.028	0.003	5.01E+11		0	20.3
212.75	0.259	0.028	0.003	5.09E+11		0	8
230.5	0.249	0.029	0.003	5.38E+11	4.70E+11	0	16.5
235	0.246	0.029	0.003	5.45E+11		0	16.5
257	0.233	0.029	0.003	5.82E+11	4.34E+11	0	15.4
301.5	0.206	0.030	0.003	6.59E+11	2.72E+11	0	27.9
305.5	0.204	0.030	0.003	6.66E+11		0	27.1
310.5	0.201	0.031	0.003	6.75E+11		0	27.3
324.5	0.193	0.031	0.003	7.00E+11	2.37E+11	0	27.9
328.5	0.19	0.031	0.003	7.07E+11		0	26.4
333.5	0.187	0.031	0.003	7.16E+11		0	26.9
348.5	0.178	0.032	0.002	7.43E+11	1.41E+11	0	24.2
352.5	0.176	0.032	0.002	7.51E+11		0	24.7
355.5	0.174	0.032	0.002	7.56E+11		0	25.5
371.5	0.152	0.032	0.002	7.86E+11	1.44E+11	0.126	24.7

Run 2

0	0.212	0.017	0.004	2.46E+11	2.46E+11	0	21.37
7	0.209	0.017	0.0039	2.53E+11		0	24.42
23.9	0.203	0.017	0.0037	2.70E+11	3.68E+11	0	25.34
67.9	0.188	0.018	0.0033	3.15E+11	5.81E+11	0	22.9
70.9	0.187	0.018	0.0033	3.18E+11		0	26.71
75.9	0.185	0.018	0.0032	3.23E+11		0	24.59

91.4	0.180	0.018	0.0031	3.39E+11	6.33E+11	0	26.22
95.9	0.178	0.018	0.0031	3.44E+11		0	26.21
100.9	0.176	0.018	0.003	3.49E+11		0	24.39
115.4	0.171	0.019	0.003	3.65E+11	7.30E+11	0	25.61
118.9	0.170	0.019	0.0029	3.69E+11		0	27.59
139.4	0.163	0.019	0.0028	3.91E+11	5.78E+11	0	26.58
143.4	0.161	0.019	0.0028	3.95E+11		0	27.07
147.9	0.160	0.019	0.0028	4.00E+11		0	25.76
162.9	0.154	0.019	0.0027	4.17E+11	5.84E+11	0	28.23
166.9	0.153	0.019	0.0027	4.22E+11		0	26.98
172.07	0.151	0.019	0.0026	4.27E+11		0	30.75
190.07	0.145	0.020	0.0026	4.48E+11		0	26.99
234.9	0.129	0.021	0.0024	5.00E+11	6.86E+11	0	31.4
239.15	0.127	0.021	0.0024	5.05E+11		0	31.46
245.4	0.125	0.021	0.0023	5.13E+11		0	31.84
258.9	0.120	0.021	0.0023	5.29E+11	7.27E+11	0	30.69
264.4	0.118	0.021	0.0023	5.36E+11		0	32.04
268.4	0.117	0.021	0.0023	5.41E+11		0	22.94
287.4	0.110	0.022	0.0022	5.64E+11		0	30.08
308.4	0.103	0.022	0.0021	5.91E+11	5.46E+11	0	32.94
312.9	0.101	0.022	0.0021			0	33.36

Table 5. Biomass production rate $r_{x(substrates)}$, fitted biomass production rate $r_x(t)_{fit}$ growth rate μ, fitted biomass x(t)fit, measured cell numbers, and substrate concentrations in acetate-limited retentostats for **Figure 3-9**

Run 1

Time, h	r_x(substrates) [mmol C h^{-1}]	r_x(t) fit [mmol C h^{-1}]	μ [h^{-1}]	Fitted biomass, x(t)fit total	Cells measured, total	acetate [mM]	benzoate [mM]	Fe II [mM]
10	0.026	0.030	0.007	2.34E+11	2.51E+11	0	0.13	35.97
24	0.032	0.030	0.006	3.83E+11	2.76E+11	0	0.03	38.57
28	0.029	0.030	0.006		2.83E+11	0	0.02	36.67
33	0.025	0.030	0.006		2.91E+11	0	0.03	38.12
48	-0.012	0.031	0.006	4.16E+11	3.18E+11	0	0.05	37.9
52	-0.063	0.031	0.006		3.25E+11	0.252586	0.09	38.72
57.3	-0.031	0.031	0.005		3.35E+11	0.522974	0.16	37.02
72	-0.012	0.032	0.005	5.21E+11	3.62E+11	0	0.23	36.46
77.9	0.027	0.032	0.005		3.72E+11	0	0.18	36.01
104.8	0.035	0.032	0.004	5.63E+11	4.22E+11	0	0.09	34.67
120	0.036	0.033	0.004	5.89E+11	4.51E+11	0	0.08	35.62
124	0.034	0.033	0.004		4.59E+11	0	0.08	35.94
129	0.040	0.033	0.004		4.68E+11	0	0.09	35.11
144	0.043	0.034	0.004	5.59E+11	4.97E+11	0	0.08	33.65
149	0.044	0.034	0.004		5.07E+11	0	0.08	33.42
153	0.027	0.034	0.004		5.15E+11	0	0.08	30.11
167.3	0.044	0.034	0.004	5.36E+11	5.43E+11	0.211175	0.08	31.34
173.3	0.043	0.034	0.004		5.55E+11	0	0.09	34.74
180.3	0.048	0.035	0.004		5.69E+11	0	0.1	36.62
193	0.043	0.035	0.003	4.39E+11	5.95E+11	0	0.1	34.65
196.3	0.041	0.035	0.003		6.01E+11	0	0.11	37.4

Time, h	r_x(substrates) [mmol C h^{-1}]	r_x(t) fit [mmol C h^{-1}]	μ [h^{-1}]	Fitted biomass, x(t)fit total	Cells measured, total	acetate [mM]	benzoate [mM]	Fe II [mM]
201.3	0.048	0.035	0.003		6.11E+11	0	0.12	34.84
216.3	0.049	0.036	0.003	3.83E+11	6.42E+11	0	0.11	33.71
220.8	0.037	0.036	0.003		6.52E+11	0	0.11	35.98
225.3	0.051	0.036	0.003	3.21E+11	6.61E+11	0.15	0.11	33.15
243	0.081	0.036	0.003	3.03E+11	6.98E+11	0	0.12	33.79
266.55	0.090	0.037	0.003	2.50E+11	7.48E+11	0	0.06	19.42
286.9	0.093	0.038	0.003	2.49E+11	7.93E+11	0	0.05	32.54
291.15	0.093	0.038	0.003		8.02E+11	0	0.04	35.67
293.9	0.097	0.038	0.003		8.08E+11	0	0.04	34.06
296.9	0.102	0.038	0.003		8.15E+11	0	0.03	32.11
310.9	0.098	0.039	0.003		8.46E+11	0	0.03	29.00
314.9	0.098	0.039	0.003	2.15E+11	8.55E+11	0	0.04	32.04
320.9	0.095	0.039	0.003		8.68E+11	0	0.05	31.90
333.9	0.100	0.039	0.003		8.98E+11	0	0.07	31.01
341	0.100	0.040	0.003	1.37E+11	9.14E+11	0	0.06	29.52

Run 2

0	0.22	0.029	0.009	1.90E+11	1.90E+11	0.15	0.193	22.07
25.5	0.24	0.030	0.007	2.34E+11	2.25E+11	0	0.171	25.91
28.3	0.25	0.030	0.007	2.38E+11	2.53E+11	0	0.152	24.19
33	0.26	0.030	0.007	2.47E+11		0.07	0.084	1.47
49.5	0.19	0.030	0.006	2.75E+11	5.16E+11	0	0.282	18.97
71.5	0.28	0.031	0.006	3.14E+11	5.16E+11	0	0.003	3.76
75.5	0.28	0.031	0.006	3.21E+11	5.56E+11	0	0.001	17.10
81	0.27	0.031	0.005	3.31E+11		0.02	0.003	19.39
94.4	0.27	0.031	0.005	3.56E+11	5.56E+11	0	0.002	23.11

98	0.26	0.032	0.005	3.62E+11		0	0.001	23.35
104.5	0.26	0.032	0.005	3.74E+11	6.32E+11	0	0.006	26.66
121.4	0.24	0.032	0.005	4.05E+11		0	0.038	1.40
124.4	0.23	0.032	0.005	4.11E+11	6.29E+11	0.01	0.050	23.68
167	0.2	0.033	0.004	4.92E+11		0.04	0.060	28.16
171	0.2	0.034	0.004	5.00E+11	6.32E+11	0	0.058	21.89
176	0.16	0.034	0.004	5.10E+11		0.05	0.145	14.38
190.5	0.19	0.034	0.004	5.38E+11	5.10E+11	0.01	0.070	30.61
195	0.19	0.034	0.004	5.47E+11		0	0.068	31.41
200	0.19	0.034	0.004	5.57E+11	2.14E+11	0	0.062	31.81
214.5	0.19	0.035	0.003	5.86E+11		0	0.038	23.00
218.17	0.19	0.035	0.003	5.94E+11	2.93E+11	0	0.034	21.69
238.5	0.16	0.036	0.003	6.35E+11		0	0.076	28.28
242.5	0.15	0.036	0.003	6.43E+11	2.87E+11	0.01	0.105	24.16
247	0.15	0.036	0.003	6.53E+11	1.28E+11	0	0.094	27.10
262	0.15	0.036	0.003	6.84E+11		0	0.054	25.74
266	0.15	0.036	0.003	6.92E+11	2.14E+11	0	0.051	26.03
271.17	0.15	0.037	0.003	7.03E+11		0	0.045	25.56
289.17	0.15	0.037	0.003	7.42E+11		0	0.033	25.16
338.25	0.12	0.039	0.003	8.49E+11	2.86E+11	0	0.039	26.62
344.5	0.11	0.039	0.003	8.64E+11		0	0.042	31.47
358	0.1	0.039	0.003	8.94E+11	1.28E+11	0	0.071	29.68
363.5	0.09	0.039	0.003	9.07E+11	1.28E+11	0	0.082	27.50

Run 3

Time, h	r_x(substrates) [mmol C h^{-1}]	r_x(t) fit [mmol C h^{-1}]	μ [h^{-1}]	Fitted biomass, x(t)fit total	Cells measured, total	acetate [mM]	benzoate [mM]	Fe II [mM]
0	-0.23	0.033	0.004	4.7E+11	4.7E+11	1.3	0.5	35.9
23	-0.07	0.034	0.004	5.2E+11	5.1E+11	0.3	0.4	33.8
29	-0.23	0.034	0.004	5.3E+11	5.0E+11	1.5	0.5	34.1
32	-0.03	0.034	0.004	5.3E+11		0.2	0.4	29.1
53	0.00	0.035	0.003	5.8E+11	6.0E+11	0.3	0.2	31.3
81	0.04	0.035	0.003	6.3E+11	6.6E+11	0.0	0.0	35.9
99	0.01	0.036	0.003	6.7E+11	7.2E+11	0.0	0.1	37.9
107	0.09	0.036	0.003	6.9E+11		0.0	0.0	32.3
122	0.01	0.037	0.003	7.2E+11		0.0	0.1	37.4
130	0.07	0.037	0.003	7.3E+11		0.0	0.0	33.5
145	0.08	0.037	0.003	7.7E+11	8.5E+11	0.0	0.0	32.6
148	0.14	0.038	0.003	7.7E+11		0.0	0.0	27.9
154	0.03	0.038	0.003	7.9E+11		0.5	0.1	32.5
171	-0.01	0.038	0.003	8.2E+11	8.7E+11	0.3	0.1	37.3
180	0.12	0.039	0.003	8.4E+11		0.2	0.0	28.6
193	0.06	0.039	0.003	8.7E+11	9.0E+11	0.8	0.0	28.4
199	0.09	0.039	0.003	8.9E+11		1.1	0.0	24.0
202	0.15	0.039	0.003	8.9E+11		0.4	0.0	24.6
219	0.16	0.040	0.002	9.3E+11	9.7E+11	0.3	0.0	24.9
236	0.18	0.040	0.002	9.7E+11	1.0E+12	0.3	0.0	22.7
253	0.19	0.041	0.002	1.0E+12	9.0E+11	0.4	0.0	21.6
256	0.23	0.041	0.002	1.0E+12	7.9E+11	0.2	0.0	19.6
262	0.21	0.041	0.002	1.0E+12		0.2	0.0	21.1
276	0.23	0.042	0.002	1.1E+12	9.2E+11	0.2	0.0	19.6
282	0.21	0.042	0.002	1.1E+12		0.2	0.0	22.0

299	0.27	0.043	0.002	1.1E+12	9.2E+11	0.2	0.0	16.7
305	0.22	0.043	0.002	1.1E+12		0.1	0.0	21.0
326	0.18	0.044	0.002	1.2E+12	8.3E+11	0.3	0.0	23.3
331	0.19	0.044	0.002	1.2E+12	8.9E+11	0.5	0.0	20.5

Table 6. Bacterial 16S rRNA gene T-RFLP fingerprints for **Figure** 3-18

	Indigenous communities									Communities in dialysis bags							
TRF/ sample	**10 cm**	**15 cm**	**20 cm**	**25 cm**	**35 cm**	**40 cm**	**45 cm**	**50 cm**	**60 cm**	**1 bag (25 cm)**	**2 bag (40 cm)**	**3 bag (35 cm)**	**4 bag (20 cm)**	**5 bag (20 cm)**	**6 bag (40 cm)**	**7 bag (20 cm)**	***G. metallireducens***
61B	2.93	2.7	1.185	1.02	1.32	0.84	0.86	0.98	1.01	0	0	0	0	0	0	0	0
66B	0	0	0.38	0.84	0.675	0.82	0.75	0.85	0.395	3.46	0.5	5.44	0	4.09	0	0	0
71B	0.57	0	0	0.41	0	0.3	0.26	0.46	0.27	0	0	0	0	0	0	0	0
72B	1.17	1.765	0.555	0.53	0.33	0.3	0	0	0.23	0	0	0	0	0.54	0	0	0
74B	1.19	1.875	1.13	0.64	0.335	0.25	0.54	0.48	1.05	0.17	0	0	0	0	0	0	88.7
77B	0	0	1.075	3.24	10.48	17.48	20.91	6.39	1.445	0.37	15.7	0.39	0	0	0.53	0	0
79B	0	0.47	0	0.4	0.245	0.62	1.25	0.77	0.1	0.81	0	0.32	0	0	0	0	0
80B	0	0	0	0	0	0	0	0.35	1.33	0	0	0	0	0	0.17	0	0
82B	0.94	0.13	0	0	0.24	0.22	0	0	0.19	0	0	0	0	0	0	0	0
87B	0	0	0	0.61	0.72	2.17	2.51	2.35	0.445	0.85	1.21	1.47	0	0	0.52	0	0
88B	0	0	0	0	0	0	0	0	0	0.3	3.56	0.54	0	0	0.41	0	0
90B	0.63	0.535	0	0	0	0	0	0	0.56	0	0	0	0	0	0	0	0
91B	1.64	0.79	0.835	0.4	0.28	0.6	0.99	0.28	0.37	0.41	0	0.19	0	4.07	0.39	0	0
103B	0.3	0	0.55	0.49	0.52	0.83	0.99	0.69	0	0	0	0	0	0	0	0	0
106B	0.47	0.105	0.16	0.23	0.09	0	0	0	0	0	0	0	0	0	0	0	0
110B	1.67	1.68	0.765	0.35	0	0	0	0.31	0.515	0	0	0	0	0	0	0	0
113B	0	0	0.25	0.32	1.1	2.29	2.57	4.98	0.655	2.33	1.45	3.97	0	1.65	0.93	0	0
121B	0	0.85	0.385	0.29	0.86	0.7	0.38	1.32	4.985	0	0	0	0	0	0	0	0
122B	0	0.195	0.395	0.41	0.33	0.34	0.37	0.34	0	0	0	0	48.01	0	0	6.97	0
126B	0.5	0	0	0	0.31	0.25	0	0.31	0.25	0	0	0	0	0	0	0	0
128B	2.99	2.895	1.07	1.43	2.23	1.64	1.25	1.2	1.275	0	0	0	0	0	0	0	0
129B	4.5	3.155	2.635	1.44	1.13	1.36	0	1.02	1.29	0	0	0	0	0	0	0	0
132B	0	0	0.185	0.98	2.215	0.31	0	0	0	0	0	0	0	0	0	0	0
135B	0	0	0.19	0	0.975	2.99	1.71	1.22	1.145	0	0	0	0	5.16	0.43	0	0
136B	2.37	4.985	1.15	0.76	1.685	0.6	0	0	0	0.25	0	0	0	0	0	0	0
137B	1.02	0.76	0.78	0.88	0.97	0.78	0.92	0.53	0.485	0	0	0	0	0	0	0	0
138B	2.25	2.435	1.6	2.39	4.25	5.12	4.54	6.65	4.15	0	0	0	0	0	6.59	0	0
139B	0.69	1.98	3.335	2.37	4.81	0	0	0	1.22	0	0	0	0	0.55	0	0	0
141B	0.38	0	0	0	0	0.2	0	0	15.86	0.37	0	0	0	0	0	11.97	0
142B	3.22	0.1	0	0	0.47	0.56	0	0.25	0	0	0	0	0	0	0	0	0
143B	0	0	0	0.39	0.225	0.95	2.82	0.96	0	0	0	0	0	1.04	0	0	0
144B	0	0	0	0	0.135	0.94	0.78	0.65	0	0	0	0.95	9.62	1.05	0.32	0	0
146B	0	0	0	0	0	0	0.89	1.03	0	0	1.61	0	0	1.3	0	0	0
147B	21.69	17.715	8.78	5.24	3.675	2.57	3.74	5.66	6.185	1.9	0.61	0.6	0	0	3.69	0	0
149B	1.21	1.145	0.36	2.13	1.435	0.34	0.67	0.24	7.075	0	0.48	0	0	0	0.15	0	0
150B	4.57	0	0	0	0.095	0	0	0.28	0	0	0	0	0	0	0	0	0
154B	0	0.84	1.37	0.9	0.96	2.09	3.84	2.24	0.635	4.51	0	4.19	0	0	5.17	0	0
156B	0	0	0	0.37	1.495	3.37	0.87	0.84	0	0	0	0	0	0	0.56	0	0
157B	0.6	1.16	0	0	0	0	0	0	0.255	0	0	0	0	0	0	0	0
159B	2.16	2.735	2.095	3.51	4.695	2.95	3.8	3.28	2.495	0	0	0	0	0	0.93	0	5.84
160B	0	0.295	0.595	0.47	0.15	0.26	0	0	0	0	0	0	0	0	0	0.45	0
161B	0	0	0.5	0.69	0.205	0.42	0.37	0.41	6.12	0.71	0	0.22	0	0	0.27	1.86	0

	Indigenous communities									Communities in dialysis bags							
TRF/ sample	**10 cm**	**15 cm**	**20 cm**	**25 cm**	**35 cm**	**40 cm**	**45 cm**	**50 cm**	**60 cm**	**1 bag (25 cm)**	**2 bag (40 cm)**	**3 bag (35 cm)**	**4 bag (20 cm)**	**5 bag (20 cm)**	**6 bag (40 cm)**	**7 bag (20 cm)**	***G. metallireducens***
162B	1.4	0	0	0	0.745	0	1.19	0.9	0	0.17	0	0.18	0	0	2.9	0	0
163B	0	0.995	1.29	0	0	0	0	0	0	0	0	0	0	0	0	0	0
167B	0	3.27	2.775	1.34	0.93	0.96	0.81	1.23	0.93	0	0	0	0	0	0	0	0
169B	0.41	0.43	0.195	0	0.095	0	0	0	0	0	0	0	0	0	0	3.98	0
170B	0	0.1	0.17	0.3	0.08	0	0	0	0.575	0	0	0	0	0	0	0	0
172B	0.85	1.035	0.67	0.62	0.355	0	0	0	0.475	0	0	0	0	0	0	0	0
174B	0.37	0.195	0	0	0.45	0.22	0	0.2	0	0	0	0	0	0	0	0	0
175B	0.32	0.255	0.43	0.28	0.31	0.53	0.64	0.37	0	0	0	0	0	0	0	0	0
178B	0.7	0.8	0.93	0.43	0	0	0	0	0	0	0	0	0	0	0	0.62	0
180B	2.53	3.975	2.335	1.67	5.005	0.54	0.23	0.41	0.345	0	0	0	0	0	0	0	0
191B	0	0.27	0.765	0.24	0.625	0.44	0.33	0	0.75	0	0	0	0	0	0	0	0
192B	1.69	0	0	0	0	0	0	0	0	2.57	0	0.49	0	6.36	13.76	0	0
198B	0	0.22	0.57	0.48	0.09	0	0	0.26	0.25	0	0	0	0	0	0	0	0
201B	0	0.125	0.71	0	0.39	0	0	0.24	0.15	0	0	0	0	0	0	0	0
205B	0	0.19	0.73	0.51	0.415	0.63	0.95	1.2	2.545	0	0.54	0	0	0.18	0	0	0
206B	0	0.09	0.595	0.53	0	0.19	0	0	0.32	0	0	0	0	0	0	0.54	0
209B	0.64	0.2	0.19	0.22	0	0	0.21	0	0	0	0	0	0	0	0	0	0
219B	0.48	0	0	0	0	0	0.29	0.32	0	0	0	0	0	0	0	0	0
223B	0.8	0.73	0.955	0.45	0.29	0.26	0.27	0.18	0.415	0	0	0	0	0	0	0	0
268B	0	0.105	0	0	0	0	0	0	0.315	0	0	0	0	0	0.3	0	0
275B	0	0	0	0	0.23	0.5	0.34	0.51	0.09	0	0	0	0	0	0.31	0	0
280B	1.88	1.67	2.41	4.01	2.375	4.06	4.54	2.49	1.675	0	0	0	0	0.44	0.56	0	0
285B	0	0.135	0	1.2	0	0	0.24	0.19	0.57	0	0	0	0	0	0	0	0
287B	1.49	1.32	0.67	0.36	0.345	0.4	0	0.17	0.285	0	0	0	0	0	0	63.25	0
288B	0	0	0	0	0	0	0	0	0	10.14	0	10.58	0	0.18	1.27	0	0
294B	0	0	0	0	0	0	0	0.26	0.37	0	0	0	0	0	0	0	0
305B	0	0.56	0.875	0.78	1.01	0.57	0.4	0.31	0.44	0	0	0	0	0	0	9.58	0
401B	2.62	0.82	0	0	2.275	0	0	0	0	0.34	2.7	0.21	0	0.85	0.56	0	0
402B	0	0.99	2.31	4.29	0.74	1.26	2.32	1.7	1.54	0	0	0	0	0	0	0	0
422B	0.52	0.17	0.38	0.75	0.295	0.2	0.86	0.39	0.6	0	0	0	0	0	0	0	0
428B	0.91	0.855	0.8	0.64	0.49	0.23	0.51	0.38	1.25	6.68	0.32	19.8	0	25.51	3.77	0	0
429B	0	0	0	0	0	0	0	0	0	0	0.34	0	0	0	0	0	0
433B	0.7	0	0	0	0.21	0.27	0.28	0.27	0	0	0	0	0	0	0	0	0
434B	0	0	0	0.85	0	0	0	0	0.63	0.27	0	0.12	0	0	0.27	0	0
437B	0	1.76	1.84	3.18	2.585	3.2	3.03	2.53	0	0	0.39	0	0	0.29	0.25	0	0
438B	8.6	0	0	2	0.37	0	0	0	1.07	0.18	0	0.13	0	0	0	0	0
442B	0	0	0	0	0.095	0	0	0.3	0.285	0	0	0	0	0	0	0	0
448B	0.83	0	0	0.72	0.72	0.77	0.83	1.78	0.365	0	0	0	0	0	0	0	0
454B	0	1.115	1.875	0.46	0.47	0	0	0	0	0	0	0	0	0	0	0	0
455B	1.62	0	0	0	0	0.2	0	0.18	2.87	0	0	0	0	0	0	0	0
457B	0	0.65	1.09	0.37	0.715	0	0	0	0	0	0	0	0	0	0	0	0
460B	0	0.145	0	0	0.08	0.36	1.37	0.4	0	0.55	0	0.13	0	0	0.3	0	0
469B	3.93	0	0	0	1.085	2.81	2.33	2.39	1.19	0	0	0	0	0	1.3	0	0
469B	0	0.67	0.93	2.1	0	0	0	0	0	0	0	0	0	0	0	0	0

	Indigenous communities									Communities in dialysis bags							
TRF/ sample	**10 cm**	**15 cm**	**20 cm**	**25 cm**	**35 cm**	**40 cm**	**45 cm**	**50 cm**	**60 cm**	**1 bag (25 cm)**	**2 bag (40 cm)**	**3 bag (35 cm)**	**4 bag (20 cm)**	**5 bag (20 cm)**	**6 bag (40 cm)**	**7 bag (20 cm)**	***G. metallireducens***
473B	1.29	0.495	0.695	2.16	2.15	0.83	0.24	0.63	0	0	0	0	0	0	0	0	0
475B	0	0	0	0	0	0	0	0	0.23	0.52	0	1.81	0	3.77	1.05	0	0
478B	0	0	0	0	0	0	0	0	0.245	0.21	0	0.7	0	0.43	0.36	0	0
486B	0	0	0	1.09	0	0	0	0	0.565	25.91	32.28	23.37	0	0	12.81	0	0
488B	0	0	0.345	0.84	6.405	6.41	4.9	2.09	0.455	5.25	1.14	2.29	35.98	20.2	0.61	0	0
490B	0	20.295	35.415	15.4	10.265	11.33	5.76	17	7.4	15.88	2.79	11.73	0	14.09	26.94	0	0
492B	0	0	0	5.58	1.095	0	0	0	3.665	0	0	0.66	0	0	0	0	0
493B	0	0	0	0	0	0.25	0.43	2.84	0	0.6	1.35	0	0	6.34	3.15	0	0
494B	0	0.085	0	0	0	0	0	0	0	9.36	8.26	6.49	0	0	3.39	0	0
495B	0	0	0	0	0.595	0.78	0.78	1.17	0	0	0	0	0	1.3	0	0	0
496B	0	0	0.25	0.9	0.35	0	0	0	0	0	0	0	6.38	0	0	0	0
499B	1.22	0.885	0.735	2.44	1.55	2.09	1.62	3.28	0.305	2.21	13.62	0.39	0	0	1.33	0	0
502B	0	0	0.17	0.9	0.32	0.52	0	0	0	0	0	0	0	0	0	0	0
505B	0	0	0.59	0.26	0	0	0	0	0.205	0.59	0	1.18	0	0.15	0.26	0	5.45
508B	1.93	1.1	0	0.22	0.545	0	0.47	0	1.895	0.35	0	0.19	0	0	1.23	0	0
517B	0.65	0.09	0	0.42	0.29	0.27	0	0.48	0.245	0	0	0	0	0	0	0	0
521B	0	0	0	0.37	0.855	0.67	0	0.53	0	0	0	0	0	0	0.16	0	0
525B	0.7	0.105	0	0.48	0.37	0	0	0	0	0	0	0	0	0	0	0	0
529B	0	0	0	0	0	0.23	0	0.36	0.31	0	0	0	0	0	0	0	0
533B	0	0	0	0	0.26	0.82	0.92	1.04	0	0.22	0.47	0	0	0	0	0	0
542B	0.63	0.13	0	0.22	0	0	0	0	0.195	0.19	9.71	0	0	0	0	0	0
549B	0.6	0	0	0.36	0.09	0	0	0	0.08	0	0	0	0	0	0	0.78	0
596B	0	0	0	0	0	0	0	0	0	0.53	0.99	0.55	0	0	0.41	0	0
601B	0	0.935	2	1.63	0.135	0	0	0.68	0.625	0.26	0	0.29	0	0.29	0.9	0	0
610B	0	0	0	0.23	0	0	0	0.2	0.17	0	0	0	0	0	0	0	0
668B	0	0.74	0.835	1.1	0.815	0.64	0.66	0.94	0.35	0	0	0	0	0	0	0	0
676B	0	0	0	0.3	0.395	1.05	3.68	1.57	0	0	0	0.12	0	0.16	0.28	0	0
686B	0	0	0.2	2.21	0	0	0	0.31	0.785	0.58	0	0.31	0	0	0.54	0	0

Table 7. Median values of relative protein abundances assigned to respective metabolic pathways expressed in chemostats relative to batch for **Figure 3-22**

Pathways/median	A2/B1	A1/B3	A1/B1	A1/B1_	F2/B3	F3/B1	F1/B1	F2/B1	F4/B1_	F4/B1	L1/B3	L2/B1
16.1%, Unknown	1.5	1.8	1.5	2.3	1.5	1.3	1.4	1.5	0.9	1.9	1.2	1.5
10.4%, Protein synthesis	0.5	0.3	0.4	0.3	0.4	0.5	0.5	0.3	0.2	0.4	0.5	0.5
9.9%, Amino acids metabolism	1.3	1.0	0.9	1.0	0.9	0.9	0.8	0.9	1.4	0.9	1.2	1.0
8.6%, Carbohydrate metabolism	2.0	1.6	1.1	1.3	1.2	1.2	1.9	1.5	1.80	1.3	1.3	1.1
7.4%, Biosynthesis of cofactors	1.3	1.3	1.0	1.7	1.1	1.1	2.0	1.4	1.7	1.2	1.0	1.1
6.7%, Regulation	0.9	1.0	1.2	1.0	1.1	1.1	0.9	1.0	1.1	1.0	0.9	1.0
5.7% Energy metabolism	2.0	2.0	1.5	1.6	1.7	1.8	1.2	1.8	1.8	1.9	1.3	1.6
4.5%, DNA met and transcriptio	0.8	0.9	0.9	0.8	0.6	1.0	0.8	1.1	0.7	1.2	1.2	1.1
4.4%, Nucleotide metabolism	0.6	0.7	0.6	0.6	0.5	0.5	0.9	0.6	0.8	0.6	0.7	0.7
4.4%, Protein degradation	0.833	0.6	0.9	0.5	0.8	1.0	0.6	0.6	0.6	0.6	0.9	1.0
4.3%, Transport	0.9	1.0	0.9	0.7	0.6	0.7	0.8	0.8	1.7	1.2	1.0	1.0
4%, Cell envelope	1.2	1.9	1.6	1.5	0.8	1.4	0.8	1.2	2.3	1.6	1.0	1.4
2.8%, Chemotaxis and motility	1.2	1.0	1.2	1.4	1.1	0.8	1.3	1.0	0.9	0.8	0.8	0.7
2,8%, Wood-Ljungdahl pathway	4.5	5.9	4.0	4.4	5.4	3.6	2.6	10.7	9.8	11.2	8.9	4.0
2.2%, Signaling	1.0	1.4	1.1	1.9	1.2	1.1	1.6	1.5	1.1	1.5	1.0	0.9
1.6%, Nitrogen metabolism	0.5	1.0	1.5	1.0	1.1	1.7	1.6	1.1	0.7	0.9	1.3	2.3
1.2%, Cell division	0.7	0.9	1.2	1.6	1.9	0.9	1.8	1.3	1.1	0.9	1.1	1.2
1.2%, Sporulation	8.0	11.8	5.9	1.8	8.2	6.5	1.5	5.0	1.3	13.1	5.3	13.0
1.2%, Stress	1.5	3.7	2.0	1.9	4.8	2.2	1.0	4.0	1.9	4.2	2.9	2.8
0.6%, Sulfur metabolism	1.9	3.3	1.6	1.9	7.9	6.6	1.9	7.7	5.6	12.7	2.0	1.0

Table 8. Median values of relative protein abundances assigned to respective catabolic pathways expressed in chemostats relative to batch for **Figure 3-23**

Pathways	**Number of detected proteins**				**Median of the ratios**											
	Number of predicted proteins	**Lactate lim.**	**Fumarate lim.**	**Ammonium plus fimarate lim.**	**L1/B3**	**L2/B1**	**F2/B3**	**F3/B1**	**F1/B1**	**F2/B1**	**F4/B1_**	**F4/B1**	**A2/B1**	**A1/B3**	**A1/B1**	**A1/B1_**
Valine, leucine and isoleucine degradation	21	3	3	3	0.8	1.6	0.9	1.9		0.6		0.4	0.5	0.6	0.4	
Amino sugar and nucleotide sugar metabolism	36	17	17	17	1.1	1.5	0.6	1.4	0.7	0.8	2.3	1.2	2.1	1.1	1.0	1.5
Butanoate metabolism	48	11	11	11	1.6	1.3	1.6	1.0	2.3	1.8	2.3	2.5	4.5	2.2	1.3	2.3

Pathways	Number of detected proteins				Median of the ratios											
	Number of predicted proteins	Lactate lim.	Fumarate lim.	Ammonium plus fimarate lim.	L1/B3	L2/B1	F2/B3	F3/B1	F1/B1	F2/B1	F4/B1_	F4/B1	A2/B1	A1/B3	A1/B1	A1/B1_
C5-Branched dibasic acid metabolism	18	6	6	6	1.3	1.3	2.4	1.3	1.9	2.2	3.2	2.3	4.1	2.6	1.4	1.7
Citrate cycle (TCA cycle)	27	11	11	11	0.9	0.8	1.9	2.4	3.7	2.0	1.0	1.9	2.4	1.4	1.0	2.0
Fructose and mannose metabolism	14	6	6	6	1.5	1.0	1.4	1.4	2.6	1.8	2.8	1.9	1.3	2.2	1.2	3.3
Galactose metabolism	8	4	4	4	1.3	0.9	0.8	0.5		0.9		1.1	0.7	0.6	0.4	
Glycolysis / Gluconeogenesis	32	13	13	13	1.3	1.8	1.3	1.1	2.3	1.7	2.6	1.1	1.2	1.3	0.8	1.1
Glyoxylate and dicarboxylate metabolism	31	13	13	13	2.1	1.1	0.9	1.9	3.3	1.6	7.4	1.3	3.1	2.4	1.5	6.8
Pentose and glucuronate interconversions	14	4	3	3	1.0	0.7	0.9	0.8		0.4		0.7	1.8	0.4	0.9	
Pentose phosphate pathway	20	13	12	12	1.2	1.4	1.0	1.2	2.3	1.3	2.6	1.1	1.0	1.0	0.8	1.1
Propanoate metabolism	30	9	9	9	0.8	0.7	0.8	0.8	1.0	0.8	0.8	0.7	2.6	0.7	1.0	1.4
Pyruvate metabolism	38	13	13	14	1.1	0.7	0.7	0.7	1.1	0.8	2.0	0.6	1.9	0.9	1.0	1.3
Starch and sucrose metabolism	14	7	7	7	1.1	3.9	0.8	7.8		0.9		0.9	1.3	0.6	0.8	
Carbon fixation in photosynthetic organisms	15	11	11	11	1.1	1.3	1.0	1.1	1.9	1.7	3.1	1.2	1.3	1.1	1.1	1.3
Carbon fixation pathways in prokaryotes	73	21	21	21	2.2	1.0	1.5	1.8	2.0	2.0	1.6	1.9	2.7	1.7	1.3	3.0
Methane metabolism	68	23	25	25	1.4	1.6	1.0	1.7	2.3	1.2	1.5	1.4	1.0	1.4	1.5	1.4
Xenobiotics degradation	91	19	20	21	3.8	1.7	4.4	1.8	2.3	3.6	5.0	4.0	3.0	3.2	1.4	3.0
ethanol degradation under L1 and F2	6	1	1	1	4.2		1.3			49.2			0.3			
Lactate degradation	15	8	8	8	2.4	3.2	4.2	5.4	4.3	5.0	5.1	5.4	6.1	10.5	8.6	7.9
Galactose degradation	3	2	2	2	0.6	0.3	0.5	0.6		0.4		0.4	0.1	0.4	0.7	
Glycogen degradatation	3	2	2	2	1.3	6.3	1.1	7.2		0.9		1.1	2.1	0.6	6.1	